Tryptophan catabolism and amino acid transporter reprogramming in the tumour microenvironment

Elina Timošenko

Radcliffe Department of Medicine
Wolfson College
University of Oxford

A thesis submitted for the degree of Doctor of Philosophy

Trinity 2016

Abstract

A large proportion of human tumours exploit tryptophan catabolism as a means to suppress T cell activity in the tumour microenvironment. However, the mechanisms that allow tumour cells to resist the detrimental effects of local tryptophan depletion have so far remained obscure. Here we demonstrate that shortage of tryptophan induced by the expression of tryptophan-degrading enzymes indoleamine 2,3-dioxygenase (IDO) and tryptophan 2,3-dioxygenase (TDO) results in ATF4-dependent reprogramming of the amino acid transporter expression profile in tumour cells. Specifically, we show that tumour cells undergoing tryptophan starvation enhance the expression of several amino acid transporters including SLC1A5 and its truncated isoforms through activation of the ATF4 stress response pathway. While upregulation of SLC1A5 leads to improved glutamine and tryptophan uptake, the knockdown of this amino acid transporter inhibits tumour cell proliferation under low tryptophan conditions. In contrast to tumour cells, T cells fail to upregulate SLC1A5 during tryptophan starvation, but can enhance its expression upon cognate antigen T cell receptor engagement. SLC1A5 expression is also enriched in T regulatory cells and IDO-expressing dendritic cells, as well as in tumours growing under conditions of IDO-mediated tryptophan degradation *in vivo*. Finally, SLC1A5 expression correlates with IDO expression in several human tumours *in silico*, which is associated with poor prognosis in brain lower grade glioma. In conclusion, our results highlight key differences in the ability of tumour cells and T cells to adapt to tryptophan starvation and shed light on the previously unappreciated role of amino acid transport in IDO- and TDO-mediated immune escape.

Acknowledgement

First and foremost, I would like to thank my supervisor, Prof Vincenzo Cerundolo, for giving me the opportunity to work in his lab. His continued guidance and support have allowed me to develop both personally and professionally, for which I am immensely grateful. I am also grateful to Enzo's lab members, from whom I have learnt so much over the years. In particular, I would like to thank Hemza Ghadbane, Dawn Shepherd and Jon Silk, who have so generously shared their scientific expertise with me and taught me the right approach to science. My thanks also go to the Medical Research Council, Cancer Research UK, the Ludwig Institute for Cancer Research and the Harry Mahon Cancer Research Trust, which have funded this work. And, last but not least, I would like to thank my family – my mum and my husband in particular, who have supported me through all the ups and downs of this challenging yet rewarding journey, and to whom I dedicate this work.

Table of contents

Table of figures

Table of tables

Table of abbreviations

1MT	1-methyl-tryptophan
3-HAO	3-hydroxyanthranilate-3,4-dioxygenase
AhR	Aryl hydrocarbon receptor
AML	Acute myeloid leukemia
APC	Antigen presenting cell
ARNT	AhR nuclear translocator
ASNS	Asparagine synthetase
ATF4	Activating transcription factor 4
BCA	Bicinchoninic acid
BCR	B cell receptor
BenSer	*O*-Benzyl-L-serine
bHLH-PAS	Basic helix-loop-helix Per-Arnt-Sim
C/EBPβ	CCAAT/enhancer binding protein β
CAR	Chimeric antigen receptor
CARS	Cysteinyl-tRNA synthetase
CCL	C-C motif chemokine ligand
CCR	C-C chemokine receptor
CD	Cluster of differentiation
CD98hc	CD98 heavy chain
ChiP	Chromatin immunoprecipitation
CTH	Cystathionine gamma-lyase
CTL	Cytotoxic T lymphocyte
CTLA-4	Cytotoxic T-lymphocyte-associated protein 4
CXCL	C-X-C motif chemokine ligand
DAP12	DNAX activation protein of 12kDa
DC	Dendritic cell
DMEM	Dulbecco's Modified Eagle Medium
dsRNA	Double-stranded RNA
EAA	Essential amino acid
EDTA	Ethylenediaminetetraacetic acid

ER	Endoplasmic reticulum
FBS	Fetal bovine serum
FICZ	6-formylindolo[3,2-*b*]carbazole
FoxP3	Forkhead transcription factor
FW primer	Forward primer
GARS	Glycyl-tRNA synthetase
GAS	IFNγ-activated site
GCN2	General control nonderepressible protein 2
GFP	Green fluorescent protein
GFPT	Glutamine fructose-6-phosphate transaminase
GIST	Gastrointestinal stromal tumour
GITR	Glucocorticoid-induced TNF-receptor
GITRL	Glucocorticoid-induced TNF-receptor-related protein
GPT2	Glutamic pyruvate transaminase 2
HOXB9	Homeobox B9
HPLC	High performance liquid chromatography
HRI	Haem-regulated inhibitor
HRP	Horseradish peroxidise
HSP90	Heat shock protein 90
IDO	Indoleamine 2,3-dioxygenase
IFN	Interferon
IL	Interleukin
iNKT cell	Invariant natural killer T cell
iNOS	Inducible nitric oxide synthase
IRF1	IFN-regulatory factor 1
ISR	Integrated stress response
ISRE	IFN-stimulated response element
JAK	Janus kinase
KAT	Kynurenine aminotransferase
KYN-OHase	Kynurenine hydroxylase
KYNase	Kynureninase
LB broth	Luria-Bertani broth
LMP	Latent membrane protein
LPS	Lipopolysaccharide

MCT1	Monocarboxylate transporter 1
MDSC	Myeloid-derived suppressor cell
MEM	Minimum Essential Medium
MHC	Major histocompatibility complex
MICA	MHC class I polypeptide-related sequence A
MoDC	Monocyte-derived dendritic cell
mTOR	Mammalian target of rapamycin
NAD	Nicotinamide adenine dinucleotide
NF-κB	Nuclear factor κB
NK cell	Natural killer cell
NLR	NOD-like receptor
PB	Permeabilization Buffer
PBMC	Peripheral blood mononuclear cell
PBS	Phosphate buffered saline
PERK	PKR-like endoplasmic reticulum kinase
PFA	Paraformaldehyde
PGE2	Prostaglandin E2
PRK	Protein kinase RNA-dependent
PRR	Pattern recognition receptor
PSAT1	Phosphoserine aminotransferase 1
PSPH	Phosphoserine phosphatase
QPRTase	Quinolinate phosphoribosyl-transferase
RBD	Receptor Binding Domain
RT	Room temperature
RV primer	Reverse primer
SLC	Solute carrier
STAT1	Signal transducer and activator of transcription 1
TAA	Tumour-associated antigen
TAM	Tumour-associated macrophage
TAP	Transporter associated with antigen processing
TCA	Trichloroacetic acid
TCDD	2,3,7,8-tetrachloro-dibenzo-p-dioxin
TCR	T cell receptor
TDLN	Tumour-draining lymph node

TDO	Tryptophan 2,3-dioxygenase
Th cell	T helper cell
TLR	Toll-like receptor
TM	Transmembrane
TNF	Tumour necrosis factor
v-ATPase	Vacuolar H^+-adenosine triphosphatase
WARS	Tryptophanyl-tRNA synthetase
XAP2	Hepatitis B virus X-associated protein 2
XBE	Xenobiotic response element
αGalCer	α-galactosylceramide

CHAPTER 1: Introduction and aims of the project

1.1. Immune system: a brief overview

1.1.1. Myeloid and lymphoid lineages

The immune system is comprised of a complex network of organs (such as thymus, bone marrow and lymph nodes), cells and molecules, which function to provide defense against infectious organisms and other potentially damaging elements. The immune response can be broadly classified into the innate and adaptive immunity. The cells of the immune system originate in the bone marrow and derive from a common hematopoietic stem cell, which gives rise to erythroid, myeloid and lymphoid lineages. The erythroid lineage includes red blood cells and megakaryocytes, which distribute oxygen to body tissues and play a role in blood coagulation, respectively. Myeloid lineages, on the other hand, include the inflammatory and phagocytic cells of the innate immunity – granulocytes (neutrophils, eosinophils, basophils and mast cells), macrophages and dendritic cells (DCs), while lymphoid lineages include T lymphocytes, B lymphocytes and NK cells. Notably, both myeloid and lymphoid lineages can give rise to DCs (DeFranco et al., 2007).

1.1.2. Innate immunity

1.1.2.1. Pattern recognition receptors and the inflammatory response

Cells of the innate immune system are able to recognise foreign bodies through expression of pattern recognition receptors (PRRs) that bind to conserved microbial components. PRRs can be classified into membrane-bound PRRs, which include Toll-like receptors (TLRs) and C-type lectin receptors, and cytoplasmic PRRs, such as NOD-like receptors (NLRs) and RIG-I-like receptors (DeFranco et al., 2007). PRRs are designed to facilitate

recognition of a wide range of pathogens. TLRs, for example, are able to recognise diverse ligands both at the cell surface and intracellularly, including bacterial lipopolysaccharide (LPS), peptidoglycan, lipoteichoic acid, lipoarabinomannan and flagellin, as well as nucleic acids, such as viral double-stranded RNA (dsRNA) (Takeda et al., 2003). NLRs, on the other hand, specialise in recognising the substructures of bacterial peptidoglycan, among other ligands (Ferrand and Ferrero, 2013). PRR activation in tissue macrophages, mast cells and DCs induces initiation of the inflammatory immune response through production of numerous inflammatory mediators, including cytokines (e.g. tumour necrosis factor (TNF), interleukin 1 (IL-1), IL-6 and interferon (IFN)), chemokines (e.g. C-C motif chemokine ligand 2 (CCL2), CCL3, CCL5 and C-X-C motif chemokine ligand 8 (CXCL8)), lipid molecules (e.g. prostaglandin I2 (PGI2), PGE2 and leukotriene B4) and vasoactive amines (e.g. histamine) (DeFranco et al., 2007). These mediators increase vascular permeability and modulate the adhesive properties of the endothelium to attract more immune cells to the site of inflammation, as well as activate the incoming immune cells to stimulate their microbicidal functions. CXCL8, for example, promotes the recruitment of neutrophils – one of the first cells to arrive at the site of infection, which employ several killing mechanisms, including the production of reactive oxygen species through respiratory burst and phagocytosis (Kolaczkowska and Kubes, 2013). The latter is triggered by the activation of phagocytic receptors, such as mannose receptor and dectin-1, expressed on macrophages, DCs and neutrophils. Phagocytosis involves actin polymerization-mediated engulfment of the foreign body, its internalization through phagosome formation, and destruction of the phagosomal content via fusion with lysosomes and primary and secondary granules. Such granules contain numerous microbicidal mediators, including several proteases, defensins and the peptidoglycan-degrading lysozyme, among many others (DeFranco et al., 2007).

Activation of the complement cascade represents another important function of the innate immune system, which can be triggered by the formation of antibody-antigen immune complexes (classical pathway), by mannose-binding lectin and ficolin interaction with their ligands (lectin pathway), as well as through direct complement binding to the microbial surface (alternative pathway). The complement cascade involves approximately 30 serum and membrane proteins and can facilitate foreign substance destruction through multiple mechanisms, including the induction of inflammation, chemoattraction, phagocytosis and promotion of antibody generation. In addition, complement system plays a role in apoptotic cell clearance and the prevention of antibody-antigen complex accumulation (DeFranco et al., 2007).

1.1.2.2. Dendritic cells

DCs are specialised phagocytic cells that play a key role in the activation of the adaptive immune response through a process termed antigen presentation. Immature DCs reside in the peripheral tissues, where they constantly probe their tissue environment for potentially dangerous elements through expression of an arsenal of phagocytic receptors, including several TLRs, C-type lectin receptors, complement and Fc receptors. Antigens taken up by DCs are processed intracellularly and presented on the cell surface in the form of peptide-major histocompatibility complex (MHC) complexes. Importantly, antigen presentation can be classified into the endogenous and exogenous pathways, mediated by MHC class I and MHC class II molecules, respectively. While (endogenous) peptide fragments produced in the cytosol are presented by MHC class I molecules expressed on almost all cells, MHC class II molecules, which acquire their peptide fragments in endosomes, are mainly expressed by professional antigen presenting cells (APCs) – DCs, macrophages and B cells (DeFranco et al., 2007). Notably, immature tissue-resident DCs express low levels of MHC class II molecules but high levels of chemokine receptors CCR1, CCR2 and CCR5, which

allow their recruitment into the sites of infection/injury. Maturation of DCs can be triggered by microbial signals, such as LPS or dsRNA, inflammatory mediators, such as TNFα, IL-1β, IL-6 and PGE2, as well as mechanistic injury or necrosis (DeFranco et al., 2007; Mellman and Steinman, 2001). Upon maturation, DCs downregulate their phagocytic activity, upregulate cell surface expression of MHC class I and class II molecules, as well as cluster of differentiation (CD)40 and costimulatory molecules of the B7 family B7-1 (CD80) and B7-2 (CD86), and replace the receptors for inflammatory chemokines by CCR7, which facilitates DCs migration to T cell-rich zones of the lymph nodes, where they can present their antigens to T cells. DCs maturation in the presence of infection is also associated with the secretion of pro-inflammatory cytokines (e.g. IL-12, IFNα) and chemokines (e.g. TARC, RANTES, MIP-1α) (DeFranco et al., 2007; Mellman and Steinman, 2001).

1.1.3. Adaptive immunity

1.1.3.1. Lymphocyte antigen receptors

While cells of the innate immune system recognise antigens through a limited repertoire of receptors detecting conserved constituents of microorganisms, T and B lymphocytes, which represent the adaptive arm of the immune response, are able to recognise a myriad of different antigens through the expression of a single receptor, the T cell receptor (TCR) or B cell receptor (BCR), respectively, with a virtually unlimited repertoire of variants. This diversity is achieved during lymphocyte development in the thymus through a process called V(D)J recombination, by which T cells and B cells randomly assemble different combinations of distinct gene segments (variable (V), diversity (D) and joining (J) genes), each found in multiple copies, in order to generate unique antigen receptors, which collectively provide specificity for different antigens (DeFranco et al., 2007). Another

unique feature of the adaptive immune response is generation of immunological memory – the ability of the immune system to mount a stronger attack upon repeat antigen exposure.

1.1.3.2. Antigen recognition by T cells

αβT cells (further referred to as T cells) recognise antigens through binding of their αβTCR (a heterodimer composed of an α and β chain) to peptide-MHC complexes presented by APCs. There are two major T cell subsets – the MHC class I-restricted $CD8^+$ cytotoxic T lymphocytes (CTLs) and the MHC class II-restricted $CD4^+$ T helper (Th) cells. Commitment to CD8/CD4 T cell lineage occurs during T cell development in the thymus, where early lymphoid progenitors undergo positive and negative selection based on their affinity for ligand-MHC complexes. During this key process thymocytes expressing TCRs recognising self-peptide-MHC complexes with sufficient affinity get positively selected, while strong binding to self-peptide-MHC complexes leads to thymocyte negative selection and cell death by apoptosis (DeFranco et al., 2007). Notably, in the periphery, recognition of a specific peptide-MHC complex by the TCR (signal 1) is not sufficient for the induction of naïve T cell activation, as it also requires costimulation (signal 2), which is facilitated by the interaction of CD28 receptor on T cells with one of the costimulatory molecules of the B7 family, B7-1 (CD80) or B7-2 (CD86). B7-1 and B7-2 are expressed abundantly on professional APCs, particularly mature DCs (June et al., 1994). Of note, these molecules can also provide inhibitory signals to T cells by binding to the cytotoxic T-lymphocyte-associated protein 4 (CTLA-4) receptor on their surface, which is homologous to CD28 (Krummel and Allison, 1995). Importantly, T cell activation in the absence of costimulation or in the presence of strong inhibitory signals can lead to T cell anergy – the state of unresponsiveness characterised by incomplete activation and low IL-2 production (Crespo et al., 2013). In addition to the CD28:B7 interaction, T cell activation is assisted by the CD40L:CD40 interaction, and the CD4 and CD8 T cell coreceptors, which bind to the

invariant regions of the MHC class I and MHC class II molecules, respectively, focusing the T cell on the relevant MHC molecule and facilitating a prolonged Tcell:APC interaction. T cell activation is associated with initiation of the TCR signaling transduction cascade, which involves multiple mediators, including Lck, ZAP-70 and phospholipase Cγ1. Notably, it leads to actin polymerization and activation of a gene transcription program required for T cell clonal expansion, cytokine secretion and differentiation into effector subsets (DeFranco et al., 2007).

1.1.3.3. T cell effector subsets

$CD8^+$ CTLs are key effector cells of the adaptive immunity, which are specialised to provide immunity against viruses and other intracellular pathogens through secretion of IFNγ and TNFα, activation of the FasL-dependent pro-apoptotic pathway and granzyme-perforin cytotoxicity, which involves the release of cytotoxic granzymes (e.g. granzyme A and granzyme B) into the target cells through perforin-mediated pore formation (DeFranco et al., 2007). $CD4^+$ Th effector T cell subsets also play an important role in the adaptive immune response, and can be classified into Th1, Th2 and Th17 cells. Th cells mediate immunity through secretion of a range of cytokines, specific for each Th subset, which can activate different immune cell populations. Th1 cells, for example, secrete pro-inflammatory cytokines like IFNγ and facilitate the destruction of several pathogens, including bacteria, viruses and protozoa, by activated CTLs, macrophages and NK cells. In addition, Th1-type cytokines can promote antibody production by activated B cells. Th2 cells, on the other hand, abundantly secrete IL-4, and mediate the elimination of parasitic worm infections by eosinophils, basophils and mast cells, while Th17 cells produce IL-17 and coordinate neutrophil acute inflammatory responses (DeFranco et al., 2007). Another subset of $CD4^+$ T cells is represented by T regulatory (Treg) cells, which are characterised by the expression of the CD25 cell surface marker and forkhead transcription factor

(FoxP3) transcriptional activator. $CD4^+CD25^+FoxP3^+$ Treg cells can be generated in the thymus (naturally occurring Treg cells) or induced in the periphery in response to various tolerogenic stimuli (induced Treg cells). Treg cells play an important role in the suppression of pro-inflammatory effector T cell responses, which is achieved through multiple mechanisms, including anti-inflammatory IL-10 and TGFβ cytokine secretion and cell contact-dependent stimuli (Nishikawa and Sakaguchi, 2010; Zou, 2006).

1.1.3.4. Specialised T cell subsets

1.1.3.4.1. Invariant natural killer T cells

Invariant natural killer T (iNKT) cells represent a distinct subset of T cells recognising lipid (rather than peptide) antigens presented to them in conjunction with the non-classical MHC class I-like molecule CD1d, which is expressed on a range of hematopoietic cells, including DCs and B cells. The semi-invariant TCR of iNKT cells can be characterised by the expression of a conserved Vα24 chain and one of a limited number of conserved Vβ chains, predominantly Vβ11 (McEwen-Smith et al., 2015). iNKT cells can recognise glycosphingolipids from mycobacteria (Sada-Ovalle et al., 2008), α-proteobacteria like *Sphingomonas* (Kinjo et al., 2005; Mattner et al., 2005), and fungi (Albacker et al., 2013). α-galactosylceramide (αGalCer), derived from a marine sponge, was identified as the first iNKT cell glycosphingolipid agonist (Kawano et al., 1997). Following stimulation, iNKT cells are capable of mounting rapid responses in the form of abundant IFNγ and IL-4 secretion, which, in contrast to conventional T cells, does not require priming. iNKT cells can also act as potent activators of natural killer (NK) cells (directly through release of IFNγ) and conventional T cells (indirectly through interaction with APCs) (Cerundolo et al., 2009).

1.1.3.4.2. γδ T cells

γδ T cells are distinct from conventional $CD4^+$ and $CD8^+$ αβT cells, as they express the products of γ and δ rather α and β TCR genes and exhibit a more constrained TCR repertoire. γδ T cells develop early in ontogeny in a series of developmentally programmed waves and are thought to be particularly important for immune protection during perinatal period. In adults, γδ T cells are much less abundant than αβT cells but are present in high numbers at mucosal sites, including dermis, intestine, lungs and uterus. γδ T cells can be activated by bacterial and host intracellular metabolites, including phosphoantigens, as well as by molecules associated with cellular stress, such as MHC class I polypeptide-related sequence A (MICA), leading to rapid pro-inflammatory cytokine secretion and perforin-mediated cytotoxicity; however, the mechanisms of their activation still remain poorly understood. In addition to pathogen clearance, γδ T cells may also contribute to tissue integrity (DeFranco et al., 2007; Vantourout and Hayday, 2013).

1.1.3.5. Natural killer cells

Like T cells and B cells, NK cells also belong to lymphoid lineage, and share some effector functions with CTLs, such as granzyme-perforin cytotoxicity and IFNγ release. In addition, NK cells express Fc receptors that can recognise infected cells opsonised with antibodies and initiate killing by antibody-dependent cellular cytotoxicity. NK cells lack variable receptors for antigen recognition, but express inhibitory and activating receptors of the KIR family, which allow NK cells to differentiate between normal and abnormal cells. While binding of inhibitory KIR receptors to the constitutively expressed surface molecules, such as self MHC class I found on all uninfected healthy cells, prevents NK cell-mediated killing, recognition of ligands associated with DNA damage and other cellular stresses (e.g. MICA and MICB) by activating KIR receptors, such as NKG2D, promotes NK cell immune response (DeFranco et al., 2007; Smyth et al., 2005).

1.2. Tumour immunosurveillance and immune evasion

1.2.1. Anti-tumour immunity

The concept of tumour immunosurveillance, first proposed by Ehrlich (Ehrlich, 1909) and later formally postulated by Burnet and Thomas (Burnet, 1970; Thomas, 1959), implies that the immune system is able to protect the host against the development of cancer. After years of challenging the validity of this hypothesis, it has been established that the immune system can indeed detect and destroy transformed cells through recognition of tumour-associated antigens (TAAs). TAAs can be classified into those that arise as a result of protein overexpression or mutation in cancer; differentiation antigens that are typically associated with the cancer cell type of origin; viral proteins related to the neoplastic process and cancer-testis antigens (DeFranco et al., 2007). Anti-tumour immunity involves both innate and adaptive arms of the immune system, although NK cells and T cells – αβ T cells, (particularly $CD8^+$ CTLs), iNKT cells and γδ T cells are considered to be the main cellular effectors. The immune response against the tumour can be initiated by TAA recognition by host $CD8^+$ CTLs, as well as by NKG2D-mediated activation of NK cells and certain γδ T cells by ligands like MICA and MICB, which can be upregulated in response to tumour-associated cellular stress (Waldhauer and Steinle, 2008). In line with the concept of immunosurveillance, mice lacking the immune cell subsets mentioned above demonstrate increased susceptibility to tumour formation (Girardi et al., 2001; Smyth et al., 2001; Smyth et al., 2000), as do animals treated with NKG2D-neutralising antibodies (Smyth et al., 2005) or those deficient in genes encoding IFNγ, IL-12 or perforin (Kaplan et al., 1998; Shankaran et al., 2001; Smyth et al., 2000; Street et al., 2001; Street et al., 2002) – the critical mediators of the anti-tumour immune response executed by NK cells and tumour-specific T cells.

1.2.2. Strategies of tumour immune escape

Despite the evidence for the tumour-suppressor role of the immune response, it has become clear that the immune system can also aid tumour progression by selecting for tumour escape variants with lower immunogenicity and hence increased capacity to survive the immune attack. To incorporate the concept of immunity's dual role in cancer development, the cancer immunosurveillance theory has been refined into cancer immunoediting, which consists of elimination (tumour immunosurveillance), equilibrium and escape phases (Dunn et al., 2004). Notably, the immunoediting theory incorporates the notion of tumour immune escape, which is now classified as a hallmark of cancer (Hanahan and Weinberg, 2011). A wide range of tumour immune evasion mechanisms has been identified to date, which target several aspects of the anti-tumour immune response, as well as exploit host immunosuppressive mechanisms. One of the most well-documented strategies of tumour immune escape is impairment of tumour antigen presentation, which hampers MHC-dependent TAA recognition by tumour-specific T cells. This can be caused by a variety of mechanisms including downregulation or complete loss of MHC class I expression due to mutations in the β_2-microglobulin gene (Wang et al., 1993) or selective loss of individual HLA alleles (Natali et al., 1989). Other causes are mutations in transporter associated with antigen processing (TAP) and proteasome subunit-encoding latent membrane protein (LMP)2 and LMP7 genes (Johnsen et al., 1999; Restifo et al., 1993; RotemYehudar et al., 1996) implicated in the antigen processing machinery. Furthermore, tumour cells commonly fail to express costimulatory molecules of the B7 family, leading to T cell anergy as a result of TCR engagement in the absence of costimulation (Staveley-O'Carroll et al., 1998). In contrast, negative costimulatory signals in the tumour microenvironment, such as CTLA-4:B7 are readily engaged by cancer cells, delivering inhibitory signals to tumour-specific T cells (Leach et al., 1996). In addition, tumours can interfere with

proximal TCR signaling via downregulation of CD3ζ chain, $p56^{lck}$ and $p59^{fyn}$ kinases in tumour-infiltrating T cells (Mizoguchi et al., 1992), and activate pro-apoptotic pathways, such as FasL (Hahne et al., 1996), TRAIL (Giovarelli et al., 1999) an RCAS1 (Nakashima et al., 1999), leading to the induction of T cell apoptosis.

1.2.2.1. Tumour microenvironment

There is a growing body of evidence indicating that tumours also promote the development of an immunosuppressive microenvironment to escape from immune-mediated destruction. This is achieved by the production of anti-inflammatory mediators, including VEGF, PGE2, gangliosides and cytokines like TGFβ and IL-10; exploitation of inhibitory molecules of the B7 family, such as PD-L1, which can interact with PD-1 on tumour-specific T cells, leading to their anergy or apoptosis; and recruitment of immunoregulatory cells, such as Treg cells, tolerogenic DCs and myeloid-derived suppressor cells (MDSCs) (Zou, 2005). Accumulation of Treg cells has been observed in several cancers, and a low effector T cell to Treg cell ratio has been shown to correlate with poor prognosis (Nishikawa and Sakaguchi, 2010; Zou, 2006). In addition to Treg cell differentiation and expansion, tumours are able to promote trafficking of Treg cells from the peripheral blood, thymus, lymph nodes and bone marrow to the tumour site through release of CCL22, which engages C-C chemokine receptor type 4 (CCR4) on Treg cells (Curiel et al., 2004). Tolerogenic myeloid populations are also major contributors to the tumour-induced tolerance in the local microenvironment. These populations include specific subsets of myeloid DCs, plasmacytoid DCs (pDCs), tumour-associated macrophages (TAMs) and MDSCs capable of secreting anti-inflammatory cytokines and expressing immunosuppressive metabolic enzymes, such as inducible nitric oxide synthase (iNOS), arginase and indoleamine 2,3-dioxygenase (IDO), which produce nitric oxide and catalyse the degradation of arginine and tryptophan, respectively (Zou, 2005). Some of these

inhibitory mediators, particularly the amino acid-degrading enzymes arginase and IDO, can also be expressed by tumour cells themselves, leading to further establishment of immunological tolerance.

1.3. Introduction to tryptophan-degrading enzymes

1.3.1. Tryptophan metabolism

Out of 20 amino acids, 9 are considered essential (essential amino acid, EAA), as they cannot be synthesised endogenously by mammalian cells and so have to be obtained from external sources. Tryptophan is the least abundant of all EAAs, with plasma concentrations ranging from 40 to 80μM in humans (Armstrong and Stave, 1973) and from 60 to 100μM in mice (Demarte and Enesco, 1985; Rivera et al., 1987). Tryptophan obtained from the diet enters the liver through the hepatic portal system, where it can be used for protein synthesis (Sidransky, 1976). About 5% of the dietary tryptophan that is not used for protein synthesis in the liver or in the blood stream enters the methoxyindole pathway for the generation of neurotransmitter serotonin via the action of tryptophan hydroxylase **(Figure 1-1)**. In turn, serotonin can be used as a precursor for the neurohormone melatonin synthesis. The remaining 95% of tryptophan obtained from the diet, on the other hand, is shuttled down the kynurenine pathway, which represents the principal route of tryptophan degradation (Oxenkrug, 2010). IDO and tryptophan 2,3-dioxygenase (TDO) are cytosolic haem dioxygenase enzymes that catalyze the initial and rate-limiting step of the kynurenine pathway, which involves the oxidative cleavage of tryptophan indole ring **(Figure 1-1)**. This reaction yields *N*-formylkynurenine, which is rapidly converted to kynurenine, either spontaneously under acidic conditions or via formamidase activity, and can be further metabolised into other biologically active tryptophan metabolites, such as kynurenic acid, anthranilic acid, 3-hydroxykynurenine, 3-hydroxyanthranilic acid and quinolinic acid

(Thomas and Stocker, 1999) **(Figure 1-1)**. The end product of the kynurenine pathway is quinolinic acid-derived nicotinamide adenine dinucleotide (NAD) – a cellular cofactor key for redox metabolism, cellular function and survival. NAD^+ is involved in such critical biological processes as ATP synthesis and DNA repair, for example (Khan et al., 2007).

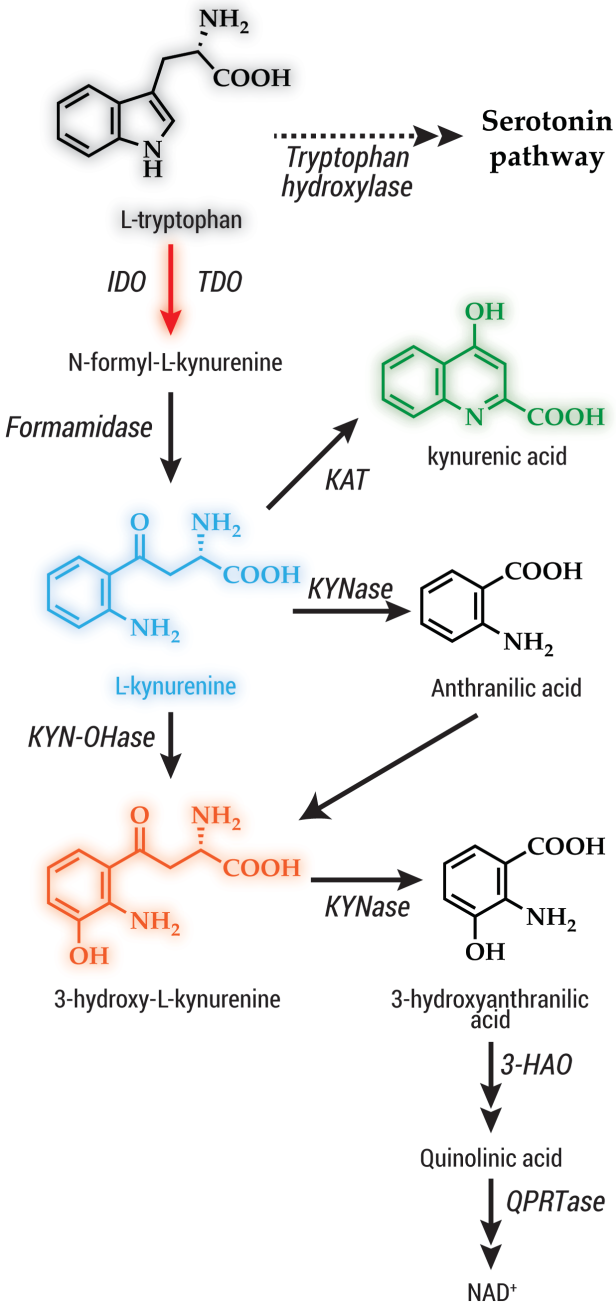

Figure 1-1. The kynurenine pathway

The kynurenine pathway describes the conversion of the EAA tryptophan into NAD^+. IDO and TDO enzymes catalyse the dioxygenation of tryptophan into N-formylkynurenine, which is followed by its spontaneous or formamidase-mediated conversion into kynurenine. Kynurenine can be further metabolised into 3-hydroxykynurenine, kynurenic acid or anthranilic acid through the action of kynurenine hydroxylase (KYN-OHase), kynurenine aminotransferase (KAT) or kynureninase (KYNase), respectively. Anthranilic acid can also be converted into 3-hydroxykynurenine through non-specific hydroxylation. Once 3-hydroxykynurenine is generated, KYNase can metabolise it into 3-hydroxyanthranilic acid, which can be used to synthesise NAD^+ through reactions involving 3-hydroxyanthranilate-3,4-dioxygenase (3-HAO) and quinolinate phosphoribosyl-transferase (QPRTase). Alternatively, tryptophan can be shuttled into the serotonin synthesis pathway catalysed by tryptophan hydroxylase.

1.3.2. The distinct characteristics of IDO1, IDO2 and TDO enzymes

There are two isoforms of the IDO enzyme, IDO1 and the less studied IDO2 isoform, which shares 43% sequence identity with IDO1 and is likely to have arisen from evolutionary gene duplication (Ball et al., 2007). IDO1 and TDO enzymes are even less structurally related and only share 10% sequence identity (Forouhar et al., 2007). Although these three haem dioxygenases catalyze the same reaction in the kynurenine pathway, there are substantial differences in their biochemical properties, molecular regulation and expression pattern. For example, while IDO1 exhibits broad substrate specificity, TDO only accepts a small range of tryptophan analogues for oxidation, including L-tryptophan, 5-fluorotryptophan and 6-fluorotryptophan but not serotonin or melatonin (Basran et al., 2008; Forouhar et al., 2007). Furthermore, IDO1 is widely expressed in various tissues, such as the placenta (including syncytiotrophoblasts, cytotrophoblasts and fetal membranes), gut, lung and pancreas (Kudo et al., 2004; Sarkar et al., 2007; Sedlmayr et al., 2002; Theate et al., 2015), and can be induced in several cell types in response to IFNγ (Carlin et al., 1989a; Munn et al., 1999; Takikawa et al., 1988). In contrast, TDO expression is mainly restricted to the liver (Knox and Mehler, 1950; Pilotte et al., 2012) and the brain (Haber et al., 1993; Kanai et al., 2009), and is largely unresponsive to immunological stimuli. On the other hand, TDO expression can be induced by dietary tryptophan and steroid hormones (Knox, 1966; Schimke et al., 1965). Like TDO, IDO2 also shows distinct tissue distribution (Fukunaga et al., 2012), but exhibits reduced enzymatic activity, compared to that of IDO1 (Austin et al., 2010; Ball et al., 2007).

1.3.3. Regulation of IDO expression

1.3.3.1. IDO induction stimuli

IDO1 expression can be found in various cell types, particularly APCs, such as macrophages (Munn et al., 1999) and DCs (Munn et al., 2002), but also neutrophils (De

Ravin et al., 2010; Lewkowicz et al., 2013), eosinophils (Odemuyiwa et al., 2004), epithelial cells (Barcelo-Batllori et al., 2002), endothelial cells (Xiao et al., 2013), fibroblasts (Curran et al., 2014) and smooth muscle cells (Pantoja et al., 2000). Several physiological inducers of IDO1 have been identified, of which IFNγ is the most potent. IFNγ-dependent *IDO1* gene expression relies on the presence of IFN-stimulated response elements (ISREs) and IFNγ-activated sites (GASs) in the *IDO1* promoter region, which interact with IFN-regulatory factor 1 (IRF1) and signal transducer and activator of transcription 1 (STAT1), respectively. In line with this, optimal *IDO1* gene transcription in response to IFNγ requires Janus kinase (JAK), STAT1 and IRF1 (Chon et al., 1995; Jeong et al., 2009; Konan and Taylor, 1996). Other soluble inducers of *IDO1* transcription include pro-inflammatory cytokines, e.g. TNFα, which synergises with IFNγ through activation of the nuclear factor κB (NF-κB) pathway (Robinson et al., 2006; Robinson et al., 2003), type I IFNs, IFNλ, IL-1 (Babcock and Carlin, 2000; Carlin et al., 1987; Fox et al., 2015; Hu et al., 1995) and tumour growth factor (TGF)β (Pallotta et al., 2011); several TLR ligands, e.g. LPS (Fujigaki et al., 2006; Hissong et al., 1995; Hissong and Carlin, 1997) and CpG-rich oligodeoxynucleotides (Fallarino and Puccetti, 2006; Volpi et al., 2012); hormones, e.g. oestrogen (Xiao et al., 2004; Zhu et al., 2007) and human chorionic gonadotropin (Ueno et al., 2007); and lipid molecules like PGE2 (Braun et al., 2005; Sayama et al., 1981). The latter has been shown to synergise with TNFα or TLR ligands in the induction of IDO expression in DCs through activation of adenylate cyclase (Braun et al., 2005), while TGFβ has been reported to trigger Fyn kinase-dependent IDO phosphorylation in pDCs, followed by NF-κB pathway activation and type I IFN signaling (Pallotta et al., 2011). In addition to soluble molecules, cell-contact dependent stimuli can also mediate IDO induction. In DCs, IDO expression can be triggered by the interaction of costimulatory molecules B7-1/B7-2 with CTLA-4 on Treg cells (Fallarino et al., 2003; Grohmann et al.,

2002; Munn et al., 2004b), engagement of glucocorticoid-induced TNF-receptor-related protein (GITRL) by glucocorticoid-induced TNF-receptor (GITR) on Treg cells (Grohmann et al., 2007), as well as by the activation of the CD200 receptor (Fallarino et al., 2004).

1.3.3.2. Negative regulators of IDO expression

Negative regulators of *IDO1* gene transcription include IL-4 (Musso et al., 1994), BLIMP-1, which has been reported to inhibit IFNγ-dependent *IDO1* gene transcription by binding to *IDO1* promoter (Barnes et al., 2009), and the *Tyrobp*-encoded DNAX activation protein of 12kDa (DAP12), downregulation of which is required for IDO functional competence (Orabona et al., 2006). Moreover, histone deacetylation has also been shown to repress *IDO1* transcription, as evidenced by the increased expression of *IDO1* in murine bone-marrow-derived DCs treated with histone deacetylase inhibitors (Reddy et al., 2008).

1.3.4. Regulation of IDO activity

In addition to transcriptional and epigenetic regulation, there is evidence of post-translational modulation of IDO activity. For example, phosphorylation of IDO has been shown to regulate its proteasomal degradation (Orabona et al., 2008) and signaling activity (Pallotta et al., 2011). IDO enzymatic activity is also subject to regulation by several biochemical factors, e.g. intracellular availability of haem, which IDO may need to compete for with enzymes like haem oxygenase 1 (Hill et al., 2005).

1.4. Physiological roles of tryptophan-degrading enzymes

1.4.1. The role of IDO in infection

IDO expression is commonly induced in infection, and the role of this enzyme in host defense against infection has been long recognised (Byrne et al., 1986; Carlin et al., 1989b; Pfefferkorn, 1984). The antimicrobial function of IDO has now been demonstrated for several pathogens *in vitro* and *in vivo*, including *Toxoplasma gondii* (Divanovic et al.,

2012), *Chlamydia trachomatis* (Leonhardt et al., 2007), *Candida albicans* (Bozza et al., 2005), flavivirus (Yeung et al., 2012) and measles virus (Obojes et al., 2005). In line with these findings, certain gain-of-function *IDO1* gene polymorphisms have been associated with increased protection against recurrent vulvovaginal candidiasis in humans (De Luca et al., 2013). On the other hand, IDO activity can also exert a counter-regulatory role and promote immunosuppression during infection by some pathogens, including, *Leishmania major* (Divanovic et al., 2012; Makala et al., 2011) and murine leukemia virus (Hoshi et al., 2010), leading to increased pathogen burden. These studies highlight the complex role of IDO pathway in infection, suggesting that its antimicrobial or immunoregulatory actions may be pathogen-specific.

1.4.2. The role of IDO in pregnancy

Although the importance of IDO activity for inhibition of pathogen growth has been known for many years, the biological significance of tryptophan catabolism in other physiological settings has only been addressed more recently, starting with pioneering work by Munn and Mellor, who demonstrated that IDO, which is highly expressed in the placenta, protects the fetus from maternal T cell attack during pregnancy (Munn et al., 1998). Notably, treatment of pregnant mice with the IDO inhibitor 1-MT leads to rapid rejection of allogeneic but not syngeneic concepti, which is dependent on maternal T cell infiltration and T cell-mediated complement activation (Mellor et al., 2001; Munn et al., 1998). In line with these findings, IDO induction at the maternal-fetal interface has been shown to improve pregnancy outcome in an abortion-prone mouse model (Li et al., 2009). Furthermore, pregnant women with pre-eclampsia exhibit a significantly increased tryptophan-to-kynurenine ratio in plasma (Kudo, 2013), suggesting impaired IDO expression/activity in this maternal syndrome. Consistent with these data, symptoms typical of pre-eclampsia have also been reported in $IDO^{-/-}$ mice (Santillan et al., 2015). Altogether, these studies highlight the key

role of IDO in the regulation of maternal T cell immunity during pregnancy and provide therapeutic opportunities for pregnancy conditions such as pre-eclampsia.

1.4.3. The role of IDO in autoimmunity

In addition to infection and pregnancy, IDO-mediated tryptophan catabolism has been implicated in autoimmunity. In contrast to *Foxp3* (Brunkow et al., 2001; Godfrey et al., 1991; Wildin et al., 2001) and *Ctla4* knockout mice (Waterhouse et al., 1995), *IDO1*-deficient animals do not exhibit spontaneous autoimmunity (Mellor et al., 2003), suggesting that IDO is dispensable for the maintenance of self-tolerance under homeostatic conditions. Rather, IDO appears to be important for establishing acquired tolerance to new or foreign antigens. Pharmacological inhibition or genetic disruption of IDO exacerbate clinical symptoms and inflammation in several models of autoimmune disease, including experimental autoimmune encephalitis (Kwidzinski et al., 2005; Sakurai et al., 2002; Yan et al., 2010), inflammatory bowel disease (Gurtner et al., 2003; Matteoli et al., 2010; Takamatsu et al., 2013) and insulin-dependent diabetes mellitus (Grohmann et al., 2003). Interestingly, autoimmunity in non-obese diabetic mice has been linked to the inability of IFNγ to induce IDO in DCs as a result of impaired STAT1 signaling, and rescuing tryptophan catabolism has been shown to restore tolerance in these mice (Grohmann et al., 2003). Moreover, induction of IDO has been shown to alleviate symptoms and reduce severity in several other autoimmune disease models, such as colitis (Ciorba et al., 2010; Coquerelle et al., 2009) and uveoretinitis (Choi et al., 2006). Interestingly, IDO has also been implicated in the induction of tolerance to self-antigens expressed by apoptotic cells, as evidenced by the development of lupus-like pathology and serum autoreactivity to double-stranded DNA in *IDO1*-deficient mice chronically exposed to apoptotic cells (Ravishankar et al., 2012).

1.4.4. IDO expression by APCs

At the cellular level, IDO-competent professional APCs, such as macrophages (Munn et al., 1999) and DCs (Munn et al., 2002), play a key role in the metabolic control of the adaptive immune response, in particular inhibition of antigen-specific T cell immunity, as has been demonstrated in autoimmunity (Grohmann et al., 2003), transplantation (Miki et al., 2001) and other immunological settings. IDO competence is confined to specific DC subsets, including $CD8\alpha^+$ DCs and $CD19^+$ pDCs in mice, and $CD123^+$ $CCR6^+$ pDCs and activated monocytes and macrophages in humans (Carlin et al., 1989a; Fallarino et al., 2002a; Mellor et al., 2003; Munn et al., 1999; Munn et al., 2004a; Munn et al., 2002). Notably, IDO expression and activity are induced upon DC maturation (Braun et al., 2005), and are important for optimal DC activation and migration (Hill et al., 2007; Hwang et al., 2005).

1.4.5. Other emerging physiological roles of IDO

Some reports suggest that IDO1 may also be involved in vascular homeostasis (due to the vasodilating properties of its metabolite kynurenine) (Wang et al., 2010), neurological functions like pain perception (Kim et al., 2012) and bone remodeling, as evidenced by the osteopenic phenotype of *IDO1*-deficient mice (Bozec et al., 2014).

1.4.6. Physiological roles of IDO2 and TDO

In contrast to the plethora of biological functions attributed to IDO1, physiological roles of IDO2 remain largely unknown due to the low activity of this more recently discovered enzyme (Austin et al., 2010; Ball et al., 2007) and the common presence of functionally attenuating *IDO2* polymorphisms in the Caucasian population (Metz et al., 2007). However, some evidence suggests that IDO2 may be involved in B cell autoimmunity (Merlo et al., 2014) and could support IDO1-mediated immunoregulatory functions (Metz et al., 2014). TDO, on other hand, is responsible for regulating systemic tryptophan concentrations, as well as the levels of neuroactive tryptophan catabolites in the brain, e.g.

quinolinic acid (Guillemin, 2012). In line with this, *TDO2* gene polymorphisms are associated with neurological disorders such as depression (Comings, 2001) and autism (Nabi et al., 2004), while *TDO2*-deficient mice exhibit increased anxiety-related behavior (Kanai et al., 2009).

1.5. IDO and TDO expression in the tumour microenvironment

1.5.1. IDO and TDO expression by tumours

In the past decade, tryptophan catabolism has emerged as an important mechanism of cancer immune escape. A significant proportion of human cancers constitutively express IDO (Theate et al., 2015; Uyttenhove et al., 2003), particularly endometrial and cervical carcinomas, among many others **(Figure 1-2)**. The immunosuppressive role of tryptophan catabolism in cancer was revealed by a key study conducted by Benoit Van den Eynde and co-workers, who showed that acquisition of IDO by immunogenic tumours prevents their rejection in pre-immunised mice through inhibition of tumour-specific $CD8^+$ T cell responses (Uyttenhove et al., 2003). An analogous immunosuppressive effect has been demonstrated *in vivo* for TDO (Pilotte et al., 2012) – another tryptophan catabolising enzyme that can be hijacked by human tumours (Opitz et al., 2011; Pilotte et al., 2012). Although the expression of TDO in human cancers has not been studied as extensively as that of IDO, it has been shown to be commonly overexpressed in hepatocellular carcinoma and glioblastoma **(Figure 1-2)**. Notably, constitutive TDO expression in glioblastoma not only inhibits the anti-tumour immune response but also enhances tumour cell survival and motility (Opitz et al., 2011). IDO2 expression has also been detected in some cancers (Lob et al., 2009; Witkiewicz et al., 2009b), however, the role of this isoform in tumour immune escape is yet to be determined.

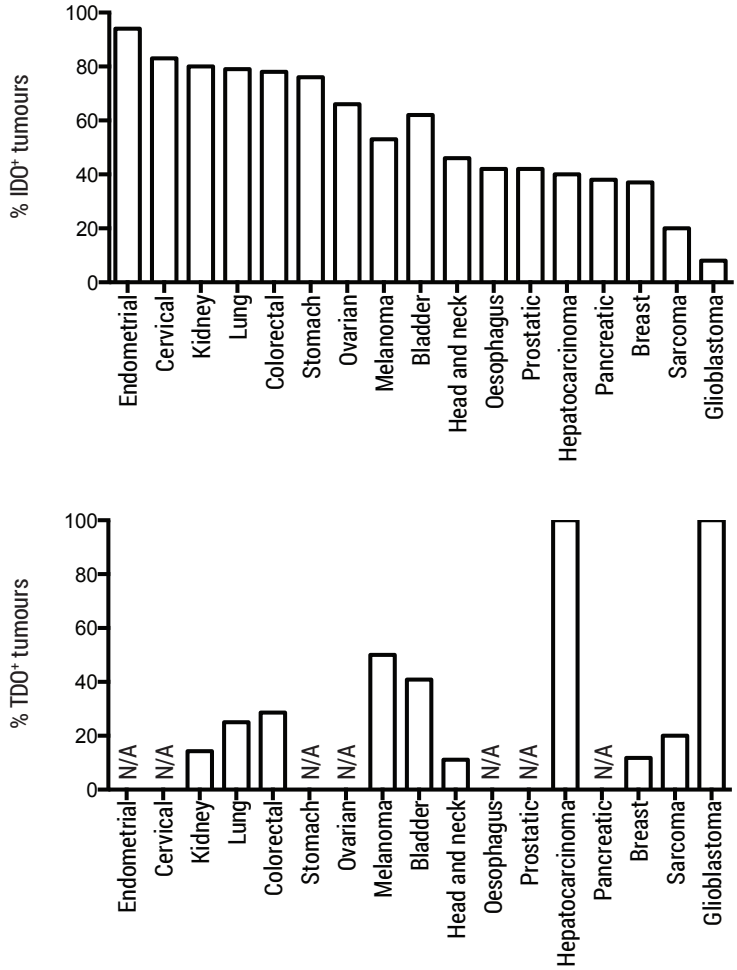

Figure 1-2. IDO and TDO expression in human tumours

IDO and TDO expression in primary human cancers was determined by immuno-histochemistry and/or q-RT-PCR. Adapted from (Opitz et al., 2011; Pilotte et al., 2012; Theate et al., 2015; Uyttenhove et al., 2003). N/A, non-applicable (data not available for this tumour type).

1.5.2. IDO expression by tumour-associated cells

Apart from tumour cells themselves, IDO can be expressed by other cells in the tumour microenvironment. IDO can be detected in tumour-infiltrating DCs and macrophages, for example, as well as in DCs in tumour-draining lymph nodes (TDLNs), as has been observed in patients with malignant melanoma and breast carcinoma (Lee et al., 2003; Munn et al., 2004a; Munn et al., 2002). Notably, such IDO-competent DCs exhibit immunosuppressive properties (discussed in Chapter 1.7) (Munn et al., 2004a; Sharma et al., 2007). In addition, IDO can be expressed by mesenchymal stem cells in the tumour microenvironment, which are able to suppress anti-tumour T cell responses and promote tumour growth in a manner dependent on IDO-mediated tryptophan catabolism (Ling et al., 2014). Notably, the upregulation of IDO in tumour-associated cells is of importance, as it may contribute to the tumour-induced tolerance in the local microenvironment.

1.5.3. Implications of IDO and TDO expression for tumour prognosis

Importantly, IDO expression is associated with poor clinical prognosis in several human cancers and typically correlates with decreased survival, e.g. in melanoma (Brody et al., 2009; Munn et al., 2004a; Speeckaert et al., 2012), colorectal (Gao et al., 2009), endometrial (Ino et al., 2008; Ino et al., 2006), ovarian (Inaba et al., 2009; Okamoto et al., 2005; Takao et al., 2007) and non-small cell lung carcinoma (Astigiano et al., 2005). Furthermore, in some cancers, such as colorectal (Brandacher et al., 2006; Huang et al., 2002), endometrial (Ino et al., 2006) and breast cancer (Mansfield et al., 2009; Yu et al., 2011), IDO expression correlates with increased risk of metastasis, which points to its active contribution to tumour progression. The association between TDO expression and clinical parameters in cancer has not been examined in as much detail yet, however, there is evidence of decreased survival of patients with TDO-expressing gliomas (Opitz et al., 2011).

1.5.4. IDO induction stimuli in the tumour microenvironment

A key question regarding IDO dysregulation in cancer is the nature of the molecular signaling events and stimuli controlling IDO expression in the tumour microenvironment. Evidence suggests that these factors can be intrinsic to the tumour or host immune cells. One cause of IDO upregulation in tumour cells is loss of the tumour-suppressor gene *Bin1* (Muller et al., 2005). *Bin1* acts as a negative regulator of *IDO1* expression, and is commonly deleted, aberrantly spliced or downregulated in cancer (Ge et al., 1999; Ge et al., 2000a; Ge et al., 2000b; Tajiri et al., 2003). Genetic loss of *Bin1* activates STAT1- and NF-κB-dependent transcription of *IDO1* in transformed cells, and promotes tumour immune escape through suppression of anti-tumour T cell responses (Muller et al., 2005). IDO expression in tumours can also be driven by cancer-specific signaling pathways, such as the constitutively activated oncogenic KIT-PI3K-AKT pathway in gastrointestinal stromal tumour (GIST) (Balachandran et al., 2011). Others have shown that PGE2 is also able to induce IDO expression in tumour cells (Basu et al., 2006) and tumour-associated dendritic cells (von Bergwelt-Baildon et al., 2006). IFNγ produced by tumour-infiltrating T cells is another potent stimulus for IDO upregulation in the tumour microenvironment (Spranger et al., 2013). Importantly, it has been demonstrated that the induction IDO as well as PD-L1 expression in melanoma is caused by the immune pressure imposed on tumour cells by $CD8^+$ T cells (Spranger et al., 2013), demonstrating that some major mechanisms of tumour immune escape can be intrinsically driven by the immune system itself.

1.6. Sensing of tryptophan catabolism

IDO enzyme activity not only depletes tryptophan from the local microenvironment but also leads to the production of biologically active tryptophan metabolites, such as kynurenine. It has become clear that these outcomes of the kynurenine pathway –

tryptophan deprivation and accumulation of kynurenine, mediate their immunosuppressive effects through activation of distinct metabolic pathways.

1.6.1. The GCN2-ATF4 pathway

Depletion of tryptophan (and other amino acids) is sensed through two amino acid responsive pathways – the general control nonderepressible protein 2 (GCN2) kinase pathway and the mammalian target of rapamycin (mTOR) pathway. The GCN2 pathway is designed to detect amino acid deficiency and is directly activated by uncharged tRNA, the levels of which increase upon amino acid starvation (Dong et al., 2000; Wek et al., 1995). Aminoacyl-tRNA synthetases are a family of enzymes that interpret the genetic code by covalently linking amino acids to their specific tRNA molecules. For example, *WARS* gene-encoded tryptophanyl-tRNA synthetase adds tryptophan onto $tRNA^{TRP}$, and the resulting tryptophan-$tRNA^{TRP}$ complex (tryptophanyl-tRNA) can be subsequently used for protein synthesis. Notably, inhibition of tRNA charging via loss of aminoacyl-tRNA synthetase function, activates GCN2 even under amino acid-sufficient conditions (Wek et al., 1995). Once activated, GCN2 kinase undergoes autophosphorylation (Romano et al., 1998) and dimerization (Qiu et al., 2001; Qiu et al., 1998), and phosphorylates the translation initiation factor eIF2α on Ser51, leading to a global translational reduction (Dever et al., 1992). However, a number of selected transcripts can still be translated under conditions of eIF2α phosphorylation due to the presence of alternative upstream open reading frames in the 5'UTR of the mRNA (Harding et al., 2000a; Lu et al., 2004; Vattem and Wek, 2004). One of such transcripts is the activating transcription factor 4 (ATF4) **(Figure 1-3)**, a master transcriptional regulator of the integrated stress response (ISR) – a pro-survival gene expression program critical for adaptation to cellular stress. By binding to the amino acid response elements in the promoters of ATF4-dependent genes, ATF4 regulates transcription of a spectrum of genes involved in amino acid synthesis and import, resistance

to oxidative stress, apoptosis and other functions (Harding et al., 2000a; Harding et al., 2003). ATF4 also induces expression of other transcription factors, such as ATF3 (Jiang et al., 2004), CHOP/DDIT3/GADD153 (Han et al., 2013; Wang et al., 1998; Zinszner et al., 1998), TRIB3 (Ohoka et al., 2005), HERPUD1 (Kokame et al., 2000) and the negative regulator of the eIF2α kinase response GADD34 (Ma and Hendershot, 2003; Novoa et al., 2001), to assist in the regulation of the ISR transcriptional program **(Figure 1-3)**. Although GCN2 is the most relevant eIF2α kinase in the context of amino acid starvation, ATF4 can be activated in response to eIF2α phosphorylation triggered by other type of stresses. Mammalian cells have four kinases that phosphorylate eIF2α – GCN2, PKR-like endoplasmic reticulum kinase (PERK), haem-regulated inhibitor (HRI) and protein kinase RNA-dependent (PKR), each responsive to distinct stress conditions, namely amino acid deficiency (Dong et al., 2000; Wek et al., 1995), accumulation of unfolded proteins in the endoplasmic reticulum (ER) (Harding et al., 2000b; Harding et al., 1999) and hypoxia (Koumenis et al., 2002), haem deprivation (Chen et al., 1991; Han et al., 2001), and infection with RNA viruses (Meurs et al., 1990), respectively **(Figure 1-3)**. All of these environmental stresses activate ATF4, albeit through distinct pathways upstream. In addition to nutrient deprivation, GCN2 can also be activated in response to UV irradiation, however, this does not lead to ATF4 activation but rather NFκB signaling (Deng et al., 2002; Dey et al., 2012; Jiang and Wek, 2005).

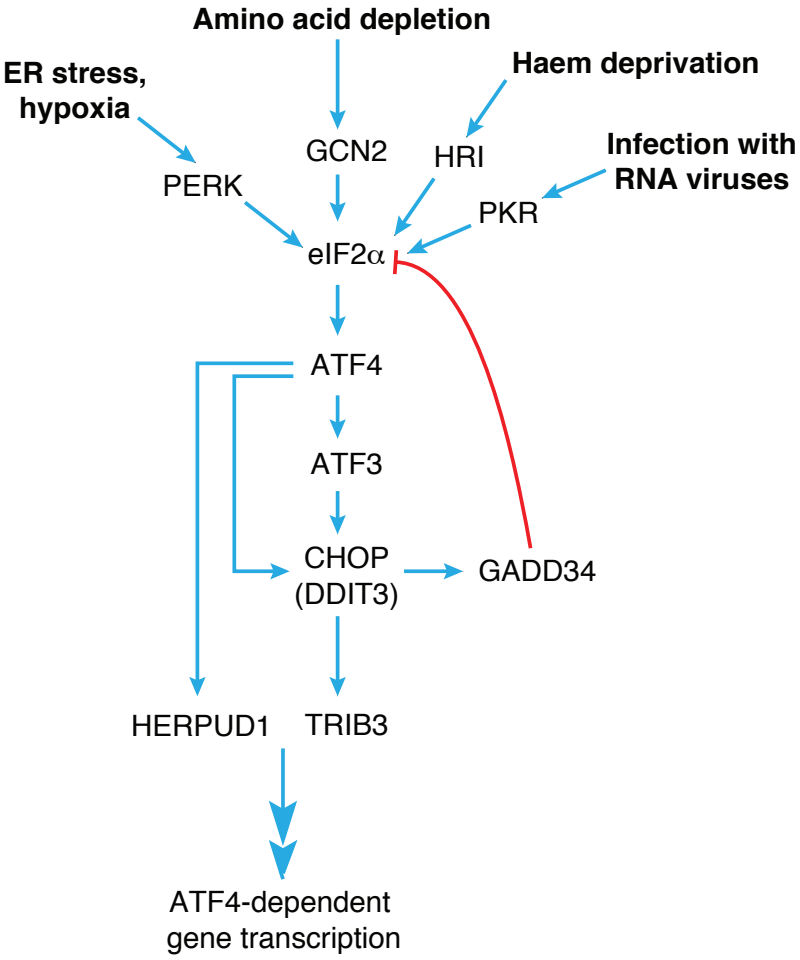

Figure 1-3. Activation of the ATF4 pathway by distinct cellular stresses
GCN2, PERK, HRI and PKR are eIF2α kinases that activate the ATF4 ISR pathway in response to specific environmental stresses – amino acid starvation, ER stress/hypoxia, haem deprivation and RNA virus infection, respectively. ATF4 cooperates with the downstream transcription factors ATF3, CHOP (DDIT3), TRIB3 and HERPUD1 to initiate the transcription of ATF4 target genes. GADD34, on the other hand, constitutes part of the negative feedback regulatory loop of the ISR response, which promotes protein synthesis recovery through eIF2α dephosphorylation.

1.6.1.1. The role of the GCN2-ATF4 pathway in adaptation to nutrient starvation and tumour development

The role of GCN2 in adaptation to nutrient deprivation conditions has been demonstrated *in vivo*, as evidenced by the enhanced loss of body mass and increased mortality of $GCN2^{-/-}$ mice fed leucine-free diet (Anthony et al., 2004). In addition, GCN2 has been shown to play a role in managing nutritional stress during embryogenesis (Zhang et al., 2002). The GCN2-eIF2α-ATF4 pathway has also been implicated in cancer. It has been shown to be activated in several human and mouse tumours (Ye et al., 2010) and capable of promoting survival and proliferation of tumour cells under amino acid starvation conditions. In line with this, tumours with silenced GCN2 or ATF4 exhibit significantly reduced growth *in vivo* (Ye et al., 2010).

1.6.2. The mTOR pathway

Amino acid starvation can also affect the mTOR pathway, which functions to confirm amino acid availability and maintain protein synthesis and cell growth. In addition to amino acids, mTOR activity can be modulated by such stimuli as growth factors, cytokines, energy status, hypoxia and DNA damage (Thomson et al., 2009). However, amino acids appear to be the most potent inducers of mTOR, as evidenced by the inability of growth factors to activate mTOR under conditions of amino acid starvation (Sancak et al., 2008). Amino acid-induced mTOR activation takes place at the lysosomal surface and involves Ragulator- and Rag GTPase-dependent translocation of mTORC1 to the lysosome, where it can interact with its direct upstream activator Rheb (Bar-Peled et al., 2012; Kim et al., 2008b; Sancak et al., 2010; Sancak et al., 2008), leading to the phosphorylation of the mTOR downstream substrates 4E-BP1/eIF4E and p70 S6 kinase (and its targets S6 ribosomal protein and eEF2, among others), and translation initiation (Beretta et al., 1996; Brunn et al., 1997; Hara et al., 1998; Holz et al., 2005). Although the molecular events

involved in the detection of amino acid availability in the mTOR pathway are still poorly understood, the lysosomal amino acid sensing machinery regulating mTOR is thought to involve vacuolar H^+-adenosine triphosphatase (v-ATPase) (Zoncu et al., 2011) and SLC38A9-(Rebsamen et al., 2015; Wang et al., 2015b) and SLC36A1 (PAT1)-mediated (Ogmundsdottir et al., 2012) amino acid transport. Notably, tryptophan unavailability and IDO-mediated tryptophan catabolism have been reported to suppress mTOR signaling, which can be rescued by tryptophan supplementation or pharmacological inhibition of IDO (Cobbold et al., 2009; Metz et al., 2012).

1.6.3. The AhR pathway

While GCN2 and mTOR pathways are responsible for sensing IDO-mediated tryptophan depletion, the biologically active tryptophan metabolites kynurenine and kynurenic acid act on a different pathway, having been identified as endogenous ligands of the aryl hydrocarbon receptor (AhR) (DiNatale et al., 2010; Opitz et al., 2011). AhR is a highly conserved transcription factor of the basic helix-loop-helix Per-Arnt-Sim (bHLH-PAS) family activated in response to environmental xenobiotic toxic chemicals like 2,3,7,8-tetrachloro-dibenzo-p-dioxin (TCDD) and 6-formylindolo[3,2-*b*]carbazole (FICZ). In the cytoplasm, AhR is found as part of a chaperone complex consisting of heat shock protein 90 (HSP90), p23 and Hepatitis B virus X-associated protein 2 (XAP2). Upon ligand binding, AhR translocates to the nucleus and forms a heterodimer with its dimerisation partner AhR nuclear translocator (ARNT), which allows it to bind to xenobiotic response elements (XREs) and induce transcription of target genes like cytochrome *P4501A1*, which is involved in xenobiotic metabolism (Bersten et al., 2013; Esser et al., 2009). Similarly to AhR high-affinity ligand TCDD, kynurenine has been shown to increase AhR nuclear translocation (Opitz et al., 2011), while both kynurenine and kynurenic acid have been reported to activate the transcription of AhR-dependent genes (DiNatale et al., 2010; Opitz

et al., 2011).

1.6.3.1. The role of AhR in tumour development

Although best known for mediating environmental toxicity, AhR has several physiological roles, including immunological settings like autoimmunity and infection (Esser et al., 2009). Notably, mice with constitutive AhR expression are highly susceptible to tumour development (Moennikes et al., 2004), suggesting a role for AhR in cancer. Evidence exists that AhR may be specifically implicated in TDO-related tumour tolerance. One study reported that tumour TDO-derived kynurenine can inhibit tumour-specific $CD8^+$ T cell infiltration and enhance tumour cell survival and motility through activation of AhR in human glioblastoma (Opitz et al., 2011). These findings suggest that kynurenine-dependent AhR activation may be responsible, at least in part, for mediating the immunosuppressive effects of tryptophan-degrading enzymes.

1.7. Inhibition of the anti-tumour immune response by tryptophan catabolism

There is a growing body of evidence indicating that IDO and TDO expression in the tumour microenvironment leads to induction of localised immune tolerance, which provides the tumour with a selective growth advantage (Friberg et al., 2002; Ling et al., 2014; Muller et al., 2005; Muller et al., 2008; Opitz et al., 2011; Pilotte et al., 2012; Uyttenhove et al., 2003). Recent findings demonstrate that IDO- and TDO-mediated tryptophan catabolism contributes to tumour-induced tolerance through multiple mechanisms.

1.7.1. Induction of T cell proliferative arrest by tryptophan catabolism

One important aspect of immune regulation by IDO is inhibition of T cell proliferation. In T cells, IDO-mediated tryptophan depletion induces a proliferative arrest, inhibiting the

G1-to-S phase transition (Kudo et al., 2001; Munn et al., 1999; Munn et al., 2005; Silk et al., 2011). Notably, GCN2 activation is instrumental for this phenomenon, as T cells from $GCN2^{-/-}$ mice remain resistant to IDO-mediated suppression and continue to proliferate even in the presence of IDO-competent pDCs (Munn et al., 2005). The inhibitory effect of IDO- and TDO-mediated tryptophan catabolism on tumour-specific $CD8^{+}$ T cell infiltration has also been demonstrated in various tumour models *in vivo*, and can be reversed by pharmacological inhibition of IDO or TDO (Ling et al., 2014; Opitz et al., 2011; Pilotte et al., 2012; Uyttenhove et al., 2003).

1.7.2. Pro-apoptotic properties of tryptophan metabolites

Tryptophan metabolites, including kynurenine, 3-hydroxykynurenine, 3-hydroxyanthranilic acid and quinolinic acid can also exhibit immunosuppressive properties, particularly the induction of apoptosis in activated T cells and NK cells (Fallarino et al., 2002b; Frumento et al., 2002; Lee et al., 2010; Terness et al., 2002). Interestingly, such cytotoxic action appears to be selective to certain T cell subsets. 3-hydroxyanthranilic acid and quinolinic acid, for example, induce cell death in Th1 but not Th2 cells (Fallarino et al., 2002b). In addition to Th2 cells, DCs also exhibit resistance to tryptophan metabolite cytotoxicity (Terness et al., 2002). Consistently, administration of tryptophan metabolites *in vivo* induces selective depletion of specific immune cell subsets (Fallarino et al., 2002b). The molecular mechanisms mediating this selective cytotoxicity are not fully understood, but may involve caspase-8 activity (Fallarino et al., 2002b), glutathione depletion (Lee et al., 2010) and inhibition of TCR engagement-induced NF-κB activation (Hayashi et al., 2007). There is also evidence that tryptophan metabolites may synergise with tryptophan depletion in the induction of some immunosuppressive effects, e.g. TCR ζ-chain downregulation and the associated reduction in effector T cell cytotoxic function (Fallarino et al., 2006).

1.7.3. Other effects of tryptophan catabolism on effector T cells

IDO-catalyzed tryptophan metabolism may also hamper anti-tumour effector T cell responses by inducing anergy (Munn et al., 2005; Munn et al., 2004a), suppressing T cell activation through disruption of calcium signaling (Iken et al., 2012), and interfering with T cell metabolism, namely inhibiting glucose uptake, aerobic glycolysis and glutaminolysis (Eleftheriadis et al., 2014; Eleftheriadis et al., 2013).

1.7.4. The effect of tryptophan catabolism on Treg cells

1.7.4.1. Induction of Treg cell conversion by tryptophan catabolism

In contrast to the inhibitory effects of tryptophan catabolism on effector T cell responses, IDO activity strongly promotes Treg cell differentiation and function. Both pDCs and monocyte-derived DCs (MoDCs) expressing IDO have been shown to induce Treg cells (Chen et al., 2008; Chung et al., 2009; Jurgens et al., 2009). Tryptophan deficiency, in synergy with tryptophan metabolites, is also able to trigger the conversion of naïve $CD4^+$ $CD25^-$ T cells into a regulatory phenotype (Fallarino et al., 2006). Furthermore, IDO expression in human tumours often correlates with the increased number of Treg cells, e.g. in acute myeloid leukemia (AML), non-Hodgkin's lymphoma, cervical cancer, melanoma and breast cancer (Curti et al., 2007b; Liu et al., 2014; Nakamura et al., 2007; Spranger et al., 2013; Witkiewicz et al., 2009a; Yu et al., 2011). Evidence exists that such bias towards a Treg cell phenotype is tumour-driven. In line with this concept, exposure of $CD4^+$ $CD25^-$ T cells to tumour cell conditioned medium is able to induce Treg cell generation (Curti et al., 2007b; Liu et al., 2007). Moreover, AML cells and leukemic dendritic cells that express IDO can directly promote Treg cell conversion, generating Treg cells capable of suppressing leukemia-specific effector T cell responses (Curti et al., 2007a; Curti et al., 2007b; Curti et al., 2010). Treg cell conversion in this system is dependent on IDO, as it can be suppressed by pharmacological inhibition of the enzyme (Curti et al., 2007b; Curti

et al., 2010). Acquisition of the regulatory phenotype by naïve $CD4^+CD25^-$ T cells under low tryptophan conditions is thought to depend on TGFβ-mediated induction of FoxP3 (Cobbold et al., 2009; Fallarino et al., 2006) and GCN2 activation (Fallarino et al., 2006), although there is some evidence that inhibition of mTOR signaling may also be involved (Cobbold et al., 2009). In addition to tryptophan depletion, Treg cell generation can be induced by AhR activation by kynurenine or other AhR ligands (Funatake et al., 2005; Gandhi et al., 2010; Mezrich et al., 2010), revealing another molecular mechanism employed by IDO to signal for a Treg cell phenotype. Finally, the ability of tumour-derived IDO to increase Treg cell numbers has been confirmed in mouse tumour models *in vivo* (Curti et al., 2007b; Wainwright et al., 2012).

1.7.4.2. Treg cells activation by tryptophan catabolism

In addition to *de novo* generation of Treg cells (Chen et al., 2008), IDO-expressing pDCs in TDLNs are able to activate pre-existing Treg cells and enhance their suppressor function in an IDO-, GCN2- and CTLA-4-dependent manner (Munn et al., 2004a; Sharma et al., 2007). Such IDO-induced Treg cells appear to utilise the PD-1/PD-L1 pathway for immunosuppression (Sharma et al., 2007). In addition, IDO-competent pDCs contribute to the maintenance of a stable Treg cell phenotype, limiting Treg cell plasticity and preventing Treg cell conversion into pro-inflammatory Th17 cells through GCN2-dependent inhibition of IL-6 production (Baban et al., 2009; Sharma et al., 2010; Sharma et al., 2009).

1.7.4.3. Reciprocal IDO induction by Treg cells

In turn, Treg cells can induce IDO expression in DCs by initiating the CTLA-4 interaction with DC costimulatory molecules B7-1/B7-2. CTLA-4 ligation triggers reverse signaling by B7-1/-B7-2, leading to IFNγ- and STAT1-dependent IDO production (Fallarino et al., 2003; Grohmann et al., 2002; Munn et al., 2004b). Importantly, constitutive IDO expression by mesenteric lymph node DCs is dependent on this Treg cell-mediated

induction mechanism (Onodera et al., 2009). Upregulation of IDO can also be achieved by direct cross-linking of B7-1/-B7-2 molecules on DCs through administration of soluble fusion protein CTLA-4-immunoglobulin (CTLA-4-Ig), which promotes tolerance *in vivo* (Grohmann et al., 2002). Consistently, prevention of allograft rejection by CTLA-4-Ig requires tryptophan catabolism and is abolished upon pharmacological inhibition of IDO (Grohmann et al., 2002). In addition to CTLA-4-dependent mechanisms, expression of IDO in DCs can be self-amplified through IDO enzymatic activity-independent immune signaling triggered by TGFβ (Pallotta et al., 2011), of which Treg cells are major producers.

1.7.5. The central role of IDO in tumour tolerance

The bias towards the Treg cell phenotype in IDO-expressing tumours is of importance not only due to the inhibitory function of these cells but also due to their potential to cooperate with IDO in amplifying the immunosuppressive network in the tumour microenvironment. Treg cells can achieve this by imposing tolerogenic properties on DCs through induction of IDO, as discussed above, as well as by recruiting and activating other immunosuppressive cell populations, such as MDSCs, which can suppress anti-tumour effector T cell responses through arginase and iNOS activity and generation of immunosuppressive cytokines like TGFβ (Holmgaard et al., 2015) **(Figure 1-4)**. Importantly, inhibiting IDO activity (or depleting FoxP3$^+$ Treg cells) prevents MDSC infiltration in human melanoma, releasing immunosuppression and delaying tumour growth (Holmgaard et al., 2015), which highlights the central role of IDO in the regulation of tumour-induced immune tolerance **(Figure 1-4)**.

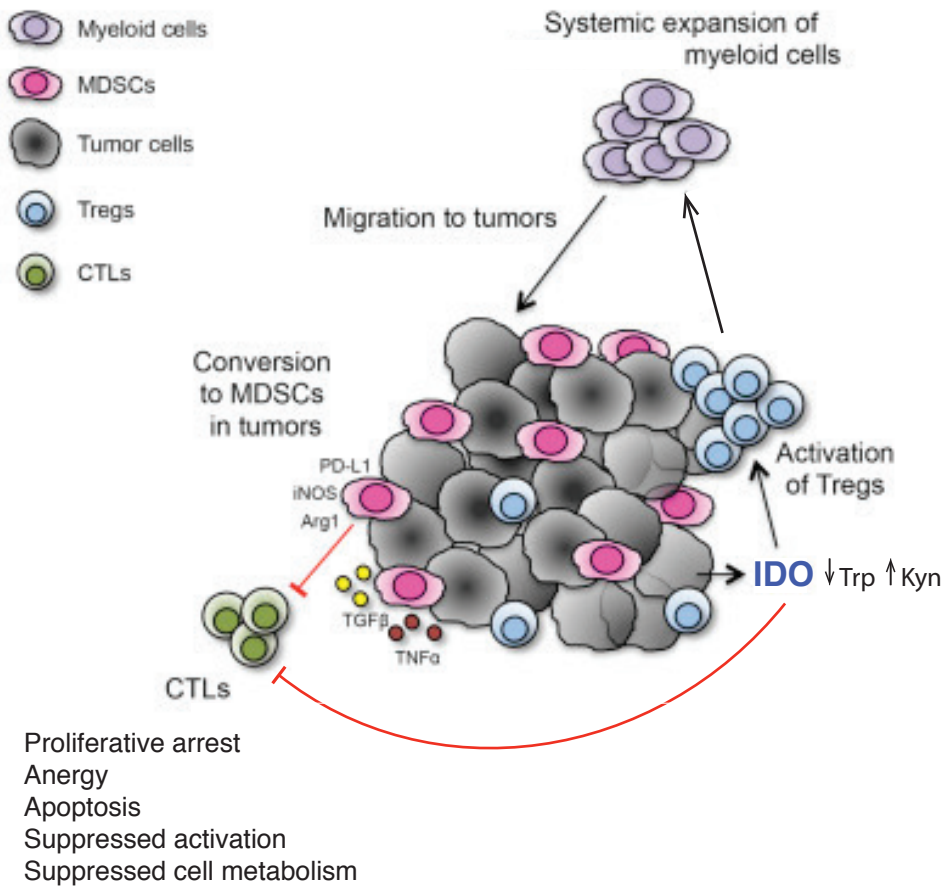

Figure 1-4. IDO-induced immunosuppression in the tumour microenvironment
IDO-mediated tryptophan catabolism in the tumour microenvironment can hamper the anti-tumour immune response through multiple mechanisms, including the induction of tumour-infiltrating CTL proliferative arrest, anergy and apoptosis, interference with optimal CTL activation and metabolic function, as well as promotion of Treg cell differentiation and activation. Activated Treg cells, in turn, can induce expansion and intra-tumoural recruitment of immunosuppressive myeloid populations like MDSCs, which further inhibit anti-tumour effector T cell responses through PD-L1-, iNOS-, arginase- and inhibitory cytokine-dependent mechanisms. Adapted from (Holmgaard et al., 2015), by permission of Elsevier.

1.7.5.1. Inhibition of the anti-tumour immune response by arginase

Arginase enzyme, expressed or secreted by tumour cells and tumour-associated cells, such as TAMs and MDSCs, converts the semi-essential amino acid arginine into ornithine and urea. Similarly to tryptophan, arginine is required for effector T cell proliferation, and its depletion from the local microenvironment through arginase activity leads to T cell proliferative arrest, impaired T cell activation and cytokine production (Kropf et al., 2007; Munder et al., 2006; Rodriguez et al., 2002), as well as to the polarization of myeloid populations into tolerogenic phenotypes (Mussai et al., 2013). Notably, arginase expression and release from AML blasts has been shown to play a key role in AML-induced immunosuppression (Mussai et al., 2013).

1.7.6. The effect of tryptophan catabolism on other lymphoid effectors of anti-tumour immunity

Notably, the immunosuppressive effects of IDO are not limited to αβ T cells. IDO activity has been reported to restrict γδ T cell reactivity (Romani et al., 2008), modulate cytokine responses by iNKT cells, favoring Th2-type cytokines IL-4 and IL-13 over pro-inflammatory IFNγ (Molano et al., 2008), induce apoptosis of NK cells (Frumento et al., 2002; Terness et al., 2002), and inhibit NK cell cytolytic function through downregulation of activating receptors, including NKG2D (Della Chiesa et al., 2006; Pietra et al., 2012). IDO expression in melanoma and ovarian cancer has also been shown to hamper NK cell-mediated anti-tumour immunity (Pietra et al., 2012; Wang et al., 2012). Others, however, argue that IDO is required for (rather than inhibitory of) NK cell cytolytic function (Kai et al., 2004) and anti-tumour response (Kai et al., 2003). Further research is required to resolve these discrepancies.

In summary, there is a growing body of evidence demonstrating the immunosuppressive role of IDO in the tumour microenvironment. Immunoregulation by tryptophan catabolism involves several pathways, including GCN2, AhR and mTOR, and affects diverse aspects of the anti-tumour immune response, ranging from tolerogenic status of APCs to viability, differentiation and function of T cells.

1.8. Therapeutic targeting of tryptophan catabolism in cancer

1.8.1. Inhibition of IDO enzymatic activity

The key role of IDO in the regulation of tumour-induced immune tolerance makes it a promising therapeutic target. One approach of targeting the immunosuppressive tryptophan catabolism in cancer is to disrupt the enzymatic activity of IDO. Numerous IDO-targeted inhibitors have shown promising results in pre-clinical animal studies, particularly in melanoma and breast cancer (Banerjee et al., 2008; Hou et al., 2007; Kumar et al., 2008; Metz et al., 2010; Muller et al., 2010), but also in other tumour models, such as glioblastoma (Li et al., 2014; Wainwright et al., 2012), lung (Smith et al., 2012), pancreatic (Koblish et al., 2010; Liu et al., 2010) and colon cancer (Koblish et al., 2010). IDO represents a particularly attractive target for cancer immunotherapy due to its well-studied biochemistry (Littlejohn et al., 2003; Sono et al., 1980), resolved crystal structure (Sugimoto et al., 2006) and lack of autoimmune disease observed in *IDO1*-deficient mice (Mellor et al., 2003), which is predictive of minimal side effects induced by pharmacological IDO blockade. The first IDO inhibitor, 1-methyl-tryptophan (1MT) showed best efficacy in tumour rejection when used in combination with chemotherapy (Hou et al., 2007; Li et al., 2014; Muller et al., 2005), and has also been reported to synergise with anti-CTLA-4 immunotherapy *in vivo* (Holmgaard et al., 2013). Several IDO inhibitors are currently undergoing Phase I/II clinical trials in humans, including NLG8189,

INCB024360 and NLG919, among others (http://ClinicalTrials.gov). 1-$_D$-MT (also referred to as indoximod or NLG8189), the racemic isoform that demonstrated higher anti-tumour efficacy *in vivo* than 1-$_L$-MT (Hou et al., 2007), has completed the first small-scale Phase I clinical trial, showing no substantive toxicity and some anti-tumour activity in combination with chemotherapy in patients with metastatic solid tumours (Soliman et al., 2014a). The efficacy and safety of indoximod is currently being evaluated in combination with other therapies, such as CTLA-4-targeting drug ipilimumab (Zakharia et al., 2015) and anti-cancer vaccines (Jha and Miller, 2014; Soliman et al., 2014b; Soliman et al., 2015). Another promising clinical candidate is the second-generation IDO inhibitor epacadostat (also referred to as hydroxyamidine or INCB024360), which has shown efficacy in pancreatic (Koblish et al., 2010; Liu et al., 2010) and colon (Koblish et al., 2010) tumour models, and is currently being tested in several Phase I/II combination drug trials, including its combination with anti-CTLA-4 immunotherapy in metastatic melanoma (Gibney et al., 2015). In addition to the inhibitors of IDO enzymatic activity, tryptophan catabolism in the tumour microenvironment can be targeted using TDO inhibitors, the development of which is also underway (Dolusic et al., 2011; Pilotte et al., 2012).

1.8.2. Inhibition of IDO induction stimuli in the tumour microenvironment

An alternative strategy to disrupt the IDO-dependent immunosuppressive network is to target the molecular signaling events regulating IDO expression in the tumour microenvironment. One successful example of such an approach is the tyrosine kinase inhibitor imatinib, which has been shown to suppress IDO expression through inhibition of oncogenic KIT signaling (Balachandran et al., 2011). Interestingly, the anti-tumour effects of imatinib in GIST have been attributed, at least in part, to the downregulation of tumour-derived IDO expression (Balachandran et al., 2011). Furthermore, IDO induction in the tumour microenvironment can be prevented through inhibition of COX-2 activity – an

enzyme key for the production of PGE2, which is capable of inducing IDO expression (Braun et al., 2005; Sayama et al., 1981; von Bergwelt-Baildon et al., 2006). Quite promisingly, early pre-clinical studies have demonstrated that COX-2 inhibition is able to reduce the levels of IDO, suppress tumour growth and metastasis, and improve the anti-tumour efficacy of a dendritic cell-based cancer vaccine (Basu et al., 2006; Lee et al., 2009). Notably, therapeutic targeting of the upstream pathways controlling IDO expression represents an important area of research, as, in addition to IDO enzymatic activity, it could be used to block IDO non-enzymatic immune signaling, which has been shown to promote immune tolerance (Pallotta et al., 2011) and is likely to be refractory to IDO enzymatic inhibitors.

1.9. Amino acid transport

1.9.1. The SLC superfamily

Amino acid entry into cells is mediated by substrate-specific transmembrane transport proteins or solute carriers (SLCs). Human SLCs are grouped into a large, complex superfamily, which comprises 55 families and more than 360 putatively functional members able to transport a wide range of substrates, including not only amino acids but also inorganic cations and anions (SLC4, SLC8, SLC9, SLC12, SLC20, SLC24, SLC26 and SLC34 families), sugars (SLC2/GLUT, SLC5, SLC37 and SLC45 families), fatty acids, prostaglandins and steroid sulphates (SLC27 and SLCO2 families), vitamins and cofactors (SLC19, SLC23, SLC33 and SLC46 families) and metal ions (SLC11, 30, SLC31, SLC39, SLC40 and SLC41 families) (He et al., 2009). Amino acid transport is mediated by the members of SLC1, SLC6, SLC7, SLC15, SLC16, SLC32, SLC38, SLC36 and SLC43 families. Notably, amino acid transporters vary in structure, localisation and function, and display promiscuous substrate specificities, as outlined in **Figure 1-5**. system

L constitutes the main neutral amino acid transport system in mammalian cells, importing large hydrophobic amino acids with branched or aromatic side chains, several of which are essential, for example, leucine and tryptophan (Verrey, 2003).

1.9.2. CD98hc-mediated amino acid transport

1.9.2.1. system L

system L is a ubiquitously expressed, sodium-independent transporter composed of the type II membrane glycoprotein CD98 heavy chain (CD98hc, or SLC3A2) covalently attached to one of several described light chains (Verrey, 2003; Verrey et al., 2004), including LAT1 (SLC7A5) (Kanai et al., 1998; Mastroberardino et al., 1998), LAT2 (SLC7A8) (Pineda et al., 1999; Rossier et al., 1999; Segawa et al., 1999) and LAT3 (SLC43A1) (Babu et al., 2003), which exhibit distinct tissue distribution (Verrey et al., 2004) and substrate specificity **(Figure 1-5)**. For example, while LAT1 is highly expressed in the brain, ovary and placenta, LAT2 is particularly abundant in the kidney and small intestine (Rossier et al., 1999). Furthermore, LAT2 exhibits broader substrate specificity than LAT1 – while the latter prefers large neutral amino acids like tryptophan, phenylalanine, valine, leucine, isoleucine, methionine and histidine for its substrates (Kanai et al., 1998), LAT2 also accepts small amino acids like alanine, serine and threonine (Segawa et al., 1999) **(Figure 1-5)**. LAT3, on the other hand, mainly transports phenylalanine, valine, leucine, isoleucine and, to a lesser extent, methionine (Babu et al., 2003) **(Figure 1-5)**. Moreover, in contrast to LAT1 and LAT2, which require heterodimerisation with CD98hc to achieve functional expression, LAT3 can also function by itself (Babu et al., 2003).

1.9.2.2. system y^+L

In addition to SLC7A5 (LAT1) and SLC7A8 (LAT2), CD98hc can associate with other members of the SLC7 family, such as SLC7A6 (y^+LAT2) and SLC7A7 (y^+LAT1) (known

as system y^+L). Such heterodimeric transporters accept cationic amino acids like lysine, arginine and histidine, while other members of the SLC7 family, including SLC7A1 (CAT1), SLC7A2 (CAT2) and SLC7A3 (CAT3), are able to transport these amino acids independently of CD98hc (Verrey et al., 2004) **(Figure 1-5)**.

1.9.2.3. system x^-_c

Another transporter able to associate with CD98hc is SLC7A11 (xCT) (known as system system x^-_c) – a sodium-independent obligatory exchanger, which couples the uptake of cystine to glutamate release, thus maintaining the intracellular cystine pool required for the synthesis of the reducing agent glutathione (Sato et al., 1999; Verrey et al., 2004).

1.9.3. The amino acid transport-independent function of CD98hc

Interestingly, in addition to other amino acid transporters, CD98hc can also form complexes with integrins (Kolesnikova et al., 2001) and mediate integrin signaling (Fenczik et al., 1997; Feral et al., 2005). The latter function of CD98, which is independent of its amino acid transport function, has been implicated in cancer (Cantor and Ginsberg, 2012) and shown to be important for T and B cell clonal expansion (Cantor et al., 2009; Cantor et al., 2011).

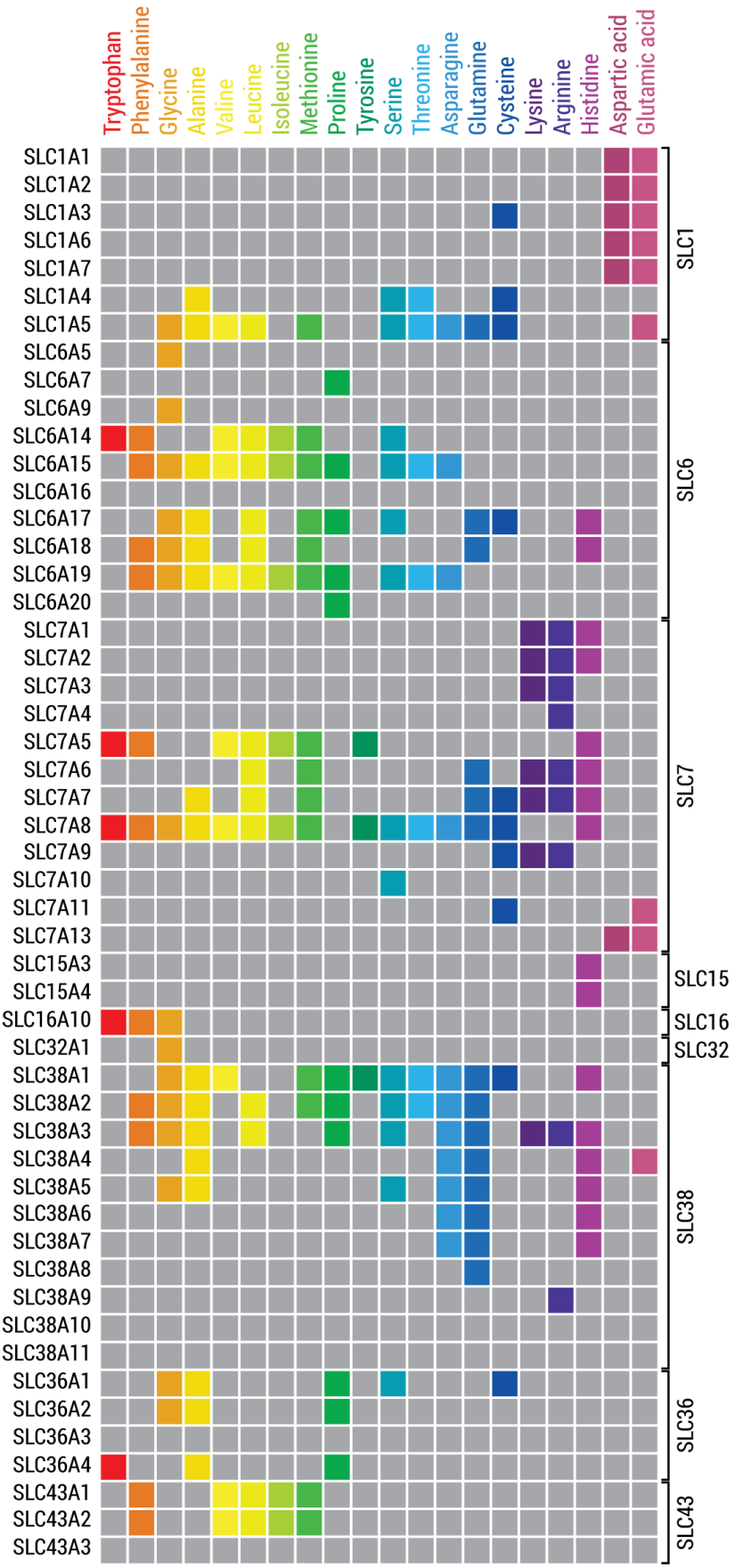

Figure 1-5. Substrate specificities of human SLC amino acid transporters

1.9.4. system L as an obligate amino acid exchanger

system L is an obligate amino acid exchanger, and its function relies on the expression of other amino acid transporters that can provide intracellular substrates like glutamine, for which tryptophan and other large amino acids can be subsequently exchanged (Verrey, 2003). In the SLC superfamily, the high-affinity glutamine transporters are mainly represented by the members of the SLC38 (SNAT) family and one member of the SLC1 family – SLC1A5, although some members of the SLC6 and SLC7 families are also able to transport this amino acid (Pochini et al., 2014) **(Figure 1-5)**. Notably, glutamine influx facilitated by SLC1A5 has been shown to be critical for system L exchange function, as evidenced by the inhibition of LAT1-mediated EAA uptake and the suppression of mTOR signaling caused by SLC1A5 silencing or pharmacological blockade (Nicklin et al., 2009).

1.9.5. The SLC1 family

SLC1 family consists of seven members, five of which (SLC1A1, SLC1A2, SLC1A3, SLC1A6 and SLC1A7) are high-affinity glutamate transporters extensively expressed in the brain, which contribute to glutamatergic transmission and protect against glutamate excitotoxicity in the central nervous system (Kanai and Hediger, 2004). The other two members of the SLC1 family, SLC1A4 (ASCT1) and SLC1A5 (ASCT2), are sodium-dependent AlaSerCys (ASC) system transporters exhibiting high affinity for small neutral amino acids alanine, serine, cysteine and threonine (Kanai and Hediger, 2004) **(Figure 1-5)**. In contrast to SLC1A4, SLC1A5 also accepts several other amino acids at high affinity, one of which is glutamine **(Figure 1-5)**.

1.9.5.1. SLC1A5 (ASCT2)

SLC1A5 was originally cloned from human placental choriocarcinoma cell cDNA library (Kekuda et al., 1996) and from mouse testis (Utsunomiya-Tate et al., 1996) and is expressed in a wide range of tissues (apart from the placenta and testis), including kidney,

brain, lung, large intestine and skeletal muscle, among others (Pochini et al., 2014). Interestingly, SLC1A5 amino acid transporter can act as a receptor for RD114/simian type D retroviruses, facilitating viral cell entry (Rasko et al., 1999; Tailor et al., 1999). SLC1A5 has also been reported to bind to the fusogenic protein syncytin-1/HERV-W, mediating fusions between placental trophoblasts (Blond et al., 2000), as well as between cancer cells and endothelial cells (Bjerregaard et al., 2006).

1.9.6. The role of SLCs in human pathology

The members of the SLC superfamily play key roles in physiology, including nutrient and ion transport and waste removal. Many drug classes also depend on SLCs for cell entry. Statin transport, for example, is mediated by SLCO1B1 (Cesar-Razquin et al., 2015). SLCs have also been extensively implicated in human pathology. Mutations in *SLC6A3, SLC12A3* and *SLC6A19* genes, for example, have been associated with Parkinsonism disease (Kurian et al., 2009), Gitelman's syndrome (Simon et al., 1996) and Hartnup disorder (Seow et al., 2004), respectively. Furthermore, reduced expression of SLC22A5 and SLC10A2, has been linked to inflammatory bowel disease (Wojtal et al., 2009), while SLC15A4 has been shown to be involved in the pathogenesis of lupus-like disease (Kobayashi et al., 2014).

1.9.6.1. The role of SLCs in tumour development

1.9.6.1.1. Amino acid transporters

Notably, several amino acid transporters exhibit strong overexpression in cancer, including CD98hc, SLC7A5, SLC1A5, SLC7A11 and SLC6A14 (Bhutia et al., 2015; Cantor and Ginsberg, 2012; Fuchs and Bode, 2005; Ganapathy et al., 2009), all of which constitute either direct or indirect targets of Myc, as well as other oncogenes, such as Ets-1 (Bhutia et al., 2015). CD98hc, for example, appears to promote tumour cell proliferation, invasion, anchorage-independence and apoptosis resistance, although these effects may depend on

the integrin signaling rather than amino acid transport function of CD98hc (Cantor and Ginsberg, 2012). The expression of CD98hc-associated light chain LAT1 has also been reported to correlate with tumour cell proliferation (Kobayashi et al., 2008). Consistently, pharmacological blockade or genetic disruption of LAT1 suppresses tumour cell growth in several model systems (Cormerais et al., 2016; Kim et al., 2008a; Oda et al., 2010; Yun et al., 2014). A similar effect is also exerted by the inhibition or knockdown of the high-affinity glutamine amino acid transporter SLC1A5, which demonstrates elevated expression in various cancer types, including breast cancer (van Geldermalsen et al., 2016), escpecially HER2 type (Kim et al., 2013), melanoma (Wang et al., 2014), neuroblastoma (Ren et al., 2015), lung cancer (Hassanein et al., 2013; Hassanein et al., 2015), colorectal cancer (Huang et al., 2014) and prostate cancer (Wang et al., 2015a). Furthermore, SLC7A11 cysteine/glutamate transporter, which is upregulated in triple-negative breast cancer (Timmerman et al., 2013), has been reported to facilitate tumour growth through promotion of glutathione-mediated reduction of oxidative damage (Ishimoto et al., 2011). Consistently with the role of SLC7A11 in tumorigenesis, its overexpression is inhibited by the tumour suppressor gene p53 (Jiang et al., 2015).

1.9.6.1.2. Glucose and lactate transporters

In addition to amino acid transporters, glucose transporters are also commonly upregulated in cancer, particularly, SLC2A1 (GLUT1) and SLC5A1 (SGLT1), which enhance glucose entry into tumour cells, leading to increased anaerobic glycolysis typical of transformed cells (Ganapathy et al., 2009). Moreover, cancer cells also commonly exhibit elevated levels of the lactate transporter SLC16A1 (monocarboxylate transporter 1, MCT1), which allows to prevent cellular acidification as a result of lactate (the end of product of anaerobic glycolysis) accumulation (Ganapathy et al., 2009).

1.9.7. Therapeutic targeting of SLCs

The diverse biology of the SLC superfamily provides exciting opportunities for therapeutic intervention. Notably, a number of FDA-approved drugs are known to target specific SLCs, including members of the SLC6 neurotransmitter transporter family (treatment of depression, epilepsy and addiction), members of the SLC12 ion transporter family (treatment of diuresis) and members of the SLC22 organic anion transporter family (treatment of uricosuresis and gout), among others (Cesar-Razquin et al., 2015; Rask-Andersen et al., 2013). Although there are some clinical trials assessing safety and efficacy of SLC-targeting drugs in cancer (e.g. SLC2 and SLC5 family glucose transporters) (Rask-Andersen et al., 2013), this still remains a relatively under-studied field. Thus, improving our understanding of SLC involvement in neoplasia would be critical for the identification of novel anti-cancer targets.

1.10. Aims of the project

A large proportion of human tumours exploit tryptophan catabolism as a means to induce an immunosuppressive microenvironment. However, it remains unclear how tumour cells themselves are able to resist the dramatic tryptophan shortage that they impose on the main effectors of anti-tumour immunity – T lymphocytes. We hypothesised that IDO- and TDO-expressing tumour cells may be able to compensate for local tryptophan depletion in the tumour microenvironment through upregulation of amino acid transport.

To address this hypothesis, we set the following aims for this study:

a) to investigate the effect of tryptophan catabolism on tumour cell whole transcriptome profile, particularly the amino acid transporter expression profile
b) to study the biological function of the most interesting amino acid transporter candidate(s) upregulated in IDO- and TDO-expressing tumour cells
c) to assess whether amino acid transporter reprogramming confers tumour cells with a functional advantage in a low tryptophan microenvironment
d) to determine the mechanisms mediating the changes in amino acid transporter profiling in IDO- and TDO-expressing tumour cells
e) to assess amino acid transporter expression in resident immune cells of the tumour microenvironment
f) to study T cell response to tryptophan starvation
g) to study the association between tryptophan catabolism and amino acid transporter expression *in vivo* and in primary human tumour samples

CHAPTER 2: Materials and Methods

2.1. Cell lines and culture media

The HeLa, A431, DX3, HPAF and DU145 tumour cell lines were obtained from Cancer Research UK. HeLa cells were cultured in Minimum Essential Medium (MEM) supplemented with 10% fetal bovine serum (FBS), 1% penicillin/streptomycin and 2mM glutamine (Sigma-Aldrich). A431, DX3 and HPAF cells were maintained in Dulbecco's Modified Eagle Medium (DMEM) supplemented with 10% FBS, 1% penicillin/streptomycin and 2mM glutamine. DU145 cells were cultured in RPMI-1640 medium supplemented with 10% FBS, 1% penicillin/streptomycin and 2mM glutamine (further referred to as R10). Customised DMEM depleted of tryptophan, glutamine, arginine, leucine, isoleucine, glycine and serine (Life Technologies) was supplemented with 15mg/ml phenol red (Sigma-Aldrich), 10% dialysed FBS (Life Technologies), 1% penicillin/streptomycin and the missing amino acids accordingly. Tryptophan, glutamine, arginine, leucine, isoleucine, glycine and serine were supplemented to the following final concentrations in the medium: 80μM, 2mM, 400μM, 800μM, 800μM, 400μM and 400μM, respectively. Tryptophan, glutamine, leucine, isoleucine and serine solutions were prepared from powder (Sigma-Aldrich), while 1M glycine and 100mM arginine hydrochloride were purchased in solution (Sigma-Aldrich). Before being resuspended in amino acid-depleted medium, cells were washed twice in ice-cold phosphate buffered saline (PBS) (Sigma-Aldrich).

HeLa cells overexpressing human *IDO1* with green fluorescent protein (GFP), human *TDO2* with GFP or GFP alone, as well as EG7 cells overexpressing mouse *IDO1* with GFP or GFP alone had been generated previously (Silk et al., 2011). Transduced EG7 cells were

cultured in R10 supplemented with 0.1% β-mercaptoethanol and 0.4mg/ml G418 (Sigma-Aldrich). Transduced HeLa and EG7 cells were regularly FACS re-sorted on the basis of GFP expression. IDO expression and enzymatic activity were verified by quantitative PCR and high performance liquid chromatography (HPLC), respectively.

2.2. Antibodies and chemicals

2.2.1. Antibodies used for Western blotting

Primary Western blotting antibodies were obtained from the following sources: SLC1A5 #ABN73 (Merck Millipore); β-actin #8457 (Cell Signaling Technology); β-tubulin #15115 (Cell Signaling Technology); FLAG tag #14793 (Cell Signaling Technology); HA tag #3724 (Cell Signaling Technology); pS6 (Ser240/244) #5364 (Cell Signaling Technology); S6 #2217 (Cell Signaling Technology); LAT1 #5347 (Cell Signaling Technology); ATF4 #11815 (Cell Signaling Technology); GCN2 #3302 (Cell Signaling Technology); WARS #EPR3424 (Abcam). Primary antibodies (all anti-rabbit) were used at 1:1000. Donkey anti-rabbit horseradish peroxidise (HRP)-conjugated affinity-purified F(ab')2 Fragment (H+L) secondary antibody #711-036-152 (Jackson ImmunoResearch laboratories) was used at 1:10,000.

2.2.2. Antibodies used for flow cytometry

Target	Conjugated fluorophore	Company	# number	Dilu-tion	Type of staining
Anti-human					
CD25	Brilliant Violet 421™	Biolegend	#302629	1:40	Surface
CD3	APC	BD Biosciences	#555335	1:40	Surface
CD3	PE	eBioscience	#12-0037	1:40	Surface
CD4	FITC	eBioscience	#11-0048	1:40	Surface

CD4	PE	BD Biosciences	#347327	1:40	Surface
CD4	PerCP-eFluor® 710	eBioscience	#46-0047	1:80	Surface
CD45	PE/Cy7	BD Biosciences	#557748	1:200	Surface
CD8	APC/Cy7	Biolegend	#344714	1:40	Surface
CD8	FITC	BD Biosciences	#555634	1:40	Surface
CD80	PE	BD Biosciences	#557227	1:40	Surface
FoxP3	PE	eBioscience	#12-4777	1:40	Intranuclear
HA tag	None	Cell Signaling Technology	#3724	1:1000	Surface/ cytoplasmic
HLA-ABC	FITC	BD Biosciences	#555552	1:40	Surface
Ki67	PECy7	Biolegend	#350525	1:40	Intranuclear
TCR Vα24	FITC	Beckman Coulter	#IM1589	1:80	Surface
TCR Vβ11	APC	Beckman Coulter	#A66905	1:80	Surface
Anti-mouse					
CD45.2	APC	eBioscience	#17-0454-82	1:300	Surface
Secondary antibodies					
Goat anti-mouse	Alexa Fluor® 647	ThermoFisher Scientific	A21235	1:500	Surface
Goat anti-rabbit	Alexa Fluor® 647	ThermoFisher Scientific	A21245	1:500	Surface/ cytoplasmic

Table 2-1. Antibodies used for flow cytometry analysis

2.2.3. Chemicals

O-Benzyl-L-serine and kynurenine were purchased from Sigma-Aldrich. 6-formylindolo[3,2-*b*]carbazole (FICZ) was from Enzo Life Sciences. Recombinant human IFNγ was purchased from PeproTech and was used at 1000 U/ml. IL-1β, IL-6, TNFα were from PeproTech. LPS from *Escherichia coli* and PGE2 were from Sigma-Aldrich.

2.3. Analysis of gene expression

2.3.1. Transcriptome sequencing (RNA-seq)

RNA was isolated from untreated WT, WT treated with 1000 U/ml IFNγ, GFP-transduced and *IDO1*-transduced HeLa cells seeded at density of $1x10^5$ cells per ml in 1.5ml complete Minimum Essential Medium per well in a 12-well plate for 48 or 72 hours (h).

Sequencing library was made by following standard protocol:

http://www.illumina.com/documents/products/technotes/technote-truseq-rna-access.pdf.

Superscript III reverse transcriptase (Life Technologies) and Illumina's TruSeq Stranded Total RNA Sample Prep Kit (Illumina) were used for making the cDNA library. 2x100 bp paired-end reads were produced with Illimina Hi-seq sequencer. After quality and adaptor trimming, an average of ~115 million reads were generated for each sample of which there was a single replicate. Reads were trimmed using TrimGalore (http://www.bioinformatics.babraham.ac.uk/projects/trim_galore/) and aligned with TopHat version 1.1.4 (Trapnell et al., 2009). Reads were aligned to the GRCh37/hg19 human reference genome build and quantified by Cufflinks (Trapnell et al., 2010) as fragments per kilobase million (FPKM). Using MetaCore (https://portal.genego.com/), pathways that contained SLC transporter genes and showed interactions with tryptophan were enriched for and the candidates' FPKM and read coverage were assessed by visualizing the data as a bigwig file in the UCSC Genome Browser (Kent et al., 2002), which showed SLC1A5 to have a distribution of reads across exons that suggested potential isoform expression.

Unsupervised clustering of the normalised data of the 2000 genes with highest upregulation in all four conditions (*IDO1*-transduced vs GFP-transduced HeLa cells cultured for 48h; *IDO1*-transduced vs GFP-transduced HeLa cells cultured for 72h; IFNγ-treated vs untreated WT HeLa cells cultured for 48h; IFNγ-treated vs untreated WT HeLa cells cultured for 72h) was performed using GENE-E

(http://www.broadinstitute.org/cancer/software/GENE-E/index.html), with all the clustering analyses performed using one minus Pearson correlation.

The data has been deposited in the GEO database (GEO accession GSE75956).

2.3.2. Real-time quantitative reverse transcription PCR (q-RT-PCR)

RNA for q-RT-PCR analysis was isolated using the NucleoSpin® RNA kit (Macherey Nagel) and cDNA was synthesised in the presence of oligo-dT primers using the RETROscript® Kit (Ambion) according to the manufacturer's instructions. Human *SLC1A5(L), SLC1A5(M)* and *SLC1A5(S)* q-RT-PCR probes and primers were designed manually using Primer Express® Software (Life Technologies):

SLC1A5(L)_q-RT-PCR_FW 5'-CAAGAGCCAAGGAACTTCAG-3'

SLC1A5(L)_q-RT-PCR_RV 5'-CCTAGGACTGAGTTGAGTAACA-3'

SLC1A5(L)_q-RT-PCR_probe 5'-TGGAGACTGGAACTTTGGAGGGC-3'

SLC1A5(M)_q-RT-PCR_FW 5'- CGGGCTGAGGCATGAGTAG-3'

SLC1A5(M)_q-RT-PCR_RV 5'-GTTTTAAGGCAGCGAGTGGAA-3'

SLC1A5(M)_q-RT-PCR_probe 5'- TGTATTTGCGTGCAGGC-3'

SLC1A5(S)_q-RT-PCR_FW 5'-TTAGGAAAACTCGACAGGATATTGAG-3'

SLC1A5(S)_q-RT-PCR_RV 5'-CCAGGTTGGAAGGGAAGATATTT-3'

SLC1A5(S)_q-RT-PCR_probe 5'-CTCCAGCCCTCGGGA-3'

Forward (FW) and reverse (RV) primers were used at the final concentration of 900nM, and the probe – at 250nM.

The rest of the mRNA expression analysis was performed using commercially available TaqMan® probes described in **Table 2-2** (Life Technologies), following the manufacturer's instructions. The reactions were run on the 7500 Fast Real-Time PCR System (Applied Biosystems).

Gene	Amplicon length	# number
Human		
18S	187	Hs99999901_s1
ACTB	171	Hs99999903_m1
ASNS	69	Hs04186194_m1
GAPDH	122	Hs99999905_m1
GPT2	71	Hs00370287_m1
HOXB9	65	Hs00256886_m1
HPRT	100	Hs99999909_m1
IDO1	66	Hs00984148_m1
SLC1A4	74	Hs00983079_m1
SLC1A5	68	Hs01056542_m1
SLC7A11	57	Hs00921938_m1
TDO2	74	Hs00194611_m1
WARS	60	Hs00188259_m1
Mouse		
ACTB	143	Mm02619580_g1
IDO1	83	Mm00492590_m1
SLC1A5	59	Mm00436603_m1

Table 2-2. TaqMan® probes used for q-RT-PCR analysis

2.4. Gene overexpression using lentiviral vectors

2.4.1. Cloning of SLC1A5 isoforms

2.4.1.1. The pHR-SLC1A5(L)-IRES-GFP and pHR-SLC1A5(S)-IRES-GFP constructs

To generate a lentiviral vector coding for human SLC1A5(L) or SLC1A5(S) under a strong spleen focus-forming virus (SFFV) promoter and internal ribosomal entry site element (IRES) driving the expression of GFP as a reporter gene, parental vector pHR-SIN-IRES-GFP (see vector map in Appendix I) was digested with *Bam*HI and *Xho*I (New England Biolabs) at 37°C for 1.5h, and the digested product was gel-purified using the QIAquick® Gel Extraction Kit (Qiagen) according to the manufacturer's instructions. cDNA for SLC1A5(L) and SLC1A5(S) was PCR amplified with the Phusion® High-Fidelity DNA Polymerase (New England Biolabs), using one of the FW primers, SLC1A5(L)_*Bgl*II_FW or SLC1A5(S)_*Bgl*II_FW, and a universal RV cloning primer SLC1A5_*Xho*I_RV (**Table 2-3**). SLC1A5(L)_*Bgl*II_FW primer was also used to introduce a silent point mutation

(T→A) to destroy an internal *Xho*I recognition site at the 5' end of the SLC1A5(L) sequence to ease the cloning process. The PCR products were digested with *Bgl*II and *Xho*I (New England Biolabs) at 37°C for 1.5h and gel-purified using the QIAquick® Gel Extraction Kit (Qiagen) according to the manufacturer's instructions. The digested pHR-SIN-IRES-GFP vector and SLC1A5(L) or SLC1A5(S) insert were ligated using T4 DNA ligase (New England Biolabs) at 14°C overnight **(Figure 2-1)**.

2.4.1.2. The pHR-SLC1A5(L)-HA-IRES-GFP and pHR-SLC1A5(L)-FLAG-IRES-GFP constructs

To generate lentiviral vectors coding for human SLC1A5(L) or SLC1A5(S) tagged with HA or FLAG at the C-terminus, parental vector pHR-SIN-IRES-GFP was digested with *Bam*HI and *Xho*I and gel-purified as described in 2.4.1.1. cDNA for SLC1A5(L) fused at the 3' end to a sequence encoding either HA or FLAG epitope was PCR amplified using SLC1A5(L)_*Bgl*II_FW and one of the reverse primers: SLC1A5_HA_*Bgl*II_*Xho*I_RV or SLC1A5_FLAG_*Bgl*II_*Xho*I_RV, respectively (**Table 2-3**). The PCR products were then digested with *Bgl*II and *Xho*I, gel-purified and ligated with the *Bam*HI/*Xho*I-flanked pHR-SIN-IRES-GFP vector as described in 2.4.1.1 **(Figure 2-1)**.

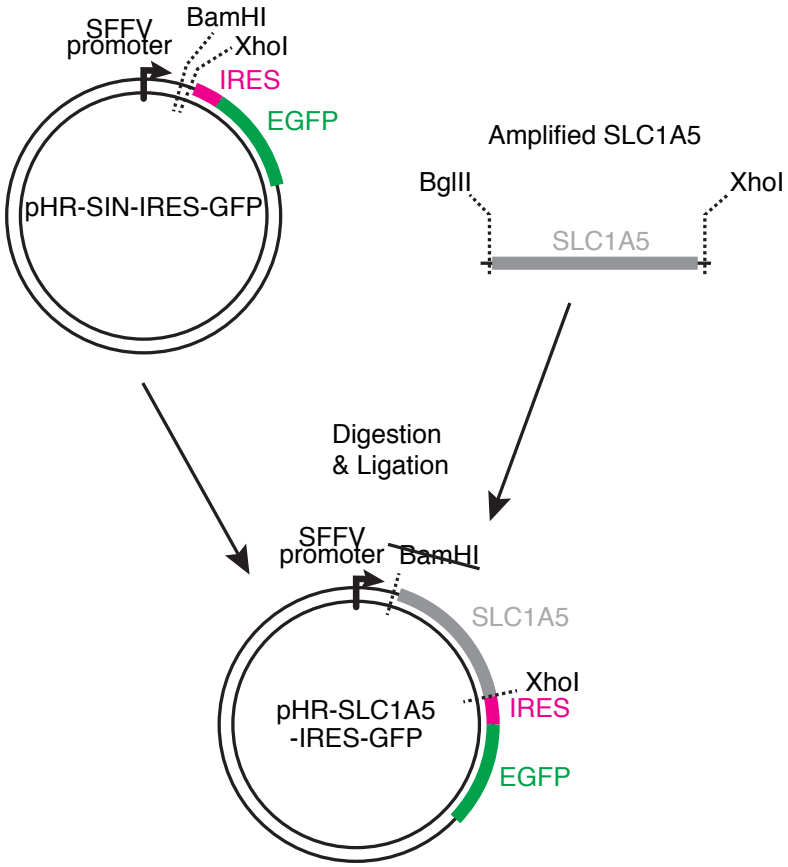

Figure 2-1. Cloning of SLC1A5 into the pHR-SIN-IRES-GFP expression vector
Cloning strategy used for the generation of pHR-SLC1A5(L)-IRES-GFP, pHR-SLC1A5(S)-IRES-GFP, pHR-SLC1A5(L)-HA-IRES-GFP and pHR-SLC1A5(L)-FLAG-IRES-GFP constructs. Cloning was performed as described in Chapters 2.4.1.1 and 2.4.1.2.

2.4.1.3. The pHR-SLC1A5(S)-HA-IRES-mCherry construct

pHR-SLC1A5(S)-HA-IRES-mCherry construct was generated by inserting the ligated SLC1A5(S)-HA-IRES cDNA product into the pHR-SIN-mCherry lentiviral vector (see vector map in Appendix II). Parental vector pHR-SIN-mCherry was digested with *Mlu*I and *Bam*HI (New England Biolabs) at 37°C for 1.5h, and the digested product was gel-purified using the QIAquick® Gel Extraction Kit according to the manufacturer's instructions. cDNA for SLC1A5(S) fused at the 3' end to a sequence encoding HA epitope was PCR amplified using SLC1A5(S)_*Mlu*I_FW and SLC1A5_HA_*Bgl*II_*Xho*I_RV (**Table 2-3**), and digested with *Bgl*II (New England Biolabs) at 37°C for 1.5h. cDNA for IRES was PCR amplified using IRES_*Bcl*I_FW and IRES_*BamH*I_RV **(Table 2-3)**, and digested with *Bcl*I. The digested products were then ligated using T4 DNA ligase (New England Biolabs) at 14°C overnight to create the SLC1A5(S)-HA-IRES cDNA product. The latter was PCR amplified using SLC1A5(S)_*Mlu*I_FW and IRES_*BamH*I_RV, digested with *Mlu*I and *BamH*I (New England Biolabs) at 37°C for 1.5h and gel-purified using the QIAquick® Gel Extraction Kit according to the manufacturer's instructions. The digested product was then inserted into *Mlu*I/*BamH*I-flanked pHR-SIN-mCherry plasmid through ligation with T4 DNA ligase at 14°C overnight **(Figure 2-2)**.

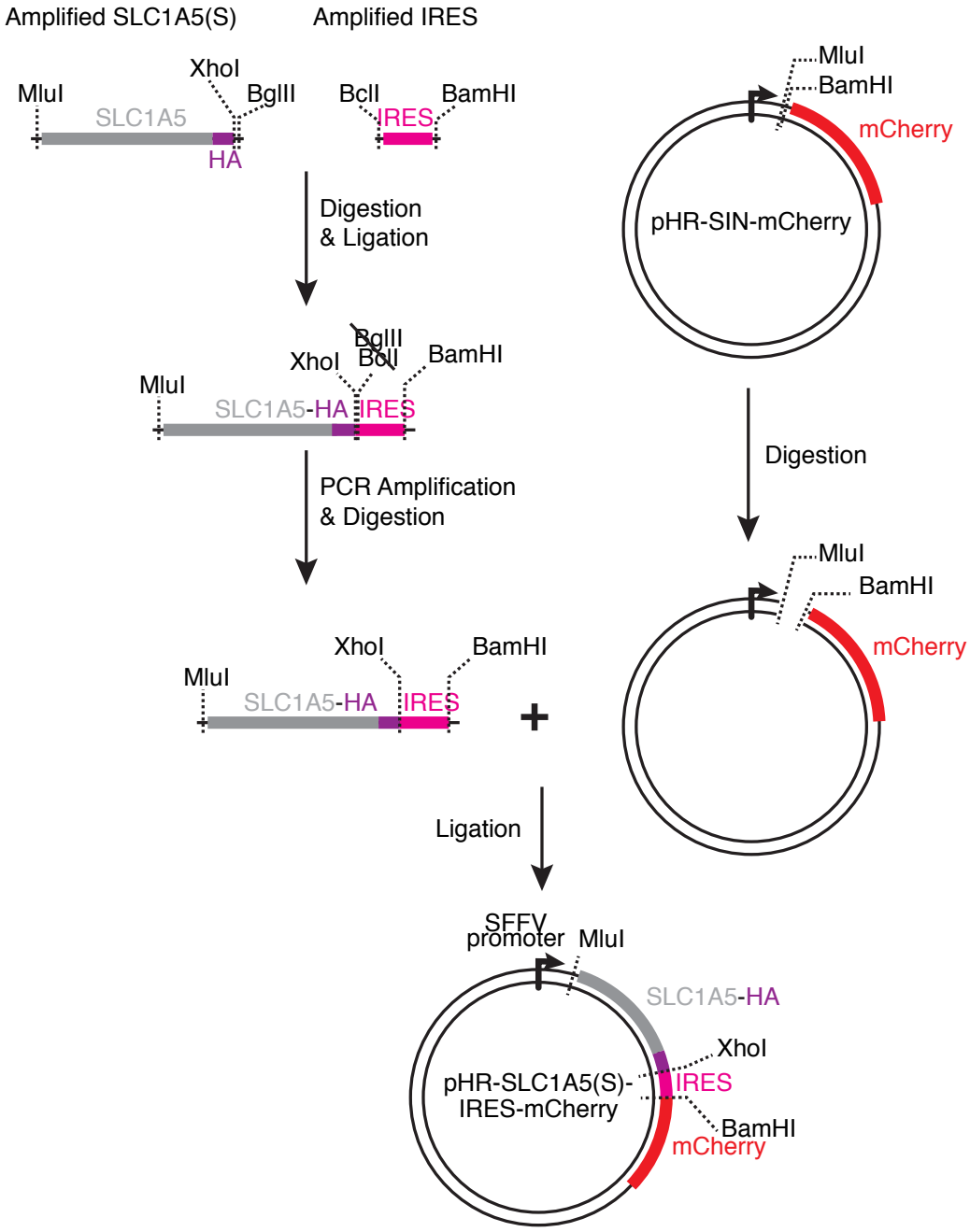

Figure 2-2. Cloning of SLC1A5 into the pHR-SIN-mCherry expression vector
Cloning strategy used for the generation of the pHR-SLC1A5(S)-HA-IRES-mCherry construct. Cloning was performed as described in Chapter 2.4.1.3.

2.4.2. Transformation of competent bacteria and plasmid purification

Chemically-competent DH5α *E. coli* cells (25–50µl) were transformed with the ligation mixture (1–10µl) by incubating for 10 min on ice, 45 sec at 42°C and another 2 min on ice. After transformation bacteria were incubated shaking horizontally in 200µl Luria-Bertani (LB) broth for 45 min at 37°C. Transformed bacteria were then plated on LB agar plates containing 100µg/ml ampicillin. Following an overnight incubation at 37°C, ampicillin-resistant single colonies were picked and screened for the correct insertion of the sequence of interest with the MangoTaq™ DNA Polymerase PCR kit (Bioline), using primers from the first cDNA PCR amplification step. Colonies positive for the desired insert expression were picked and grown in 5ml LB broth containing 100µg/ml ampicillin in a shaking incubator at 37°C and 200 rpm overnight. Plasmids were purified using the QIAprep® Spin Miniprep kit (Qiagen) according to the manufacturer's instructions and sequence-verified with primers SFFV_FW and IRES_RV **(Table 2-3)**. Once the insert sequence was confirmed in full, the QIAGEN Plasmid Midi Kit (Qiagen) was used for plasmid purification from 500ml cultures of bacteria that had been grown in LB containing 100µg/ml ampicillin at 37°C and 200 rpm overnight.

2.4.3. Lentiviral transduction

Human embryonic kidney (HEK293T) cells were used as a packaging cell line for lentiviral particles encoding SLC1A5(L) or SLC1A5(S). To produce lentiviral particles, HEK293T cells were co-transfected with packaging plasmids encoding VSV-G and Gag-Pol, as well as the appropriate lentiviral vectors using the X-tremeGENE 9 transfection reagent (Roche) according to the manufacturer's instructions. WT HeLa cells were transduced by adding 48h supernatants to the cells. Alternatively, the virus was concentrated by layering pooled 24, 48 and 72h supernatants onto 20% (w/v) sucrose solution in sterilised oak ridge tubes (Nalgene) and centrifuging at 24,000 rpm in a fixed-angle JA-25.50 rotor (Beckman

Coulter) for 2h at 4°C. Concentrated virus pellet was then resuspended in PBS, aliquoted, and stored at -80ºC. WT HeLa cells were transduced by adding concentrated virus directly to the cells.

Where applicable, transduced cells were FACS sorted on the basis of GFP/mCherry expression. Double transfected HeLa cells were generated by simultaneously transducing the cells with two lentiviruses (one encoding FLAG-tagged SLC1A5(L) with GFP and the other encoding HA-tagged SLC1A5(S) with mCherry, Chapter 3.2.1.) and sorting on the GFP^+ $mCherry^+$ population. SLC1A5 expression in transduced cells was confirmed by Western blotting and/or flow cytometry.

2.4.4. Primers

All primers were obtained from MWG Eurofins and resuspended to 100µM in double-distilled water. Primer working concentration was 5µM. Primers used for cloning and sequencing are outlined in **Table 2-3**.

Primer name	Primer sequence
Primers used for cloning	
SLC1A5(L)_*Bgl*II_FW	5'-CCG**AGATCT**ATGGTGGCCGATCCTCCACGAGAC TCC-3'
SLC1A5(S)_*Bgl*II_FW	5'-CCG**AGATCT**ATGAACATCCTGGGCTTGGTAGTG-3'
SLC1A5_*Xho*I_RV	5'-CCGCTCGAGTTACATGACTGATTCCTTCTCAG-3'
SLC1A5_FLAG_*Bgl*II_ *Xho*I_RV	5'-CCG**AGATCT**CTCGAGTTACTTATCGTCGTCATCCTT GTAATCCATGACTGATTCCTTCTCAG-3'
SLC1A5_HA_*Bgl*II_*Xho* I_RV	5'-CGA**GATCT**CTCGAGTTAAGCGTAATCTGGAACATCG TATGGGTACATGACTGATTCCTTCTCAG-3'
SLC1A5(S)_*Mlu*I_FW	5'- CCG**ACGCGT**ATGAACATCCTGGGCTTGGTAGTG-3'
IRES_*Bcl*I_FW	5'-GCG**TGATCA**TTATCTGCAACTCC-3'
IRES_*BamH*I_RV	5'-CCG**GGATCC**TTGTGGCCATATTATCATCGTG-3'
Primers used for sequencing	
SFFV_FW	5'-TGCTTCTCGCTTCTGTTCG-3'
IRES_RV	5'-ACATATAGACAAACGCACACCG-3'.

Table 2-3. Primers used for cloning and sequencing
Restriction enzyme recognition sites are shown in bold (black bold: *Bgl*II restriction site; grey bold: *Xho*I; purple bold: *Mlu*I; blue bold: *Bcl*I; red bold: *BamH*I) and introduced silent point mutations are underlined. Sequences encoding FLAG and HA epitopes are shown in red and orange, respectively. FW = forward primer, RV = reverse primer.

2.5. CRISPR-Cas9-mediated gene silencing

CRISPR-Cas9 technology was used to silence SLC1A5, ATF4, and LAT1 by targeting unique sequences in the coding region of exon 4 of SLC1A5, exon 1 of ATF4, and exon 1 of LAT1. Cas9 and the chimeric guide RNA were delivered to WT HeLa cells using a pX330 construct or the lentiCRISPRv2 construct (Addgene plasmid #52961). All oligonucleotides used to generate CRISPR guide sequences were purchased from MWG Eurofins and IDT, and are described in **Table 2-4**.

Primer name	Genomic target	Primer sequence (5' to 3')
SLC1A5_gs_sense	SLC1A5 exon 4	CACCGGTAGTGTTTGCCATCGTCTT
SLC1A5_gs_antisense	SLC1A5 exon 4	AAACAAGACGATGGCAAACACTAC C
ATF4_gs_sense	ATF4 exon 1	CACCGCCACTCACCCTTGCTGTTGT
ATF4_gs_antisense	ATF4 exon 1	AAACACAACAGCAAGGGTGAGTGG C
LAT1_gs_sense	LAT1 exon 1	CACCGGGGAACATCACGCTACTCA
LAT1_gs_antisense	LAT1 exon 1	AAACTGAGTAGCGTGATGTTCCCC

Table 2-4. Oligonucleotides used for generation of CRISPR guide sequences targeting SLC1A5, ATF4 or LAT1

2.5.1 Lentiviral CRISPR-Cas9-mediated gene knockdown

SLC1A5 and ATF4 knockdown cell lines were generated using the lentiCRISPRv2 construct (a gift from Feng Zhang; Addgene plasmid #52961). In short, SLC1A5- or ATF4-specific guides were designed using crispr.mit.edu server (Hsu et al., 2013) and added to the lentiCRISPR vector as previously described (Sanjana et al., 2014; Shalem et al., 2014). Lentiviral particles expressing Cas9 and the guide RNA were generated by co-transfection of HEK293T cells with the lentiCRISPRv2 plasmid alongside the packaging vectors encoding VSV-G and Gag-pol. The virus particles were concentrated and used to transfect WT HeLa cells (as described in Chapter 2.4.3) followed by selection with 1μg/ml puromycin. The efficiency of the knockdowns was confirmed by Western blotting.

2.5.2 Generation of monoclonal CRISPR-Cas9 knockout cell lines

LAT1$^{-/-}$ monoclonal cell lines were generated using the pX330-EGFP-P2A-Neo construct (modified from pX330 and kindly provided by Dr. Joey Riepsaame); the parent plasmid, pX330-U6-Chimeric_BB-CBh-hSpCas9, was a gift from Feng Zhang (Addgene plasmid #42230) (Cong et al., 2013). A LAT1-specific guide was designed and inserted into the pX330-EGFP-P2A-Neo plasmid, and then used to transfect WT HeLa cells using Lipofectamine® 2000 following the manufacturer's instructions (Life Technologies). Single-cell FACS sorting was performed 24–48h post-transfection on the basis of GFP positivity. The monoclones were grown and screened for the success of LAT1 knockout by Western blotting.

2.6. shRNA-mediated gene silencing

GCN2 shRNA

(sequence CCGGGCCTAACTGGTGAAGAAGTATCTCGAGATACTTCTTCACCAGT TAGGCTTTTTG) and ATF4 shRNA (sequence CCGGGCCTAGGTCTCTTA GATGATTCTCGAGAATCATCTAAGAGACCTAGGCTTTTT) lentiviral transduction particles were obtained from Sigma-Aldrich. The shRNA, under the control of the U6 promoter, were expressed using pLKO.1 plasmids, allowing selection of transduced cells with 1μg/ml puromycin. MISSION® pLKO.1-puro Non-Mammalian shRNA vector (Sigma-Aldrich) served as shRNA control, which targets no known mammalian genes. Lentiviral transduction was performed as described in Chapter 2.4.3.

2.7. Analysis of protein expression

2.7.1. Cell lysis

Adherent cells were washed twice in ice-cold PBS, after which ice-cold lysis buffer (20mM Tris-HCl [pH 7.5], 150mM NaCl, 1mM ethylenediaminetetraacetic acid (EDTA), 1% Triton X-100, 1mM EGTA, 2.5mM sodium-pyrophosphate decahydrate, 1mM β-glycerophosphate) supplemented with protease inhibitors (Roche) was added directly to the plates and the cells were harvested using a cell scraper. Non-adherent cells were harvested and washed twice in ice-cold PBS, after which supernatant was aspirated entirely and the cells were resuspended in ice-cold lysis buffer supplemented with protease inhibitors. 25µl lysis buffer was used for 10^6 cells. Cells were then vortexed and incubated for 30 min on ice, vortexing periodically. Cell debris and nuclei were removed by centrifugation at 13,000 rpm for 30 min at 4°C. Supernatant was collected.

2.7.2. Determination of protein concentration

Protein concentration in lysates was established using the bicinchoninic acid (BCA) protein assay kit (Pierce). The assay was performed according to the manufacturer's instructions on cell lysates diluted 1:5 and/or 1:10 in double-distilled water. 10-30µg of each sample was then mixed 3:1 with 3X SDS sample buffer (New England Biolabs) and 125µM DTT (New England Biolabs), boiled for 5 min at 70°C, replaced on ice and centrifuged at 13,000 rpm for 1 min.

2.7.3. Western blotting

Samples were resolved on NuPAGE Novex 4–12% Bis-Tris gels (Invitrogen), assembled in a running chamber filled with MES running buffer (Invitrogen). Separation was performed for 1h at a constant voltage of 170V. The resolved proteins were then transferred onto a Hybond-P PVDF membrane (GE Healthcare), which was subsequently blocked with 5%

milk powder dissolved in PBS supplemented with 0.5% (v/v) Tween-20 (Sigma-Aldrich) (further referred to as PBS-T) for 30 min at room temperature (RT). The membrane was then incubated with a primary antibody (Chapter 2.2.1) in 2.5% milk powder in PBS-T for 1h at RT, or at 4°C overnight. After three 10 min washes in PBS-T, the membrane was incubated with a secondary HRP-conjugated secondary antibody (Chapter 2.2.1) in PBS-T for 1h at RT, or at 4°C overnight. This was followed by three 15 min washes in PBS-T and a final 5 min wash in PBS. HRP activity was detected by chemiluminescence using ECL Plus Western blotting Substrate (Pierce) or SuperSignal West Femto Chemiluminescent Substrate (Thermo Scientific) according to the manufacturer's instructions. Luminescence was captured on FUJI SUPER-RX films (Fleischhacker) and with an ImageQuant (GE Healthcare). Band intensity analysis was performed using ImageJ software (NIH) and Microsoft Excel, and included normalization of the band intensity to the loading controls.

2.7.3.1 Membrane stripping

For reprobing the same blot with a different antibody, Hybond-P PVDF membranes were stripped by incubation in 62.5mM Tris-HCl [pH 6.8], 2% SDS and 0.7% β-mercaptoethanol solution for 30 min at 50°C, followed by at least three 10 min washes in PBS-T. The membranes were then re-blocked with 5% milk powder dissolved in PBS-T and stained with primary and secondary antibodies as described above.

2.7.4. PNGase F and EndoH treatment

Where indicated, samples were digested with Endoglycosidase H (EndoH) or *N*-Glycosidase F (PNGase F) (New England Biolabs) according to the manufacturer's instructions. Briefly, lysates were first denatured in 10X Glycoprotein Denaturing Buffer (New England Biolabs) for 10 min at 95°C, followed by EndoH or PNGase F digesion for 1h at 37°C.

2.7.5. Immunoprecipitation

Cell lysates were obtained as described in Chapter 2.7.1 and pre-cleared for 1h at 4°C with mouse IgG-Agarose (#A0919, Sigma-Aldrich). For immunoprecipitation, samples were incubated for 2h at 4°C with anti-FLAG (M2)–Agarose (#A2220, Sigma-Aldrich). Agarose was then washed 4 times with ice-cold co-immunoprecipitation buffer made of 50mM Tris-HCl [pH 7.5], 1mM EDTA, 150mM NaCl and 0.5% Nonidet P-40. Bound proteins were eluted by incubation with 3X FLAG peptide (#F4799, Sigma-Aldrich) and analysed by Western blotting.

2.8. Flow cytometry

2.8.1. Cell viability and cell surface staining

Cells were harvested, transferred to a 96 well plate and washed twice in PBS. Cells were stained with LIVE/DEAD® Fixable Aqua Dead Cell Stain (#L34957, ThermoFisher Scientific) for 20 min at 4°C. The stock was made up according to the manufacturer's instructions and diluted 1:250 in PBS for the staining. After live/dead staining, cells were washed in PBS containing 1% FBS (further referred to as FACS buffer). In experiments with amino acid-depleted medium FACS buffer was made up with 1% dialysed FBS. Antibodies were added to the cells at the indicated concentrations (**Table 2-1**) and incubated for 25-30 min at 4°C. Cells were then washed twice in FACS buffer, transferred to FACS tubes and run on Cyan analyser.

2.8.1.1. Propidium iodide cell viability staining

Where indicated, 10µg/mL propidium iodide (#P3566, ThermoFisher Scientific) was added to the cells just prior to flow cytometry analysis.

2.8.2. Cytoplasmic staining

Where indicated, live/dead and cell surface staining were performed as described above. Cells were then fixed in 100µl Intracellular Fixation Buffer (eBioscience) for 20 min at RT, and washed in 1X Permeabilization Buffer (PB) (eBioscience). Cells were blocked in 1X PB supplemented with 1% BSA, 5% FBS, 5% human serum, 5% goat serum and human BD Fc block (BD Biosciences) used at 1:100 for 30 min at RT. Intracellular antibodies were diluted in 1X PB and added to the cells at the indicated concentrations (**Table 2-1**) for 25–30 min at RT. Cells were then washed in 1X PB and FACS buffer, resuspended in FACS buffer, transferred to FACS tubes and run on Cyan analyzer.

2.8.3. Intranuclear staining

Where indicated, live/dead and cell surface staining were performed as described above. Cells were then fixed in 100µl FOXP3 Fix/Perm buffer (Biolegend) working solution (prepared according to the manufacturer's instructions) for 45 min at RT, and washed in 1X FOXP3 PB (Biolegend). Cells were blocked in 1X FOXP3 PB supplemented with 1% BSA, 5% FBS, 5% human serum, 5% goat serum and human BD Fc block (BD Biosciences) used at 1:100 for 30 min at RT. Intranuclear antibodies were diluted in 1X FOXP3 PB and added to the cells at the indicated concentrations (**Table 2-1**) for 45 min at RT. Cells were then washed in 1X FOXP3 PB and FACS buffer, resuspended in FACS buffer, transferred to FACS tubes and run on Cyan analyser.

2.8.4. CFSE staining

Cells were washed in ice-cold PBS, followed by another wash in RT PBS. CellTrace™ CFSE staining solution (ThermoFisher Scientific) was added to the cells ($1x10^7$ cells/ml) at the final concentration of 0.5µM in RT PBS. Cells were incubated for 8 min in the dark,

after which the staining was quenched by adding FBS. Cells were then centrifuged and washed in R10.

2.8.5. SLC1A5 cell surface staining using RD114-RBD mFc

Mouse Fc-fused SLC1A5 cell surface Receptor Binding Domain (RBD) ligand (RD114-RBD mFc) was obtained from METAFORA biosystems. Staining was performed according to the manufacturer's instructions – for 20 min at 37°C in the presence of sodium azide and EDTA. Goat anti-mouse IgG (H+L) Alexa Fluor® 647 **(Table 2-1)** was used as a secondary antibody for flow cytometry analysis.

2.9. Confocal microscopy

Coverslips were pre-washed in ethanol, dried and placed into a 24-well plate. HeLa cells were plated and left to adhere overnight. Cells were then washed in ice-cold PBS and fixed with 4% (paraformaldehyde) (PFA) for 15 min at RT. Following another two washes in PBS, cells were permeabilised by adding 0.5% Triton-X100 PBS for 1 min (two times). Cells were then blocked with 0.1% Triton-X100 PBS supplemented with 5% FBS, 5% human serum, 5% goat serum and human BD Fc block (BD Biosciences) used at 1:100 (blocking buffer) for 45 min to 2h at RT or at 4°C overnight. Primary rabbit anti-HA tag antibody (#3724, Cell Signaling Technology) was added in blocking buffer at 1:1000 for 20 min at RT, followed by three 5 min washes in 0.1% Triton-X100 PBS. Secondary goat anti-rabbit IgG (H+L) Alexa Fluor® 647 (#A21245, ThermoFisher Scientific) was added in blocking buffer at 1:200 for 20 min at RT. Cells were then washed two times in 0.1% Triton-X100 PBS and mounted with DAPI Fluoromount G (Southern Biotech). Pictures were acquired using a Zeiss LSM-780 inverted confocal microscope.

2.10. Measurement of IDO enzymatic activity by HPLC

Culture supernatants were spun down and proteins were precipitated using trichloroacetic acid (TCA). Samples were incubated with chilled 30% w/v TCA at 4°C for 15 min, followed by a 30 min centrifugation at 13,000 rpm at 4°C. The clear supernatant was then injected onto a Spherisorb S5-ODS1 column, 4.6 x 150mm (Waters, Milford, MA). The HPLC system consisted of a Knauer pump, a variable wavelength detector and a BioTek 565 autosampler. The mobile phase constituted of 40mM sodium citrate buffer [pH 2.25], 50% methanol and 0.4mM SDS. Kynurenine and tryptophan were detected at 365 nm and 280nm wavelengths, respectively.

2.11. Measurement of ^{3}H-labelled amino acid uptake

HeLa cells were washed twice in PBS, followed by a 20 min incubation at 37°C. [^{3}H]L-tryptophan or [^{3}H]L-glutamine (both from PerkinElmer) were added to the cells at 50pmol/ml and 200pmol/ml, respectively, for a fixed time at 37°C. Uptake was stopped by removing the solution and adding 20mM L-lysine in ice-cold PBS. The cells were lysed with 1% NaOH, 0.1% SDS. [^{3}H]L-tryptophan/[^{3}H]L-glutamine uptake was determined by liquid scintillation.

2.12. ELISA

Human IFNγ ELISA was performed according to the manufacturer's instructions. Briefly, enhanced binding ELISA plates (Greiner) were coated with 2 μg/ml anti-human IFNγ capture monoclonal antibody (#551221, BD Biosciences) diluted in coating buffer (100mM $NaHCO_3$ [pH 7.9]) at 4°C overnight. The plates were washed 3–4 times in PBS-T and blocked in PBS 10% FBS for 1.5–2h at RT. 4ng/ml standard and the diluted samples were

then added to the plates and incubated for 3–4h at RT, or at 4°C overnight. Next, the plates were washed 6 times in PBS-T and coated with 1 μg/ml biotinylated anti-human IFNγ detection monoclonal antibody (#554550, BD Biosciences) diluted in PBS 10% FBS. Following a 2h incubation at RT and 6 washes in PBS-T, 2.5 μg/ml avidin-peroxidase (#A-3151, Sigma-Aldrich) was added in PBS 10% FBS for 45 min at RT. The plates were washed 6–8 times in PBS-T and 2 times in water, after which the ABTS substrate was added. Colour reaction was allowed to develop for 10–80 min and was stopped by addition of SDS/SMF. Plate absorbance at OD 405nm was measured on a BMG SPECTROstar plate reader. A 4-parameter standard curve was generated and used to determine the concentration of IFNγ in each sample (MARS data analysis software, BMG).

2.13. Isolation and stimulation of primary immune cells

2.13.1. Isolation of peripheral blood mononuclear cells from leukocyte cones

Peripheral blood mononuclear cells (PBMCs) were isolated from commercially available leukocyte cones (NHS Blood and Transplant, Bristol) by density gradient centrifugation. 30ml diluted blood was layered onto 15ml Lymphoprep (Fresenius Kabi Norge AS) and centrifuged at 2000 rpm for 30 min with the centrifuge brake turned off. PBMCs were collected from the interface between plasma and Lymphoprep with a Pasteur pipette and centrifuged at 1500 rpm for 15 min, followed by a 10min spin at 1500 rpm and another two 10 min spins at 1200 rpm to remove platelets and debris. Red blood cells were lysed in Red Blood Cell Lysis buffer (Qiagen) for 5 min at RT and the cells were washed in R10.

2.13.2. Isolation and stimulation of human $CD4^+$ and $CD8^+$ T cells

$CD4^+$ and $CD8^+$ T cells were purified from PBMCs using magnetic cell separation. $CD4^+$ T cells were separated by positive selection using human CD4 MicroBeads (#130-045-101, Miltenyi Biotec), and $CD8^+$ T cells were separated by negative selection using human

$CD8^+$ T Cell Isolation Kit (#130-096-495, Miltenyi Biotec) according to the manufacturer's instructions. Buffer used for magnetic cell separation consisted of 90% PBS, 10% FBS and 2mM EDTA. Pre-coating with anti-human CD3 and CD28 antibodies (eBioscience) was used for T cell stimulation. Plates were coated with 5μg/ml anti-human CD3 and CD28 antibodies for 1h at 37°C, or at 4°C overnight, after which the antibody-containing solution was removed and plates were washed twice with PBS.

2.13.3. Stimulation of a tumour-specific T cell clone

NY-ESO-1-specific $CD8^+$ T cell clone (4D8), kindly provided by Ji-Li Chen (MRC Human Immunology, WIMM, Oxford), was activated by co-culture with B cells pre-pulsed with NY-ESO-$1_{157–165}$ (9V) peptide analogue for 2h, also provided by Ji-Li Chen. NY-ESO-$1_{157–165}$ (9V) peptide analogue has the carboxyl-terminal cysteine substituted for valine (Chen et al., 2000).

2.13.4. Isolation and stimulation of iNKT cells

PBMCs were stained with TCR Vα24 and TCR Vβ11 antibodies **(Table 2-1)** as described in Chapter 2.8.1. iNKT cells were FACS sorted from PBMCs by gating on the $Vα24^+Vβ11^+$ population. iNKT cell agonists αGalCer, PI-3 and OCH-9, as well as the biotinylated hCD1d–αGalCer monomer (Denkberg et al., 2008) were kindly provided by Mariolina Salio (MRC Human Immunology, WIMM, Oxford). $Vα24^+Vβ11^+$ cells were stimulated by co-culture with B cells pre-pulsed with αGalCer analogues for 2h. Alternatively, $Vα24^+Vβ11^+$ cells were stimulated with plate-bound hCD1d–αGalCer monomer by pre-coating streptavidin plates (ThermoFisher Scientific) with 10μg/ml biotinylated hCD1d–αGalCer monomer for 1h at 37°C, or at 4°C overnight, after which the monomer-containing solution was removed, streptavidin plates were washed twice with PBS and $Vα24^+Vβ11^+$ cells were added.

2.13.5. Isolation and differentiation of MoDCs

$CD14^+$ cells were purified from PBMCs by magnetic cell separation with human CD14 MicroBeads (#130-050-201, Miltenyi Biotec), which was performed according to the manufacturer's instructions. Buffer used for magnetic cell separation consisted of 90% PBS, 10% FBS and 2mM EDTA. $CD14^+$ monocytes were differentiated into MoDCs by addition of 50ng/ml recombinant human GM-CSF (PeproTech) and 100ng/ml recombinant human IL-4 (PeproTech) to the culture medium for 5 days.

2.14. Processing of primary human tumour samples

Samples obtained from renal cell carcinoma patients (ethical approval 13/A093) and melanoma patients (ethical approval 09/H0606/5) were processed in gentleMACS™ Dissociator using Tumour disassociation kit (#130-095-929, Miltenyi Biotec) according to the manufacturer's instructions. The resulting cell suspension was applied onto an appropriate cell strainer, washed in RPMI-1640 and centrifuged at 1500 rpm for 7 min. Red blood cells were lysed in Red Blood Cell Lysis buffer (Qiagen) for 5 min at RT and the cells were washed in R10. The samples were then either frozen or stained immediately for flow cytometry analysis.

2.15. Chromatin immunoprecipitation (ChIP)

ATF4 ChIP experiments were performed as previously described (Milne et al., 2009; Wilkinson et al., 2013). Briefly, cells were washed twice in ice-cold PBS and fixed in 2mM disuccinimidyl glutarate (#80424-50MG-F, Sigma-Aldrich) for 30 min, followed by 30 min in 1% formaldehyde. Cells were then lysed in 1% SDS, 10mM EDTA, 50mM Tris [pH 8.1] lysis buffer supplemented with protease inhibitors (#P8340, Sigma-Aldrich) for 10 min on ice. Samples were fragmented using a Bioruptor sonicator (Diagenode) for 20 min at high

in a constantly circulating 4°C water bath to an average size of 200-500bps. Chromatin was cleared using Dynabeads (Life Technologies) diluted in ChIP dilution buffer (0.01% SDS, 1.1% TritonX-100, 1.2mM EDTA, 16.7mM Tris-HCl [pH 8.1], 167mM NaCl) supplemented with protease inhibitors. 50µl aliquots were taken from 1ml of the sonicated, diluted chromatin before antibody incubation (this serves as total input; the signal from the input samples represents 5% of the total chromatin used in each ChIP). The rest of the chromatin was incubated with the anti-ATF4 antibody (#11815, Cell Signaling Technology) at 4°C overnight. Samples were then incubated with the 1:1 mixture of protein A and protein G Dynabeads (Life Technologies) for 3–5h. Antibody:chromatin complexes were collected with a magnet, and washed twice with a solution of 50mM HEPES-KOH [pH 7.6], 500mM LiCl, 1mM EDTA, 1% NP-40 and 0.7% Na-Deoxycholate. After a wash in 10mM Tris-HCl [pH 8.0], 1mM EDTA, samples were eluted in 50mM Tris-HCl [pH 8.0], 10mM EDTA and 1% SDS, treated with RNase (ThermoFisher Scientific) and Proteinase K (ThermoFisher Scientific), and purified using a PCR purification kit (Qiagen). ChIP samples were quantified by q-RT-PCR relative to inputs as previously described (Milne et al., 2009; Wilkinson et al., 2013). 'The amount of genomic DNA coprecipitated with antibody was calculated as a percentage of total input using the following formula $\Delta C_T = C_T$ (input) – C_T (chromatin IP), % total = $2^{\Delta CT}$ X 5.0%' (Milne et al., 2009). SLC1A5-specific primers were designed using the previously reported ATF4 binding site (Ren et al., 2015).

2.16. *In vivo* studies

B6.SJL-*Ptprc*^{a} (CD45.1) mice were bred in house and originally obtained from The Jackson Laboratory. EG7 cells ($4x10^{6}$) were injected subcutaneously in the back of male B6.SJL-*Ptprc*^{a} mice. All mice were sex-matched and aged between 6 and 8 weeks at the

time of the injection. After 5 days, mice were euthanised and tumours were harvested and processed using collagenase (type 2, #LS004202, Worthington Biochemical Corporation) and DNAse I (#D4513, Sigma-Aldrich). All studies were carried out in accordance with Animals (Scientific Procedures) Act 1986, and the University of Oxford Animal Welfare and Ethical review Body (AWERB) under project licence 40/3636.

2.17. Analysis of mRNA expression in primary human tumours

Expression of mRNA measured by RNA sequencing was downloaded from the TCGA data portal for LIHC (n = 374), OV (n = 309), GBM (n = 169), LGG (n = 534), UCEC (n = 177), ACC (n = 79), CESC (n = 306), BRCA (n = 1102), and KIRC (n = 534), and the Spearman's rank correlation coefficient was calculated between the expressions of *SLC1A5* and *WARS, TDO2, IDO1*, and *ATF4* for each tumour type. Additionally, clinical data was downloaded for the LGG samples, and Kaplan-Meier curves comparing survival of patients with low and high expression of *SLC1A5, IDO1*, and the combinations thereof were made. High and low expression of *SLC1A5* or *IDO1* was defined as above and below median expression, respectively. Median expression is an arbitrary cut-off but in cases where no a-priory knowledge of a clinically useful cut-off is available it offers balanced groups for analysis. Statistical analysis was performed using log-rank test.

2.18. Statistical analysis

Other than RNA-seq analysis, for which methods are provided above, statistical analysis was performed using Prism software (GraphPad, San Diego, CA). Unpaired, two-tailed Student's t-test was used to determine statistical significance. The threshold for rejection of the null hypothesis was $p<0.05$. *$p < 0.05$; **$p < 0.01$, ***$p < 0.001$, ***$p < 0.0001$.

CHAPTER 3: Modulation of the amino acid transporter expression profile by tryptophan catabolism in tumour cells

3.1. RNA-seq analysis of IDO-expressing tumour cells

3.1.1. Tumour cells expressing tryptophan-degrading enzymes metabolise tryptophan into kynurenine

To investigate the effect of tryptophan catabolism on tumour cell whole transcriptome profile, we developed an *in vitro* system where IDO expression was induced either by transducing HeLa cells with a lentivirus encoding human IDO (IDO^+ HeLa) (Silk et al., 2011) or by treating HeLa cells with IFNγ (IFNγ HeLa). As expected, *IDO1*-transduced and IFNγ-treated wild-type (WT) HeLa cells upregulated *IDO1* gene expression **(Figure 3-1A)**. In addition, HeLa cells were transduced with human *TDO2* (TDO^+ HeLa), which exhibited enhanced *TDO2* but not *IDO1* transcription **(Figure 3-1A)**.

We then confirmed that IDO and TDO were biologically active by measuring tryptophan and kynurenine levels in the supernatants obtained from IFNγ, IDO^+ and TDO^+ HeLa cells, as compared to untreated WT HeLa cells or HeLa cells transduced with a lentivirus encoding GFP alone (GFP HeLa). While conditioned medium from HeLa cells that did not express *IDO1* or *TDO2* (WT and GFP HeLa) **(Figure 3-1A)** contained about 25μM tryptophan, this amino acid was virtually undetectable in the supernatants obtained from IFNγ HeLa and TDO^+ HeLa cells cultured in conventional culture medium for 72h **(Figure 3-1B)**. Tryptophan concentration also fell substantially in the conditioned medium obtained from IDO^+ HeLa cells – from about 25μM to 2μM **(Figure 3-1B)**. On the contrary, tryptophan metabolite kynurenine was virtually undetectable in WT and GFP HeLa cell

supernatants, while it reached 13-15μM in the conditioned medium derived from IFNγ, IDO$^+$ and TDO$^+$ HeLa cells **(Figure 3-1B)**. We thus confirmed that tryptophan-degrading enzyme induction in our *in vitro* system, either though IFNγ treatment or *IDO1/TDO2* gene overexpression, leads to functional enzymatic activity, as evidenced by the decreased tryptophan-to-kynurenine ratio in the supernatants from IFNγ, IDO$^+$ and TDO$^+$ HeLa cells.

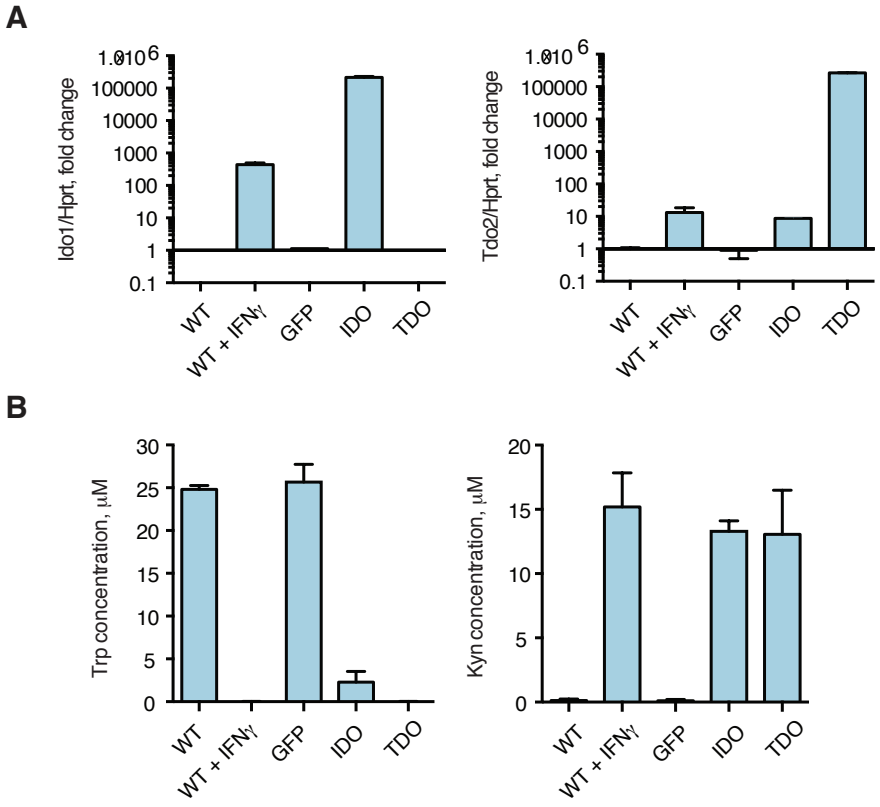

Figure 3-1. Induction of IDO or TDO expression in HeLa cells results in functional enzymatic activity

(A) WT, IFNγ-treated, GFP-transduced, *IDO1*-transduced and *TDO2*-transduced HeLa cells were cultured for 72h. *IDO1* and *TDO2* mRNA expression levels were analysed by quantitative PCR, and are shown as fold change in expression relative to *Hprt*. Bars represent the mean ± SEM. **(B)** Supernatants were collected from WT, IFNγ-treated, GFP-transduced, *IDO1*-transduced and *TDO2*-transduced HeLa cells cultured for 72h in complete tissue culture medium. Tryptophan and kynurenine concentrations were determined by HPLC. Bars represent the mean ± SEM.

3.1.2. Tumour cells expressing IDO upregulate the expression of several amino acid transporter genes

Using RNA-seq, we identified the genes modulated in IDO^+ HeLa cells under conditions of nutritional stress caused by incubation in limited amount of culture medium, and compared them with the gene profiling of IFNγ HeLa cells. After 72h of culture, IDO^+ HeLa cells increased transcription of several genes that were also upregulated in IFNγ HeLa cells **(Figure 3-2)**. Such shared genetic signature between IDO^+ HeLa and IFNγ HeLa cells was more evident at 72h rather than at 48h **(Figure 3-3)**, which could be accounted for by differences in the kinetic required by IDO^+ HeLa cells to degrade tryptophan contained in the culture medium. At 72h, this shared transcriptional signature included the expression of genes involved in several biological functions, such as regulation of cellular redox signaling and apoptosis (e.g. *TXNIP* (Spindel et al., 2012), *FAS* (Nagata and Golstein, 1995), *HERPUD1* (Kokame et al., 2000) and *DDIT3/CHOP/GADD153* (Han et al., 2013; Zinszner et al., 1998)), hemopoiesis (e.g. *JAG1* (Poulos et al., 2013) and *EPAS1* (Scortegagna et al., 2003)), inflammatory response (e.g. pro-inflammatory cytokine-, chemokine- and transcription factor-encoding genes *TNF*, *CXCL2* and *CXCL3,* and CCAAT/enhancer binding protein β (*C/EBPβ)*), amino acid biosynthesis (e.g. asparagine synthetase-encoding *ASNS,* cystathionine gamma-lyase-encoding *CTH***,** phosphoserine aminotransferase 1-encoding *PSAT1* and phosphoserine phosphatase-encoding *PSPH*, which are involved in the production of asparagine, cysteine and serine, respectively), metabolism (e.g. glutamine fructose-6-phosphate transaminase 1-encoding *GFPT1* and glutamine fructose-6-phosphate transaminase 2-encoding *GFPT2*, which regulate the flux of glucose into the hexosamine pathway, and glutamic pyruvate transaminase 2-encoding *GPT2* involved in the production of pyruvate and glutamate), as well as tRNA amino acylation and amino acid transport **(Figures 3-2, 3-3)**. The most abundantly upregulated

gene involved in tRNA amino acylation was *WARS* (tryptophanyl-tRNA synthetase) followed by *GARS* (glycyl-tRNA synthetase) and *CARS* (cysteinyl-tRNA synthetase), while the most abundantly upregulated genes associated with amino acid transport were *SLC7A11* (cystine/glutamate exchanger), *SLC1A4* (glutamate/neutral amino acid transporter), *SLC1A5* (glutamine/neutral amino acid transporter) and, to a lesser extent, *SLC6A9* (glycine neurotransmitter transporter) (**Figures 3-2B, 3-3**). Of note, consistent with the hypothesis that changes in the gene profiling of SLC and amino acid metabolism genes are dependent on conditions of sufficient nutritional stress, overexpression of these genes in IDO^+ HeLa cells was only induced after 72h but not after 48h incubation **(Figure 3-3)**. Other major amino acid transporters, including CD98hc (*SLC3A2*), LAT1 (*SLC7A5*) and SNAT2 (*SLC38A2*) showed a less pronounced differential expression in HeLa cells expressing IDO (**Figure 3-3**). Notably, out of the top four upregulated SLC genes, SLC1A5 was the only amino acid transporter associated with EAA transport (Nicklin et al., 2009) and tryptophan transport network, as determined using the MetaCore pathway analysis software (**Figure 3-4**).

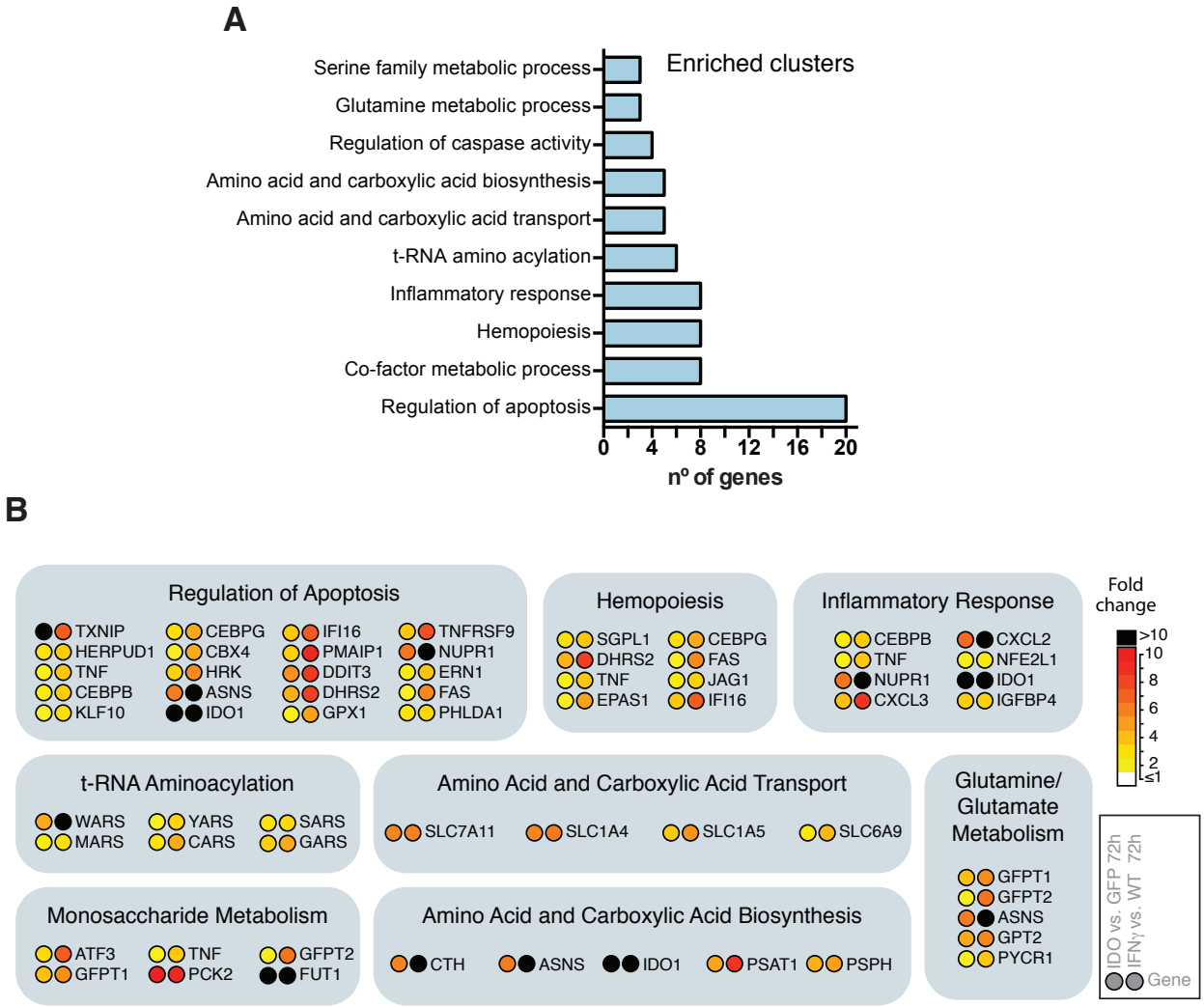

Figure 3-2. Remodeling of transcriptomic profiling in IDO-expressing tumour cells
(A) The top 2000 upregulated genes in *IDO1*-transduced vs GFP-transduced HeLa cells cultured for 72h and in IFNγ-treated vs untreated WT HeLa cells cultured for 72h, as determined by RNA-seq, were used to identify enriched biological functions in IDO^{+} tumour cells. **(B)** Clustered RNA-seq expression data showing the fold change in the expression of genes upregulated in both *IDO1*-transduced vs GFP-transduced HeLa cells cultured for 72h (left circles) and IFNγ-treated vs untreated WT HeLa cells cultured for 72h (right circles), as indicated in the legend box on the right.

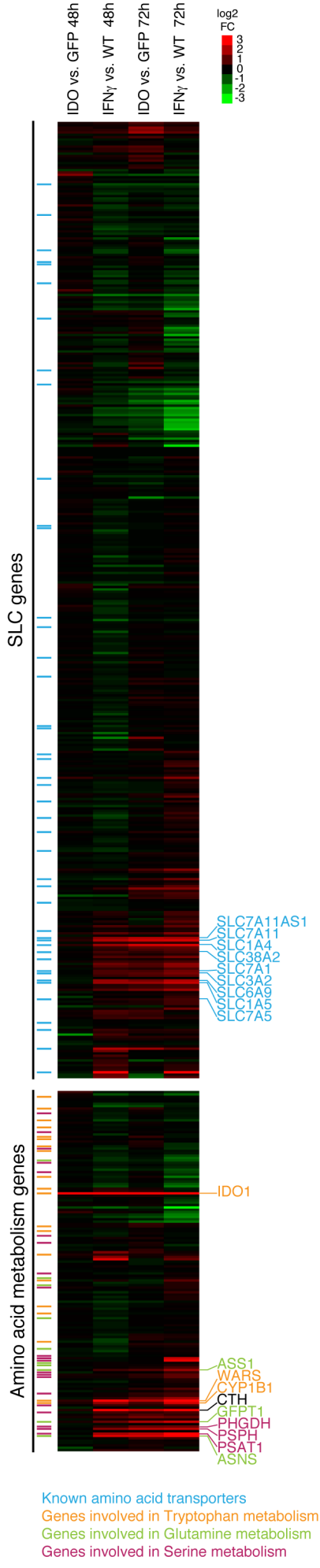

Figure 3-3. IDO-expressing tumour cells demonstrate extensive remodeling of amino acid transport and metabolism genes

RNA-seq profiles of SLC (top) and amino acid metabolism (bottom) genes in *IDO1*-transduced vs GFP-transduced and IFNγ-treated vs untreated WT HeLa cells cultured for 48h or 72h. Amino acid transporter genes are denoted by blue bars; genes involved in tryptophan, glutamine and serine metabolism are denoted by orange, green, and maroon bars, respectively. The hierarchical clustering of genes was performed using GENE-E package, with distance determined by the Pearson correlation coefficient.

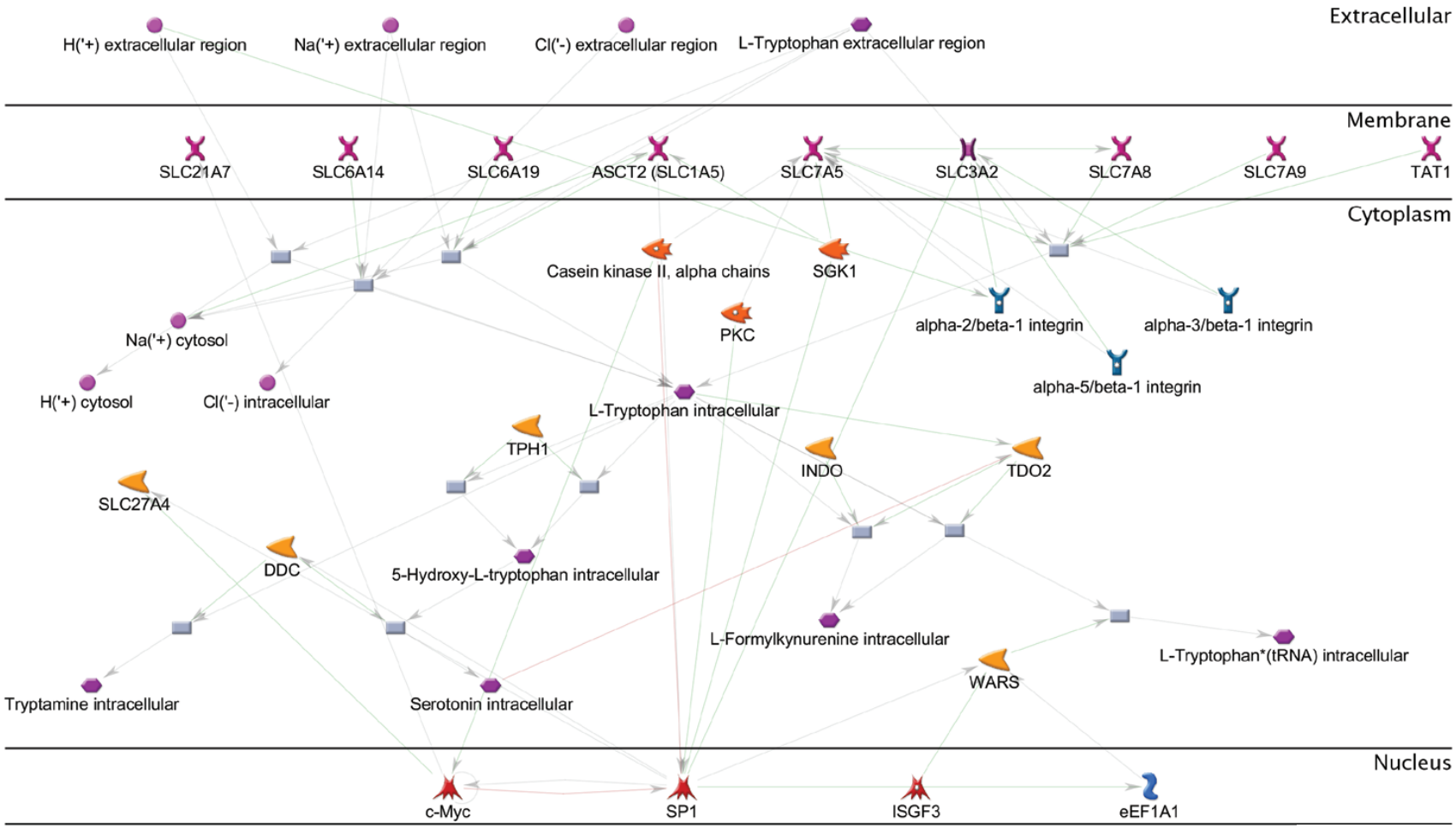

Figure 3-4. Tryptophan network MetaCore analysis

MetaCore pathway analysis showing the members of the tryptophan metabolism and transport network. Symbols are explained in the MetaCore legend found at https://portal.genego.com/legends/MetaCoreQuickReferenceGuide.pdf

3.1.2.1. Tumour cells expressing tryptophan-catabolising enzymes exhibit enhanced expression of novel SLC1A5 isoforms

Further analysis demonstrated that, in addition to the full-length *SLC1A5* transcript, hereafter referred to as *SLC1A5* long (*SLC1A5(L)*), there are truncated splice variants of *SLC1A5* – *SLC1A5* middle (*SLC1A5(M)*) and *SLC1A5* short (*SLC1A5(S)*). Both SLC1A5(L) and SLC1A5(S) are encoded by eight exons, but in SLC1A5(S), the original exon one (1a) is replaced by a short unique sequence (1b). Sequence 1b, however, does not constitute part of the coding region, as SLC1A5(S) mRNA translation starts at the ATG codon in exon four **(Figure 3-5A)**. SLC1A5(M), on the other hand, is encoded by seven exons, contains a unique exon one sequence (1c), from which its translation is initiated **(Figure 3-5A)**. The predicted membrane topology of SLC1A5 isoforms is shown in **Figure 3-5B**. According to this model, the full-length SLC1A5 protein is composed of eight transmembrane (TM) domains (TM1-TM8) and two hairpins of different lengths (H1 and H2) **(Figure 3-5B)**. SLC1A5(S) and SLC1A5(M) isoforms lose approximately 230 and 200 amino acids of the original N-terminus sequence, respectively, which form TM1-TM3 **(Figure 3-5B)**. Of note, the transport activity of the SLC1 family amino acid transporters is thought to take place in the mobile hairpin-containing domain at the C-terminus (Kanai et al., 2013; Pingitore et al., 2013; Reyes et al., 2009) which remains intact in the truncated SLC1A5(S) and SLC1A5(M) isoforms **(Figure 3-5B)**.

Next, we utilised the unique sequences in the non-coding regions of the *SLC1A5(S)* and *SLC1A5(M)* transcripts (1b and 1c, respectively, **Figure 3-5A**) to design a quantitative PCR (q-RT-PCR) assay for specific amplification of *SLC1A5(L)*, *SLC1A5(S)*, and *SLC1A5(M)* mRNA. This assay allowed us to demonstrate that IFNγ-treated WT, *IDO1*-transduced HeLa, as well as HeLa cells overexpressing the tryptophan-degrading enzyme TDO exhibit increased expression of all three *SLC1A5* variants **(Figure 3-6A)**. In agreement with the

RNA-seq data, the expression of transcripts associated with *SLC7A11* and *SLC1A4* was also upregulated in IFNγ, IDO^+ and TDO^+ HeLa cells **(Figure 3-6A)**. We then assessed SLC1A5 protein expression in tumour cells exhibiting IDO or TDO activity using an antibody specific for the N-terminus of the full-length SLC1A5, which is expected to detect SLC1A5(L) but not the other isoforms (see predicted SLC1A5 membrane topology in **Figure 3-5B**). SLC1A5 expression levels increased substantially in tumour cells treated with IFNγ and those transduced with *IDO1* or *TDO2* (**Figure 3-6B**).

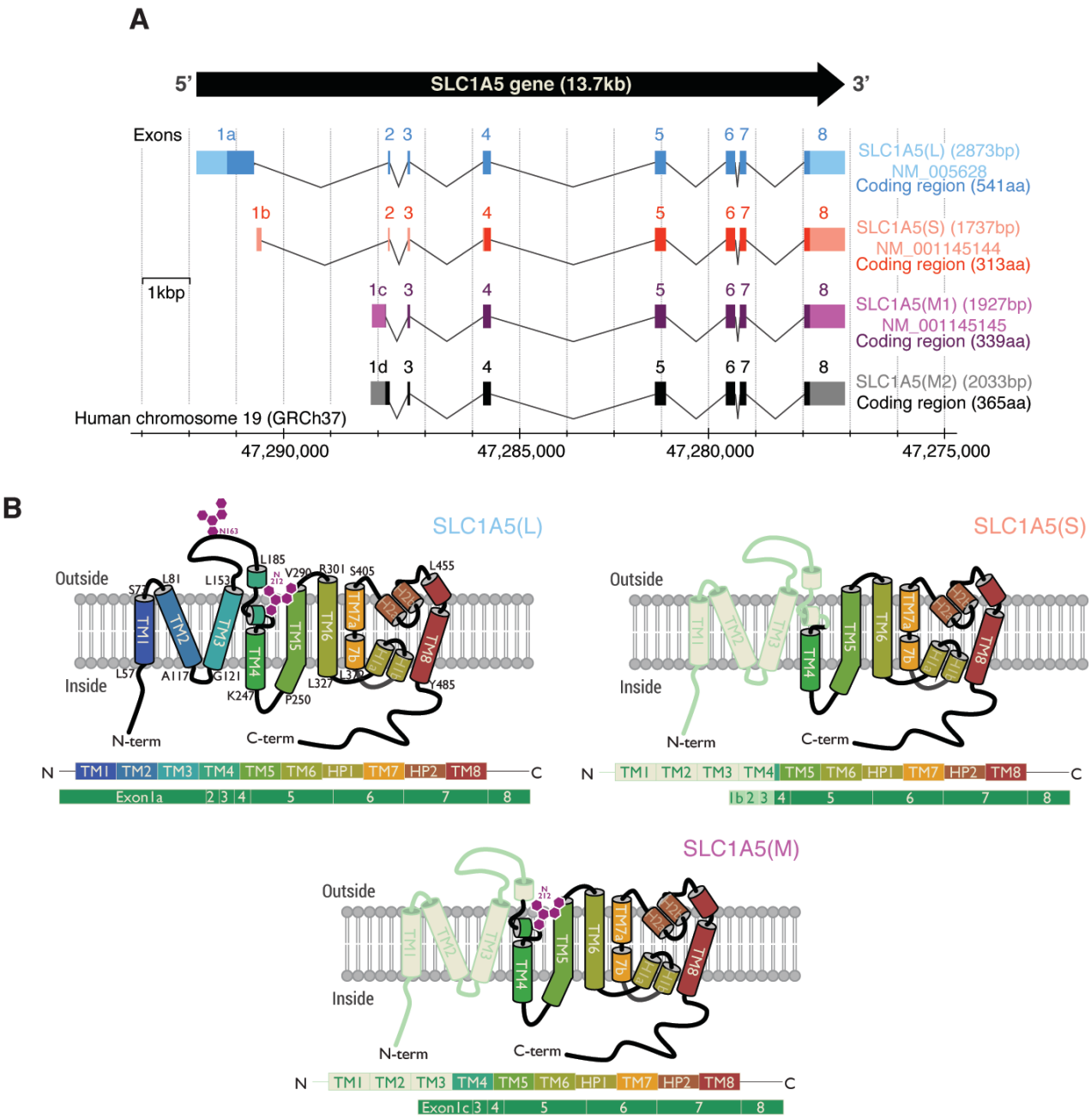

Figure 3-5. Genomic organisation and predicted membrane topology of SLC1A5 isoforms

(A) Genomic organisation of SLC1A5 isoforms. Introns are represented as lines, exons as boxes; coding region is shown in a darker colour. **(B)** Gene to protein sequence alignments and predicted membrane topology of SLC1A5 isoforms, based on a putative 3D-structure generated in Swiss-Model server (Biasini et al., 2014), with the structure of the thermophilic archaeal (*Pyrococcus horikoshii* and *Thermococcus kodakarensis*) glutamate transporter Glt_{Ph} (Jensen et al., 2013; Verdon et al., 2014; Yernool et al., 2004), homologous to SLC1A5, as a template (PDB: 4OYF and 4KY0). Each transmembrane/hairpin domain is shown in a different colour. Missing regions are shown in a faded colour. The putative *N*-linked glycosylation sites, N163 and N212 (shown in purple), are located between TM3 and TM4 (Console et al., 2015; Wollscheid et al., 2009). TM, transmembrane domain; H, hairpin.

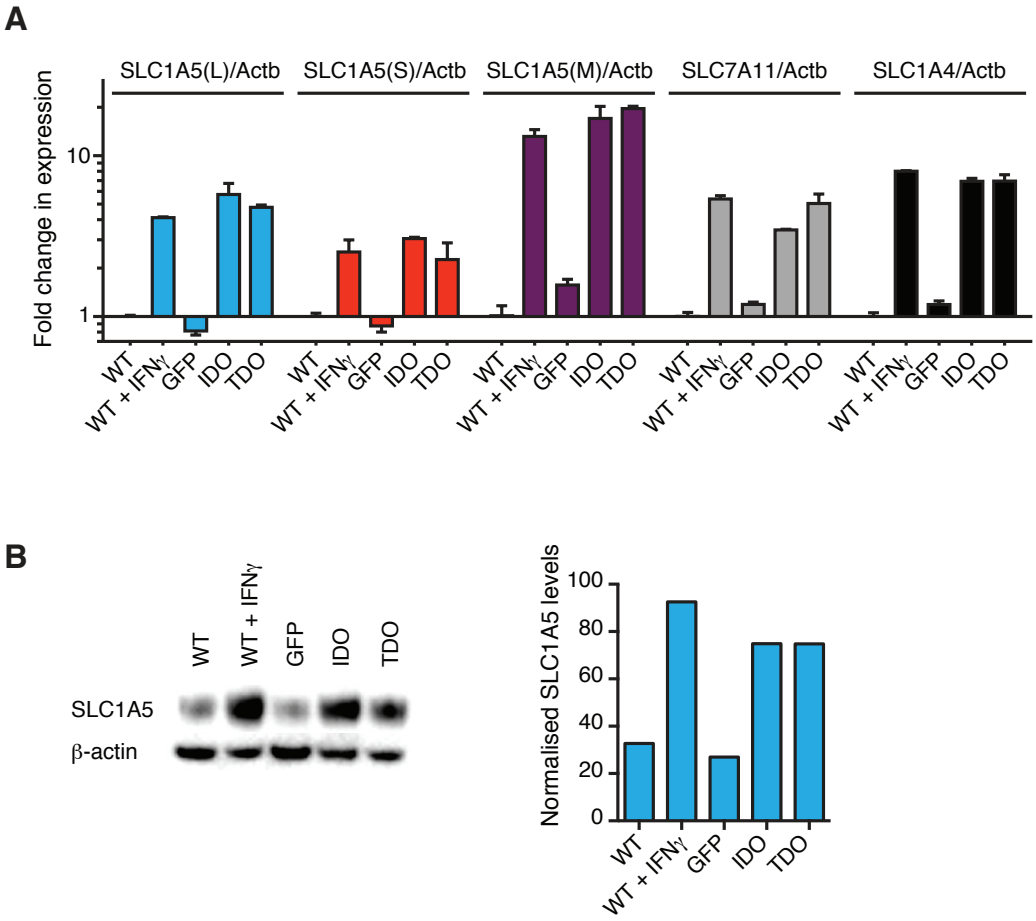

Figure 3-6. SLC1A5, SLC7A11 and SLC1A4 expression is increased in IDO- and TDO-expressing tumour cells

WT, IFNγ-treated, GFP-transduced, *IDO1*-transduced and *TDO2*-transduced HeLa cells were cultured for 72h. *SLC1A5(L)*, *SLC1A5(S), SLC1A5(M), SLC7A11* and *SLC1A4* mRNA expression levels were analysed by quantitative PCR, and are shown as fold change in expression relative to *Actb*. Bars represent the mean ± SEM **(A)**. Western blotting was performed with indicated antibodies and protein levels were quantified by densitometry **(B)**.

3.2. Biochemical properties and localisation of SLC1A5 isoforms

3.2.1. Cloning of SLC1A5 isoforms and generation of tumour cell lines with stable SLC1A5 isoform overexpression

To study the biological function of SLC1A5 transporter, we overexpressed SLC1A5(L) and its most truncated isoform, SLC1A5(S), in HeLa cells. The pHR-SLC1A5(L)-IRES-GFP and pHR-SLC1A5(S)-IRES-GFP constructs, in which SLC1A5(L) or SLC1A5(S) expression is driven by SFFV promoter and GFP is used as a reporter gene, were generated as described in Materials and Methods (Chapter 2.4.1.1). WT HeLa cells transduced with a lentiviral vector encoding SLC1A5(L) with GFP, SLC1A5(S) with GFP or GFP alone, as a control, acquired GFP fluorescence, as determined by flow cytometry **(Figure 3-7A)**. SLC1A5(L) protein overexpression was also confirmed by Western blotting with the antibody specific to the N-terminus of the full-length SLC1A5 **(Figure 3-7B)**. SLC1A5(S) could not be visualised by Western blotting due to the unavailability of good quality antibodies specific for the C-terminus of SLC1A5 (see predicted membrane topology of SLC1A5 in **Figure 3-5B**). Of note, the N-terminus specific antibody, which is not expected to detect SLC1A5(S), demonstrated some increase in SLC1A5(L) expression in HeLa cells transduced with *SLC1A5(S)* **(Figure 3-7B)**. HeLa cell lines generated using pHR-SLC1A5(L)-IRES-GFP and pHR-SLC1A5(S)-IRES-GFP constructs were used to assess the effect of SLC1A5 isoform overexpression on the amino acid uptake in tumour cells (Chapter 3.3).

To address the issue of SLC1A5(S)-specific antibody unavailability, SLC1A5(L) and SLC1A5(S) isoforms were tagged with easily identifiable affinity tags, HA and/or FLAG, to allow detection by Western blotting, as well as immuneprecipitation experiments. To this end, we generated pHR-SLC1A5(L)-HA-IRES-GFP, pHR-SLC1A5(L)-FLAG-IRES-GFP and pHR-SLC1A5(S)-HA-IRES-mCherry constructs (see Materials and Methods, Chapters

2.4.1.2 and 2.4.1.3) and transduced HeLa cells with a lentivirus encoding SLC1A5(L) tagged at the C-terminus with either HA or FLAG epitope and GFP as a reporter gene (using the SLC1A5(L)-HA-IRES-GFP and pHR-SLC1A5(L)-FLAG-IRES-GFP constructs, respectively) or with a lentivirus encoding C-terminally HA-tagged SLC1A5(S) with mCherry as a reporter gene (using the pHR-SLC1A5(S)-HA-IRES-mCherry construct). In addition, double transfectant HeLa cells were produced, which overexpressed both FLAG-tagged SLC1A5(L) with GFP and HA-tagged SLC1A5(S) with mCherry.

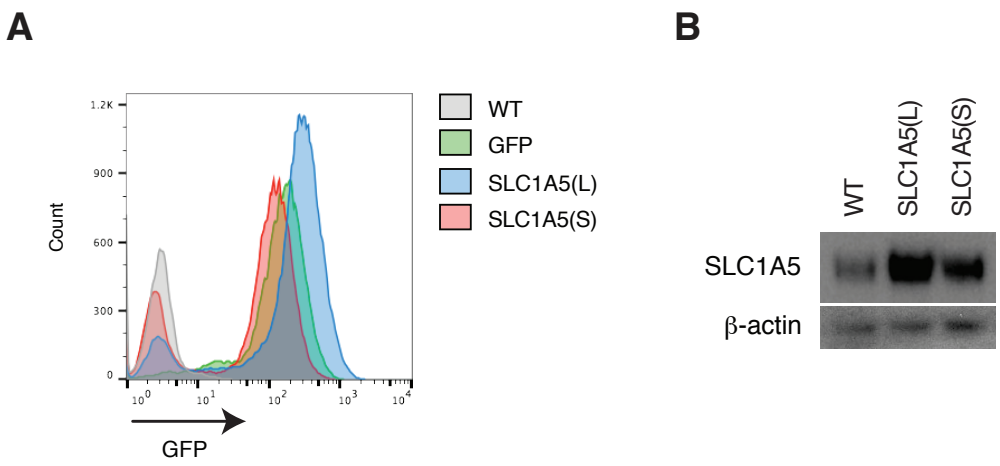

Figure 3-7. Confirmation of GFP fluorescence and protein overexpression in *SLC1A5(L)*- and *SLC1A5(S)*-transduced tumour cells
(A) GFP fluorescence in untransduced WT HeLa cells, and WT HeLa cells transduced with a lentiviral vector encoding SLC1A5(L) with GFP, SLC1A5(S) with GFP or GFP alone. Samples were analysed by flow cytometry. **(B)** Total cell lysates obtained from WT, *SLC1A5(L)*-transduced and *SLC1A5(S)*-transduced HeLa cells were analysed by Western blotting with indicated antibodies.

FLAG expression in FLAG-tagged SLC1A5(L) GFP HeLa and FLAG-tagged SLC1A5(L) GFP HA-tagged SLC1A5(S) mCherry HeLa cells was confirmed by anti-FLAG Western blotting with the appearance of a band of about 60kDa **(Figure 3-8A)**. These results are consistent with the expected molecular weight for SLC1A5(L) of 57kDa. HA expression in the transduced cells was confirmed by both Western blotting (the expected molecular

weight for SLC1A5(S) is around 30kDa) **(Figure 3-8B)** and flow cytometry **(Figure 3-8C)**. While HA expression in HA-tagged SLC1A5(L) GFP HeLa and HA-tagged SLC1A5(S) mCherry HeLa cells was undetectable at the cell surface, the transduced cells showed clear positive anti-HA staining after cell permeabilisation **(Figure 3-8C)**, which is consistent with the intracellular localisation of the SLC1A5 C-terminus predicted by the SLC1A5 membrane topology model **(Figure 3-5B)**.

3.2.2. SLC1A5(L) and SLC1A5(S) isoforms exhibit differential sensitivity to enzymatic deglycosylation

SLC1A5 full-length protein has two putative *N*-linked glycosylation sites corresponding to residues N163 and N212 located between TM3 and TM4 (Console et al., 2015; Wollscheid et al., 2009). Interestingly, the SLC1A5(S) isoform lacks these sites **(Figure 3-5B)**. To determine the sensitivity of SLC1A5(L) and SLC1A5(S) isoforms to enzymatic deglycosylation, we treated the lysates from HA-tagged SLC1A5(L) GFP HeLa and HA-tagged SLC1A5(S) mCherry HeLa cells with EndoH and PNGase F enzymes and probed them with anti-HA antibody. Of note, while EndoH specifically cleaves high mannose and some hybrid types of *N*-linked carbohydrates, PNGase F removes all types of *N*-linked glycosylation. While both SLC1A5(L) and SLC1A5(S) were resistant to EndoH-mediated deglycosylation, the two isoforms exhibited differential sensitivity to PNGase F treatment **(Figure 3-9)**. Specifically, SLC1A5(L) was PNGase F-sensitive, as demonstrated by the reduction in the molecular weight of HA-tagged SLC1A5(L) protein after PNGase F treatment **(Figure 3-9)**. The molecular weight of HA-tagged SLC1A5(S) protein, on the other hand, remained unchanged following PNGase F treatment **(Figure 3-9)**. These results are consistent with the loss of *N*-linked glycosylation sites N163 and N212 in the truncated SLC1A5(S) isoform.

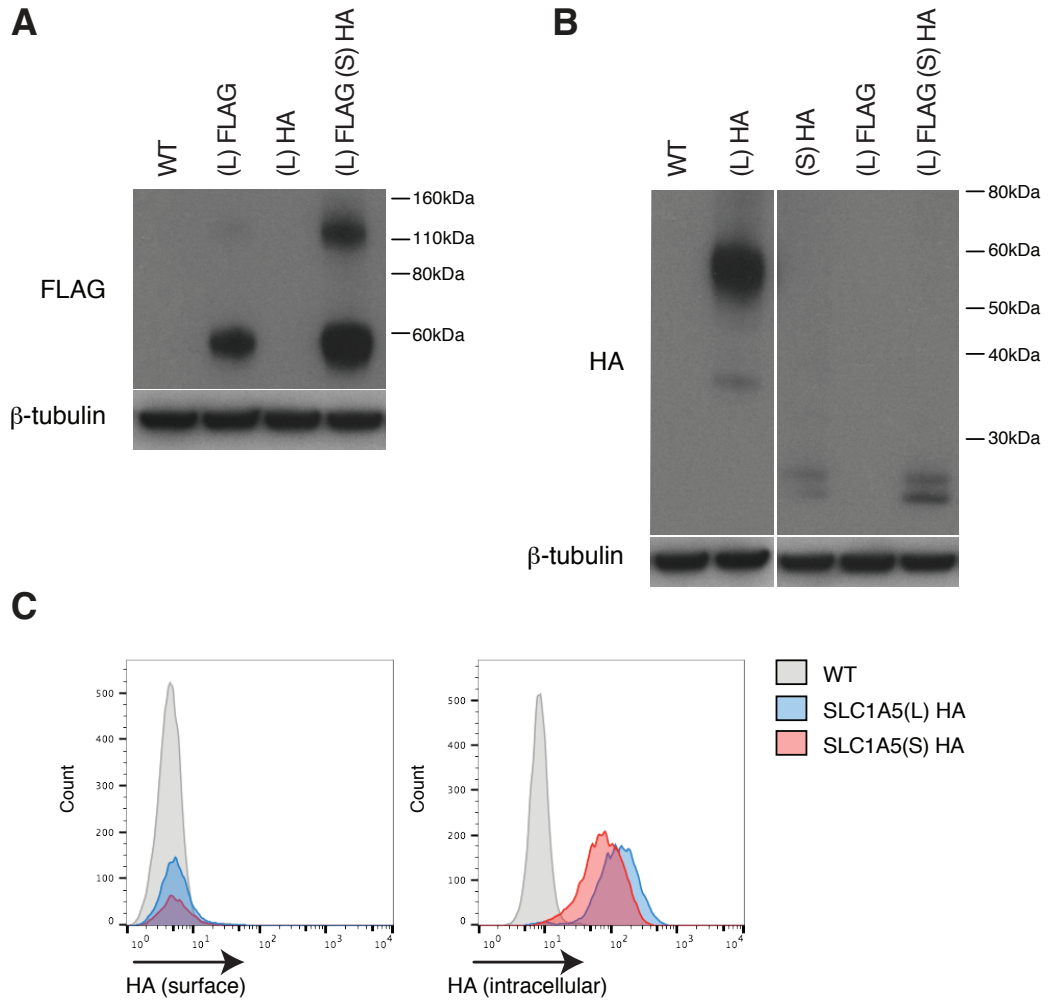

Figure 3-8. Confirmation of FLAG and HA expression in tumour cell lines expressing affinity-tagged SLC1A5(L) and/or SLC1A5(S)

(A-B) Total cell lysates obtained from untransduced WT HeLa cells, and WT HeLa cells transduced with a lentiviral vector encoding FLAG-tagged SLC1A5(L) with GFP ((L) FLAG), HA-tagged SLC1A5(L) with GFP ((L) HA), HA-tagged SLC1A5(S) with mCherry ((S) HA) or both FLAG-tagged SLC1A5(L) with GFP and HA-tagged SLC1A5(S) with mCherry ((L) FLAG (S) HA) were analysed by Western blotting with indicated antibodies. **(C)** Surface (left) and intracellular (right) anti-HA staining was performed on untransduced WT HeLa cells and WT HeLa cells transduced with a lentiviral vector encoding HA-tagged SLC1A5(L) with GFP or HA-tagged SLC1A5(S) with mCherry. Goat anti-rabbit IgG (H+L) Alexa Fluor® 647 was used as a secondary antibody. Samples were analysed by flow cytometry.

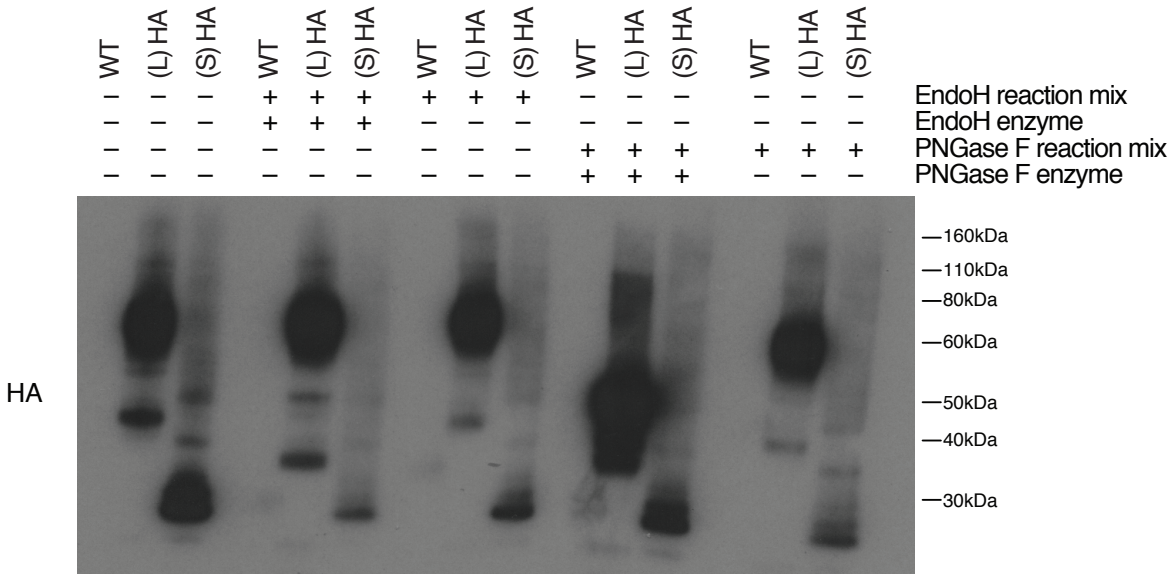

Figure 3-9. Determination of SLC1A5(L) and SLC1A5(S) protein sensitivity to EndoH- and PNGase F-mediated deglycosylation

Total cell lysates obtained from untransduced WT HeLa cells, and WT HeLa cells transduced with a lentiviral vector encoding HA-tagged SLC1A5(L) with GFP ((L) HA) or HA-tagged SLC1A5(S) with mCherry ((S) HA) were treated with EndoH reaction mix with (+) or without (-) EndoH enzyme, or PNGase F reaction mix with(+)/without(-) PNGase F enzyme, separated by SDS-PAGE and analysed by Western blotting with anti-HA antibody.

3.2.3. Evidence for SLC1A5(L) and SLC1A5(S) isoform physical interaction

To investigate the possibility of a physical interaction between the two isoforms, we used anti-FLAG antibody to immunoprecipitate the FLAG-tagged SLC1A5(L) and the associated proteins in lysates obtained from the double transfected FLAG-tagged SLC1A5(L) GFP HA-tagged SLC1A5(S) mCherry HeLa and, as a control, FLAG-tagged SLC1A5(L) GFP HeLa cells. We then analysed the anti-FLAG immunoprecipitate by Western blotting. As expected, the full-length SLC1A5 was present in the anti-FLAG immunoprecipitate obtained from FLAG-tagged SLC1A5(L) GFP HA-tagged SLC1A5(S) mCherry HeLa and FLAG-tagged SLC1A5(L) GFP HeLa but not WT HeLa cells **(Figure 3-10)**. Notably, blotting for HA revealed the presence of the HA-tagged SLC1A5(S) isoform (molecular weight of about 30kDa) in the anti-FLAG immunoprecipitate of double transfected HeLa cells. Immunoprecipitates from HeLa cells without HA-tagged SLC1A5(S), however, did not show any HA staining **(Figure 3-10)**. These results suggest that SLC1A5(S) physically associates with SLC1A5(L).

3.2.4. Subcellular localisation of SLC1A5(L) and SLC1A5(S) isoforms

We then took advantage of our affinity-tagged SLC1A5(L)- and SLC1A5(S)-overexpressing tumour cell lines to investigate the subcellular localisation of SLC1A5 isoforms using confocal microscopy. We optimised the anti-HA staining for this purpose, as described in Materials and Methods (Chapter 2.9). Staining of HA-tagged SLC1A5(L) GFP HeLa cells with anti-HA antibody revealed that SLC1A5(L) is found both at the cell surface and in intracellular compartments **(Figure 3-11)**. SLC1A5(S) on the other hand, showed increased staining in the cytosol and some at the cell surface, as determined by the anti-HA staining of HA-tagged SLC1A5(S) mCherry HeLa cells **(Figure 3-11)**.

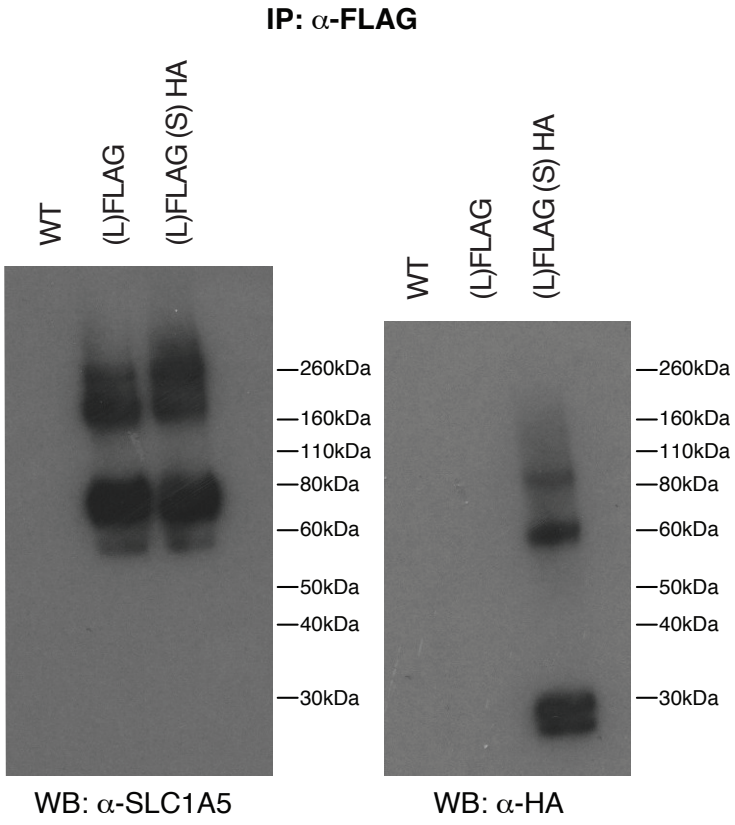

Figure 3-10. Anti-FLAG immunoprecipitation reveals physical association between SLC1A5(L) and SLC1A5(S) in tumour cell lines expressing affinity-tagged SLC1A5 isoforms

Anti-FLAG immunoprecipitation was performed on untransduced WT HeLa cells, and WT HeLa cells transduced with a lentiviral vector encoding FLAG-tagged SLC1A5(L) with GFP ((L) FLAG) or both FLAG-tagged SLC1A5(L) with GFP and HA-tagged SLC1A5(S) with mCherry ((L) FLAG (S) HA). The anti-FLAG immunoprecipitate was analysed by Western blotting with indicated antibodies.

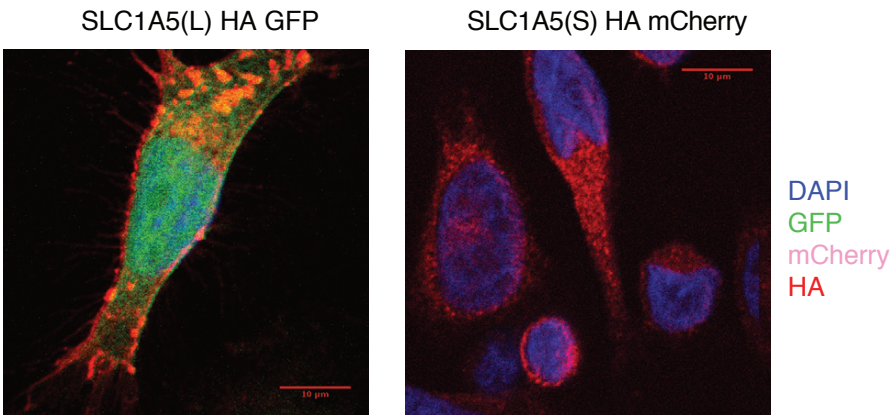

Figure 3-11. Subcellular localisation of the HA-tagged SLC1A5(L) and SLC1A5(S) isoforms in HeLa cells
WT HeLa cells transduced with a lentiviral vector encoding HA-tagged SLC1A5(L) with GFP (SLC1A5(L) HA GFP) or HA-tagged SLC1A5(S) with mCherry (SLC1A5(S) HA mCherry) were fixed, permeabilised, stained with rabbit anti-HA as a primary antibody and goat anti-rabbit IgG (H+L) Alexa Fluor® 647 as a secondary antibody, and DAPI. DAPI (shown in blue), GFP (shown in green), mCherry (shown in pink) and APC (shown in red) fluorescence was analysed using confocal imaging.

3.3. Functional implications of SLC1A5 isoform upregulation

3.3.1. SLC1A5-overexpressing tumour cells exhibit enhanced glutamine uptake capacity

We next set out to validate that tumour cells overexpressing SLC1A5 are able to upregulate their amino acid uptake. Since SLC1A5 has been reported to have high affinity for glutamine (Kekuda et al., 1996; Pingitore et al., 2013; Utsunomiya-Tate et al., 1996), we first examined the capacity of transduced cells to transport radiolabeled glutamine ([^{3}H]Gln). As expected, we observed higher levels of radiolabeled glutamine uptake in *SLC1A5(L)*-transduced tumour cells than in those expressing endogenous levels of this amino acid transporter **(Figure 3-12A)**. Notably, glutamine uptake capacity was also increased in tumour cells overexpressing SLC1A5(S) **(Figure 3-12A)**. Consistent with the reported Na^+-dependency of SLC1A5 (Kekuda et al., 1996; Utsunomiya-Tate et al., 1996),

SLC1A5(L)- and *SLC1A5(S)*-transduced tumour cells failed to upregulate glutamine uptake under Na^+-free conditions (data not shown). Furthermore, treatment of both transduced and control tumour cells with a characterised pharmacological inhibitor of SLC1A5 *O*-Benzyl-L-serine (BenSer) (Grewer and Grabsch, 2004; Wang et al., 2014) reduced glutamine uptake in a dose-dependent manner **(Figure 3-12A)**. Interestingly, IFNγ HeLa cells also exhibited increased glutamine uptake capacity **(Figure 3-12B)**, consistent with the upregulated levels of SLC1A5 observed in these cells **(Figures 3-2, 3-3, 3-6)**.

3.3.2. SLC1A5-overexpressing tumour cells exhibit enhanced tryptophan uptake capacity

Since we found SLC1A5 expression to be upregulated in the context of tryptophan degradation **(Figures 3-2, 3-3, 3-6)**, we next assessed the action of SLC1A5 on radiolabeled tryptophan ([^{3}H]Trp) uptake. Overexpression of SLC1A5(L), and particularly of SLC1A5(S) in HeLa cells, significantly improved their tryptophan uptake capacity **(Figure 3-13)**. Notably, tryptophan transport was also enhanced in IDO^+ HeLa cells **(Figure 3-13A)**. Conversely, pharmacological blockade of SLC1A5 with BenSer led to a dose-dependent reduction in radiolabeled tryptophan uptake in all cell types **(Figure 3-13B)**. In line with these results, BenSer treatment also reduced mTOR pathway activation in HeLa cells, as determined by the decreased phosphorylation of the S6 ribosomal protein (**Figure 3-14**).

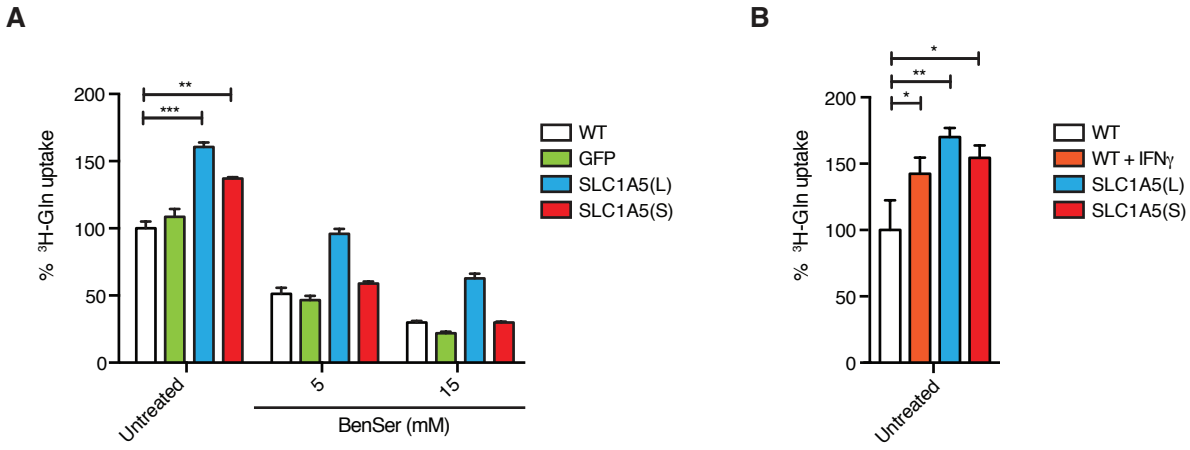

Figure 3-12. *SLC1A5(L)*- and *SLC1A5(S)*-transduced HeLa cells demonstrate improved glutamine transport

(A-B) [^{3}H]-glutamine uptake was performed in WT, IFNγ-treated WT, GFP-transduced, *SLC1A5(L)*-transduced and *SLC1A5(S)*-transduced HeLa cells over 10 min, in the presence or absence of indicated concentrations of SLC1A5 inhibitor BenSer. Bars represent the mean ± SEM.

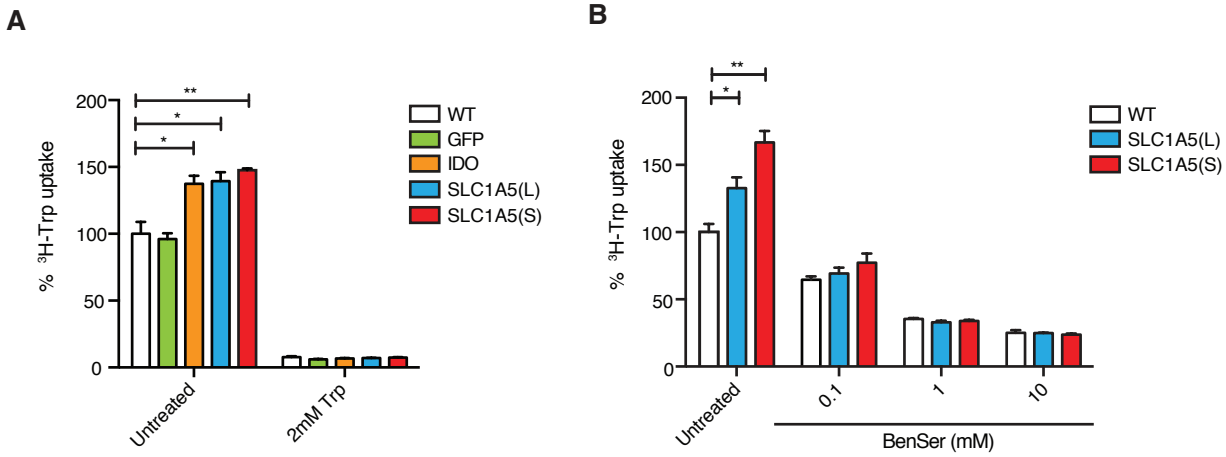

Figure 3-13. *SLC1A5(L)*- and *SLC1A5(S)*-transduced HeLa cells demonstrate improved tryptophan transport

[^{3}H]-tryptophan uptake was performed in WT, GFP-transduced, *IDO1*-transduced, *SLC1A5(L)*-transduced and *SLC1A5(S)*-transduced HeLa cells over 3 min, in the presence or absence of excess unlabeled tryptophan **(A)** or indicated concentrations of SLC1A5 inhibitor BenSer **(B)**. Bars represent the mean ± SEM.

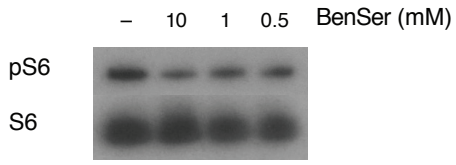

Figure 3-14. Treatment of tumour cells with SLC1A5 inhibitor BenSer reduces mTOR activation
WT HeLa cells were incubated in the presence of indicated concentrations of BenSer for 24h. Western blotting was performed with indicated antibodies.

3.3.2.1. Tryptophan uptake in HeLa cells depends on LAT1

Although not reported to transport tryptophan directly (Kekuda et al., 1996; Pingitore et al., 2013), SLC1A5 has been proposed to facilitate the activity of the dominant neutral amino acid transporter LAT1 (SLC7A5) (Kanai et al., 1998) via bidirectional transport, namely through provision of intracellular glutamine which can be used by LAT1 as an exchange substrate for EAA import (Nicklin et al., 2009). To determine the role of LAT1 in tryptophan uptake in tumour cells, we generated two LAT1$^{-/-}$ monoclonal HeLa cell lines using CRISPR-Cas9 technology. WT HeLa cells transduced with the pX330-EGFP-T2A-Neo plasmid targeting LAT1 acquired GFP fluorescence 24–48h after transduction **(Figure 3-15A)** and were single-cell sorted. The monoclones were then grown and screened for LAT1 knockout by Western blotting. As a result of screening, two monoclonal cell lines demonstrated ablated LAT1 expression **(Figure 3-15B)**, which we assessed for tryptophan uptake capacity. Notably, over 3 min, cell lines lacking LAT1 transported about 4 times less radiolabeled tryptophan than WT HeLa cells or CRISPR control HeLa cells **(Figure 3-15C)**. The difference in the tryptophan uptake capacity of LAT1-deficient and -sufficient HeLa cells became even greater when the assay time was extended from 3 to 10 min, as LAT$^{-/-}$ cell lines failed to further increase their tryptophan uptake, while WT and CRISPR control HeLa cells transported about 2 times more tryptophan over 10 min, as compared to

3 min **(Figure 3-15C)**. These findings clearly demonstrate that tryptophan uptake in HeLa cells is heavily dependent on LAT1 activity.

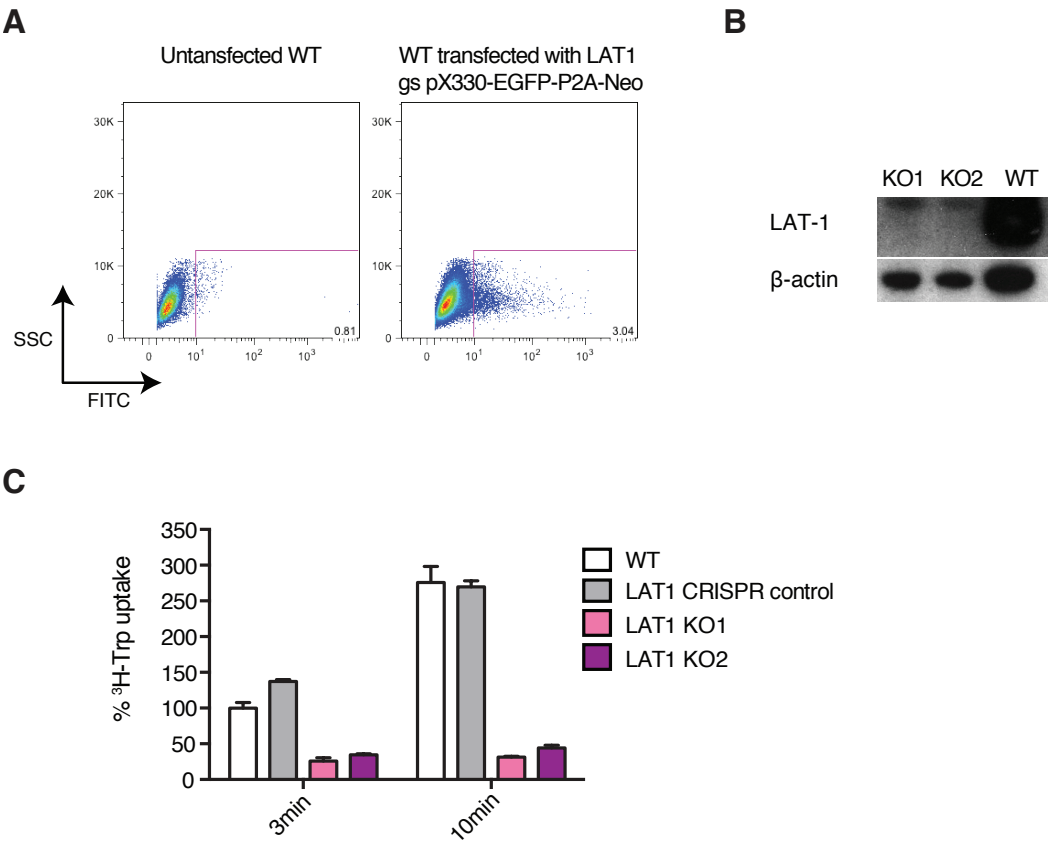

Figure 3-15. LAT1 knockout leads to impaired tryptophan uptake in tumour cells
(A) GFP fluorescence levels in WT HeLa cells 24h after transfection with pX330-EGFP-T2A-Neo targeting LAT1. **(B)** Generation of two monoclonal LAT1 knockout (KO) HeLa cell lines using CRISPR/Cas9 targeting LAT1. LAT1 CRISPR control cell line received Cas9 and LAT1-specific guide RNA but retained WT sequence. Western blotting was performed with indicated antibodies. **(C)** [^{3}H]-tryptophan uptake was measured in WT, LAT1 CRISPR control and LAT1 KO HeLa cells over 3 or 10 min. Bars represent the mean ± SEM.

3.3.3. SLC1A5 knockdown tumour cells demonstrate reduced cell proliferation under tryptophan-deficient conditions

To determine whether SLC1A5 confers tumour cells with a functional advantage under limited tryptophan conditions, we knocked down this amino acid transporter in HeLa cells using CRISPR-Cas9 lentivirus vector. WT HeLa cells successfully transduced with a lentiviral CRISPR construct containing Cas9, SLC1A5-targeting chimeric guide RNA and puromycin resistance gene were selected with 1μg/ml puromycin. Optimal puromycin concentration was determined based on puromycin killing curve **(Figure 3-16A)**. SLC1A5 knockdown HeLa cells demonstrated almost 50% reduction in SLC1A5 protein expression **(Figure 3-16B)**, which resulted in a significant impairment of cell proliferation under amino acid-sufficient conditions, as determined by the Ki67 proliferation marker intranuclear staining **(Figure 3-16C)**. Importantly, this effect was amplified even further following tryptophan withdrawal **(Figure 3-16C)**, highlighting the role of SLC1A5 in tumour cell proliferation under low tryptophan conditions.

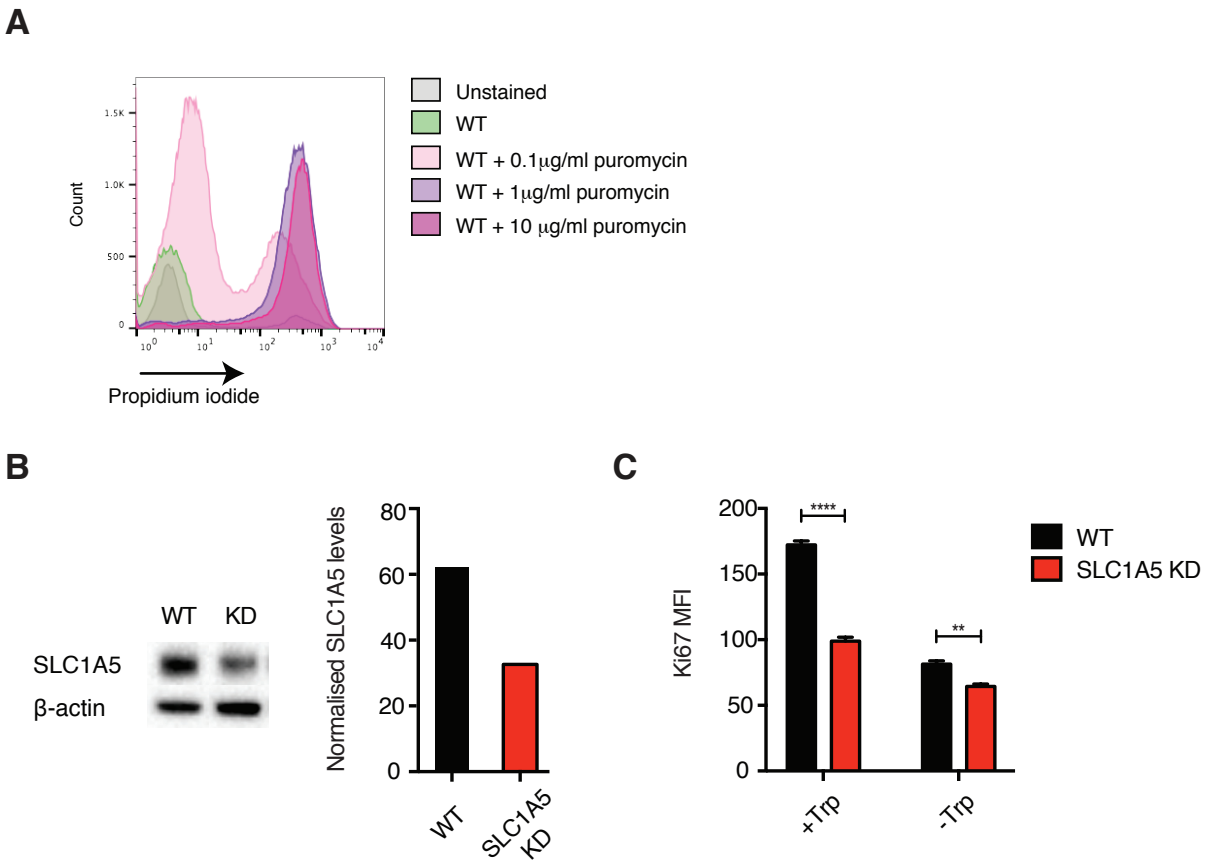

Figure 3-16. SLC1A5 knockdown tumour cells exhibit decreased proliferation in the absence of tryptophan

(A) WT HeLa cells were treated with indicated concentrations of puromycin for 48h. Propidium iodide staining was assessed by flow cytometry. **(B)** CRISPR/Cas9 targeting SLC1A5 was used to generate SLC1A5 knockdown (KD) HeLa cells. Western blotting was performed with indicated antibodies and protein levels were quantified by densitometry. **(C)** WT and SLC1A5 KD HeLa cells were incubated in tissue culture medium depleted of tryptophan for 48h. Ki67 expression was assessed by flow cytometry. Bars represent the mean ± SEM. MFI, mean fluorescence intensity.

3.4. Discussion

To study the mechanisms that allow IDO- and TDO-expressing tumour cells to withstand the effects of tryptophan starvation, we first established an *in vitro* system in which tryptophan-catabolising enzymes, induced either through stable gene overexpression or treatment with IFNγ, a known inducer of IDO, efficiently metabolised tryptophan into kynurenine in tissue culture medium. Using this system, we were able to assess the effect of tryptophan catabolism on tumour cell whole transcriptome profile using RNA-seq. The results of these experiments clearly demonstrated that IDO activity induces extensive remodeling of tumour cells' metabolism, amino acid biosynthesis and transport gene expression. In addition to changes in tryptophan starvation-associated genes, such as *WARS,* IDO^+ tumour cells exhibited vast alternations in glutamine/glutamate and monosaccharide metabolism genes, among others. Importantly, we observed a clear effect of IDO activity on SLC family member expression profile, with altered expression of several amino acid transporter-encoding genes, particularly *SLC7A11*, *SLC1A4* and *SLC1A5*, including two novel *SLC1A5* splice variants, which, to the best of our knowledge, have not been previously described. To further investigate the biological properties of the full-length SLC1A5 and its most truncated isoform, we overexpressed affinity-tagged SLC1A5(L) and SLC1A5(S) in tumour cells. This allowed us to demonstrate that the two SLC1A5 isoforms are resistant to EndoH enzymatic activity, which is indicative of their ability to migrate to the Golgi, where more complex glycan modifications occur. We also showed that SLC1A5(S), but not SLC1A5(L), remained resistant to PNGase F-mediated deglycosylation, which is consistent with the loss of the putative *N*-linked glycosylation sites in this truncated isoform. Although *N*-linked glycosylation of SLC1A5 is dispensable for its transport function (Scalise et al., 2014), it has been previously shown to facilitate trafficking to the cell membrane (Console et al., 2015). Consistent with these findings, we

observed reduced SLC1A5(S) localisation at the cell surface using confocal microscopy. However, it still remains unclear whether SLC1A5(S) localisation is modulated under conditions of amino acid starvation, and further experiments are needed to address this question. Furthermore, by performing pull-down assays on double transfected tumour cells co-expressing SLC1A5 isoforms tagged with different affinity tags, we were able to demonstrate that SLC1A5(S) physically interacts with the main isoform, possibly forming a hetero-oligomer. It is yet to be determined whether such complex formation has biological consequences, e.g. affecting SLC1A5 protein stability, and further studies in this area are warranted. Notably, SLC1A5(L) has been reported to form an oligomeric structure composed of two or three subunits similar to its homologue archaeal glutamate transporter Glt_{Ph} (Yernool et al., 2004). Hetero-oligomerisation has also been previously described for the EAAT3 (SLC1A1) and EAAT4 (SLC1A6) glutamate transporters of the SLC1 family, which can form hetero-trimers (Nothmann et al., 2011). However, this is the first report of the physical interaction between the SLC1A5 isoforms. Interestingly, SLC1A5 full-length protein has also been shown to associate with other transporters, including CD98hc (SLC3A2), LAT1 (SLC7A5) and MCT1 (SLC16A1) (Xu and Hemler, 2005), and it would be interesting to investigate whether the alternative SLC1A5 isoforms form part of such complexes.

Moreover, we have shown that upregulation of SLC1A5(L) and SLC1A5(S), in addition to enhancing the uptake of glutamine, improves tryptophan transport into tumour cells. In contrast to the described SLC1A1 isoforms of the SLC1 family, which have been reported to impede glutamate uptake from the main transporter (Porton et al., 2013), our results suggest that the alternative SLC1A5(S) isoform mimics the function of the full-length transporter. We also demonstrate that, similarly to glutamine and leucine (Wang et al., 2014), tryptophan transport in tumour cells is sensitive to SLC1A5 pharmacological

inhibitor BenSer. Since neither leucine nor tryptophan are high-affinity substrates for SLC1A5 (Kekuda et al., 1996; Pingitore et al., 2013; Utsunomiya-Tate et al., 1996), impaired uptake of these amino acids in the presence of BenSer, which is also reflected in reduced mTOR activation, is likely to be due to blockade of SLC1A5-dependent glutamine influx required for LAT1-mediated EAA import (Nicklin et al., 2009). Our results demonstrating that tryptophan uptake in HeLa cells is heavily dependent on LAT1 activity, as evidenced by the abolished radiolabeled tryptophan transport into tumour cells lacking LAT1, are consistent with this hypothesis. Of note, both SLC1A5 and LAT1 are commonly co-upregulated in human cancers (Fuchs and Bode, 2005), and the functional coupling of these amino acid transporters is also supported by the evidence of their physical interaction (Xu and Hemler, 2005). Thus, using the described bidirectional transport mechanism (Nicklin et al., 2009), IDO- and TDO-expressing tumours may be able to enhance LAT1-dependent tryptophan uptake by improving the intracellular availability of glutamine (the LAT1 exchange substrate) through upregulation of SLC1A5 isoforms.

Previous results have implicated SLC1A5 in promoting tumour cell growth and survival. The anti-proliferative effect of targeting SLC1A5 has been demonstrated in various tumour types, including hepatoma (Fuchs et al., 2007), lung cancer (Hassanein et al., 2013; Hassanein et al., 2015), acute myeloid leukemia (Willems et al., 2013), melanoma (Wang et al., 2014), neuroblastoma (Ren et al., 2015), colorectal cancer (Huang et al., 2014), prostate cancer (Wang et al., 2015a), breast cancer (van Geldermalsen et al., 2016) and multiple myeloma (Bolzoni et al., 2016). We have extended these findings by demonstrating a role for SLC1A5 in tumour cell proliferation not only under amino acid-sufficient but also tryptophan starvation conditions. These results are of importance, as they suggest that SLC1A5-mediated amino acid uptake acts as a compensatory mechanism to facilitate proliferation of IDO- and TDO-expressing cancer cells under low tryptophan conditions.

Collectively, our findings demonstrate for the first time the association between tryptophan catabolism and modulation of the amino acid transporter profiling in tumour cells, and show that increased expression levels of SLC1A5 isoforms lead to improved transport of glutamine and tryptophan into tumour cells.

CHAPTER 4: Regulation of SLC1A5 expression in tumour cells

4.1. The effect of amino acid starvation and kynurenine accumulation on SLC1A5 expression in tumour cells

4.1.1. Tryptophan deprivation induces SLC1A5 expression in tumour cells

We next set out to determine the mechanisms regulating the upregulation of SLC1A5 in tumour cells expressing tryptophan-catabolising enzymes. Since IDO and TDO enzymatic activity converts tryptophan into kynurenine **(Figure 3-1B)**, we speculated that the enhanced expression of SLC1A5 in IDO^+ and TDO^+ tumour cells could be accounted for by the reduced concentration of tryptophan in the culture medium. To investigate this possibility, we incubated WT HeLa cells, exhibiting no IDO or TDO activity **(Figure 3-1B)**, in the culture medium depleted of tryptophan. The latter was formulated using dialysed FBS, containing approximately 3.5 times less tryptophan than conventional FBS, as determined by HPLC **(Figure 4-1)**. As a control, we also showed that tryptophan was virtually undetectable in the unsupplemented tryptophan-depleted medium, and present in minute amounts (at the concentration of about 0.5μM) in complete tryptophan-depleted medium supplemented with 10% dialysed FBS, compared to almost 20μM in conventional culture medium supplemented with 10% normal FBS **(Figure 4-1)**. WT HeLa cells deprived of tryptophan for 72h strongly upregulated both *SLC1A5(L)* and *SLC1A5(S)* transcription **(Figure 4-2A)**. Importantly, this effect was abrogated when tryptophan-depleted medium was supplemented with 25μM or 10μM tryptophan **(Figure 4-2A)**. Tryptophan deprivation also induced the expression of the full-length SLC1A5 at the protein level **(Figure 4-2B)**. This effect was observable at concentrations of tryptophan

equal to or below 5μM, and was abolished at the concentration of 10μM **(Figure 4-2B)**, consistent with the quantitative PCR results **(Figure 4-2A)**. We then extended the results obtained in HeLa cells to a panel of other human tumour cell lines, including epidermoid carcinoma, prostate and pancreas cancer cell lines, which increased SLC1A5 expression to different extents. The highest upregulation in tryptophan-depleted medium was observed in HeLa (6.6-fold), DU145 (5-fold) and HPAF (3.7-fold) cell lines **(Figure 4-3A)**. Interestingly, when comparing different human tumour cell lines, we observed a degree of variability in SLC1A5 SDS mobility, which is likely to be accounted for by different levels of glycosylation, as treatment of cell lysates with the deglycosylating enzyme PNGase F abolished this variability (**Figure 4-3B**).

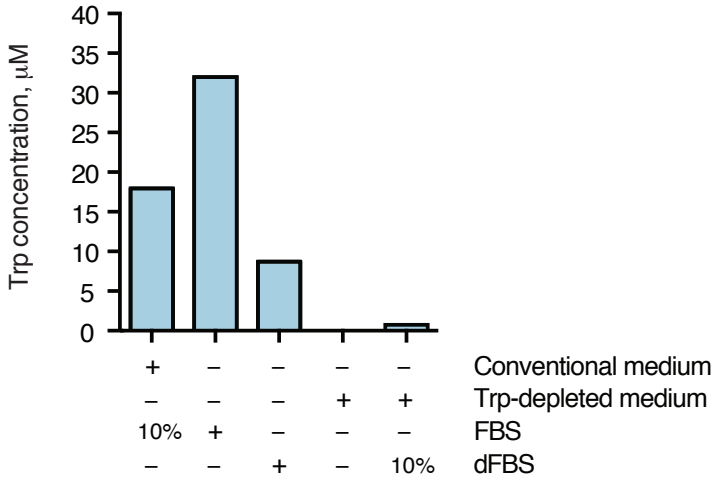

Figure 4-1. Tryptophan is present in minute amounts in the tryptophan-depleted medium supplemented with dialysed FBS

Tryptophan concentrations were measured by HPLC in FBS, dialysed FBS (dFBS), conventional medium supplemented with 10% FBS, tryptophan depleted medium and tryptophan depleted medium supplemented with 10% dFBS.

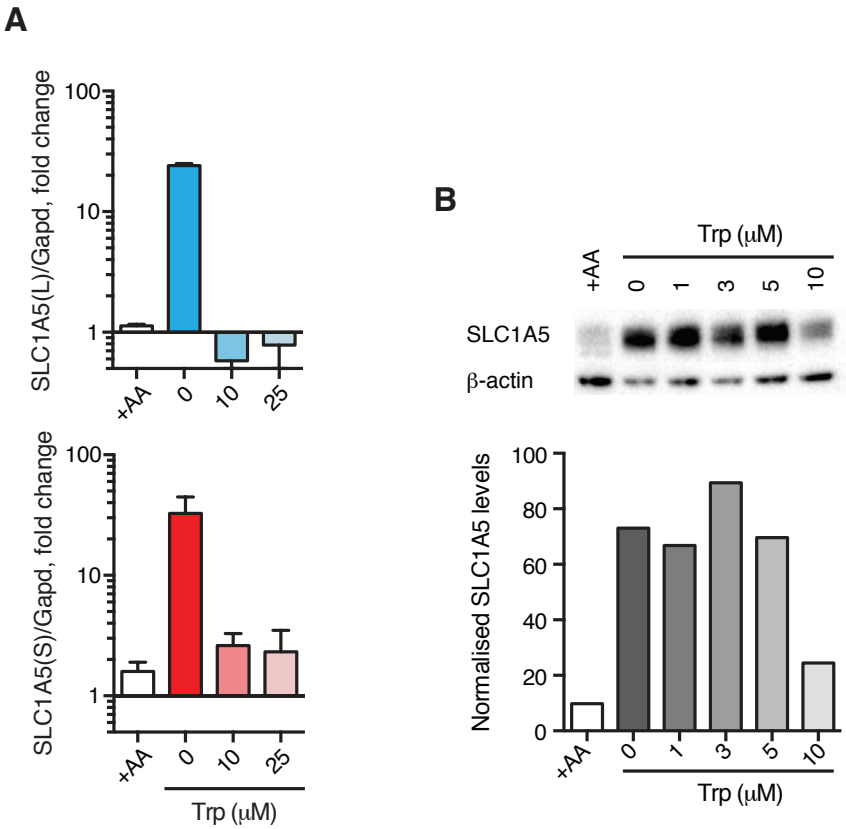

Figure 4-2. SLC1A5 expression is induced in tumour cells cultured under low tryptophan conditions

(A) WT HeLa cells were incubated in tissue culture medium containing indicated concentrations of tryptophan for 72h. *SLC1A5(L)* and *SLC1A5(S)* mRNA expression levels were analysed by quantitative PCR, and are shown as fold change in expression relative to *Gapd*. Bars represent the mean ± SEM. **(B)** WT HeLa cells were incubated in tissue culture medium containing indicated concentrations of tryptophan for 48h. Western blotting was performed with indicated antibodies and protein levels were quantified by densitometry.

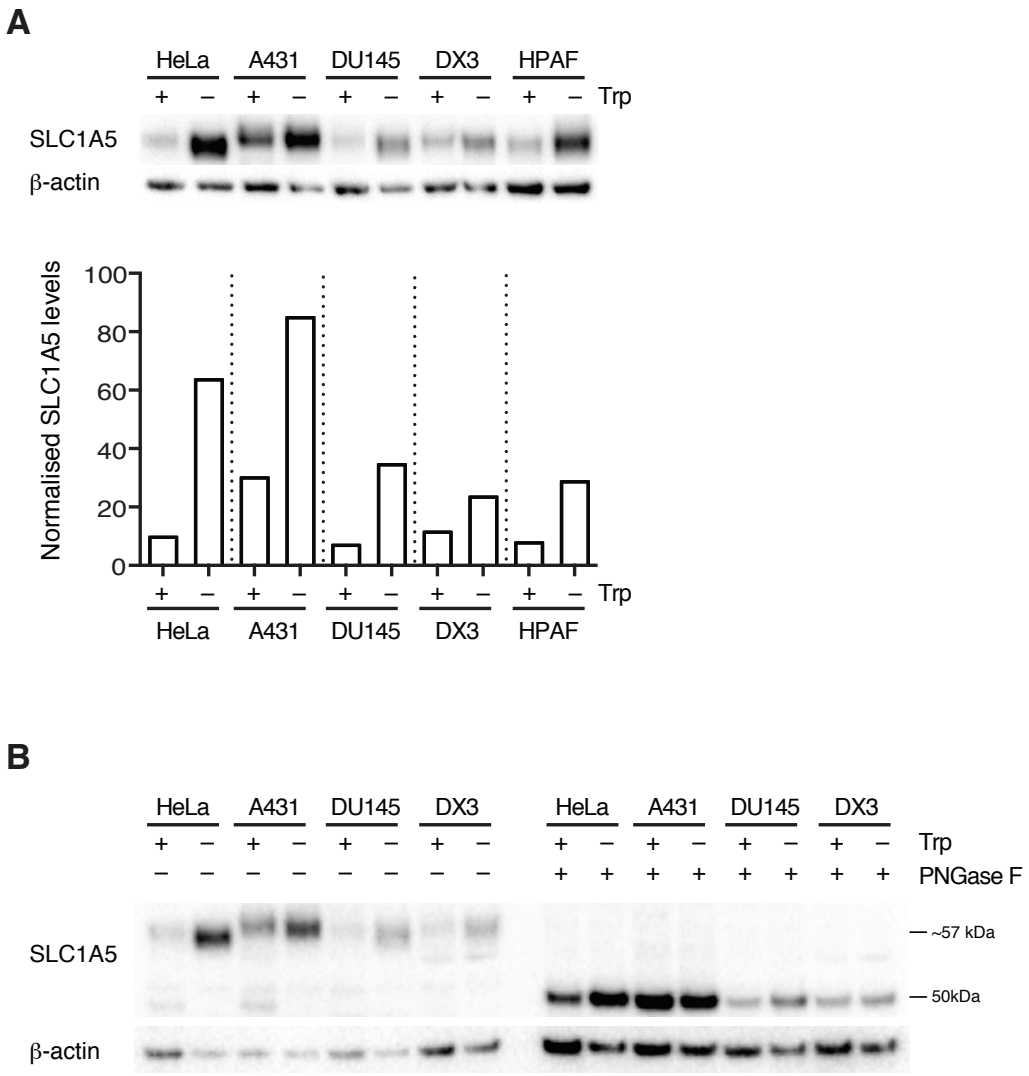

Figure 4-3. Tryptophan depletion upregulates SLC1A5 expression in a panel of IDO negative tumour cell lines

(A) HeLa, A431, DU145, DX3 and HPAF tumour cell lines were incubated in tissue culture medium depleted of tryptophan for 72h. Western blotting was performed with indicated antibodies and protein levels were quantified by densitometry. **(B)** Total cell lysates obtained from HeLa, A431, DU145 and DX3 tumour cell lines cultured in tissue culture medium depleted of tryptophan for 72h were treated with PNGase F enzyme, separated by SDS-PAGE and analysed by Western blotting with indicated antibodies.

4.1.1.1. Tryptophan deprivation modulates the expression of several amino acid transporters in tumour cells

To assess whether tryptophan depletion has a more general effect on amino acid transporter profiling in tumour cells, we tested the sensitivity of SLC7A11 and SLC1A4 transporters, which showed enhanced expression in IDO^+ and TDO^+ tumour cells **(Figures 3-2B, 3-3, 3-6A)**, to tryptophan depletion. Notably, WT HeLa cells incubated in tryptophan-depleted medium, in addition to upregulation of SLC1A5 **(Figures 4-2, 4-3)**, also increased the expression of *SLC7A11* and *SLC1A4* transcripts **(Figure 4-4)**. These results are consistent with the upregulation of these amino acid transporters in the presence of tryptophan-catabolising enzymes **(Figures 3-2B, 3-3, 3-6A)**.

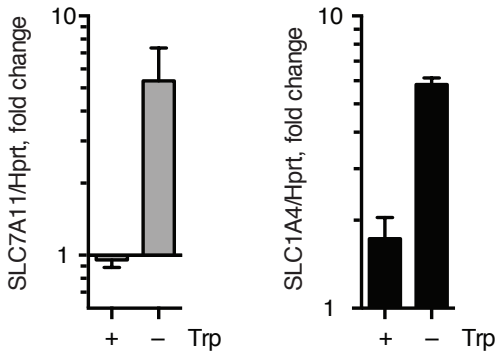

Figure 4-4. Tryptophan depletion upregulates SLC7A11 and SLC1A4 expression in tumour cells
WT HeLa cells were incubated in tissue culture medium depleted of tryptophan for 72h. *SLC7A11* and *SLC1A4* mRNA expression levels were analysed by quantitative PCR, and are shown as fold change in expression relative to *Hprt*. Bars represent the mean ± SEM.

4.1.2. SLC1A5 expression in tumour cells is unaffected by AhR agonists kynurenine and FICZ

IDO and TDO enzymatic activity not only reduces the concentration of tryptophan but also leads to accumulation of tryptophan metabolite kynurenine **(Figure 3-1B)**, which has been identified as an endogenous ligand of AhR (Opitz et al., 2011). Kynurenine has been shown to mediate several of its immunosuppressive effects through activation of AhR (Opitz et al., 2011), so we decided to investigate whether exposure of tumour cells to AhR ligands modulates their SLC1A5 expression. To test this possibility, we exposed WT HeLa cells to increasing concentrations of AhR agonists kynurenine and 6-formylindolo[3,2-*b*]carbazole (FICZ), or to tryptophan-deficient conditions, as a control, and measured their SLC1A5 expression by Western blotting. While tryptophan deprivation induced an almost 8-fold SLC1A5 upregulation, AhR agonists had no effect on the levels of SLC1A5 expression in WT HeLa cells (**Figure 4-5)**.

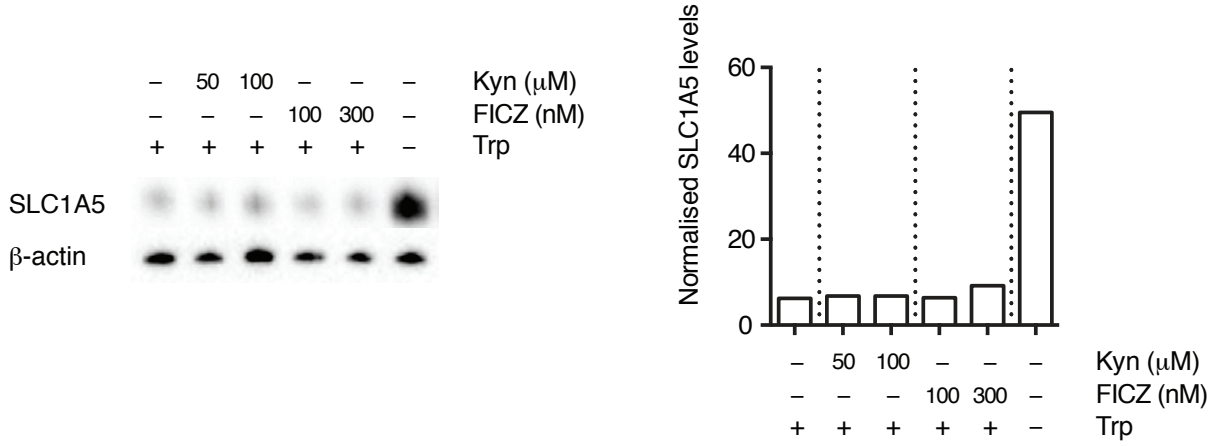

Figure 4-5. The effect of AhR agonists on SLC1A5 expression in tumour cells
WT HeLa cells were incubated in tissue culture medium depleted of tryptophan or treated with indicated concentrations of kynurenine (Kyn) or 6-formylindolo[3,2-*b*]carbazole (FICZ) for 72h. Western blotting was performed with indicated antibodies and protein levels were quantified by densitometry.

4.1.3. Differential modulation of SLC1A5 expression by the absence of distinct amino acids

Having established that shortage of tryptophan can upregulate SLC1A5, we decided to extend these results by assessing whether the lack of other amino acids could also have an effect on this transporter's expression in tumour cells. Interestingly, we found that SLC1A5 expression is differentially modulated by the deprivation of specific amino acids. Although lack of tryptophan was the most potent inducer of SLC1A5 out of the amino acids tested, incubation of WT HeLa cells in the culture medium depleted of glutamine or arginine also markedly increased their SLC1A5 expression (**Figure 4-6**). This transporter's expression was also sensitive to the extracellular concentrations of leucine and isoleucine. However, SLC1A5 induction in the absence of these EAAs was not as profound as in the absence of tryptophan (**Figure 4-6**). Notably, not all amino acids were able to induce SLC1A5 expression, as glycine or serine deprivation exerted no substantial effect on SLC1A5 levels in HeLa cells (**Figure 4-6**).

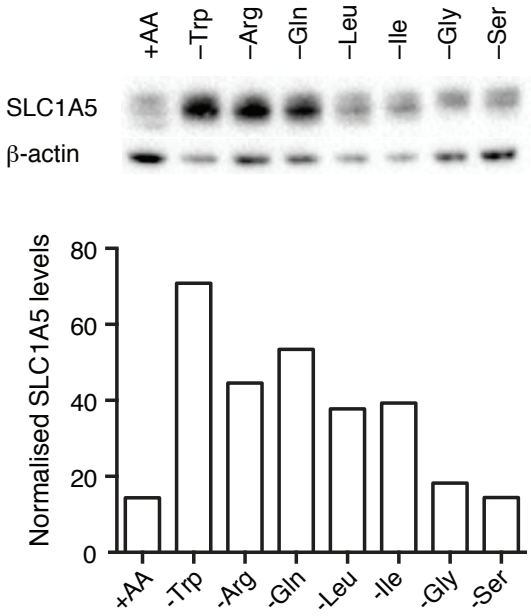

Figure 4-6. SLC1A5 expression is induced in tumour cells starved of specific amino acids

WT HeLa cells were incubated in tissue culture medium depleted of indicated amino acids for 48h. Western blotting was performed with indicated antibodies and protein levels were quantified by densitometry.

4.1.4. Kinetic of SLC1A5 upregulation under tryptophan- and glutamine-deficient conditions

To further characterise the sensitivity of SLC1A5 expression to tryptophan and glutamine withdrawal, we performed time-course experiments using tryptophan- and glutamine-depleted media. The results of these experiments demonstrated that, while 24h incubation in tryptophan-depleted medium induced some SLC1A5 upregulation in WT HeLa cells, it was more profound after 48h of tryptophan withdrawal, and peaked at 72h **(Figure 4-7A)**. We observed a similar time-dependent increase in SLC1A5 levels in WT HeLa cells cultured in the absence of glutamine, however, the difference between the 48h and 72h time points was more substantial under these conditions **(Figure 4-7B)**. We then asked whether SLC1A5 expression, enhanced following tryptophan or glutamine deprivation, could be brought back to its basal levels by re-supplementation of the missing amino acid. To test this possibility, we exposed WT HeLa cells to tryptophan- or glutamine-deficient conditions for 48h, and re-supplemented tryptophan or glutamine, respectively, for another 24h **(Figure 4-7)**. Although re-supplementation of tryptophan reduced SLC1A5 expression, it failed to downregulate it to the basal levels observed in unstarved HeLa cells **(Figure 4-7A)**, while 24h incubation was insufficient for re-added glutamine to bring down SLC1A5 upregulation triggered by glutamine starvation **(Figure 4-7B)**.

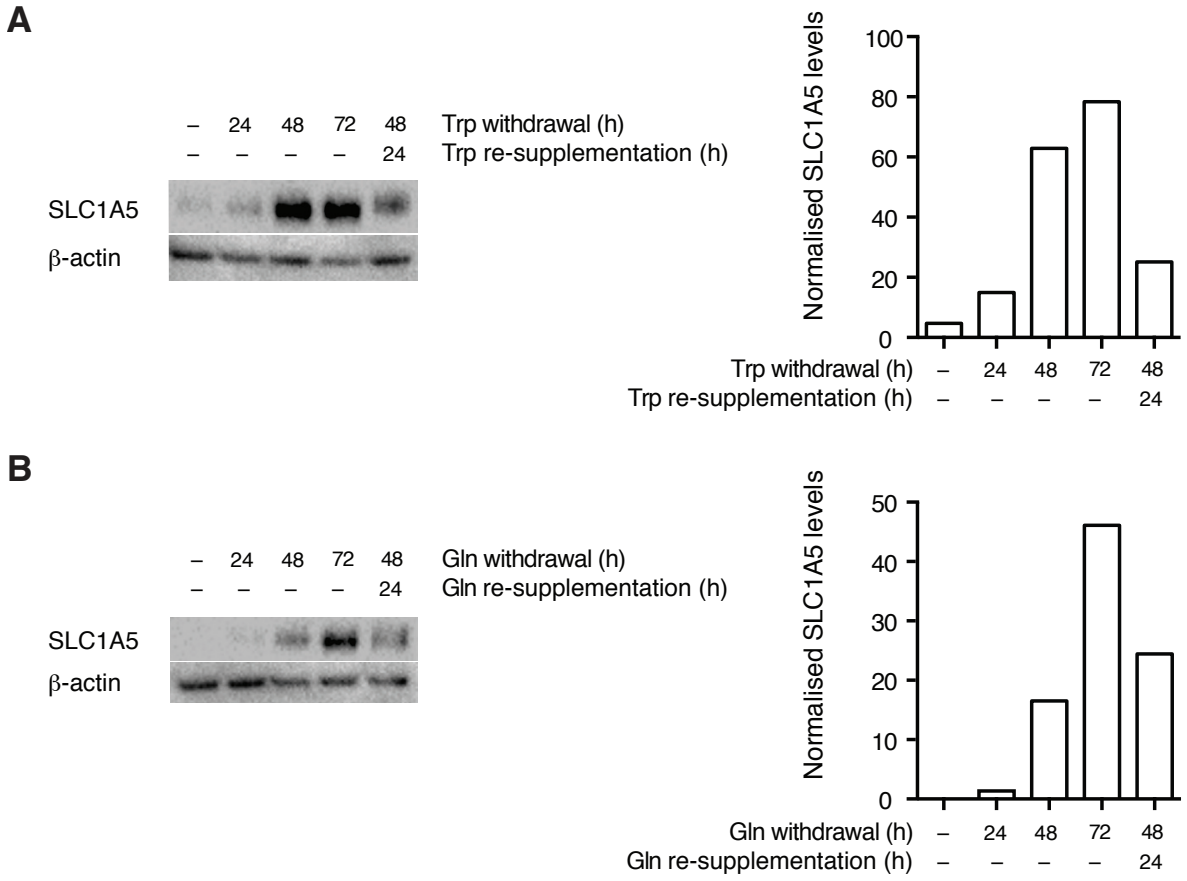

Figure 4-7. Kinetic of SLC1A5 expression in tryptophan- and glutamine-starved HeLa cells

WT HeLa cells were incubated in tissue culture medium depleted of tryptophan **(A)** or glutamine **(B)** for the time periods indicated. Where applicable, tryptophan **(A)** or glutamine **(B)** was re-supplemented into tissue culture medium for 24h following 48h tryptophan **(A)** or glutamine **(B)** withdrawal. Western blotting was performed with indicated antibodies and protein levels were quantified by densitometry. h, hours.

4.2. The role of the ATF4 pathway in tryptophan shortage-induced amino acid transporter reprogramming

4.2.1. IDO- and TDO-expressing tumour cells show evidence of ATF4 pathway activation

We next assessed the possible mechanisms that may account for the induction of SLC1A5 during tryptophan starvation. Amino acid depletion is sensed by the ATF4 pathway, which can be activated in response to increased levels of uncharged tRNA (Harding et al., 2000a; Harding et al., 2003). We interrogated our RNA-seq data for changes in the expression of stress response genes in IDO^+ tumour cells, and observed a strong transcriptional signature associated with ATF4 pathway activation, as evidenced by the upregulation of *ATF4, ATF3, CHOP, GADD34, TRIB3* and *HERPUD1* genes in IFNγ-treated WT and *IDO1*-transduced HeLa cells (**Figure 4-8**). In line with this gene expression analysis, ATF4 protein expression was enhanced in IFNγ-treated WT, *IDO1*- and *TDO2*-transduced HeLa cells, while it was virtually undetectable in untreated WT and GFP-transduced tumour cells **(Figure 4-9)** exhibiting no tryptophan-catabolising activity **(Figure 3-1B)**.

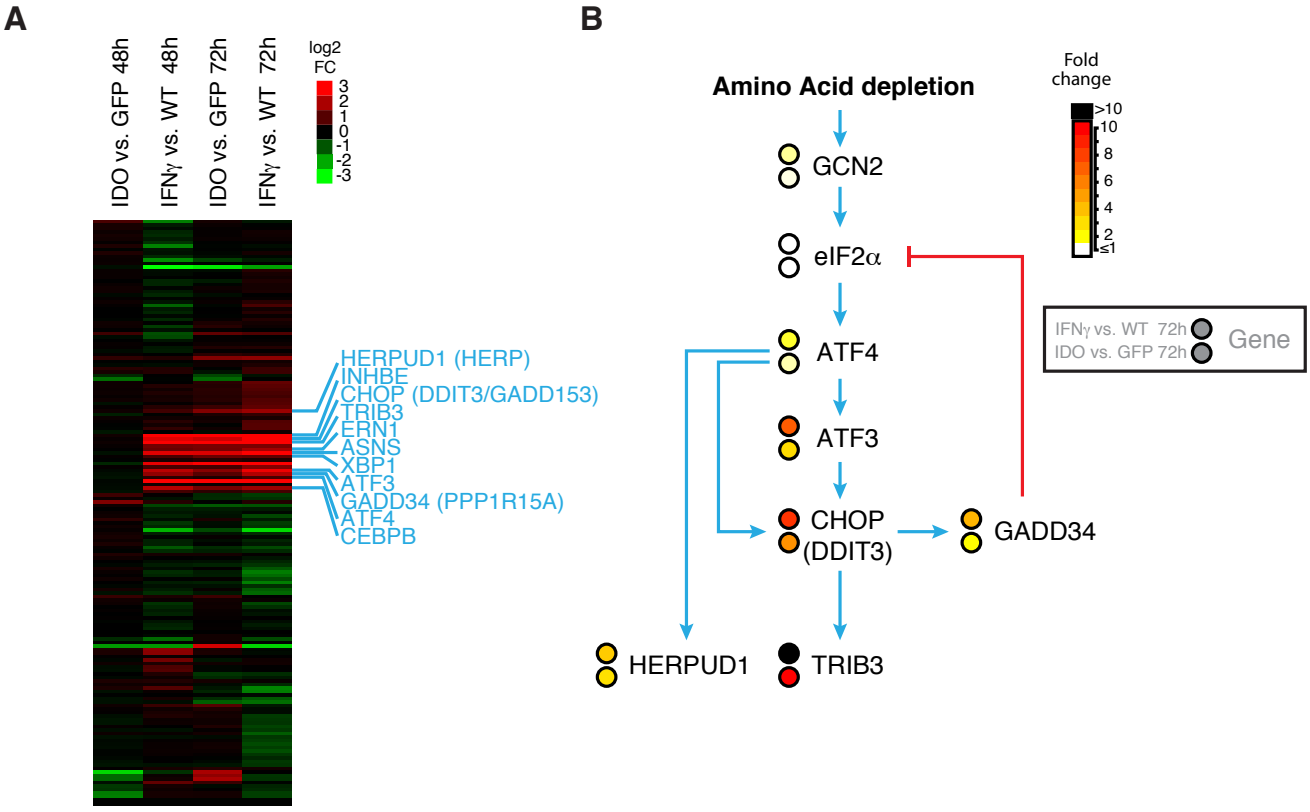

Figure 4-8. Activation of the ATF4 pathway genes in IDO-expressing tumour cells
(A) RNA-seq transcriptome profiles of the integrated stress response genes in *IDO1*-transduced vs GFP-transduced and IFNγ-treated vs untreated WT HeLa cells cultured for 48h or 72h. The hierarchical clustering of genes was performed using Gene-E package, with distance determined by the Pearson correlation coefficient. **(B)** Fold change in the expression of indicated genes in IFNγ-treated vs untreated WT HeLa cells cultured for 72h (top circles) and in *IDO1*-transduced vs GFP-transduced HeLa cells cultured for 72h (bottom circles), as indicated in the legend box on the right.

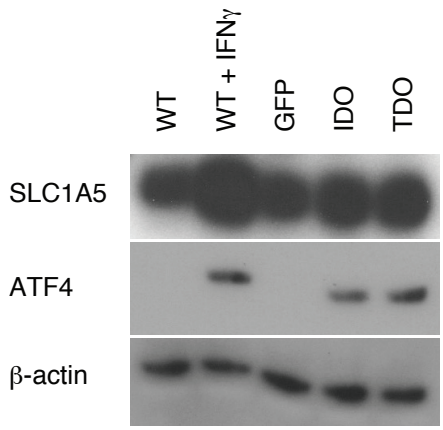

Figure 4-9. IDO- and TDO-expressing tumour cells exhibit ATF4 protein activation
WT, IFNγ-treated, GFP-transduced, *IDO1*-transduced and *TDO2*-transduced HeLa cells were cultured for 72h. Western blotting was performed with indicated antibodies.

4.2.2. ATF4 mirrors SLC1A5 expression under specific amino acid starvation conditions

To investigate whether ATF4 expression is differentially modulated by the absence of distinct amino acids, we measured ATF4 levels in WT HeLa cells cultured under various amino acid-deprived conditions. While ATF4 protein was almost undetectable in complete medium, its expression increased markedly in tumour cells cultured in the absence of tryptophan, glutamine, and, to a lesser extent, arginine and isoleucine **(Figure 4-10A)**. Lack of glycine and serine, on the other hand, failed to activate ATF4 in HeLa cells **(Figure 4-10A)**, analogous to SLC1A5 protein expression pattern **(Figure 4-6)**. ATF4 also mirrored SLC1A5 expression in tryptophan titration experiments. Similarly to SLC1A5 **(Figure 4-2B)**, the expression of this transcription factor was induced by concentrations of tryptophan lower than 5μM, as ATF4 could not be detected after supplementing the culture medium with 10μM tryptophan (**Figure 4-10B**).

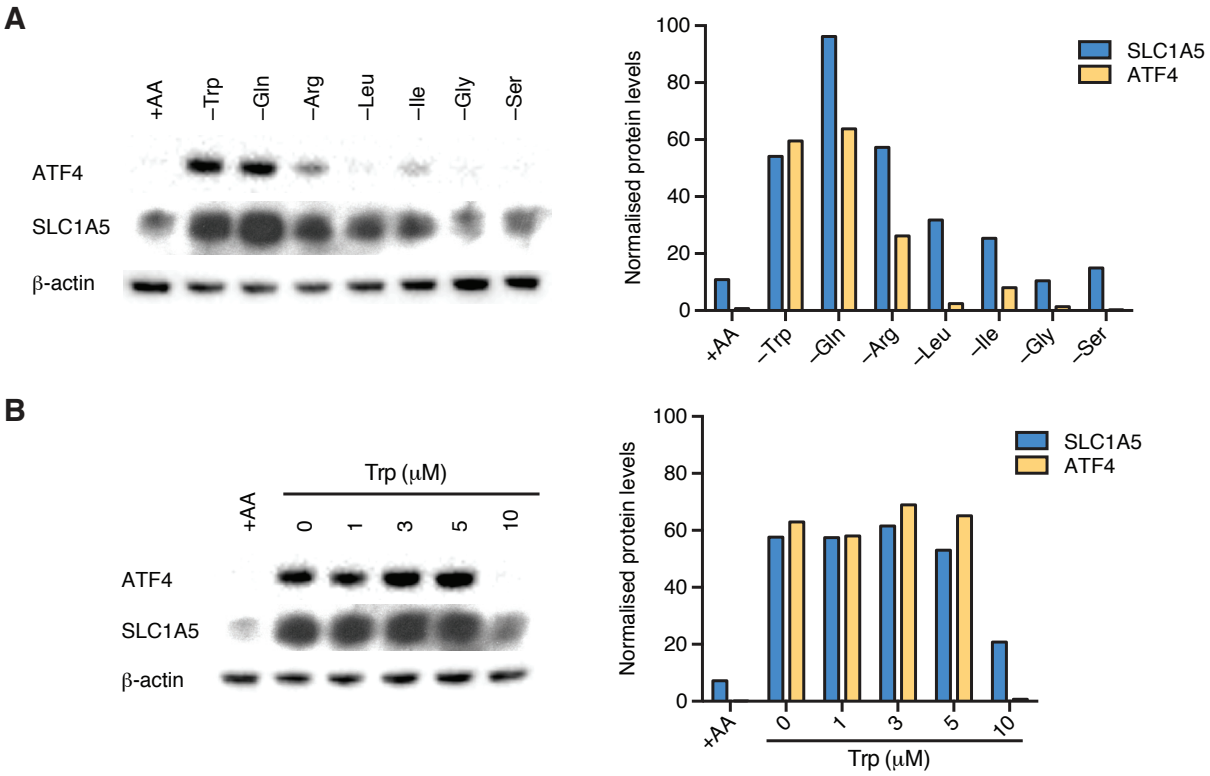

Figure 4-10. ATF4 mirrors SLC1A5 expression in tumour cells starved of tryptophan and other amino acids

WT HeLa cells were incubated in tissue culture medium depleted of indicated amino acids **(A)** or in the presence of indicated tryptophan concentrations **(B)** for 48h. Western blotting was performed with indicated antibodies and protein levels were quantified by densitometry.

4.2.3. GCN2 knockdown in tumour cells leads to impaired but not abolished SLC1A5 upregulation in the absence of tryptophan

Our observations that ATF4, in addition to being activated in IDO- and TDO-expressing tumour cells, mirrors SLC1A5 expression under tryptophan deprivation conditions proposed ATF4 pathway as a candidate regulator of SLC1A5 expression in tumour cells. Since GCN2 acts as the main eIF2α kinase activating ATF4 in response to amino acid deficiency (Dong et al., 2000; Wek et al., 1995), we decided to knock down GCN2 in tumour cells. Using GCN2 shRNA knockdown strategy, we achieved similar transduction efficiency with lentiviral supernatant and concentrated lentivirus **(Figure 4-11A)**. As a control, we also transduced WT HeLa cells with a lentivirus encoding non-target shRNA that targets no known mammalian genes. As expected, HeLa cells receiving control shRNA retained normal GCN2 expression levels **(Figure 4-11A)**. To measure SLC1A5 expression on the cell surface, we used the previously characterised SLC1A5-specific staining reagent RD114-RBD mFc (Laval et al., 2013), which utilises the binding specificity of the RD114 virus envelope glycoprotein for this amino acid transporter (Rasko et al., 1999; Tailor et al., 1999). Of note, the RD114-RBD mFc only detects the SLC1A5(L) isoform, as the extracellular loop 2, which is lost in the truncated isoforms **(Figure 3-5B)**, has been shown to be critical for RD114 virus binding (Marin et al., 2003; Rasko et al., 1999; Shimode et al., 2013). Using RD114-RBD mFc staining, we then assessed the ability of GCN2 knockdown HeLa cells to modulate SLC1A5 expression following tryptophan withdrawal. While the untreated WT and shRNA control-receiving HeLa cells readily enhanced SLC1A5 expression when cultured in tryptophan-depleted medium, GCN2 knockdown HeLa cells exhibited a partially reduced but not abrogated ability to upregulate SLC1A5 under these conditions **(Figure 4-11B)**.

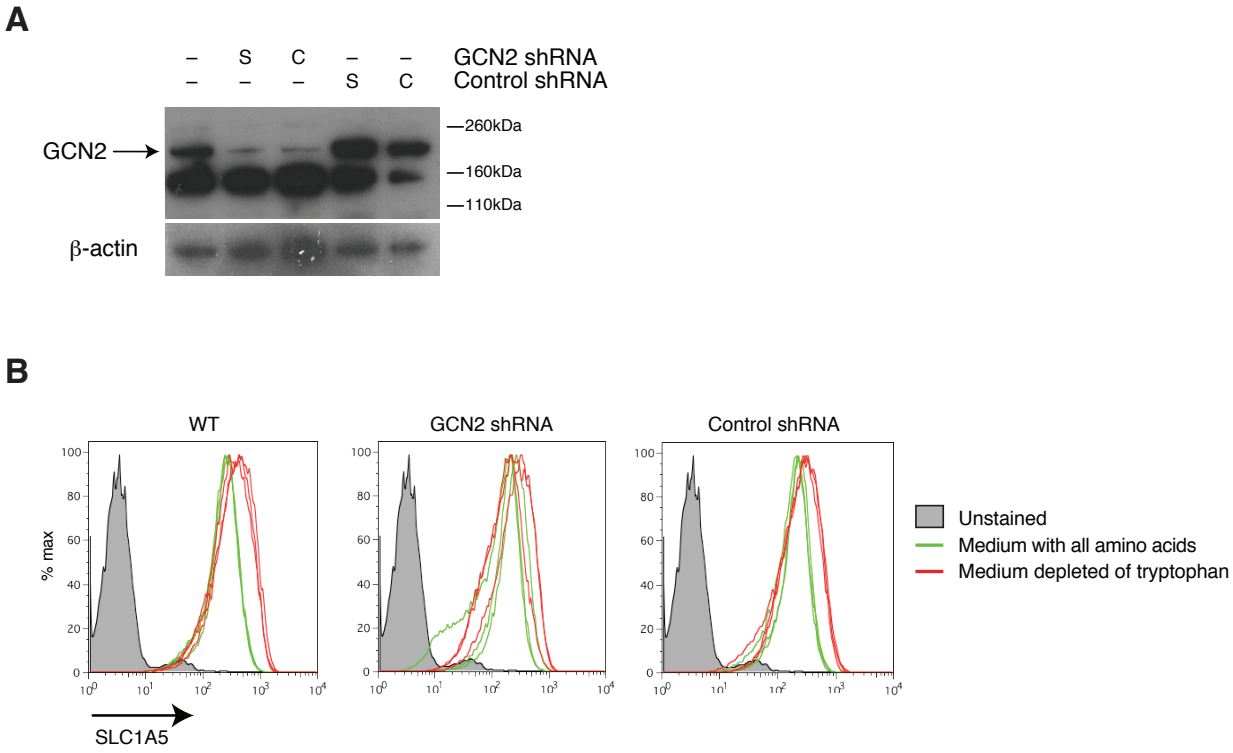

Figure 4-11. The effect of GCN2 knockdown on SLC1A5 expression in tumour cells starved of tryptophan

(A) WT HeLa cells were transduced with lentiviral supernatant (S) or concentrated lentivirus (C) encoding either GCN2-targeting shRNA or control shRNA. Transduced HeLa cells were selected with 1μg/ml puromycin. Total cell lysates obtained from WT, GCN2 shRNA- and control shRNA-transduced HeLa cells were analysed by Western blotting with indicated antibodies. The expected molecular weight of GCN2 band is 220kDa (indicated by arrow). **(B)** WT, GCN2 shRNA- and control shRNA-transduced HeLa cells were incubated in complete tissue culture medium (shown in green) or tissue culture medium depleted of tryptophan (shown in red) for 72h, in triplicate. SLC1A5 cell surface expression was assessed by flow cytometry using RD114-RBD mFc staining.

4.2.4. SLC1A5 upregulation in tryptophan-starved tumour cells is dependent on ATF4

Due to the ambiguous results observed in GCN2 knockdown HeLa cells, we decided to dissect the role of the ATF4 pathway in regulation of SLC1A5 expression under tryptophan-deficient conditions by directly targeting ATF4, rather than its upstream activators, with a lentiviral CRISPR construct. We confirmed the knockdown of ATF4 by incubating HeLa cells transduced with Cas9 and ATF4-targeting chimeric guide RNA in tryptophan-depleted medium. In sharp contrast to WT HeLa, ATF4 knockdown HeLa cells failed to efficiently express ATF4 in the absence of tryptophan, which was paralleled by complete abrogation of SLC1A5 upregulation under these conditions **(Figure 4-12)**. We also confirmed these results using ATF4 shRNA knockdown strategy, which yielded similar knockdown efficiency **(Figure 4-13)**. ATF4 shRNA knockdown HeLa cells, similarly to ATF4 CRISPR knockdown cells, showed comparable levels of SLC1A5 expression under tryptophan-sufficient and -deficient conditions, unlike untransduced WT HeLa or HeLa cells receiving control shRNA **(Figure 4-13)**. Of note, in contrast to ATF4 knockdown HeLa, GCN2 knockdown HeLa cells still exhibited considerable levels of ATF4 activation in tryptophan-depleted medium **(Figure 4-14)**, which could explain the lack of complete loss of SLC1A5 upregulation in these cells **(Figures 4-11B, 4-14)**. Furthermore, in addition to the main transcript, *SLC1A5(L)*, ATF4 knockdown tumour cells failed to upregulate the transcription of truncated SLC1A5 isoforms *SLC1A5(S)* and *SLC1A5(M)* following tryptophan withdrawal **(Figure 4-15A)**. Finally, we tested whether expression of other amino acid transporters sensitive to tryptophan depletion, SLC7A11 and SLC1A4 **(Figure 4-4)**, is also dependent on ATF4. Similarly to *SLC1A5* transcripts, upregulation of *SLC7A11* and *SLC1A4* in tryptophan-depleted medium was abolished following knockdown of ATF4 **(Figure 4-15B)**.

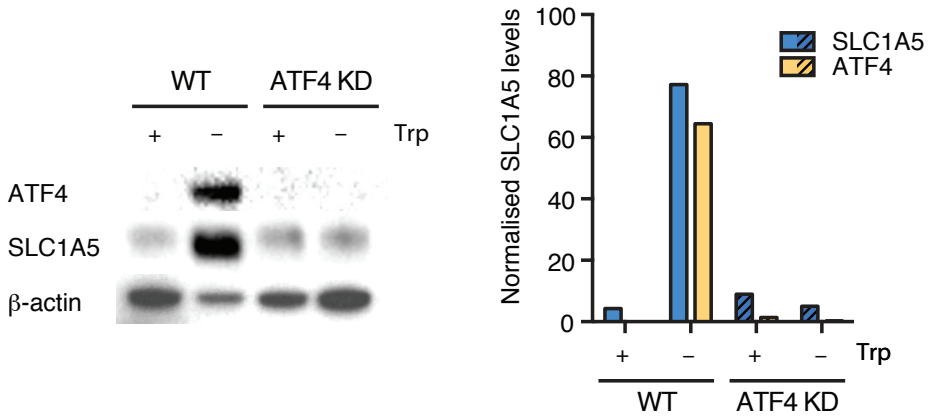

Figure 4-12. ATF4 mediates SLC1A5 upregulation upon tryptophan withdrawal
WT and ATF4 knockdown (ATF4 KD) HeLa cells generated using CRISPR/Cas9 targeting ATF4 were incubated in tissue culture medium depleted of tryptophan for 48h. Western blotting was performed with indicated antibodies and protein levels were quantified by densitometry.

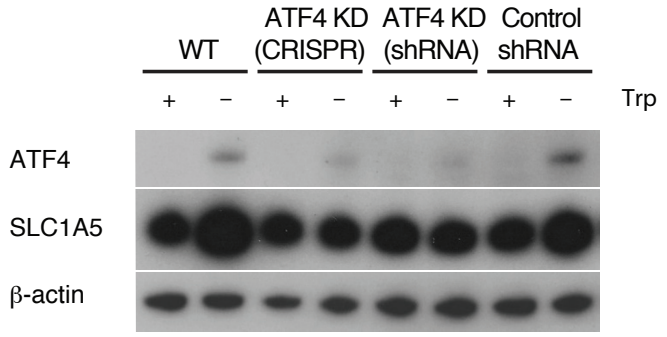

Figure 4-13. CRISPR/Cas9- and shRNA-mediated ATF4 knockdown leads to abolished SLC1A5 upregulation upon tryptophan withdrawal

WT, control shRNA-transduced and ATF4 knockdown (ATF4 KD) HeLa cells, generated using either CRISPR/Cas9 or shRNA targeting ATF4, were incubated in tissue culture medium depleted of tryptophan for 48h. Western blotting was performed with indicated antibodies.

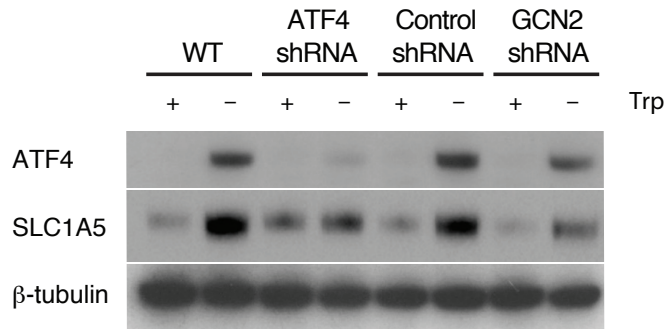

Figure 4-14. GCN2 knockdown HeLa cells exhibit remnant ATF4 activation under tryptophan-deficient conditions

WT HeLa and HeLa cells transduced with ATF4-targeting shRNA, GCN2-targeting shRNA or control shRNA were incubated in tissue culture medium depleted of tryptophan for 48h. Western blotting was performed with indicated antibodies.

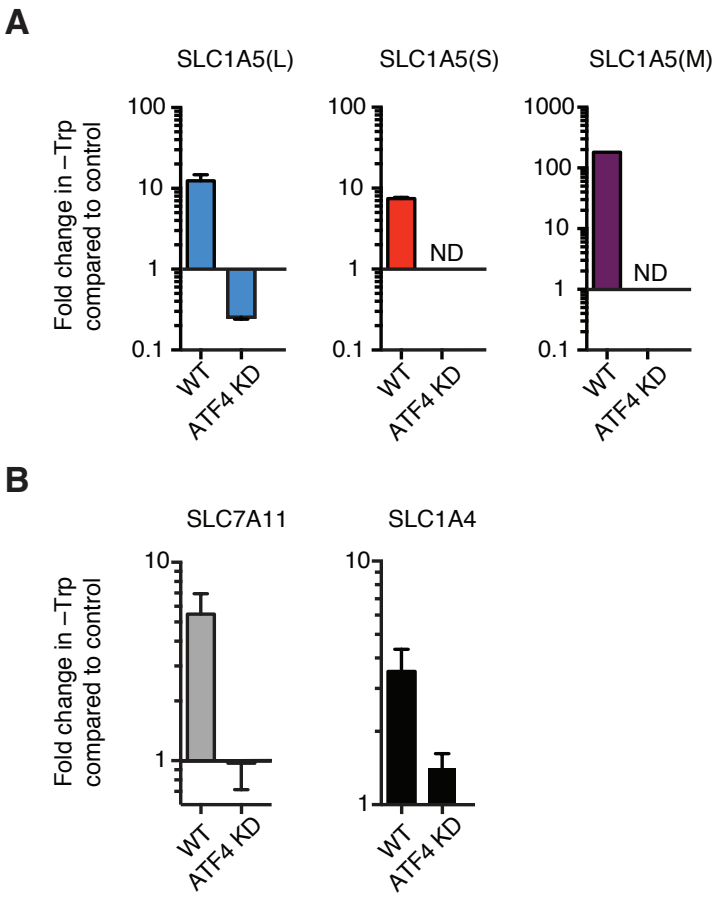

Figure 4-15. ATF4 mediates several amino acid transporter upregulation upon tryptophan withdrawal

WT and ATF4 knockdown (ATF4 KD) HeLa cells generated using CRISPR/Cas9 targeting ATF4 were incubated in tissue culture medium depleted of tryptophan for 48h. *SLC1A5(L)*, *SLC1A5(S)* and *SLC1A5(M)* mRNA expression levels **(A)**, and *SLC7A11* and *SLC1A4* mRNA expression levels **(B)** were quantified by quantitative PCR, and are shown as fold change in expression in tryptophan-depleted vs complete tissue culture medium, relative to *Hprt1*. Bars represent the mean ± SEM. ND, non-detected.

4.2.5. ATF4 ChIP assay reveals increased ATF4 binding to SLC1A5 under tryptophan-deficient conditions

Having established that SLC1A5 upregulation in tryptophan-starved tumour cells is controlled by ATF4, we next performed ATF4 ChIP-q-RT-PCR experiments in HeLa cells cultured in tryptophan-depleted medium or medium supplemented with all amino acids. Consistent with our previous findings, we observed increased ATF4 recruitment to the *SLC1A5* gene under tryptophan-deficient conditions **(Figure 4-16)**. In addition, tryptophan-starved HeLa cells exhibited enhanced ATF4 binding to the *ASNS* gene **(Figure 4-16)**, an ATF4-dependent gene (Siu et al., 2002) that we used as a positive control.

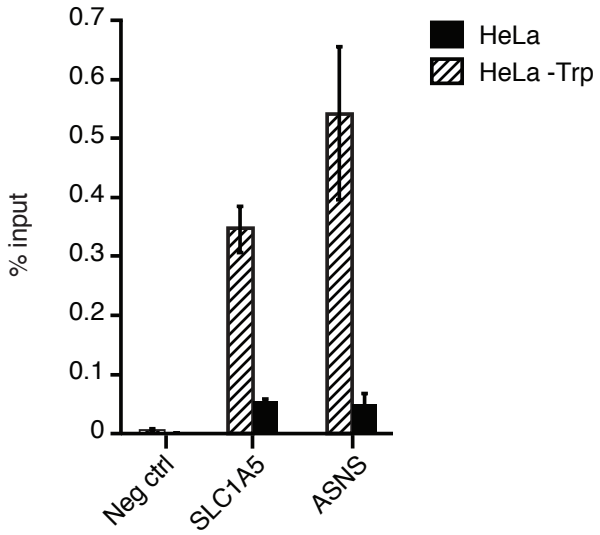

Figure 4-16. Tryptophan deprivation leads to enhanced ATF4 recruitment to SLC1A5 and ASNS genes

ATF4 ChIP was conducted on WT HeLa cells incubated in tissue culture medium depleted of tryptophan for 48h. The data are shown as percentage of total input (5% of the total chromatin, which was sonicated but not incubated with the ATF4 ChIP antibody).

4.3. Discussion

The mechanisms underlying regulation of amino acid transporters such as SLC1A5 in cancer are largely poorly understood. To elucidate the mechanisms responsible for amino acid transporter reprogramming, particularly the upregulation of SLC1A5, in cancer cells expressing tryptophan-catabolising enzymes, we exposed tumour cells to two metabolic fates of IDO/TDO enzymatic activity – tryptophan depletion and kynurenine accumulation. Tryptophan metabolite kynurenine, similarly to FICZ – a more potent AhR agonist, failed to modulate SLC1A5 levels in tumour cells, suggesting that AhR pathway is not involved in the regulation of SLC1A5 induction in the context of tryptophan catabolism. On the other hand, tryptophan starvation acted as a strong stimulus for this amino acid transporter expression, which also applied to SLC1A5 truncated isoforms. Notably, shortage of tryptophan was able to enhance SLC1A5 expression in a panel of IDO negative tumour cell lines, suggesting that the mechanisms controlling SLC1A5 upregulation are shared by transformed cells of different origin. Furthermore, we have observed that SLC1A5 is not the only transporter sensitive to the extracellular tryptophan concentration, as lack of tryptophan also enhanced the expression of SLC7A11 and SLC1A4, demonstrating a more general effect of tryptophan starvation on amino acid transporter profiling. These results suggest that modulation of the SLC1A5, SLC7A11 and SLC1A4 expression profile observed in tumour cells expressing tryptophan-catabolising enzymes are a direct consequence of tryptophan depletion induced by IDO/TDO enzymatic activity.

We have also observed differential modulation of SLC1A5 expression by the withdrawal of distinct amino acids from the culture medium. More specifically, while lack of tryptophan was one of the most potent inducers of SLC1A5, its expression was also enhanced by the absence of some other amino acids, such as glutamine and arginine. While the induction of SLC1A5 expression by the absence of glutamine is perhaps unsurprising, given its high

affinity for this amino acid (Kekuda et al., 1996; Pingitore et al., 2013; Utsunomiya-Tate et al., 1996), SLC1A5 sensitivity to the availability of its low-affinity substrates tryptophan and arginine (Kekuda et al., 1996; Pingitore et al., 2013; Utsunomiya-Tate et al., 1996) is somewhat intriguing. These results suggest that SLC1A5 upregulation represents a specific amino acid depletion response mechanism. Moreover, our findings suggest that the molecular mechanisms described in this study may also apply to tumour cells expressing the arginine-degrading enzyme arginase. Further studies investigating the SLC1A5 expression profile in tumour cells with such characteristics are warranted. Furthermore, in addition to being regulated by amino acid availability, we found that SLC1A5 expression is highly sensitive to variation in the local tryptophan concentration, with induction of this amino acid transporter observed within 0 to 5μM range. These results are consistent with the enhanced expression of SLC1A5 in IDO- and TDO-expressing tumour cells, which degrade tryptophan to concentrations below 2.5μM in tissue culture medium (Chapter 3.1). Importantly, SLC1A5 upregulation following amino acid withdrawal also appears to be persistent, as it cannot be brought down to basal levels with short-term re-supplementation of the missing amino acid. These findings could have implications for the amino acid starvation response *in vivo*, where tryptophan could still be intermittently available (e.g. from dying cells) in the presence of tryptophan-catabolising enzymes.

ATF4 is a known regulator of the nutritional stress response (Harding et al., 2000a; Harding et al., 2003), which we showed to be activated in IDO-expressing tumour cells and tumour cells exposed to culture conditions with limited amounts of tryptophan, under which ATF4 mirrored the expression of SLC1A5. Based on these findings, we hypothesised that ATF4 pathway could be involved in the induction of SLC1A5 expression under low tryptophan conditions. We undertook two approaches to test this hypothesis; one involved silencing of the ATF4-activating eIF2α kinase GCN2, and the other – a direct

knockdown of the ATF4 transcription factor. In our experimental conditions, SLC1A5 induction in response to tryptophan shortage was completely abolished in ATF4 knockdown tumour cells, which failed to efficiently activate ATF4 in tryptophan-depleted medium. In addition, we showed that tryptophan shortage induced increased ATF4 binding to the *SLC1A5* gene. Collectively, these results demonstrate that SLC1A5 upregulation in tryptophan-starved tumour cells is dependent on the ATF4 pathway. On the other hand, GCN2 knockdown tumour cells exhibited only a partial reduction in SLC1A5 upregulation in tryptophan-depleted medium. These findings are consistent with the remnant levels of ATF4 activation that we observed in GCN2 knockdown tumour cells kept under these conditions, which could be a result of signaling for ATF4 activation by the unsilenced GCN2 or through compensatory GCN2-independent mechanisms. *In vivo*, for example, loss of GCN2 in a mouse model of sarcoma has been shown to upregulate another eIF2α kinase, PERK, also able to induce ATF4 activation (Lehman et al., 2015). Alternatively, PERK and the unfolded protein response (Harding et al., 2000a; Harding et al., 2003) may contribute to the tryptophan withdrawal-induced ATF4 activation in addition to (rather than compensatory for the loss of) GCN2. Further experiments are warranted to address these possibilities.

Notably, we found that all three top upregulated amino acid transporters in IDO^+ tumour cells, SLC1A5, SLC7A11 and SLC1A4, showed evidence of regulation by the ATF4 stress response pathway. In addition to the main SLC1A5 isoform, ATF4 also controlled the induction of truncated isoforms in tryptophan-starved tumour cells. Thus, we identified ATF4 as a master transcription factor mediating the changes in amino acid transporter profiling under low tryptophan conditions. These data are in agreement with the previously reported regulation of several amino acid transporter genes by the ATF4 pathway (Harding et al., 2003; Ren et al., 2015) and with the role of ATF4 in promoting tumour cells' survival

and proliferation under amino acid starvation conditions (Ye et al., 2010). Collectively, our results suggest that tumour cells may be able to compensate for tryptophan deprivation in the tumour microenvironment through ATF4-dependent upregulation of amino acid transporters mediating cellular uptake of tryptophan, such as SLC1A5. This is consistent with the impaired adaptation of SLC1A5 knockdown tumour cells to low tryptophan conditions, as evidenced by the reduced proliferation exhibited by these cells in tryptophan-depleted medium (Chapter 3.3).

The key role of ATF4 in the adaptation of tumour cells to tryptophan starvation is further underscored by upregulation of several ATF4-dependent genes involved in biological functions other than amino acid transport in IDO-expressing tumour cells, including tryptophanyl-tRNA synthetase (*WARS*) (Han et al., 2013; Harding et al., 2003), asparagine synthetase (*ASNS*) (Siu et al., 2002), glutamic pyruvate transaminase 2 *GPT2* (Hao et al., 2016; Igarashi et al., 2007) and *C/EBPβ* (Harding et al., 2003) (Chapter 3.1). These genes could also contribute to the resistance of IDO- and TDO-expressing tumour cells to tryptophan deprivation in the tumour microenvironment. Upregulation of tryptophanyl-tRNA synthetase, for example, may allow IDO- and TDO-expressing tumour cells to replete their intracellular tryptophanyl-tRNA stocks before degrading available tryptophan, while asparagine synthetase has been previously shown to induce pro-survival and proliferation-inducing effects in tumour cells undergoing amino acid starvation (Ye et al., 2010). Further studies are needed to address the functional importance of the changes occurring in tRNA aminoacylation and amino acid biosynthesis processes in tumours expressing tryptophan-degrading enzymes.

Notably, ATF4 is unlikely to be the sole regulator of SLC1A5 expression in cancer. Overexpression of SLC1A5 has been reported in cancerous tissues of different origin (compared to normal tissues), including the brain, colon, lung, mammary gland, skin and

stomach, among others (Fuchs and Bode, 2005), which is likely to be driven by Myc oncogene, which directly targets SLC1A5 (Ren et al., 2015; Wise et al., 2008). In line with this, increased expression of 14-3-3σ, a negative regulator of c-Myc, is associated with reduced SLC1A5 expression (Phan et al., 2015). In addition to c-Myc (Wise et al., 2008) and N-Myc (Ren et al., 2015), SLC1A5 expression has been reported to be controlled by other pathways, including Rb/E2F (Reynolds et al., 2014) and EGF signaling (Avissar et al., 2008). Such cell-intrinsic mechanisms, linked to the neoplastic process, could synergise with the environmental effect of tryptophan depletion. More recently, the ubiquitin ligase RNF5 has been found to target SLC1A5 by facilitating its ubiquitinylation and degradation in paclitaxel-treated breast cancer cells undergoing ER stress (Jeon et al., 2015). Moreover, histone lysine demethylase KDM4C, which is commonly overexpressed in cancer, has been shown to cooperate with ATF4 in the transcriptional control of SLC1A5 expression (Zhao et al., 2016). These results suggest the presence and involvement of previously unknown pathways in SLC1A5 regulation, which may prove to be important therapeutic targets.

In summary, the experiments performed in Chapter 4 suggest that the modulation of amino acid profiling occurring in IDO-expressing tumour cells is induced by the shortage of tryptophan and is dependent on the activation of the transcription factor ATF4 – a master regulator of numerous stress response genes, including SLC1A5, SLC7A11 and SLC1A4 amino acid transporters. We have thus demonstrated a role for ATF4 in amino acid reprogramming and sustaining metabolic homeostasis under tryptophan starvation conditions.

CHAPTER 5: Analysis of SLC1A5 expression in resident cells of the tumour microenvironment and primary tumours

Apart from tumour cells themselves, the tumour microenvironment contains a significant infiltrate of immune cells, including lymphocytes (both tumour-specific $CD8^+$ T cells and immunosuppressive Treg cells), myeloid cells, as well as non-immune populations like fibroblasts and stromal cells, all of which may contribute to the fate of tumour progression. Importantly, in the context of an IDO/TDO-expressing tumour, these cells would also need to cope with a low tryptophan microenvironment. In this Chapter, we assess the SLC1A5 expression profile in resident immune cells of the tumour microenvironment, including conventional T cells, iNKT cells, Treg cells and IDO-competent DCs, and extend our findings describing the link between tryptophan deprivation and amino acid transporter reprogramming in human tumour cell lines to mouse tumours growing *in vivo* and primary human tumours.

5.1. SLC1A5 expression in human T cells

5.1.1. T cell response to tryptophan starvation

5.1.1.1. Human T cell proliferation is inhibited at tryptophan concentrations lower than 5μM

Tryptophan degradation by IDO-expressing tumours is a common mechanism of immune escape, which has been reported to inhibit effector T lymphocytes (Pilotte et al., 2012; Uyttenhove et al., 2003). To study T cell response to tryptophan starvation, we first examined proliferation of activated primary T cells in culture medium with graded amounts

of tryptophan using CFSE staining. $CD4^+$ T cells stimulated with αCD3/CD28 antibodies exhibited efficient proliferation at concentrations of tryptophan ranging from 25μM to 5μM, while their proliferation was strongly inhibited in tryptophan-depleted medium with no added tryptophan **(Figure 5-1)**. These findings suggested that T cell proliferative arrest is induced at concentrations of tryptophan lower than 5μM. To examine this phenomenon further, we incubated αCD3/CD28-treated $CD4^+$ T cells in culture medium containing 5, 2, 1.5, 1, 0.5 and 0μM tryptophan. Within this concentration range, we observed a dose-dependent inhibitory effect on T cell proliferation **(Figure 5-2)**. Notably, T cells exposed to low tryptophan concentrations demonstrated comparable levels of cell death **(Figure 5-2)**. These findings are consistent with the hypothesis that the effects of tryptophan deprivation on T cell proliferation are mediated through cell cycle arrest (Kudo et al., 2001; Munn et al., 1999) rather than induction of apoptosis. Furthermore, we found that addition of kynurenine to activated T cells cultured under normal or low tryptophan conditions had no substantial effect on cell division, as determined by CFSE staining, apart from a trend for a minor inhibitory effect at 25μM tryptophan, which could not be reproduced at low tryptophan concentrations (5μM and 0μM) **(Figure 5-3)**.

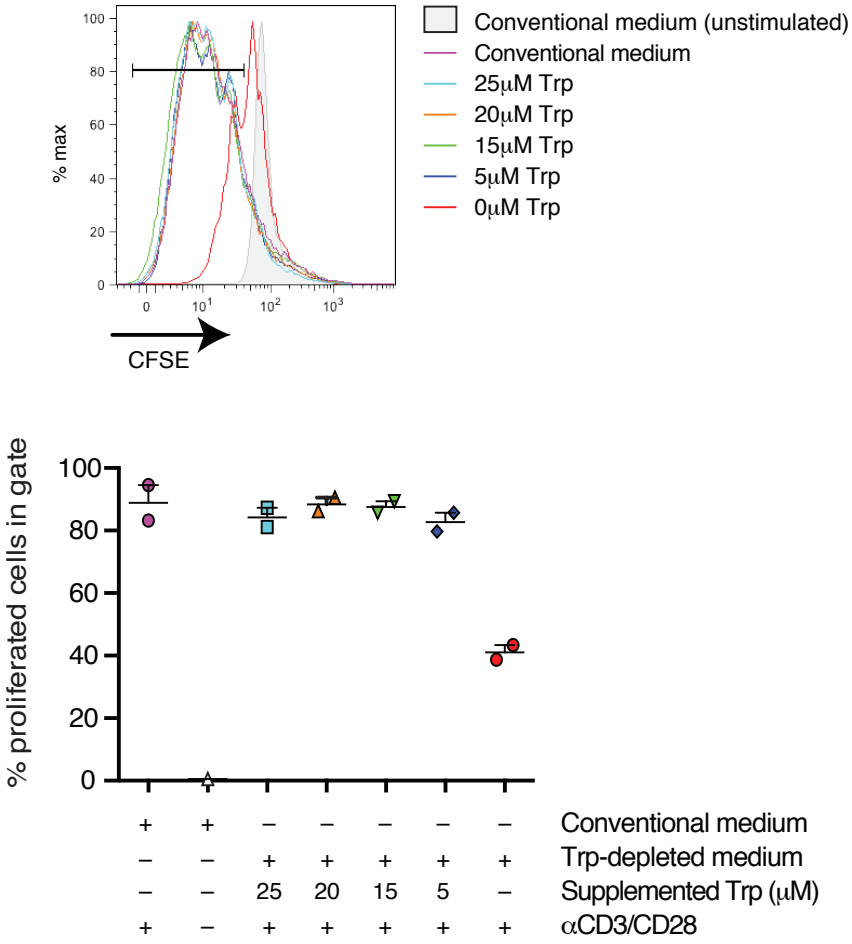

Figure 5-1. Tryptophan concentrations below 5μM inhibit human T cell proliferation
Human $CD4^+$ T cells were labeled with CFSE, stimulated with plate-bound αCD3/CD28 antibodies and incubated in conventional tissue culture medium or tryptophan-depleted tissue culture medium supplemented with indicated concentrations of tryptophan. After 96h, the cells were harvested, stained with live/dead, anti-human CD3 and CD4 antibodies and acquired by flow cytometry. CFSE levels were determined in live, $CD3^+$ $CD4^+$ cells using the gate shown (top panel). Bars represent the mean ± SEM.

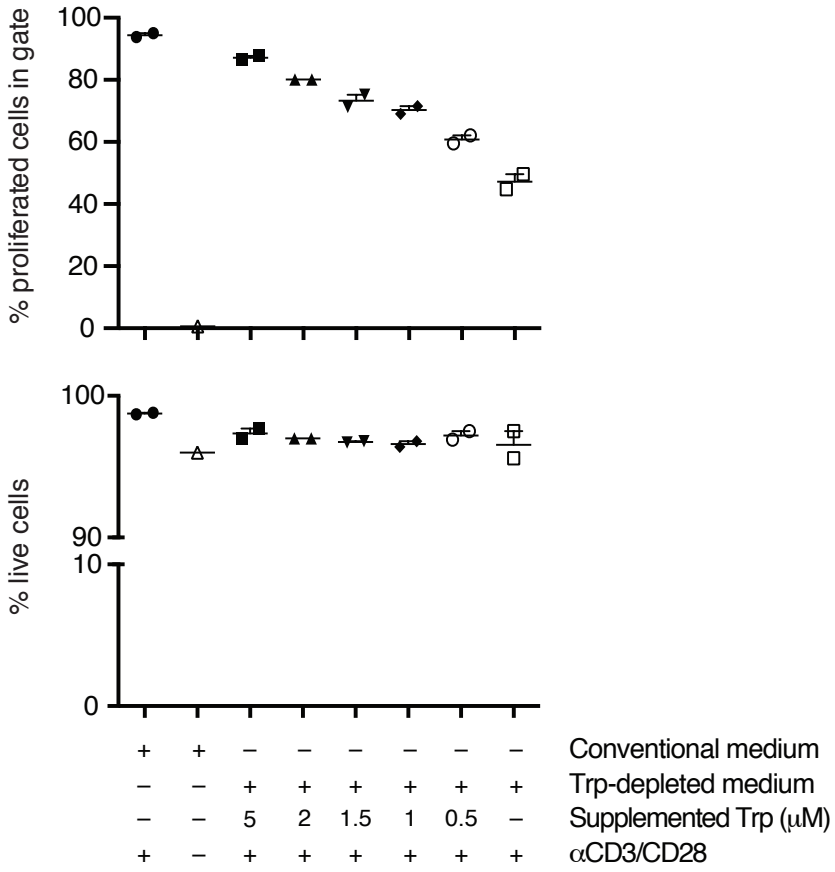

Figure 5-2. The effect of low tryptophan concentrations on human T cell proliferation and viability

Human $CD4^+$ T cells were labeled with CFSE, stimulated with plate-bound αCD3/CD28 antibodies and incubated in conventional tissue culture medium or tryptophan-depleted tissue culture medium supplemented with indicated concentrations of tryptophan. After 96h, the cells were harvested, stained with live/dead, anti-human CD3 and CD4 antibodies and acquired by flow cytometry. CFSE levels (top panel) were determined in live, $CD3^+$ $CD4^+$ cells. Bars represent the mean ± SEM.

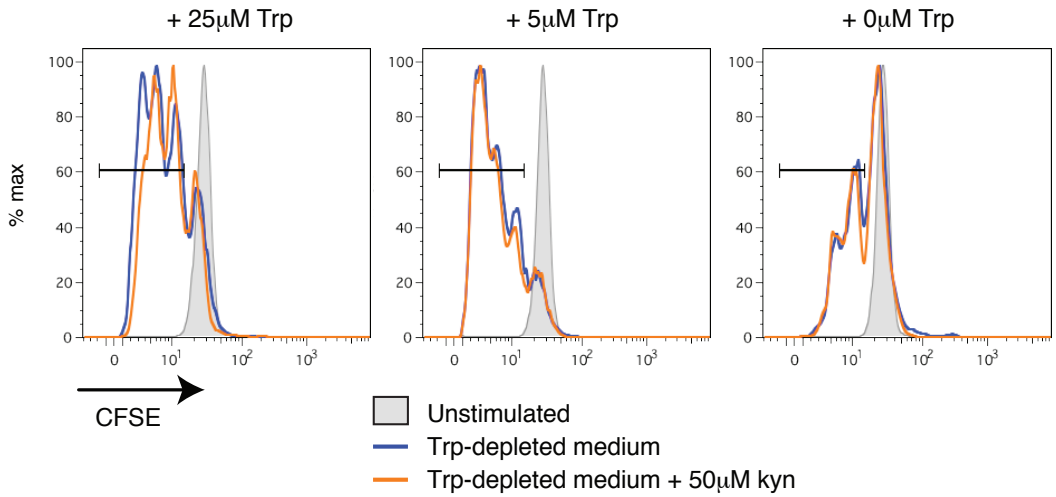

Figure 5-3. The effect of kynurenine on human T cell proliferation under normal and low tryptophan concentrations

Human $CD4^+$ T cells were labeled with CFSE, stimulated with plate-bound αCD3/CD28 antibodies and incubated in tryptophan-depleted tissue culture medium supplemented with 25, 5 or 0μM tryptophan. Where indicated, tissue culture medium was also supplemented with 50μM kynurenine (kyn). After 96h, the cells were harvested, stained with live/dead, anti-human CD3 and CD4 antibodies and acquired by flow cytometry. CFSE levels were determined in live, $CD3^+$ $CD4^+$ cells.

5.1.2. Resting human T cells fail to upregulate amino acid transporters in response to tryptophan starvation

Next, we set out to determine whether T lymphocytes, similarly to tumour cells, are able to alter their SLC1A5 expression profile when undergoing tryptophan starvation. To address this question, we first incubated resting human $CD4^+$ and $CD8^+$ T cells in tryptophan-depleted medium and measured their SLC1A5 expression using the SLC1A5-specific staining reagent RD114-RBD mFc. Notably, both $CD4^+$ and $CD8^+$ T cells exhibited low levels of SLC1A5 cell surface expression, especially when compared to tumour cells **(Figure 5-4A)**. More importantly, resting $CD4^+$ and $CD8^+$ T cells failed to enhance SLC1A5 expression in response to tryptophan depletion, in sharp contrast to the upregulation of SLC1A5 observed in HeLa cells maintained under identical conditions **(Figure 5-4A)**. In addition to the full-length isoform, human T cells kept in tryptophan-depleted medium also failed to express the alternative SLC1A5 isoform **(Figure 5-4B)**. Notably, the expression of other amino acid transporters upregulated in tryptophan-starved tumour cells, SLC1A4 and SLC7A11, were also not enhanced in T cells undergoing tryptophan starvation **(Figure 5-5)**.

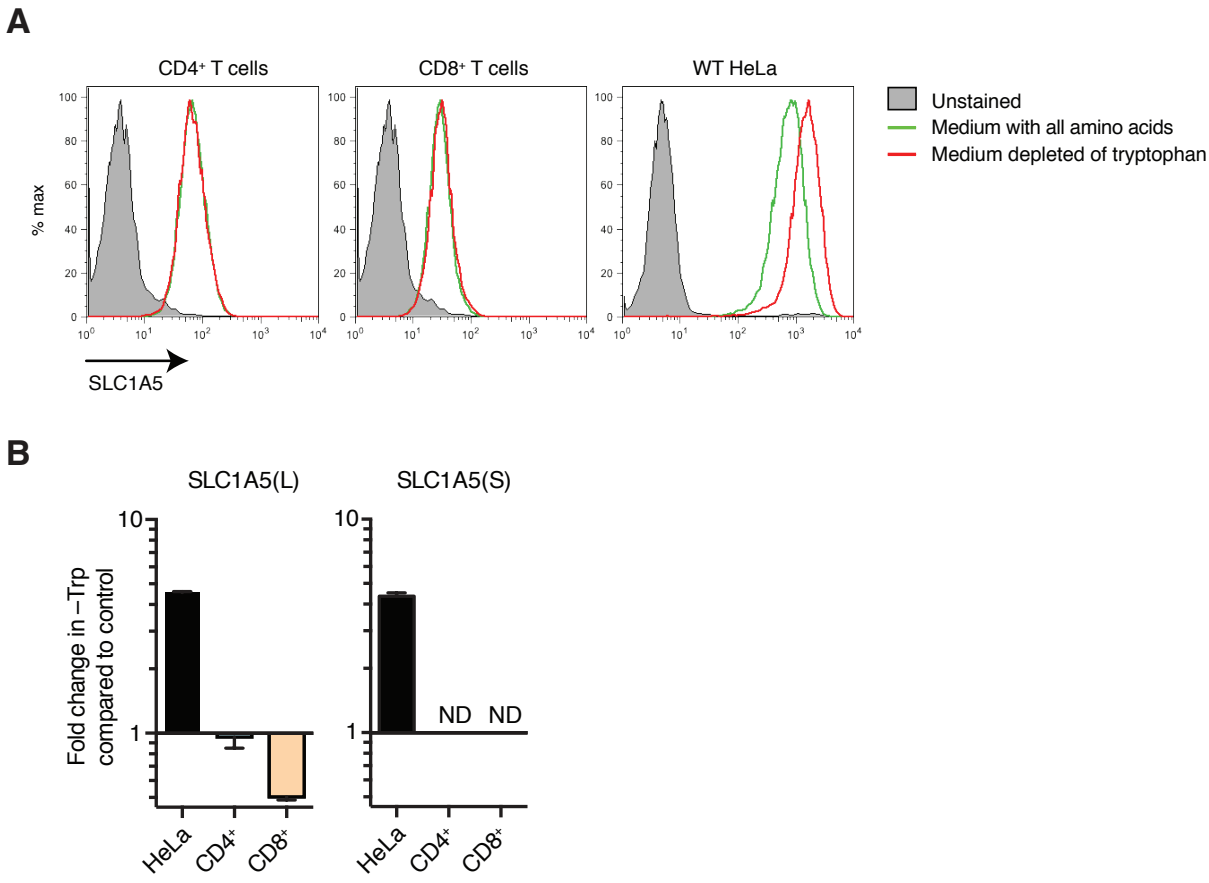

Figure 5-4. Human T cells fail to upregulate SLC1A5 expression upon tryptophan deprivation

WT HeLa and resting human $CD4^+$ and $CD8^+$ T cells were incubated in tissue culture medium depleted of tryptophan for 48h. SLC1A5 cell surface expression was assessed by flow cytometry using RD114-RBD mFc staining **(A)**. *SLC1A5(L)* and *SLC1A5(S)* mRNA expression levels were analyzed by quantitative PCR, and are shown as fold change in expression in tryptophan-depleted vs complete tissue culture medium, relative to *Hprt1*. Bars represent the mean ± SEM. ND, non-detected **(B)**.

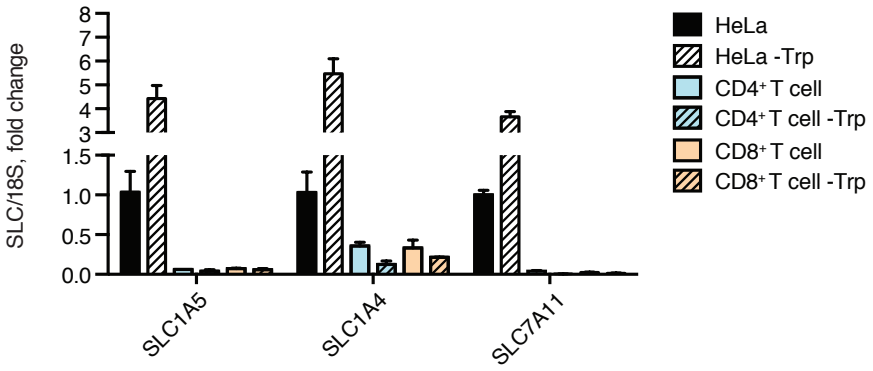

Figure 5-5. The expression of SLC1A5, SLC1A4 and SLC7A11 amino acid transporters in human T cells is unaffected by tryptophan deprivation

WT HeLa and resting human $CD4^+$ and $CD8^+$ T cells were incubated in tissue culture medium depleted of tryptophan for 48h. *SLC1A5, SLC1A4* and *SLC7A11* mRNA expression levels were analyzed by quantitative PCR, and are shown as fold change in expression relative to *18S*. Bars represent the mean ± SEM.

5.1.3. SLC1A5 expression in human T cells is enhanced upon activation and modulated by the strength of TCR engagement

We next investigated whether SLC1A5 expression in human T cells is altered upon T cell activation. The results of these experiments demonstrated that treatment with αCD3/CD28 antibodies strongly upregulated SLC1A5 expression in both $CD4^+$ and $CD8^+$ T cells (**Figure 5-6A**). While these findings are consistent with the increased metabolic demands of activated T cells (MacIver et al., 2013), it still remained unclear whether upregulation of SLC1A5 upon TCR-dependent T cell activation can be modulated by the strength of the TCR signaling events. To address this question, we stimulated an NY-ESO-1-specific human $CD8^+$ T cell clone with increasing concentrations of the cognate NY-ESO-$1_{157–165}$ peptide (Chen et al., 2000) or with αCD3/CD28 antibodies, as a control. We then used the SLC1A5-specific staining reagent RD114-RBD mFc to correlate SLC1A5 cell surface expression with T cell activation, as defined by CD25 upregulation. While low (0.1–1ng/ml) concentrations of the peptide induced very little activation (approximately 2% of the cells were activated by 1ng/ml peptide), treatment with 10–1000ng/ml of the NY-ESO-$1_{157–165}$ peptide resulted in efficient dose-dependent activation of the $CD8^+$ T cell clone **(Figure 5-6B)**. Notably, at these concentrations, we observed that upregulation of SLC1A5 directly correlated with the amount of NY-ESO-$1_{157–165}$ peptide added and with CD25 upregulation **(Figure 5-6B)**, demonstrating that it depends on the strength of TCR engagement.

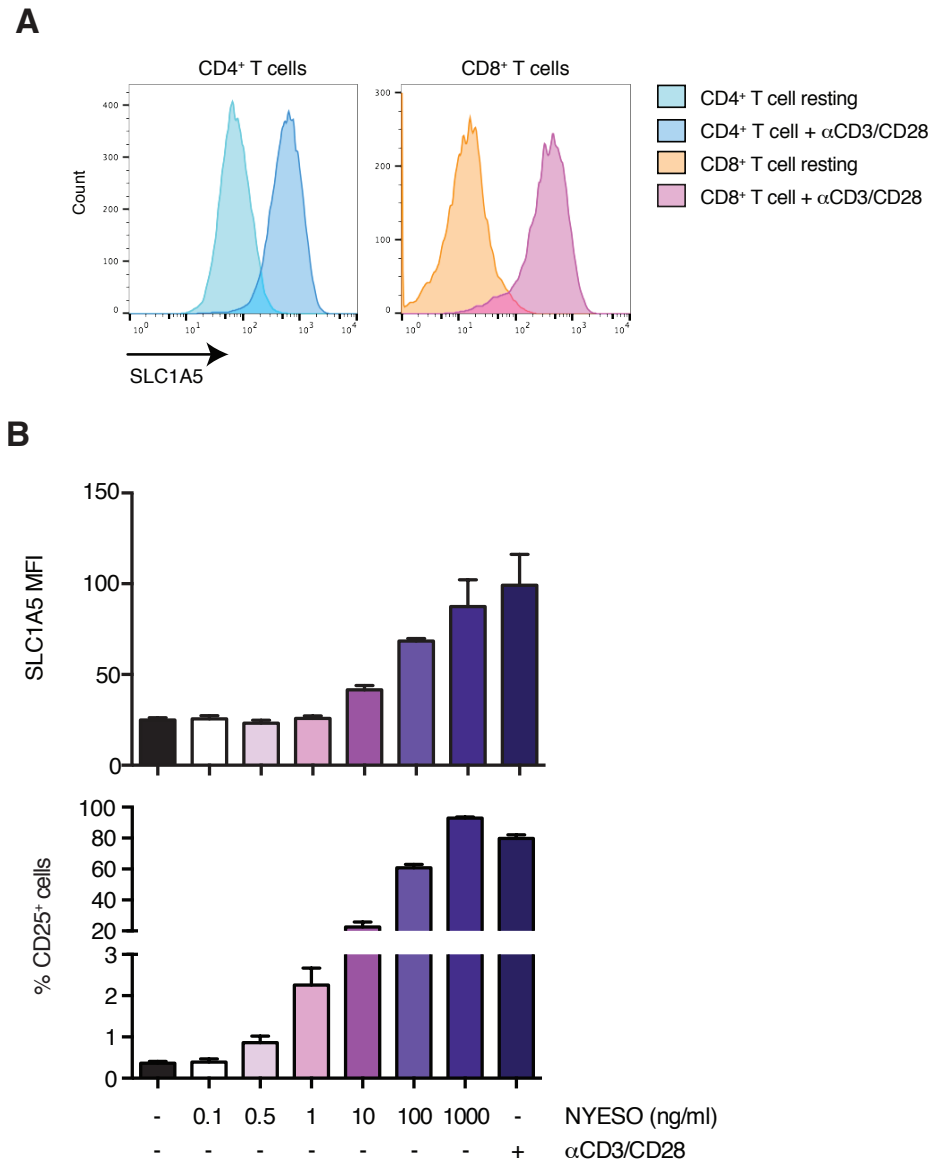

Figure 5-6. SLC1A5 upregulation in activated human T cells depends on the strength of TCR engagement

(A) Human $CD4^+$ and $CD8^+$ T cells were stimulated with plate-bound αCD3/CD28 antibodies for 96h, and SLC1A5 cell surface expression was assessed by flow cytometry using RD114-RBD mFc staining. **(B)** NY-ESO-1-specific $CD8^+$ T cell clone was stimulated with αCD3/CD28 antibodies or co-cultured with antigen presenting cells pre-pulsed with the indicated concentrations of NY-ESO-$1_{157–165}$ (9V) peptide analogue. After 48h, SLC1A5 (RD114-RBD mFc staining) and CD25 expression was assessed by flow cytometry. Bars represent the mean ± SEM. MFI, mean fluorescence intensity.

5.1.4. Pharmacological inhibition of SLC1A5 inhibits mTOR signaling in activated human T cells

Having demonstrated that SLC1A5 is upregulated in T cells receiving a strong activation stimulus, such as treatment with αCD3/CD28 antibodies or sufficient concentrations of cognate peptide, we next asked whether SLC1A5 expression in T cells played a role in mTOR pathway activation, which is reflective of the cell's amino acid uptake capacity. While phosphorylated S6 ribosomal protein was virtually undetectable in resting human T cells, its levels readily increased upon T cell activation **(Figure 5-7)**. On the other hand, pharmacological inhibition of SLC1A5 with 10mM BenSer led to a reduction in mTOR pathway activation in αCD3/CD28-treated T cells **(Figure 5-7)**. These findings are consistent with the increased metabolic demand of activated T cells for amino acids that can be transported by SLC1A5, such as glutamine (Carr et al., 2010; Nakaya et al., 2014).

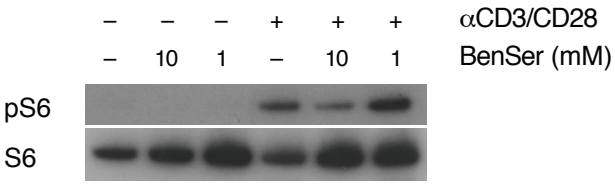

Figure 5-7. mTOR pathway activation is enhanced in activated human T cells and suppressed in the presence of SLC1A5 inhibitor BenSer
Human $CD4^+$ T cells, either stimulated (+) or unstimulated (-) with plate-bound αCD3/CD28 antibodies were incubated in the presence of indicated concentrations of BenSer for 6h. Western blotting was performed with indicated antibodies.

5.1.5. SLC1A5 expression in activated human T cells is unaffected by tryptophan starvation

We then asked whether increased SLC1A5 expression in activated T cells is further enhanced during T cell starvation response. To investigate this, we exposed resting or αCD3/CD28-treated human $CD4^+$ and $CD8^+$ T cells to low tryptophan conditions and measured their SLC1A5 transcription and protein expression by q-RT-PCR and Western blotting, respectively. Consistent with our previous results, activated T cells significantly enhanced their *SLC1A5* expression following treatment with αCD3/CD28 antibodies **(Figure 5-8A)**. On the other hand, unlike HeLa cells, both resting and activated T cells expressed comparable levels of *SLC1A5* mRNA under tryptophan-sufficient and -deficient conditions **(Figure 5-8A)**. Of note, even following activation-induced *SLC1A5* upregulation, *SLC1A5* expression was still significantly lower in T cells than in tryptophan-starved tumour cells **(Figure 5-8A)**. We observed similar results on the protein level. While resting $CD4^+$ and $CD8^+$ T cells hardly exhibited any detectable levels of SLC1A5 protein, T cell activation led to increased SLC1A5 expression **(Figure 5-8B)**. However, tryptophan depletion failed to induce further upregulation of SLC1A5 in αCD3/CD28-treated T cells **(Figure 5-8B)**. Interestingly, activated (but not resting) human $CD4^+$ and $CD8^+$ T cells also enhanced ATF4 expression when cultured in tryptophan-depleted medium, although not as efficiently as tryptophan-starved tumour cell lines **(Figure 5-8B)**. These results confirm the activation of the ATF4 stress response pathway in stimulated T cells maintained under low tryptophan conditions. We thus have extended our results in resting human T cells by demonstrating that SLC1A5 expression in activated human T cells is unaffected by tryptophan depletion despite ATF4 activation.

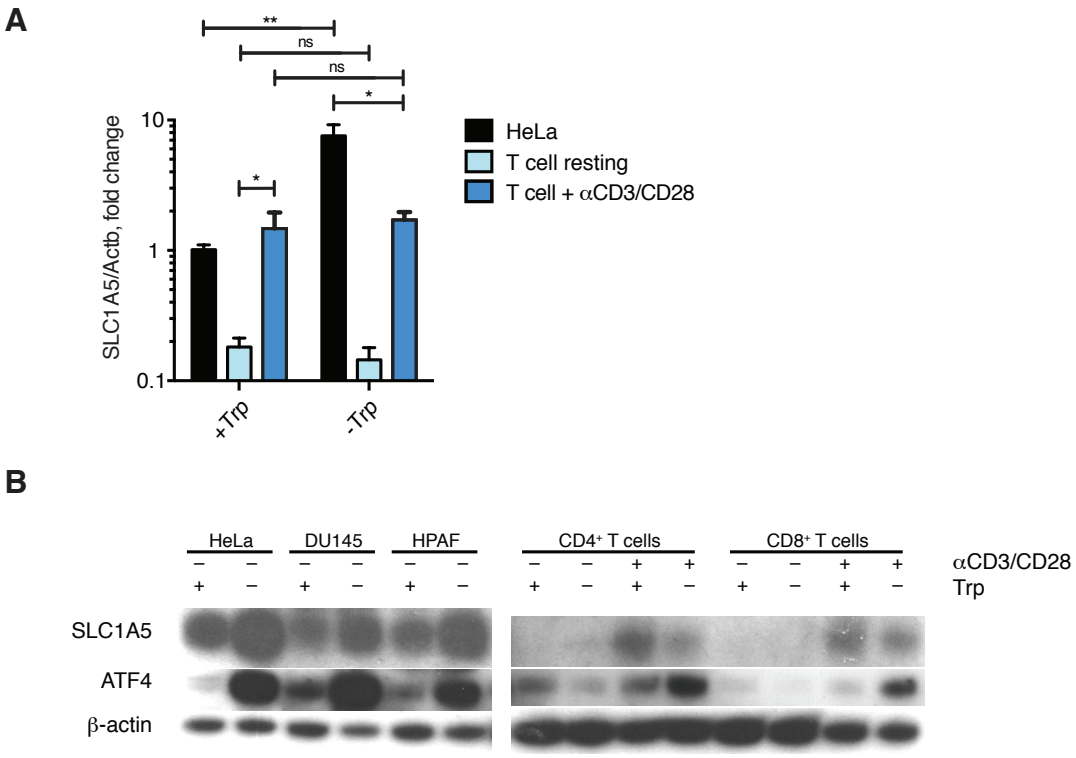

Figure 5-8. Human T cells upregulate SLC1A5 expression upon TCR stimulation, but not in response to tryptophan withdrawal

(A) WT HeLa and human $CD4^+$ T cells, either resting or stimulated with plate-bound αCD3/CD28 antibodies, were incubated in tissue culture medium with or without tryptophan for 48h. *SLC1A5* mRNA expression levels were analyzed by quantitative PCR, and are shown as fold change in expression relative to *Actb*. Bars represent the mean ± SEM. ns, non-significant. **(B)** WT HeLa, DU145, HPAF cells, and human $CD4^+$ and $CD8^+$ T cells, either stimulated (+) or unstimulated (-) with plate-bound αCD3/CD28 antibodies, were incubated in tissue culture medium with (+) or without (-) tryptophan for 48h. Western blotting was performed with indicated antibodies.

5.1.6. WARS expression in human T cells is increased upon activation but not in response to tryptophan deprivation

Having established that human T cells are unable to modulate their amino acid transporter expression profile in response to amino acid starvation, we next assessed whether T cells may exploit other potential tryptophan shortage compensatory mechanisms, such as the expression of tryptophanyl-tRNA synthetase WARS, which may help to maintain the intracellular tryptophanyl-tRNA levels, providing a reservoir for this essential amino acid under low tryptophan conditions. Similarly to SLC1A5, WARS expression at both mRNA and protein level was strongly upregulated in $CD4^+$ and $CD8^+$ T cells treated with αCD3/CD28 antibodies **(Figure 5-9A and B)**. However, tryptophan-starved T cells still failed to enhance WARS expression further when cultured in tryptophan-depleted medium, in contrast to HeLa and DU145 tumour cell lines, which readily upregulated the expression of this enzyme when exposed to identical culture conditions **(Figure 5-9A and B)**.

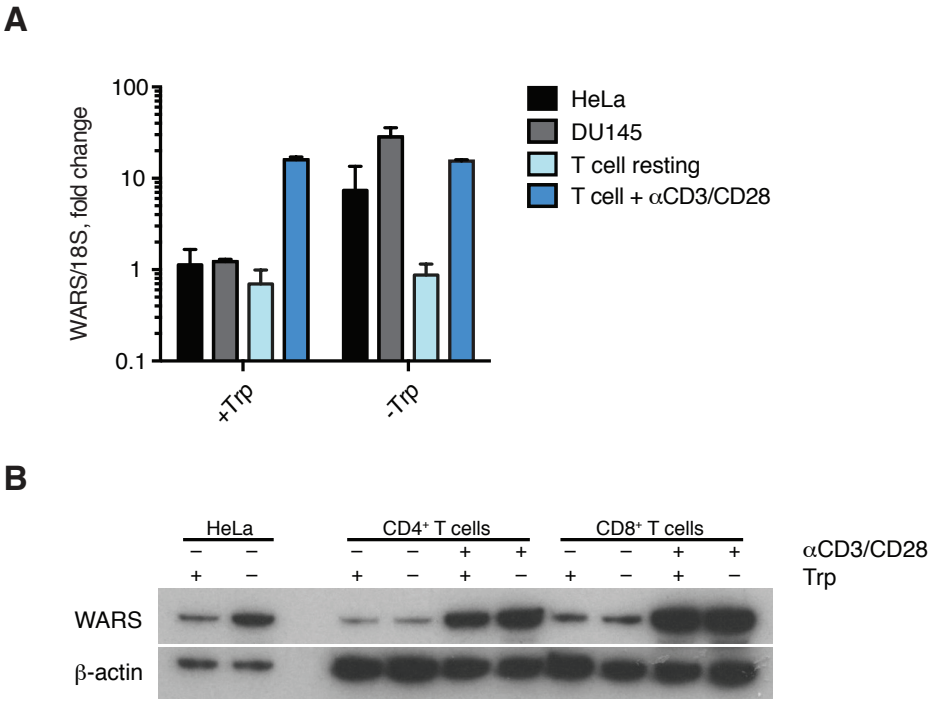

Figure 5-9. WARS expression is enhanced in human T cells upon TCR stimulation, but not in response to tryptophan withdrawal

(A) WT HeLa, DU145 and human $CD4^+$ T cells, either resting or stimulated with plate-bound αCD3/CD28 antibodies, were incubated in tissue culture medium with or without tryptophan for 48h. *WARS* mRNA expression levels were analyzed by quantitative PCR, and are shown as fold change in expression relative to *18S*. Bars represent the mean ± SEM. **(B)** WT HeLa and human $CD4^+$ and $CD8^+$ T cells, either stimulated (+) or unstimulated (-) with plate-bound αCD3/CD28 antibodies, were incubated in tissue culture medium with (+) or without (-) tryptophan for 48h. Western blotting was performed with indicated antibodies.

5.1.7. Activated human T cells increase the expression of ATF4-dependent genes GPT2 and ASNS when exposed to tryptophan deprivation

Having found ATF4 to be activated in stimulated human T cells undergoing tryptophan starvation with no associated upregulation of ATF4-dependent genes *SLC1A5* (Chapter 4.2) and *WARS* (Han et al., 2013; Harding et al., 2003), we questioned the functionality of the ATF4 stress response pathway in tryptophan-deprived T cells. To address this question, we tested the ability of T cells to upregulate other genes regulated by ATF4, such as *GPT2* (Hao et al., 2016; Igarashi et al., 2007) and *ASNS* (Siu et al., 2002). Notably, αCD3/CD28-treated T cells cultured in tryptophan-depleted medium enhanced the transcription of both *GPT2* and *ASNS* **(Figure 5-10),** suggesting a functional ATF4-dependent transcriptional program for these genes. Furthermore, in HeLa cells, tryptophan shortage induced an even stronger upregulation of *GPT2* and *ASNS* expression **(Figure 5-10)**, which is consistent with the robust activation of ATF4 in tumour cells exposed to low tryptophan conditions **(Figure 5-8B)**.

5.1.8. HOXB9 is upregulated during tryptophan starvation in both tumour cells and activated human T cells

Hayashi et al. have described homeobox B9 (HOXB9) as an ATF4-induced suppressor of human T cell response to amino acid deficiency, which interferes with cytokine production by activated T cells undergoing starvation (Hayashi et al., 2016). Based on these findings, we hypothesised that HOXB9 could prevent the changes in amino acid transporter profiling in tryptophan-deprived T cells. Consistent with Hayashi et al.'s findings, we found that activated but not resting T cells increase *HOXB9* expression when cultured in the absence of tryptophan **(Figure 5-11)**. However, *HOXB9* was also strongly upregulated in WT HeLa cells undergoing tryptophan starvation **(Figure 5-11)**, which makes it an unlikely candidate

for a negative regulator of tryptophan shortage-induced amino acid transporter reprogramming.

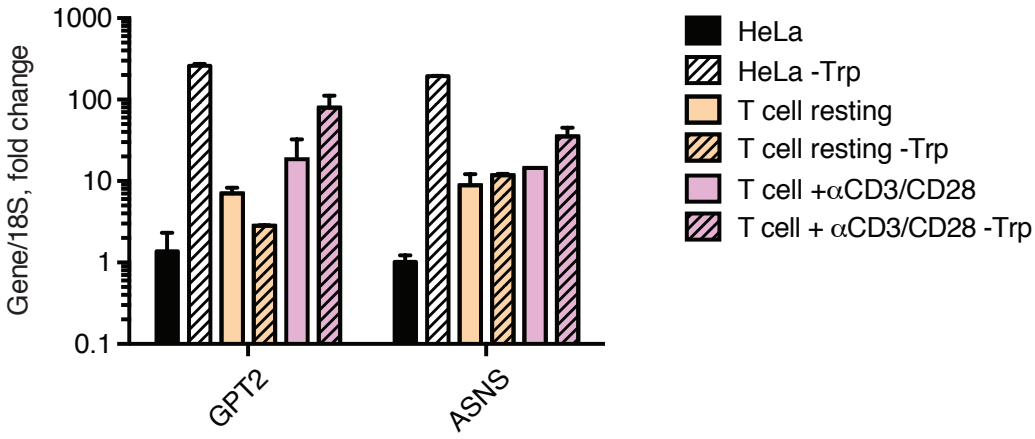

Figure 5-10. ATF4 target genes GPT2 and ASNS are upregulated in tumour cells and activated human T cells cultured under low tryptophan conditions
WT HeLa and human $CD8^+$ T cells, either resting or stimulated with plate-bound αCD3/CD28 antibodies, were incubated in tissue culture medium with or without tryptophan for 48h. *GPT2* and *ASNS* mRNA expression levels were analyzed by quantitative PCR, and are shown as fold change in expression relative to *18S*. Bars represent the mean ± SEM.

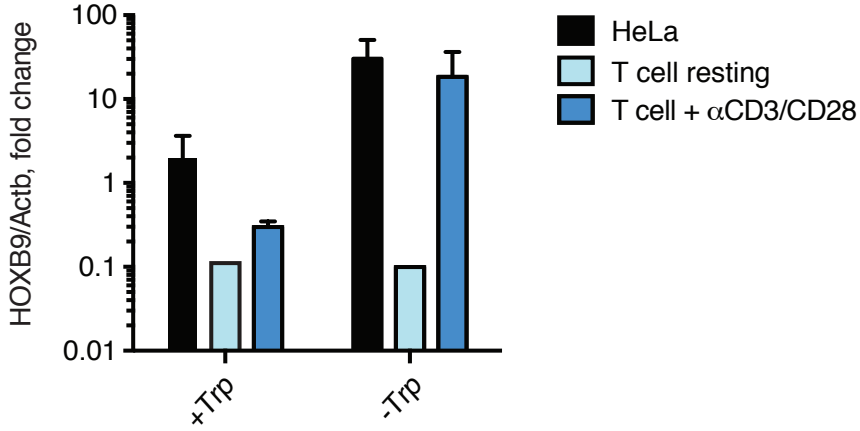

Figure 5-11. Tumour cells and activated human T cells enhance HOXB9 expression following tryptophan withdrawal
WT HeLa and human $CD4^+$ T cells, either resting or stimulated with plate-bound αCD3/CD28 antibodies, were incubated in tissue culture medium with or without tryptophan for 48h. *HOXB9* mRNA expression levels were analyzed by quantitative PCR, and are shown as fold change in expression relative to *Actb*. Bars represent the mean ± SEM.

5.1.9. Human iNKT cells exhibit a similar SLC1A5 expression profile to that of conventional T cells

5.1.9.1. SLC1A5 expression in human iNKT cells is modulated by the strength of semi-invariant TCR engagement

We then asked whether the SLC1A5 expression profile that we observed in human $CD4^+$ and $CD8^+$ T cells applied to a subset of T cells recognizing CD1d-bound lipid antigens – iNKT cells. We first assessed if, analogously to conventional T cells, iNKT cells could upregulate SLC1A5 expression upon activation with lipid antigens. To address this question, we stimulated iNKT cells with increasing concentrations of αGalCer or its analogues PI-3 and OCH-9, and measured SLC1A5 cell surface levels using RD114-RBD mFc staining. As expected, αGalCer activated iNKT cells in a dose-dependent manner, as evidenced by the increased percentage of $CD25^+$ cells. Importantly, iNKT cell activation also correlated with SLC1A5 MFI **(Figure 5-12)**. Similar results were obtained with synthetic glycolipids PI-3 and OCH-9, which also enhanced SLC1A5 expression in iNKT cells **(Figures 5-13 and 5-14)**. Notably, while αGalCer and PI-3 treatment led to abundant secretion of IFNγ by iNKT cells, OCH-9 induced approximately 5 times less IFNγ production **(Figure 5-15)** and less cell activation, as determined by CD25 staining **(Figure 5-14)**. Consistent with OCH-9 being a weaker iNKT cell agonist, it also induced a less potent SLC1A5 upregulation than αGalCer or PI-3 **(Figure 5-14)**. Collectively, our results suggest that, similarly to conventional T cells, SLC1A5 expression in iNKT cells depends on the strength of their semi-invariant TCR engagement.

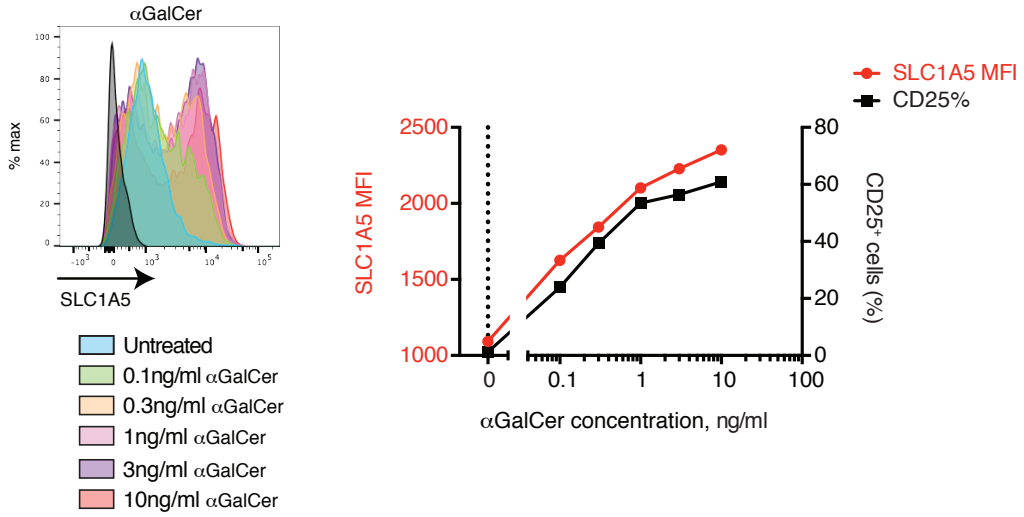

Figure 5-12. SLC1A5 expression in human iNKT cells activated with αGalCer depends on the strength of TCR engagement

Human Vα24^{+}Vβ11^{+} cells were co-cultured with antigen presenting cells pre-pulsed with the indicated concentrations of αGalCer. After 48h, SLC1A5 (RD114-RBD mFc staining) and CD25 expression was assessed by flow cytometry. MFI, mean fluorescence intensity.

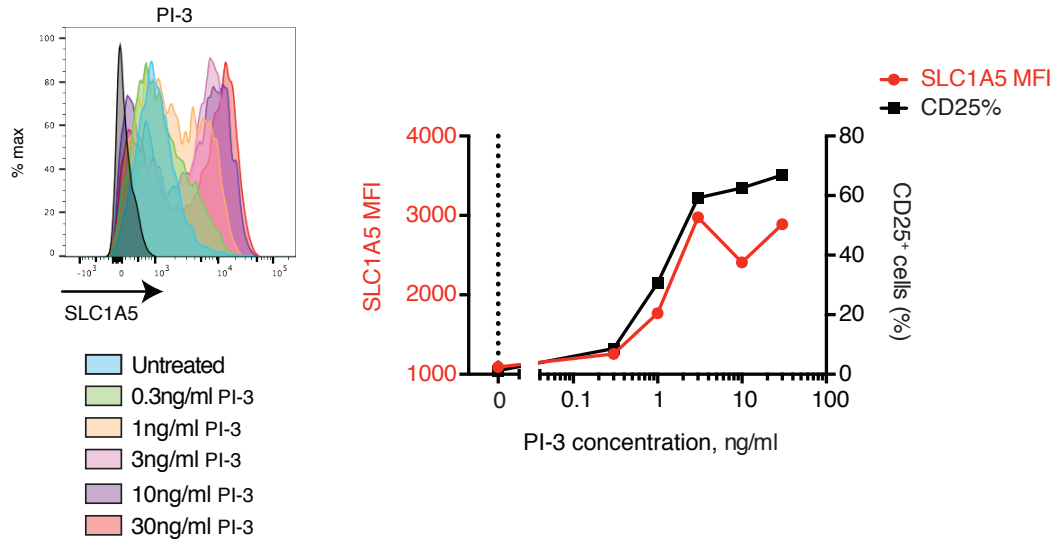

Figure 5-13. SLC1A5 expression in human iNKT cells activated with PI-3 depends on the strength of TCR engagement

Human Vα24^{+}Vβ11^{+} cells were co-cultured with antigen presenting cells pre-pulsed with the indicated concentrations of PI-3. After 48h, SLC1A5 (RD114-RBD mFc staining) and CD25 expression was assessed by flow cytometry. MFI, mean fluorescence intensity.

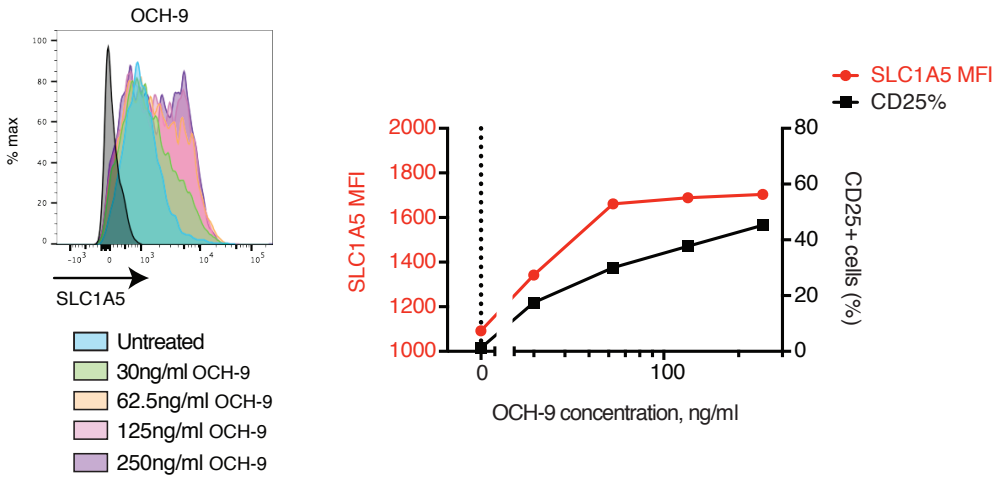

Figure 5-14. SLC1A5 expression in human iNKT cells activated with OCH-9 depends on the strength of TCR engagement

Human Vα24^{+}Vβ11^{+} cells were co-cultured with antigen presenting cells pre-pulsed with the indicated concentrations of OCH-9. After 48h, SLC1A5 (RD114-RBD mFc staining) and CD25 expression was assessed by flow cytometry. MFI, mean fluorescence intensity.

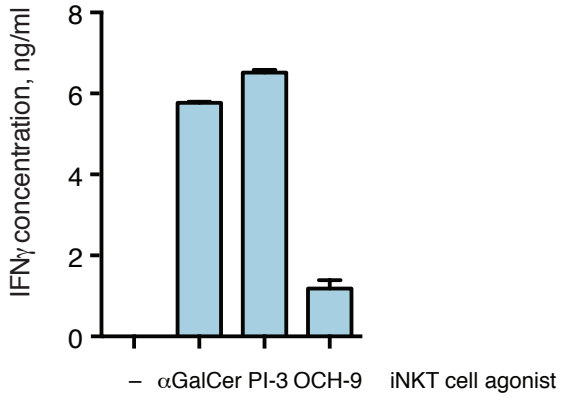

Figure 5-15. Lipid antigens induce IFNγ secretion by human iNKT cells

Human Vα24^{+}Vβ11^{+} cells were co-cultured with antigen presenting cells pre-pulsed with 10ng/ml αGalCer, 10ng/ml PI-3 or 250ng/ml OCH-9. After 48h, supernatants were collected and IFNγ concentrations were determined by ELISA. Bars represent the mean ± SEM.

5.1.9.2. SLC1A5 expression in human iNKT cells is unaffected by tryptophan starvation

To test whether human iNKT cells are able to respond to tryptophan starvation by upregulating their SLC1A5 expression, we cultured resting or αGalCer-activated iNKT cells in tryptophan-depleted medium, along with a panel of tumour cell lines, and measured SLC1A5 protein levels by Western blotting. Consistent with SLC1A5 cell surface FACS staining **(Figure 5-12)**, αGalCer acted as a strong inducer of SLC1A5 expression in iNKT cells, while resting iNKT cells expressed very low levels of this protein **(Figure 5-16)**. Despite the upregulation upon activation, iNKT cells failed to further enhance SLC1A5 expression under tryptophan-deficient conditions. Resting iNKT cells were also unable to modulate their SLC1A5 expression under these conditions, in contrast to tumour cell lines **(Figure 5-16)**. These results are consistent with our observations in conventional MHC-restricted $CD4^+$ and $CD8^+$ T cells.

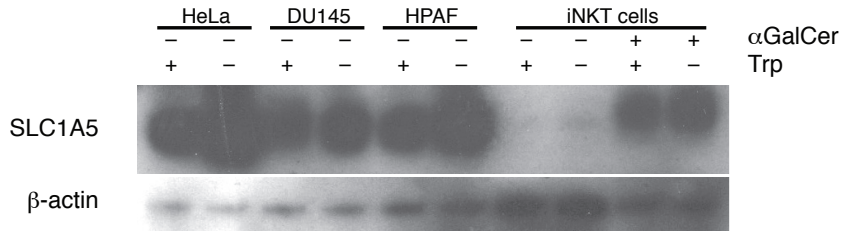

Figure 5-16. Human iNKT cells upregulate SLC1A5 expression upon TCR stimulation, but not in response to tryptophan withdrawal
WT HeLa, DU145, HPAF cells and human $V\alpha24^+V\beta11^+$ cells, either stimulated (+) or unstimulated (-) with plate-bound hCD1d–αGalCer monomer, were incubated in tissue culture medium with (+) or without (-) tryptophan for 48h. Western blotting was performed with indicated antibodies.

5.1.10. Differential expression of SLC1A5 in human renal cell carcinoma/stromal cells and tumour-infiltrating $CD8^+$ T cells *ex vivo*

Having characterised SLC1A5 expression in primary human T cells isolated from healthy blood donors, we decided to extend our findings to tumour-infiltrating T cells. Using RD114-RBD mFc staining, we measured SLC1A5 cell surface expression in primary human renal cell carcinoma samples. Specifically, we compared SLC1A5 expression levels in the $CD45^-$ population, containing tumour cells and stromal cells (which cannot be distinguished in this analysis as both cell types are negative for CD45), and in the $CD45^+$ $CD8^+$ population, representing tumour-infiltrating $CD8^+$ T cells **(Figure 5-17A)**. Flow cytometry analysis of tumours from three renal cell carcinoma patients demonstrated a trend for lower SLC1A5 expression levels in $CD45^+$ $CD8^+$ cells than the $CD45^-$ fraction **(Figure 5-17B)**.

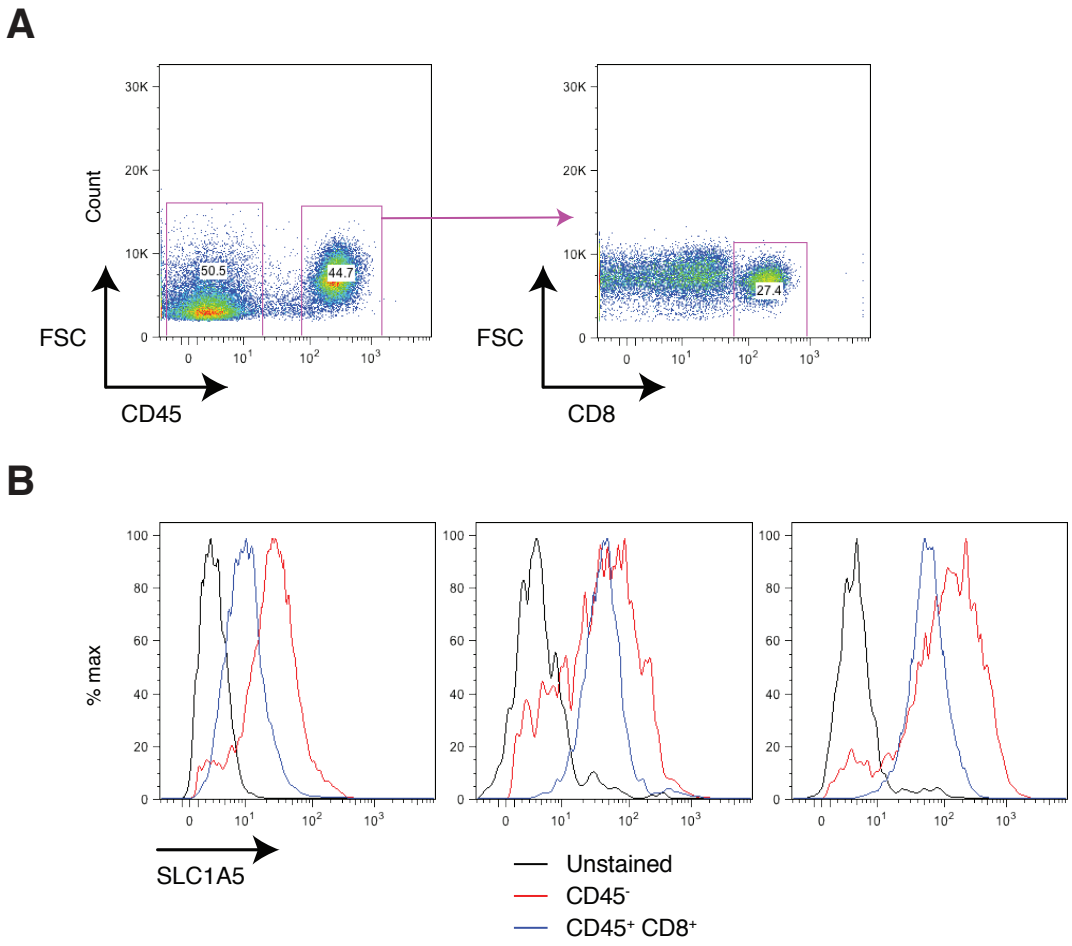

Figure 5-17. The comparison of SLC1A5 expression in CD45$^-$ and CD45$^+$ CD8$^+$ cell populations in primary human renal cell carcinoma samples

Single cell suspensions from primary human renal cell carcinoma tissues were stained with live/dead, anti-human CD45 and CD8 antibodies and RD114-RBD mFc, and acquired by flow cytometry. **(A)** Gating strategy to identify CD45$^-$ and CD45$^+$ CD8$^+$ populations. **(B)** Flow cytometry analysis of SLC1A5 cell surface expression in CD45$^-$ and CD45$^+$ CD8$^+$ populations from three renal cell carcinoma patients.

5.2. SLC1A5 expression by immunosuppressive immune cell populations

5.2.1. IDO-inducing stimuli upregulate SLC1A5 expression in human MoDCs

5.2.1.1. PGE2 and IFNγ induce IDO activity in human MoDCs

We next set out to determine whether IDO-inducing stimuli in the tumour microenvironment, such as PGE2 (Braun et al., 2005; von Bergwelt-Baildon et al., 2006) and IFNγ (Carlin et al., 1989a; Munn et al., 1999; Spranger et al., 2013; Takikawa et al., 1988), are able to modulate SLC1A5 expression in human DCs. First, we examined whether PGE2 and IFNγ can induce IDO activity in human MoDCs. PGE2-containing cytokine cocktail consisting of IL-1β, IL-6 and TNFα in addition to PGE2 is commonly used as a means of DC maturation in cancer immunotherapy trials. Consistently, we found that PGE2 was a major contributor to MoDC maturation. While over 70% of MoDCs treated with PGE2 in combination with IL-1β, IL-6 and TNFα expressed high levels of MHC class I and CD80 maturation markers, IL-1β, IL-6 and TNFα cytokines alone only induced approximately 40% of MoDCs to upregulate both these molecules **(Figure 5-18A)**. Furthermore, PGE2-containing cytokine cocktail also induced IDO activity in MoDCs, as evidenced by the reduced tryptophan-to-kynurenine ratio in the supernatants of MoDCs receiving this treatment **(Figure 5-18B)**. In addition, supernatants obtained from MoDCs treated with IFNγ or LPS also demonstrated evidence of tryptophan consumption and kynurenine production **(Figure 5-18B)**, which is indicative of IDO activity. These findings are consistent with IDO induction upon DC maturation (Braun et al., 2005).

5.2.1.2. PGE2, IFNγ and conditioned medium from activated iNKT cells induce IDO and SLC1A5 transcription in human MoDCs

Having demonstrated that IFNγ is able to induce IDO activity in MoDCs, we next asked whether activated iNKT cells, which secrete high levels of IFNγ upon stimulation with ligand **(Figure 5-15)**, can trigger the expression of this tryptophan-degrading enzyme in

MoDCs. To address this question, we treated MoDCs with the conditioned medium obtained from iNKT cells stimulated with αGalCer. Notably, similarly to PGE2-containing cytokine cocktail and recombinant IFNγ, supernatant of activated iNKT cells strongly upregulated *IDO1* transcription **(Figure 5-19)**. Even more importantly, increased *IDO1* expression in MoDCs receiving these treatments was also associated with enhanced transcription of *SLC1A5* mRNA **(Figure 5-19)**, further confirming the association between tryptophan catabolism and this amino acid transporter.

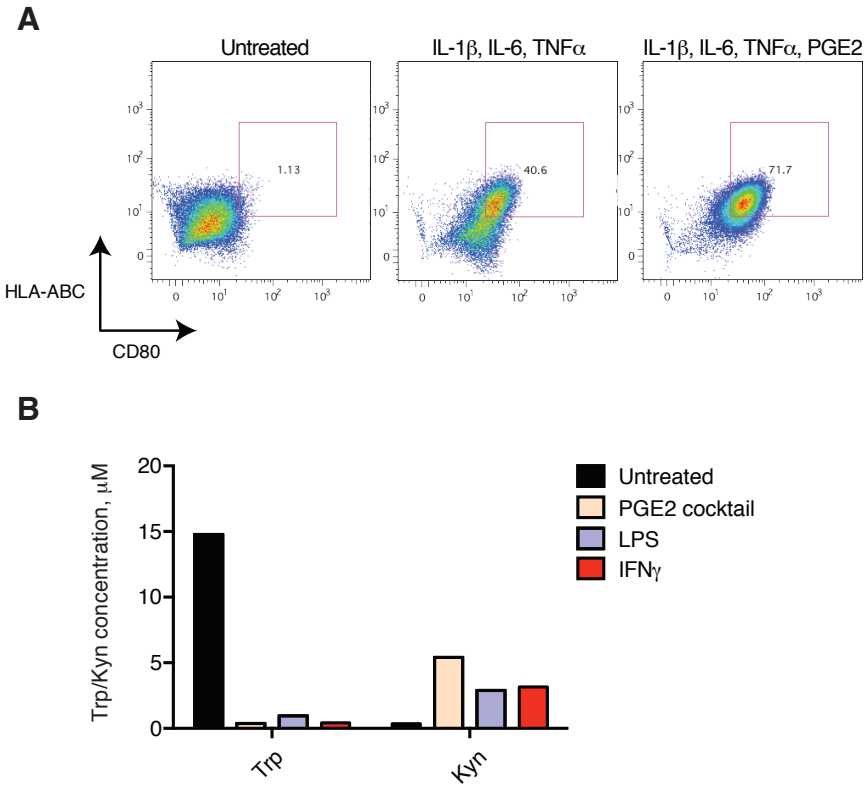

Figure 5-18. PGE2-containing cytokine cocktail induces maturation and IDO activity in human MoDCs

(A) Human MoDCs were cultured in the presence of 5ng/ml IL-1β, 15ng/ml IL-6, 10ng/ml TNFα with or without 5μg/ml PGE2. After 48h, the cells were harvested, stained with live/dead, anti-human HLA-ABC and CD80 antibodies and acquired by flow cytometry. **(B)** Human MoDCs were cultured in the presence of 5ng/ml IL-1β, 15ng/ml IL-6, 10ng/ml TNFα and 5μg/ml PGE2 (PGE2 cocktail), 1μg/ml LPS or 1000 U/ml IFNγ. After 48h, supernatants were collected, and tryptophan and kynurenine concentrations were determined by HPLC.

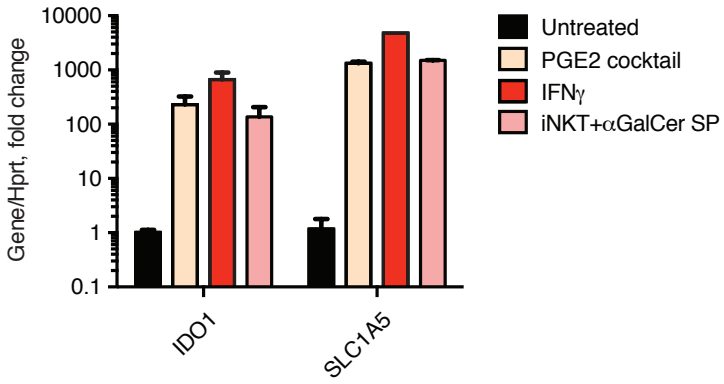

Figure 5-19. IDO-inducing stimuli enhance SLC1A5 expression in human MoDCs
Human MoDCs were cultured in the presence of 5ng/ml IL-1β, 15ng/ml IL-6, 10ng/ml TNFα and 5μg/ml PGE2 (PGE2 cocktail), 1000 U/ml IFNγ or conditioned medium obtained from $V\alpha24^{+}V\beta11^{+}$ cells co-cultured with antigen presenting cells pre-pulsed with 10ng/ml αGalCer for 48h. After 48h, the cells were harvested and *IDO1* and *SLC1A5* mRNA expression levels were analyzed by quantitative PCR, which are shown as fold change in expression relative to *Hprt*. Bars represent the mean ± SEM.

5.2.2. Treg cells exhibit enhanced SLC1A5 expression levels

Having shown enhanced SLC1A5 expression in IDO-competent DCs, we next assessed SLC1A5 expression in another key constituent of the immunosuppressive tumour microenvironment – Treg cells. To characterise SLC1A5 expression in Treg cells, we measured SLC1A5 cell surface levels in the $CD4^+$ $CD25^+$ $FoxP3^+$ population using RD114-RBD mFc staining. Our results demonstrated that human $CD4^+$ $CD25^+$ $FoxP3^+$ Treg cells exhibit higher levels of SLC1A5 expression than $CD4^+$ $CD25^-$ $FoxP3^-$ T cells from the same donors **(Figure 5-20)**. We observed this trend not only in healthy blood donors but also in lymph nodes obtained from metastatic melanoma patients **(Figure 5-20)**.

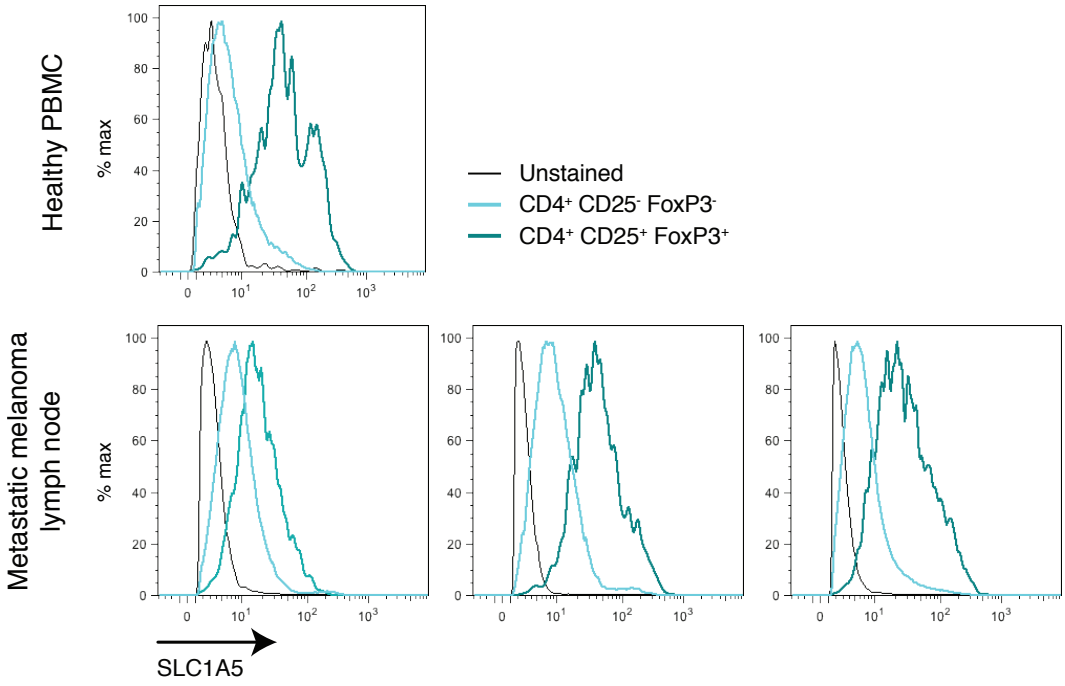

Figure 5-20. $CD4^+$ $CD25^+$ $FoxP3^+$ cells from healthy blood and metastatic melanoma lymph nodes demonstrate enriched SLC1A5 expression
PBMCs from healthy blood donors (top panel) and single cell suspensions from primary human metastatic melanoma lymph nodes (bottom panel) were stained with live/dead, anti-human CD4, CD25 and FoxP3 antibodies and RD114-RBD mFc, and acquired by flow cytometry.

5.3. SLC1A5 expression in primary mouse and human tumours

5.3.1. IDO-expressing mouse tumours upregulate SLC1A5 expression *in vivo*

To extend our findings characterising the relationship between IDO/TDO-induced tryptophan depletion and SLC1A5 upregulation in human tumour cell lines *in vitro* (Chapters 3.1 and 4.1), we next tested whether IDO-expressing tumours upregulate SLC1A5 expression *in vivo*. To address this question, we used mouse EG7 thymoma cells transduced with lentiviral vectors encoding either murine IDO with a GFP reporter (EG7 GFP IDO) or, as a control, GFP alone (EG7 GFP) (Silk et al., 2011). First, we confirmed that the transduced EG7 GFP and EG7 GFP IDO cells expressed GFP **(Figure 5-21A)**, and that IDO expression conferred functional activity, as determined by the reduced tryptophan-to-kynurenine ratio **(Figure 5-21B)**. Notably, tryptophan was virtually undetectable in the supernatant obtained from EG7 GFP IDO cells cultured for 72h **(Figure 5-21B)**, indicative of efficient enzymatic activity. Finally, we confirmed that EG7 cells expressed CD45.2 **(Figure 5-21C)**, and injected the EG7 GFP and EG7 GFP IDO cell lines into B6.SJL-*Ptprc*^{a} (CD45.1) mice. Notably, when grown *in vitro* in normal tissue culture medium, which was changed daily to prevent IDO-mediated degradation of tryptophan in the culture medium, EG7 GFP IDO and EG7 GFP cells had similar expression levels of *SLC1A5* **(Figure 5-22A)**. However, when *SLC1A5* transcription was assessed after 5 days of *in vivo* growth, EG7 GFP IDO tumours exhibited significantly higher levels of *SLC1A5* expression than the IDO-negative EG7 GFP tumours (**Figure 5-22B**). These findings demonstrate that SLC1A5 upregulation in tumours cells growing under tryptophan degradation conditions occurs not only *in vitro*, but, importantly, also *in vivo*.

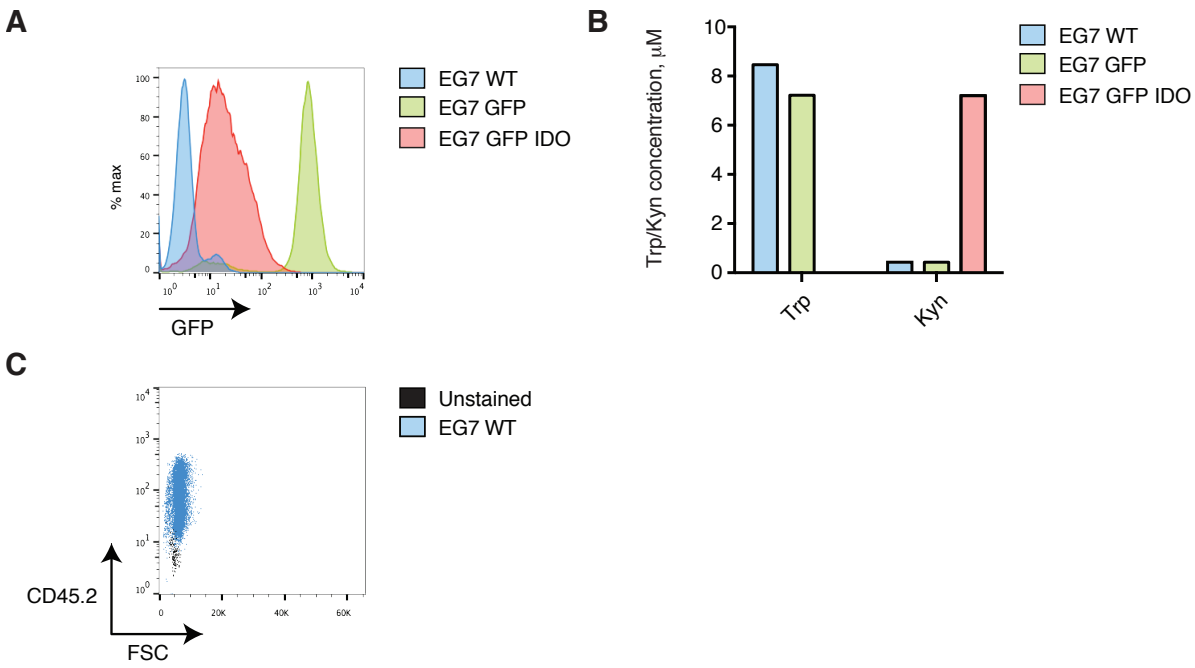

Figure 5-21. *IDO1*-transduced EG7 tumour cells acquire GFP fluorescence and metabolise tryptophan into kynurenine

(A) GFP fluorescence in untransduced WT EG7 cells and EG7 cells transduced with a lentiviral vector encoding either GFP alone (EG7 GFP) or mouse IDO linked via an IRES to GFP (EG7 GFP IDO). Samples were analysed by flow cytometry. **(B)** Supernatants were obtained from WT, GFP-transduced and *IDO1*-transduced EG7 cells cultured for 72h. Tryptophan and kynurenine concentrations were determined by HPLC. **(C)** WT EG7 cells were stained with anti-mouse CD45.2 antibody and acquired by flow cytometry.

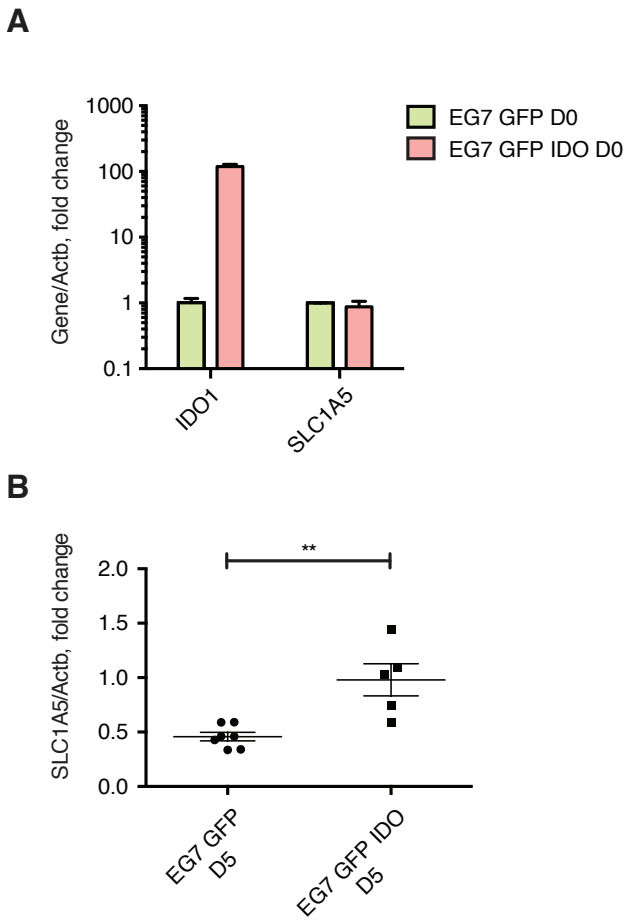

Figure 5-22. IDO-expressing EG7 tumours exhibit upregulation of SLC1A5 expression after 5 days of *in vivo* growth

(A) GFP-transduced and *IDO1*-transduced EG7 cells were cultured in fully supplemented R10 medium, which was changed daily. Mouse *IDO1* and *SLC1A5* mRNA expression levels were analyzed by quantitative PCR at day 0 (before injection *in vivo*), and are shown as fold change in expression relative to *Actb*. Bars represent the mean ± SEM. **(B)** GFP-transduced and *IDO1*-transduced EG7 cells were injected subcutaneously into B6.SJL-*Ptprc*^{a} (CD45.1) mice. Tumours were harvested after 5 days, stained with anti-mouse CD45.2 antibody and sorted on the basis of CD45.2 expression. Mouse *SLC1A5* mRNA expression levels were analyzed by quantitative PCR, and are shown as fold change in expression relative to *Actb* in EG7 GFP or EG7 GFP IDO cells at day 0. Bars represent the mean ± SEM.

5.3.2. SLC1A5 and IDO co-expression is observed in several primary human tumours

Finally, we set out to investigate whether the association between tryptophan catabolism and SLC1A5 expression can be observed in primary human tumour samples. In line with the regulation of SLC1A5 expression by the ATF4 pathway, our *in silico* analysis of available RNA-seq data demonstrated that in a large proportion of human tumours, *SLC1A5* positively correlates with *ATF4* expression **(Figure 5-23)**. However, since ATF4 activation can occur in response to several stresses, including hypoxia/anoxia and nutrient deprivation (Ameri and Harris, 2008) **(Figure 1-3)**, we assessed whether co-expression of *SLC1A5* and *ATF4* correlated with the upregulation of genes more relevant to catabolism of tryptophan in particular, such as tryptophanyl-tRNA synthetase *WARS,* which we have shown to be upregulated in IDO-expressing **(Figures 3-2 and 3-3)** and tryptophan-starved HeLa cells **(Figure 5-9)**. The results of this analysis demonstrated a strong positive correlation between *SLC1A5* and *WARS* expression in several tumours, particularly human liver hepatocellular carcinoma, ovarian serous cystadenocarcinoma, glioblastoma multiforme and brain lower grade glioma **(Figure 5-23)**. Importantly, in these tumour types *SLC1A5* also correlated significantly with the expression of one or both of the tryptophan-degrading enzyme-encoding genes *IDO1* and *TDO2* **(Figure 5-23)**, hence supporting our *in vitro* data describing the tryptophan shortage-induced SLC1A5 upregulation in IDO^+ and TDO^+ tumour cell lines (Chapters 3.1 and 4.1).

5.3.3. SLC1A5 and IDO co-expression is associated with poor survival in brain lower grade glioma

We next assessed the significance of *SLC1A5* and *IDO1* tumour expression for patient prognosis. We found that, in brain lower grade glioma, which exhibited a particularly strong positive correlation between *SLC1A5* and *IDO1* expression **(Figure 5-23)**, high expression of *SLC1A5* was significantly associated with decreased patient survival (Hazard

ratio = 0.40526; log-rank test p value = 0.00006) **(Figure 5-24A)**. We also observed a similar association between survival and high *IDO1* expression in this tumour type (Hazard ratio = 0.46179; log-rank test p value = 0.00053) **(Figure 5-24B)**. Furthermore, patients with $IDO^{hi}SLC1A5^{lo}$ lower grade gliomas survived significantly longer than those with $IDO^{hi}SLC1A5^{hi}$ tumours (Hazard ratio = 0.49285; log-rank test p value = 0.01564), while $IDO^{lo}SLC1A5^{lo}$ tumours correlated with best prognosis **(Figure 5-24C)**. These data highlight the clinical importance of IDO and SLC1A5 upregulation by human tumours such as brain lower grade glioma.

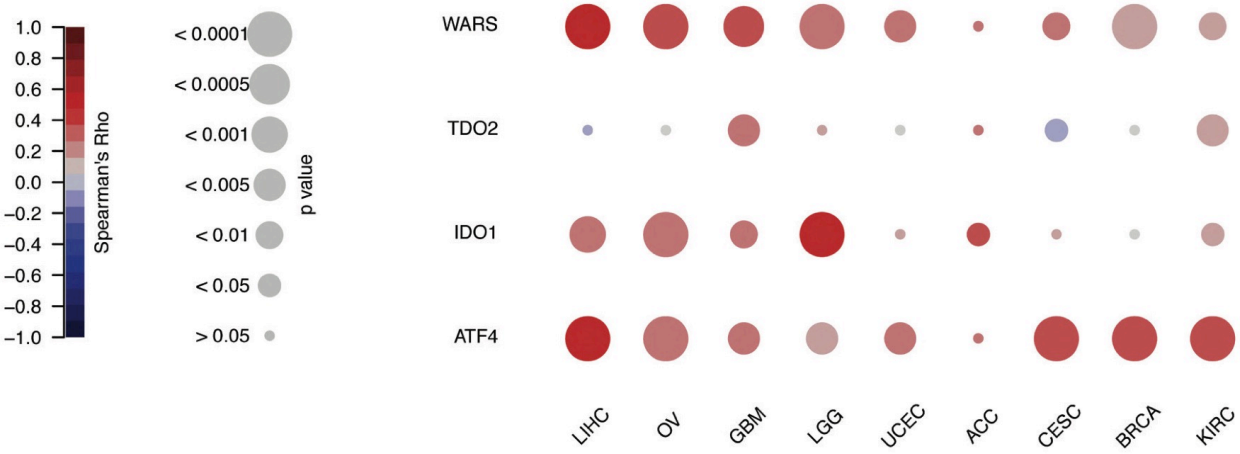

Figure 5-23. Expression of SLC1A5 correlates with the expression of tryptophan-degrading enzymes in primary human tumours

Spearman's rank correlation between *SLC1A5* and *WARS, TDO2, IDO1* or *ATF4* gene expression in RNA-seq data of human liver hepatocellular carcinoma (LIHC), ovarian serous cystadenocarcinoma (OV), glioblastoma multiforme (GBM), brain lower grade glioma (LGG), uterine corpus endometrial carcinoma (UCEC), adrenocortical carcinoma (ACC), cervical squamous cell carcinoma and endocervical adenocarcinoma (CESC), breast invasive carcinoma (BRCA) and kidney renal clear cell carcinoma (KIRC). The size of the circle indicates the significance of correlation.

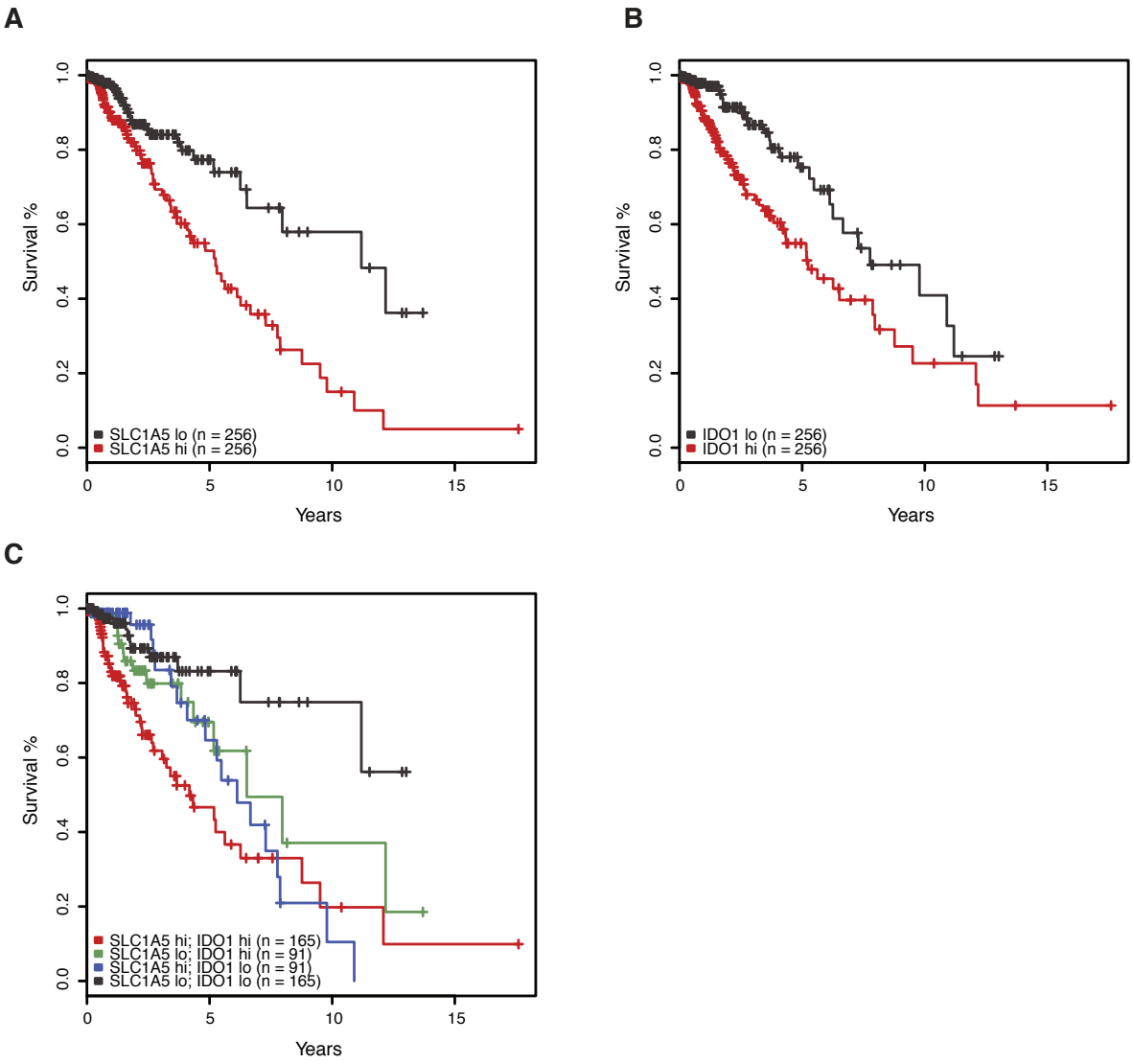

Figure 5-24. High expression of SLC1A5 and IDO1 is associated with decreased survival in brain lower grade glioma

(A) Kaplan-Meier curves comparing survival of patients with brain lower grade glioma tumours expressing high or low levels of *SLC1A5* (p value = 0.00006). **(B)** Kaplan-Meier curves comparing survival of patients with brain lower grade glioma tumours expressing high or low levels of *IDO1* (p value = 0.00053). **(C)** Kaplan-Meier curves comparing survival of patients with brain lower grade glioma tumours expressing high or low *SLC1A5* together with high or low levels of *IDO1* (p value = 0.00005). High and low expression of *SLC1A5* or *IDO1* was defined as above and below median expression, respectively.

5.4. Discussion

T cells are the major executors of the anti-tumour immune response, which is strongly hampered in the presence of tryptophan-degrading enzymes (Friberg et al., 2002; Ling et al., 2014; Muller et al., 2005; Muller et al., 2008; Opitz et al., 2011; Pilotte et al., 2012; Uyttenhove et al., 2003). Sensitivity of T cell proliferation to low tryptophan concentrations has been reported previously (Kudo et al., 2001; Munn et al., 2005; Silk et al., 2011; Uyttenhove et al., 2003). Consistently, we found that primary human T cell exposure to tryptophan-depleted microenvironment inhibited their proliferation. Specifically, this occurred at tryptophan concentrations ranging from 0μM to 5μM. Interestingly, as described in Chapter 4.1, tryptophan concentrations below 5μM also induce SLC1A5 upregulation in tumour cells, which points to a coordinated cancer immune evasion mechanism designed to inhibit T cell proliferation, while simultaneously upregulating compensatory signaling events in cancer cells.

Upon stimulation, T cells undergo extensive metabolic reprogramming to meet the increased energetic and biosynthetic demands of proliferating cells. This is reflected in the switch to anaerobic glycolysis (MacIver et al., 2013) and enhanced ability of activated T cells to transport amino acids like phenylalanine, leucine and glutamine (Carr et al., 2010; Nakaya et al., 2014; Sinclair et al., 2013). Furthermore, T cell activation is associated with upregulation of several amino acid transporters, including SLC7A5 (LAT1), SLC3A2 (CD98hc), as well as glutamine transporters SLC38A1 (SNAT1), SLC38A2 (SNAT2) and SLC1A5, among others (Carr et al., 2010; Sinclair et al., 2013). We have extended these findings by showing that SLC1A5 expression in human T cells is reflective of the T cell activation status. Specifically, we have demonstrated that SLC1A5 expression in both conventional $CD4^+$ and $CD8^+$ T cells, as well as CD1d-restricted iNKT cells, is not only positively regulated by stimulation, but is also modulated by the strength of TCR

engagement with cognate peptide or lipid antigen, respectively. Although the coupling of amino acid transporter expression to T cell activation has been previously reported (Carr et al., 2010; Sinclair et al., 2013), the molecular mechanisms regulating this phenomenon are not completely understood. A number of transporters upregulated upon T cell activation has been shown to be controlled by the transcription factor c-Myc, including glucose transporters GLUT1 and GLUT3 and amino acid transporters SLC1A5, SLC38A1, SLC7A5 and SLC3A2, as well as several enzymes involved in glucose and glutamine metabolism (Wang et al., 2011). In line with these findings, c-Myc also correlates with the expression of some amino acid transporters during asymmetric T cell division, including SLC1A5 and SLC3A2, but not SLC1A3 (Verbist et al., 2016). On the other hand, others have reported that upregulation of SLC1A5 but not SLC38A1, SLC38A2, SLC7A5 or SLC3A2 in activated T cells depends on the TCR signaling complex containing the scaffold protein CARMA1 (Nakaya et al., 2014), which is predominantly found in T cells and is involved in NF-κB and JNK pathway activation (Blonska et al., 2007; Gaide et al., 2002). CARMA1 appears to physically interact with SLC1A5 (Nakaya et al., 2014), however, the molecular mechanisms mediating SLC1A5 induction by this adaptor protein still remain unknown. So far, CARMA1 selectivity for SLC1A5 is also unexplained, and further research is required to improve our understanding of these issues. Notably, SLC1A5 upregulation following T cell activation has been shown to be important for glutamine, leucine and glucose uptake, mTOR activity and the switch to anaerobic glycolysis in stimulated T cells (Nakaya et al., 2014). A similar phenotype has also been observed in T cells lacking SLC7A5 amino acid transporter (Sinclair et al., 2013), which is functionally coupled to SLC1A5 (Nicklin et al., 2009). These studies highlight the key role of amino acid transport in the activation-induced metabolic reprogramming required for optimal T cell function.

Strikingly, although T cells were able to upregulate SLC1A5 in a TCR- and CD28-dependent manner, which could be mediated by c-Myc or CARMA1, based on previous findings (Nakaya et al., 2014; Wang et al., 2011), they failed to increase the levels of this amino acid transporter following tryptophan withdrawal, irrespectively of their activation status. Notably, this feature was not specific to MHC-restricted $CD4^+$ and $CD8^+$ T cells and also applied to CD1d-restricted iNKT cells. These findings highlight a key difference in the ability of tumour cells and T lymphocytes to adapt to tryptophan starvation.

We have shown that tryptophan shortage-induced amino acid transporter reprogramming in tumour cells is dependent on the activation of the ATF4 stress response pathway (Chapter 4.2). On the other hand, in addition to tryptophan-starved tumour cells, ATF4 activation could also be detected in T cells kept under low tryptophan conditions. Of note, in line with previous findings (Munn et al., 2005), this only occurred in activated but not resting T cells exposed to tryptophan deprivation. While the GCN2-ATF4 pathway is believed to mediate one of the major immunosuppressive effects of tryptophan catabolism – the induction of T cell proliferative arrest (Munn et al., 2005), very little is known about its effects on the amino acid transporter expression profile in T cells. Intriguingly, in tryptophan-starved T cells we observed a tailored ATF4-dependent transcriptional program, which differed from that of tumour cells exposed to low tryptophan microenvironment. We have confirmed that ATF4 pathway was functional in T cells, since tryptophan shortage was able to induce the expression of ATF4 target genes *GPT2* (Hao et al., 2016; Igarashi et al., 2007) and *ASNS* (Siu et al., 2002) in activated T cells, consistent with previous studies (Sundrud et al., 2009). In spite of this, ATF4 activation failed to trigger the transcription of ATF4-dependent genes *WARS* (Han et al., 2013; Harding et al., 2003) and *SLC1A5* in tryptophan-starved T cells. The fact that tumour cell lines readily upregulated these transcripts, paralleled by robust ATF4 expression, highlights differential regulation of the ATF4-

dependent tryptophan shortage compensatory mechanisms in tumour cells and T cells undergoing tryptophan starvation. How such differential regulation is mediated still remains unclear. One possibility is that ATF4 transcription factor fails to be efficiently recruited to the *SLC1A5* gene in tryptophan-starved T cells (in contrast to tumour cells, as described in Chapter 4.2.5) due to increased methylation of the ATF4-recognition site. ATF4-mediated transcription of *SLC1A5* could also be inhibited by a transcriptional repressor, such as FIAT (St-Arnaud et al., 2010) or DISC (Malavasi et al., 2012), or lack of epigenetic mechanisms cooperating with ATF4 in ensuring efficient transcription of ATF4-dependent genes, such as KDM4C-mediated H3K9 demethylation (Zhao et al., 2016). It would be insightful to compare the epigenetic landscape of *SLC1A5* promoter following tryptophan deficiency-induced ATF4 activation in tumour cells and T cells and perform further ATF4 ChIP studies to address these possibilities. Furthermore, it has been previously reported in the context of another amino acid transporter, SNAT2, that ATF4 binding to the C/EBP-ATF composite site of the target gene can occur without stimulation of transcriptional activity (Gjymishka et al., 2008). The authors describe a repressive signal downstream of ATF4 binding to *SNAT2* promoter, which inhibits *SNAT2* transcription in response to the unfolded protein response. It is possible that a similar mechanism may account for the lack of *SLC1A5* upregulation in tryptophan-starved T cells, and further research is required to test this hypothesis. Moreover, others have proposed that ATF4-induced transcription factors themselves, such as HOXB9, could act as negative regulators of T cell amino acid starvation response (Hayashi et al., 2016). Although we could detect HOXB9 upregulation in both tumour cells and T cells undergoing tryptophan starvation, which is inconsistent with the hypothesis that HOXB9 could prevent the changes in amino acid transporter profiling occurring under low tryptophan conditions, this transcription factor may still play an important role in nutritional stress, which is yet to be elucidated.

Consistent with the reported upregulation of SLC1A5 and other amino acid transporters in transformed versus normal cells (Fuchs and Bode, 2005), our *in vitro* experiments demonstrated abundant SLC1A5 expression in human tumour cell lines. Furthermore, although T cells upregulated SLC1A5 upon activation, under tryptophan deprivation conditions SLC1A5 expression was still significantly higher in tumour cells compared to T cells, even when the latter were given such a potent activation stimulus as treatment with αCD3/CD28 antibodies. Moreover, based on our finding that SLC1A5 expression in T cells is dependent on the strength of TCR engagement, it is very unlikely that *in vivo*, upon physiological levels of cognate MHC-peptide recognition, the levels of SLC1A5 upregulation in antigen-specific T cells can reach those induced by αCD3/CD28 antibodies. In line with this hypothesis, our *ex vivo* analysis of primary human renal cell carcinoma samples suggested that it is the tumour/stromal cells that represent the main exploiters of SLC1A5 upregulation strategies, while tumour-infiltrating $CD8^+$ T cells express low levels of SLC1A5. These data are consistent with the concepts of poor immunogenicity of tumour antigens and T cell anergy in cancer. On the other hand, we found that Treg cells from both healthy blood and cancer patient samples exhibited enhanced SLC1A5 expression. Interestingly, IDO-expressing tumours are often associated with increased Treg cell infiltration (Curti et al., 2007b; Liu et al., 2014; Nakamura et al., 2007; Spranger et al., 2013; Witkiewicz et al., 2009a; Yu et al., 2011), yet it remains largely unknown how this immunosuppressive population of T cells remains resistant to the local tryptophan depletion, which exerts detrimental effects on effector T cells, as demonstrated by our and other studies (Kudo et al., 2001; Munn et al., 1999; Munn et al., 2005; Silk et al., 2011). Although we have not assessed the ability of Treg cells to modulate their amino acid transporter expression profile upon tryptophan deprivation, the enriched basal levels of SLC1A5 expression that we observed in these cells under amino acid-sufficient conditions

suggest that Treg cells may exploit similar tryptophan shortage compensatory mechanisms to those of tumour cells. Notably, we found that both tumour cells and T cells rely on SLC1A5 for efficient amino acid import, as evidenced by the sensitivity of mTOR signaling to the pharmacological blockade of SLC1A5 in both tumour cells (Chapter 3.3) and activated T cells (Chapter 5.1). These data are consistent with the impaired activation-induced mTOR signaling reported in T cells lacking SLC1A5 (Nakaya et al., 2014), SLC7A5 (Sinclair et al., 2013) or CARMA1 (Hamilton et al., 2014) – an adaptor protein responsible for SLC1A5 upregulation in stimulated T cells (Nakaya et al., 2014). Hence, in the tumour microenvironment where the availability of tryptophan is restricted by the expression of tryptophan-degrading enzymes, SLC1A5 enrichment may allow tumour cells and Treg cells to efficiently compete for this essential amino acid. On the other hand, low levels of SLC1A5 expression in tumour-specific effector T cells, in combination with their inability to upregulate the appropriate amino acid transporters under low tryptophan conditions, may put these cells at a competitive disadvantage, compromising their function and thus contributing to further establishment of immunological tolerance. In line with these speculations, it has been recently shown that efficient metabolism is essential for the T cell anti-tumour effector function (Chang et al., 2015).

Moreover, our experiments demonstrated that IDO-inducing stimuli in the tumour microenvironment, such as PGE2 and IFNγ, can upregulate SLC1A5 expression in primary human MoDCs. Although further studies are required to dissect the role of SLC1A5 in DC maturation and function, our initial observations have further extended the link between tryptophan catabolism and amino acid transporter expression from tumour cells to IDO-competent APCs. In addition, we reported that activated iNKT cells, which are one of the major producers of IFNγ in the tumour microenvironment, also induced MoDCs to express IDO and SLC1A5. One can speculate that activated iNKT/conventional T cells may exert

similar effects on tumour cells (as well as tumour-associated myeloid cells) through IFNγ secretion, based on our findings that IFNγ acts as a potent inducer of IDO activity and amino acid transporter upregulation in tumour cells (Chapter 3.1). Such speculations would suggest that tumour-mediated activation of tryptophan-shortage compensatory mechanisms, such as upregulation of SLC1A5, may occur as a consequence of tumour-specific T cell infiltration. This hypothesis is consistent with the previously reported causative relationship between the immune pressure imposed on tumour cells by $CD8^+$ T cells and IDO induction in melanoma (Spranger et al., 2013), which suggests that tumour immune escape can be driven not only by cancer-specific pathways but also by the immune system itself.

Finally, we have extended our *in vitro* findings in human tumour cell lines by demonstrating that SLC1A5 upregulation can be observed in IDO-expressing mouse tumours growing *in vivo* under conditions of IDO-mediated tryptophan degradation. In addition, we have identified a positive correlation between IDO1 and SLC1A5 expression in several primary human tumours *in silico*, and demonstrated that such associations can be clinical important. In brain lower grade glioma, for example, we found that co-expression of IDO1 and SLC1A5 was significantly associated with decreased patient survival. Our observations complement previous studies, which have proposed high SLC1A5 expression as a marker of poor prognosis in MYCN-driven neuroblastoma (Ren et al., 2015), non-small cell lung cancer (Hassanein et al., 2015; Shimizu et al., 2014), breast cancer (Jeon et al., 2015), tongue cancer (Toyoda et al., 2014) and renal cell carcinoma (Liu et al., 2015). Our results also highlight the potential of using both SLC1A5 and IDO1 expression as prognostic biomarkers.

Collectively, our findings shed light on the biology of SLC1A5 expression in the resident cells of the tumour microenvironment, as well as primary mouse and human tumours, and

highlight the dichotomy between tumour cells and T cells in their ability to adapt to a low tryptophan microenvironment.

Final Summary

It has been known for more than 10 years that many tumours express tryptophan-degrading enzymes to suppress T cell activity in the tumour microenvironment. However, the mechanisms that allow tumour cells to resist the detrimental effects of local tryptophan depletion have so far remained elusive. This study aimed to address the hypothesis that tumour cells can adapt to a low tryptophan microenvironment through upregulation of their amino acid transport capacity. In summary, our results have demonstrated that shortage of tryptophan, induced by the expression of tryptophan-degrading enzymes IDO and TDO, initiates ATF4-dependent reprogramming of several amino acid transporter expression in tumour cells, including SLC1A5 and its truncated isoforms, which allows improved glutamine and tryptophan import into tumour cells. This previously unappreciated link between tryptophan catabolism and SLC1A5 expression can be observed not only in tumour cell lines *in vitro*, but also in primary mouse tumours *in vivo* and several primary human tumours *in silico*. Importantly, knockdown of SLC1A5 prevents optimal tumour cell proliferation under low tryptophan conditions, highlighting the key role of amino acid transport in tumour cell adaptation to nutritional stress. In contrast to tumour cells, both MHC- and CD1d-restricted human T cells fail to enhance SLC1A5 expression in response to tryptophan shortage, yet can upregulate it to some extent depending on the strength of cognate antigen TCR engagement. On the other hand, Treg cells and IDO-competent DCs exhibit enriched levels of SLC1A5, which is consistent with the ability of these cells to thrive in a tryptophan-depleted microenvironment.

In a tumour microenvironment where essential nutrients are scarce, such as in the case of an IDO/TDO-expressing tumour, cancer and immune cells' capacity for metabolic reprogramming may play a crucial role in the fate of tumour progression. It is clear that

tumour cells are able to initiate an efficient ATF4-dependent transcriptional program, which leads to the activation of compensatory mechanisms facilitating cell survival under conditions of nutritional stress. We have described SLC1A5 upregulation as one of such mechanisms; however, additional experiments are needed to assess the involvement of other potentially important tryptophan shortage compensatory strategies, such as WARS-mediated tryptophanyl-tRNA stock repletion and upregulation of enzymes involved in amino acid biosynthesis, as well as the specific roles of other amino acid transporters highly upregulated in IDO-expressing tumour cells in addition to SLC1A5 – SLC7A11 and SLC1A4. Given the roles of these proteins in cystine and glutamate transport, respectively, as well as the reported roles of cysteine-derived reducing agent glutathione and glutamate oncogenic signaling in the facilitation of tumour growth (Hu et al., 2014; Ishimoto et al., 2011), it would be insightful to determine the importance of these processes under conditions of IDO- and TDO-mediated tryptophan degradation. Notably, dissecting such pathways could provide novel therapeutic opportunities. It would be equally important to address the dichotomy between tumour cells and T cells in their ability to adapt to a low tryptophan microenvironment, as failure to employ the appropriate tryptophan shortage compensatory mechanisms may challenge T cell capacity to maintain metabolic homeostasis and mount an efficient anti-tumour immune response under conditions of tumour-imposed metabolic restriction. We speculate that the mechanisms underlying variable SLC1A5 expression in tumour cells and T cells undergoing tryptophan starvation may involve differential epigenetic regulation of ATF4-dependent transcription in these two cell types, and future studies are warranted to address this hypothesis. Furthermore, it also remains to be determined whether other resident cells of the tumour microenvironment, including Treg cells, tumour-associated myeloid cells, fibroblasts and stromal cells, all of which can contribute to immunological tolerance, are also able to

modulate their amino acid transporter expression profile in response to tryptophan deprivation, or whether such strategies are specific to tumour cells.

Finally, the results of our studies have the potential to aid in the development of novel therapeutic strategies for the treatment of cancer, such as targeting SLC1A5 in tumours expressing tryptophan-degrading enzymes IDO or TDO. Notably, such strategies would need to consider the importance of SLC1A5-mediated amino acid transport for optimal T cell function (Nakaya et al., 2014), and so would benefit from cancer cell-specific inhibition of SLC1A5 using antibody drug conjugates, for example. Furthermore, the inability of T cells to exploit strategies that can help compensate for tryptophan depletion in the tumour microenvironment may also be relevant in the context of cancer immunotherapies, as T cells expressing chimeric antigen receptors (CARs) have been reported to be susceptible to the immunosuppression mediated by tumour-derived IDO (Ninomiya et al., 2015). Thus, incorporating the capacity to upregulate the appropriate amino acid transporters as well as other potential tryptophan shortage compensatory mechanisms into CAR T cell design may improve the efficacy of such therapies. Lastly, our results demonstrating the clinical importance of IDO1 and SLC1A5 co-expression in brain lower grade glioma suggest that these genes could be exploited as prognostic biomarkers in this and possibly other cancer types.

In conclusion, our studies provide insights into the mechanisms that allow tumour cells but not T cells to withstand local tryptophan depletion in the tumour microenvironment and highlight the previously unappreciated role of amino acid transport in IDO- and TDO-mediated immune escape.

Appendix

Appendix I Map of pHR-SIN-IRES-GFP expression vector

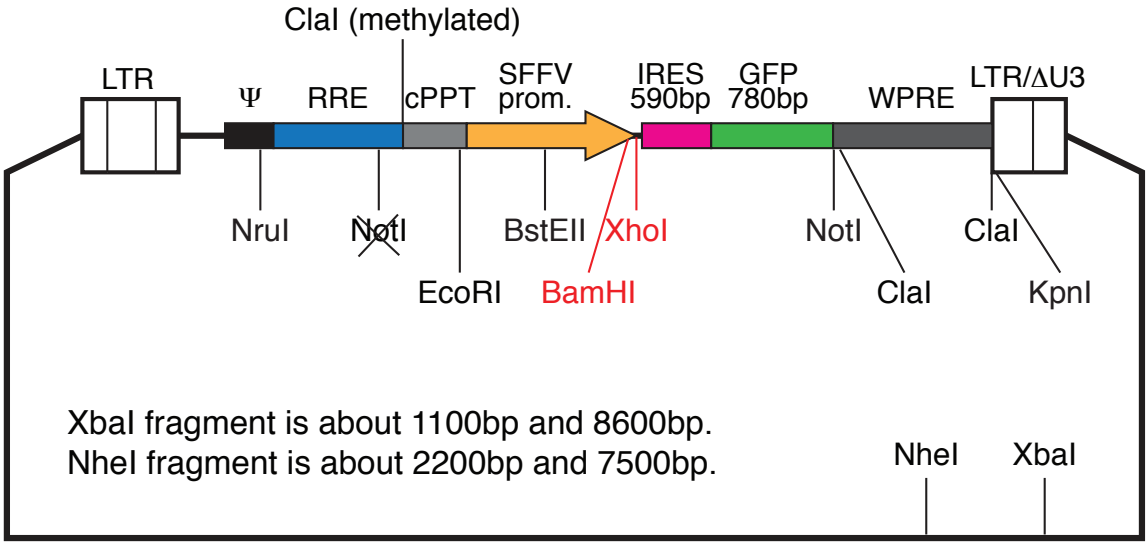

LTR	Long terminal repeat
Ψ	Packaging signal sequence
RRE	Rev-responsive element
cPPT	Central polypurine tract
SFFV prom.	Spleen focus-forming virus promoter
IRES	Internal ribosome entry site
GFP	Green fluorescent protein
WPRE	Woodchuck provirus response element
LTR/ΔU3	Transcriptional activator of HIV

pHR-SIN-IRES-GFP expression vector contains an SFFV and IRES driving the expression of GFP as a reporter gene. Inserts can be cloned between the *BamH*I and *Xho*I restriction sites downstream of the SFFV promoter (Demaison et al., 2002).

Appendix II Map of pHR-SIN-mCherry expression vector

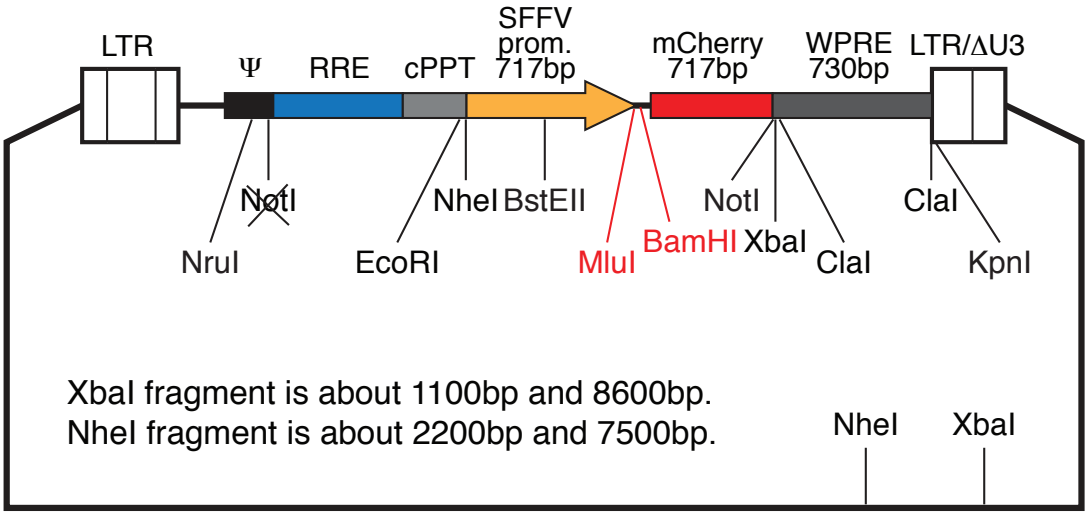

LTR	Long terminal repeat
Ψ	Packaging signal sequence
RRE	Rev-responsive element
cPPT	Central polypurine tract
SFFV prom.	Spleen focus-forming virus promoter
mCherry	mCherry red fluorescent protein
WPRE	Woodchuck provirus response element
LTR/ΔU3	Transcriptional activator of HIV

pHR-SIN-mCherry expression vector contains an SFFV driving the expression of mCherry as a reporter gene. Inserts can be cloned between the *Mlu*I and *BamH*I restriction sites downstream of the SFFV promoter (Demaison et al., 2002).

References

Albacker, L. A., Chaudhary, V., Chang, Y.-J., Kim, H. Y., Chuang, Y.-T., Pichavant, M., DeKruyff, R. H., Savage, P. B., and Umetsu, D. T. (2013). Invariant natural killer T cells recognize a fungal glycosphingolipid that can induce airway hyperreactivity. Nature Medicine *19*, 1297-1304.

Ameri, K., and Harris, A. L. (2008). Activating transcription factor 4. International Journal of Biochemistry & Cell Biology *40*, 14-21.

Anthony, T. G., McDaniel, B. J., Byerley, R. L., McGrath, B. C., Cavener, D. D. R., McNurlan, M. A., and Wek, R. C. (2004). Preservation of liver protein synthesis during dietary leucine deprivation occurs at the expense of skeletal muscle mass in mice deleted for eIF2 kinase GCN2. Journal of Biological Chemistry *279*, 36553-36561.

Armstrong, M. D., and Stave, U. (1973). Study of plasma free amino-acid levels. 2. Normal values for children and adults. Metabolism-Clinical and Experimental *22*, 561-569.

Astigiano, S., Morandi, B., Costa, R., Mastracci, L., D'Agostino, A., Ratto, G. B., Melioli, G., and Frumento, G. (2005). Eosinophil granulocytes account for indoleamine 2,3-dioxygenase-mediated immune escape in human non-small cell lung cancer. Neoplasia *7*, 390-396.

Austin, C. J. D., Mailu, B. M., Maghzal, G. J., Sanchez-Perez, A., Rahlfs, S., Zocher, K., Yuasa, H. J., Arthur, J. W., Becker, K., Stocker, R.*, et al.* (2010). Biochemical characteristics and inhibitor selectivity of mouse indoleamine 2,3-dioxygenase-2. Amino Acids *39*, 565-578.

Avissar, N. E., Sax, H. C., and Toia, L. (2008). In human entrocytes, GLN transport and ASCT2 surface expression induced by short-term EGF are MAPK, PI3K, and Rho-dependent. Digestive Diseases and Sciences *53*, 2113-2125.

Baban, B., Chandler, P. R., Sharma, M. D., Pihkala, J., Koni, P. A., Munn, D. H., and Mellor, A. L. (2009). IDO Activates Regulatory T Cells and Blocks Their Conversion into Th17-Like T Cells. Journal of Immunology *183*, 2475-2483.

Babcock, T. A., and Carlin, J. M. (2000). Transcriptional activation of indoleamine dioxygenase by interleukin 1 and tumor necrosis factor alpha in interferon-treated epithelial cells. Cytokine *12*, 588-594.

Babu, E., Kanai, Y., Chairoungdua, A., Kim, D. K., Iribe, Y., Tangtrongsup, S., Jutabha, P., Li, Y. W., Ahmed, N., Sakamoto, S.*, et al.* (2003). Identification of a novel system L amino acid transporter structurally distinct from heterodimeric amino acid transporters. Journal of Biological Chemistry *278*, 43838-43845.

Balachandran, V. P., Cavnar, M. J., Zeng, S., Bamboat, Z. M., Ocuin, L. M., Obaid, H., Sorenson, E. C., Popow, R., Ariyan, C., Rossi, F.*, et al.* (2011). Imatinib potentiates antitumor T cell responses in gastrointestinal stromal tumor through the inhibition of Ido. Nature Medicine *17*, 1094-1100.

Ball, H. J., Sanchez-Perez, A., Weiser, S., Austin, C. J. D., Astelbauer, F., Miu, J., McQuillan, J. A., Stocker, R., Jermiin, L. S., and Hunt, N. H. (2007). Characterization of an indoleamine 2,3-dioxygenase-like protein found in humans and mice. Gene *396*, 203-213.

Banerjee, T., DuHadaway, J. B., Gaspari, P., Sutanto-Ward, E., Munn, D. H., Mellor, A. L., Malachowski, W. P., Prendergast, G. C., and Muller, A. J. (2008). A key in vivo antitumor mechanism of action of natural product-based brassinins is inhibition of indoleamine 2,3-dioxygenase. Oncogene *27*, 2851-2857.

Bar-Peled, L., Schweitzer, L. D., Zoncu, R., and Sabatini, D. M. (2012). Ragulator Is a GEF for the Rag GTPases that Signal Amino Acid Levels tomTORC1. Cell *150*, 1196-1208.

Barcelo-Batllori, S., Andre, M., Servis, C., Levy, N., Takikawa, O., Michetti, P., Reymond, M., and Felley-Bosco, E. (2002). Proteomic analysis of cytokine induced proteins in human intestinal epithelial cells: Implications for inflammatory bowel diseases. Proteomics *2*, 551-560.

Barnes, N. A., Stephenson, S. J., Tooze, R. M., and Doody, G. M. (2009). Amino Acid Deprivation Links BLIMP-1 to the Immunomodulatory Enzyme Indoleamine 2,3-Dioxygenase. Journal of Immunology *183*, 5768-5777.

Basran, J., Rafice, S. A., Chauhan, N., Efimov, I., Cheesman, M. R., Ghamsari, L., and Raven, E. L. (2008). A kinetic, spectroscopic, and redox study of human tryptophan 2,3-dioxygenase. Biochemistry *47*, 4752-4760.

Basu, G. D., Tinder, T. L., Bradley, J. M., Tu, T., Hattrup, C. L., Pockaj, B. A., and Mukherjee, P. (2006). Cyclooxygenase-2 inhibitor enhances the efficacy of a breast cancer vaccine: role of IDO. Journal of immunology (Baltimore, Md : 1950) *177*, 2391-2402.

Beretta, L., Gingras, A. C., Svitkin, Y. V., Hall, M. N., and Sonenberg, N. (1996). Rapamycin blocks the phosphorylation of 4E-BP1 and inhibits cap-dependent initiation of translation. Embo Journal *15*, 658-664.

Bersten, D. C., Sullivan, A. E., Peet, D. J., and Whitelaw, M. L. (2013). bHLH-PAS proteins in cancer. Nature Reviews Cancer *13*, 827-841.

Bhutia, Y. D., Babu, E., Ramachandran, S., and Ganapathy, V. (2015). Amino Acid Transporters in Cancer and Their Relevance to "Glutamine Addiction": Novel Targets for the Design of a New Class of Anticancer Drugs. Cancer Research *75*, 1782-1788.

Biasini, M., Bienert, S., Waterhouse, A., Arnold, K., Studer, G., Schmidt, T., Kiefer, F., Cassarino, T. G., Bertoni, M., Bordoli, L., and Schwede, T. (2014). SWISS-MODEL: modelling protein tertiary and quaternary structure using evolutionary information. Nucleic Acids Research *42*, W252-W258.

Bjerregaard, B., Holck, S., Christensen, I. J., and Larsson, L. I. (2006). Syncytin is involved in breast cancer-endothelial cell fusions. Cellular and Molecular Life Sciences *63*, 1906-1911.

Blond, J. L., Lavillette, D., Cheynet, V., Bouton, O., Oriol, G., Chapel-Fernandes, S., Mandrand, B., Mallet, F., and Cosset, F. L. (2000). An envelope glycoprotein of the human endogenous retrovirus HERV-W is expressed in the human placenta and fuses cells expressing the type D mammalian retrovirus receptor. Journal of Virology *74*, 3321-3329.

Blonska, M., Pappu, B. P., Matsumoto, R., Li, H. X., Su, B., Wang, D. M., and Lin, X. (2007). The CARMA1-Bcl10 signaling complex selectively regulates JNK2 kinase in the T cell receptor-signaling pathway. Immunity *26*, 55-66.

Bolzoni, M., Chiu, M., Accardi, F., Vescovini, R., Airoldi, I., Storti, P., Todoerti, K., Agnelli, L., Missale, G., Andreoli, R.*, et al.* (2016). Dependence on glutamine uptake and glutamine addiction characterize myeloma cells: a new attractive target. Blood *128*, 667-679.

Bozec, A., Zaiss, M. M., Kagwiria, R., Voll, R., Rauh, M., Chen, Z., Mueller-Schmucker, S., Kroczek, R. A., Heinzerling, L., Moser, M.*, et al.* (2014). T Cell Costimulation Molecules CD80/86 Inhibit Osteoclast Differentiation by Inducing the IDO/Tryptophan Pathway. Science Translational Medicine *6*, 235ra260.

Bozza, S., Fallarino, F., Pitzurra, L., Zelante, T., Montagnoli, C., Bellocchio, S., Mosci, P., Vacca, C., Puccetti, P., and Romani, L. (2005). A crucial role for tryptophan catabolism at the host/Candida albicans interface. Journal of Immunology *174*, 2910-2918.

Brandacher, G., Perathoner, A., Ladurner, R., Schneeberger, S., Obrist, P., Winkler, C., Werner, E. R., Werner-Felmayer, G., Weiss, H. G., Gobel, G.*, et al.* (2006). Prognostic value of indoleamine 2,3-dioxygenase expression in colorectal cancer: Effect on tumor-infiltrating T cells. Clinical Cancer Research *12*, 1144-1151.

Braun, D., Longman, R. S., and Albert, M. L. (2005). A two-step induction of indoleamine 2,3 dioxygenase (IDO) activity during dendritic-cell maturation. Blood *106*, 2375-2381.

Brody, J. R., Costantino, C. L., Berger, A. C., Sato, T., Lisanti, M. P., Yeo, C. J., Emmons, R. V., and Witkiewicz, A. K. (2009). Expression of indoleamine 2,3-dioxygenase in metastatic malignant melanoma recruits regulatory T cells to avoid immune detection and affects survival. Cell Cycle *8*, 1930-1934.

Brunkow, M. E., Jeffery, E. W., Hjerrild, K. A., Paeper, B., Clark, L. B., Yasayko, S. A., Wilkinson, J. E., Galas, D., Ziegler, S. F., and Ramsdell, F. (2001). Disruption of a new forkhead/winged-helix protein, scurfin, results in the fatal lymphoproliferative disorder of the scurfy mouse. Nature Genetics *27*, 68-73.

Brunn, G. J., Hudson, C. C., Sekulic, A., Williams, J. M., Hosoi, H., Houghton, P. J., Lawrence, J. C., and Abraham, R. T. (1997). Phosphorylation of the translational repressor PHAS-I by the mammalian target of rapamycin. Science *277*, 99-101.

Burnet, F. M. (1970). Concept of immunological surveillance. Progress in Experimental Tumor Research *13*, 1-27.

Byrne, G. I., Lehmann, L. K., and Landry, G. J. (1986). Induction of tryptophan catabolism is the mechanism for gamma-interferon-mediated inhibition of intracellular chlamydia-psittaci replication in T24 cells. Infection and Immunity *53*, 347-351.

Cantor, J., Browne, C. D., Ruppert, R., Feral, C. C., Faessler, R., Rickert, R. C., and Ginsberg, M. H. (2009). CD98hc facilitates B cell proliferation and adaptive humoral immunity. Nature Immunology *10*, 412-419.

Cantor, J., Slepak, M., Ege, N., Chang, J. T., and Ginsberg, M. H. (2011). Loss of T Cell CD98 H Chain Specifically Ablates T Cell Clonal Expansion and Protects from Autoimmunity. Journal of Immunology *187*, 851-860.

Cantor, J. M., and Ginsberg, M. H. (2012). CD98 at the crossroads of adaptive immunity and cancer. Journal of Cell Science *125*, 1373-1382.

Carlin, J. M., Borden, E. C., Sondel, P. M., and Byrne, G. I. (1987). Biologic response modifier-induced indoleamine 2,3-dioxygenase activity in human peripheral-blood mononuclear cell-cultures. Journal of Immunology *139*, 2414-2418.

Carlin, J. M., Borden, E. C., Sondel, P. M., and Byrne, G. I. (1989a). Interferon-induced indoleamine 2,3-dioxygenase activity in human mononuclear phagocytes. Journal of Leukocyte Biology *45*, 29-34.

Carlin, J. M., Ozaki, Y., Byrne, G. I., Brown, R. R., and Borden, E. C. (1989b). Interferons and indoleamine 2,3-dioxygenase - role in antimicrobial and antitumor effects. Experientia *45*, 535-541.

Carr, E. L., Kelman, A., Wu, G. S., Gopaul, R., Senkevitch, E., Aghvanyan, A., Turay, A. M., and Frauwirth, K. A. (2010). Glutamine Uptake and Metabolism Are Coordinately Regulated by ERK/MAPK during T Lymphocyte Activation. Journal of Immunology *185*, 1037-1044.

Cerundolo, V., Silk, J. D., Masri, S. H., and Salio, M. (2009). Harnessing invariant NKT cells in vaccination strategies. Nature reviews Immunology *9*, 28-38.

Cesar-Razquin, A., Snijder, B., Frappier-Brinton, T., Isserlin, R., Gyimesi, G., Bai, X., Reithmeier, R. A., Hepworth, D., Hediger, M. A., Edwards, A. M., and Superti-Furga, G. (2015). A Call for Systematic Research on Solute Carriers. Cell *162*, 478-487.

Chang, C. H., Qiu, J., O'Sullivan, D., Buck, M. D., Noguchi, T., Curtis, J. D., Chen, Q. Y., Gindin, M., Gubin, M. M., van der Windt, G. J. W.*, et al.* (2015). Metabolic Competition in the Tumor Microenvironment Is a Driver of Cancer Progression. Cell *162*, 1229-1241.

Chen, J. J., Throop, M. S., Gehrke, L., Kuo, I., Pal, J. K., Brodsky, M., and London, I. M. (1991). Cloning of the cDNA of the heme-regulated eukaryotic initiation factor-2-alpha (EIF-2-alpha) kinase of rabbit reticulocytes - homology to yeast GCN2 protein-kinase and human double-stranded-RNA-dependent EIF-2-alpha kinase. Proc Natl Acad Sci U S A *88*, 7729-7733.

Chen, J. L., Dunbar, P. R., Gileadi, U., Jager, E., Gnjatic, S., Nagata, Y., Stockert, E., Panicalli, D. L., Chen, Y. T., Knuth, A.*, et al.* (2000). Identification of NY-ESO-1 peptide analogues capable of improved stimulation of tumor-reactive CTL. Journal of Immunology *165*, 948-955.

Chen, W., Liang, X., Peterson, A. J., Munn, D. H., and Blazar, B. R. (2008). The indoleamine 2,3-dioxygenase pathway is essential for human plasmacytoid dendritic cell-induced adaptive T regulatory cell generation. Journal of Immunology *181*, 5396-5404.

Choi, B. K., Asai, T., Vinay, D. S., Kim, Y. H., and Kwon, B. S. (2006). 4-1BB-mediated amelioration of experimental autoimmune uveoretinitis is caused by indoleamine 2,3-dioxygenase-dependent mechanisms. Cytokine *34*, 233-242.

Chon, S. Y., Hassanain, H. H., Pine, R., and Gupta, S. L. (1995). Involvement of 2 regulatory elements in interferon-gamma-regulated expression of human indoleamine 2,3-dioxygenase gene. Journal of Interferon and Cytokine Research *15*, 517-526.

Chung, D. J., Rossi, M., Romano, E., Ghith, J., Yuan, J., Munn, D. H., and Young, J. W. (2009). Indoleamine 2,3-dioxygenase-expressing mature human monocyte-derived dendritic cells expand potent autologous regulatory T cells. Blood *114*, 555-563.

Ciorba, M. A., Bettonville, E. E., McDonald, K. G., Metz, R., Prendergast, G. C., Newberry, R. D., and Stenson, W. F. (2010). Induction of IDO-1 by Immunostimulatory DNA Limits Severity of Experimental Colitis. Journal of Immunology *184*, 3907-3916.

Cobbold, S. P., Adams, E., Farquhar, C. A., Nolan, K. F., Howie, D., Lui, K. O., Fairchild, P. J., Mellor, A. L., Ron, D., and Waldmann, H. (2009). Infectious tolerance via the consumption of essential amino acids and mTOR signaling. Proc Natl Acad Sci U S A *106*, 12055-12060.

Comings, D. E. (2001). Clinical and molecular genetics of ADHD and Tourette syndrome - Two related polygenic disorders. In Adult Attention Deficit Disorder: Brain Mechanisms and Life Outcomes, J. Wasserstein, L.E. Wolf, and F.F. LeFever, eds., pp. 50-83.

Cong, L., Ran, F. A., Cox, D., Lin, S., Barretto, R., Habib, N., Hsu, P. D., Wu, X., Jiang, W., Marraffini, L. A., and Zhang, F. (2013). Multiplex Genome Engineering Using CRISPR/Cas Systems. Science *339*, 819-823.

Console, L., Scalise, M., Tarmakova, Z., Coe, I. R., and Indiveri, C. (2015). N-linked Glycosylation of human SLC1A5 (ASCT2) transporter is critical for trafficking to membrane. Biochimica Et Biophysica Acta-Molecular Cell Research *1853*, 1636-1645.

Coquerelle, C., Oldenhove, G., Acolty, V., Denoeud, J., Vansanten, G., Verdebout, J. M., Mellor, A., Bluestone, J. A., and Moser, M. (2009). Anti-CTLA-4 treatment induces IL-10-producing ICOS+ regulatory T cells displaying IDO-dependent anti-inflammatory properties in a mouse model of colitis. Gut *58*, 1363-1373.

Cormerais, Y., Giuliano, S., LeFloch, R., Front, B., Durivault, J., Tambutte, E., Massard, P. A., de la Ballina, L. R., Endou, H., Wempe, M. F.*, et al.* (2016). Genetic Disruption of the Multifunctional CD98/LAT1 Complex Demonstrates the Key Role of Essential Amino Acid Transport in the Control of mTORC1 and Tumor Growth. Cancer Res *76*, 4481-4492.

Crespo, J., Sun, H., Welling, T. H., Tian, Z., and Zou, W. (2013). T cell anergy, exhaustion, senescence, and stemness in the tumor microenvironment. Curr Opin Immunol *25*, 214-221.

Curiel, T. J., Coukos, G., Zou, L. H., Alvarez, X., Cheng, P., Mottram, P., Evdemon-Hogan, M., Conejo-Garcia, J. R., Zhang, L., Burow, M.*, et al.* (2004). Specific recruitment

of regulatory T cells in ovarian carcinoma fosters immune privilege and predicts reduced survival. Nature Medicine *10*, 942-949.

Curran, T. A., Jalili, R. B., Farrokhi, A., and Ghahary, A. (2014). IDO expressing fibroblasts promote the expansion of antigen specific regulatory T cells. Immunobiology *219*, 17-24.

Curti, A., Aluigi, M., Pandolfi, S., Ferri, E., Isidori, A., Salvestrini, V., Durelli, I., Horenstein, A. L., Fiore, F., Massaia, M.*, et al.* (2007a). Acute myeloid leukemia cells constitutively express the immunoregulatory enzyme indoleamine 2,3-dioxygenase. Leukemia *21*, 353-355.

Curti, A., Pandolfi, S., Valzasina, B., Aluigi, M., Isidori, A., Ferri, E., Salvestrini, V., Bonanno, G., Rutella, S., Durelli, I.*, et al.* (2007b). Modulation of tryptophan catabolism by human leukemic cells results in the conversion of CD25(-) into CD25(+) T regulatory cells. Blood *109*, 2871-2877.

Curti, A., Trabanelli, S., Onofri, C., Aluigi, M., Salvestrini, V., Ocadlikova, D., Evangelisti, C., Rutella, S., De Cristofaro, R., Ottaviani, E.*, et al.* (2010). Indoleamine 2,3-dioxygenase-expressing leukemic dendritic cells impair a leukemia-specific immune response by inducing potent T regulatory cells. Haematologica *95*, 2022-2030.

De Luca, A., Carvalho, A., Cunha, C., Iannitti, R. G., Pitzurra, L., Giovannini, G., Mencacci, A., Bartolommei, L., Moretti, S., Massi-Benedetti, C.*, et al.* (2013). IL-22 and IDO1 Affect Immunity and Tolerance to Murine and Human Vaginal Candidiasis. Plos Pathogens *9*.

De Ravin, S. S., Zarember, K. A., Long-Priel, D., Chan, K. C., Fox, S. D., Gallin, J. I., Kuhns, D. B., and Malech, H. L. (2010). Tryptophan/kynurenine metabolism in human leukocytes is independent of superoxide and is fully maintained in chronic granulomatous disease. Blood *116*, 1755-1760.

DeFranco, A. L., Locksley, R. M., and Robertson, M. (2007). Immunity: The Immune Response in Infectious and Inflammatory Disease: New Science Press.

Della Chiesa, M., Carlomagno, S., Frumento, G., Balsamo, M., Cantoni, C., Conte, R., Moretta, L., Moretta, A., and Vitale, M. (2006). The tryptophan catabolite L-kynurenine

inhibits the surface expression of NKp46-and NKG2D-activating receptors and regulates NK-cell function. Blood *108*, 4118-4125.

Demaison, C., Parsley, K., Brouns, G., Scherr, M., Battmer, K., Kinnon, C., Grez, M., and Thrasher, A. J. (2002). High-level transduction and gene expression in hematopoietic repopulating cells using a human immunodeficiency virus type 1-based lentiviral vector containing an internal spleen focus forming virus promoter. Human gene therapy *13*, 803-813.

Demarte, M. L., and Enesco, H. E. (1985). Influence of diet on plasma tryptophan and brain-serotonin levels in mice. Experientia *41*, 48-50.

Deng, J., Harding, H. P., Raught, B., Gingras, A. C., Berlanga, J. J., Scheuner, D., Kaufman, R. J., Ron, D., and Sonenberg, N. (2002). Activation of GCN2 in UV-irradiated cells inhibits translation. Current Biology *12*, 1279-1286.

Denkberg, G., Stronge, V. S., Zahavi, E., Pittoni, P., Oren, R., Shepherd, D., Salio, M., McCarthy, C., Illarionov, P. A., van der Merwe, A.*, et al.* (2008). Phage display-derived recombinant antibodies with TCR-like specificity against alpha-galactosylceramide and its analogues in complex with human CD1d molecules. European Journal of Immunology *38*, 829-840.

Dever, T. E., Feng, L., Wek, R. C., Cigan, A. M., Donahue, T. F., and Hinnebusch, A. G. (1992). Phosphorylation of initiation factor-2-alpha by protein-kinase GCN2 mediates gene-specific translational control of GCN4 in yeast. Cell *68*, 585-596.

Dey, S., Savant, S., Teske, B. F., Hatzoglou, M., Calkhoven, C. F., and Wek, R. C. (2012). Transcriptional repression of ATF4 gene by CCAAT/enhancer-binding protein beta (C/EBPbeta) differentially regulates integrated stress response. The Journal of biological chemistry *287*, 21936-21949.

DiNatale, B. C., Murray, I. A., Schroeder, J. C., Flaveny, C. A., Lahoti, T. S., Laurenzana, E. M., Omiecinski, C. J., and Perdew, G. H. (2010). Kynurenic Acid Is a Potent Endogenous Aryl Hydrocarbon Receptor Ligand that Synergistically Induces Interleukin-6 in the Presence of Inflammatory Signaling. Toxicological Sciences *115*, 89-97.

Divanovic, S., Sawtell, N. M., Trompette, A., Warning, J. I., Dias, A., Cooper, A. M., Yap, G. S., Arditi, M., Shimada, K., DuHadaway, J. B.*, et al.* (2012). Opposing Biological Functions of Tryptophan Catabolizing Enzymes During Intracellular Infection. Journal of Infectious Diseases *205*, 152-161.

Dolusic, E., Larrieu, P., Moineaux, L., Stroobant, V., Pilotte, L., Colau, D., Pochet, L., Van den Eynde, B., Masereel, B., Wouters, J., and Frederick, R. (2011). Tryptophan 2,3-Dioxygenase (TDO) Inhibitors. 3-(2-(Pyridyl)ethenyl)indoles as Potential Anticancer Immunomodulators. Journal of Medicinal Chemistry *54*, 5320-5334.

Dong, J. S., Qiu, H. F., Garcia-Barrio, M., Anderson, J., and Hinnebusch, A. G. (2000). Uncharged tRNA activates GCN2 by displacing the protein kinase moiety from a bipartite tRNA-Binding domain. Mol Cell *6*, 269-279.

Dunn, G. P., Old, L. J., and Schreiber, R. D. (2004). The three Es of cancer immunoediting. Annual Review of Immunology *22*, 329-360.

Ehrlich, P. (1909). Ueber den jetzigen Stand der Karzinomforschung. Ned Tijdschr Geneeskd *5*, 273–290

Eleftheriadis, T., Pissas, G., Antoniadi, G., Spanoulis, A., Liakopoulos, V., and Stefanidis, I. (2014). Indoleamine 2,3-dioxygenase increases p53 levels in alloreactive human T cells, and both indoleamine 2,3-dioxygenase and p53 suppress glucose uptake, glycolysis and proliferation. International Immunology *26*, 673-684.

Eleftheriadis, T., Pissas, G., Yiannaki, E., Markala, D., Arampatzis, S., Antoniadi, G., Liakopoulos, V., and Stefanidis, I. (2013). Inhibition of indoleamine 2,3-dioxygenase in mixed lymphocyte reaction affects glucose influx and enzymes involved in aerobic glycolysis and glutaminolysis in alloreactive T-cells. Human Immunology *74*, 1501-1509.

Esser, C., Rannug, A., and Stockinger, B. (2009). The aryl hydrocarbon receptor in immunity. Trends in Immunology *30*, 447-454.

Fallarino, F., Asselin-Paturel, C., Vacca, C., Bianchi, R., Gizzi, S., Fioretti, M. C., Trinchieri, G., Grohmann, U., and Puccetti, P. (2004). Murine plasmacytoid dendritic cells initiate the immunosuppressive pathway of tryptophan catabolism in response to CD200 receptor engagement. Journal of Immunology *173*, 3748-3754.

Fallarino, F., Grohmann, U., Hwang, K. W., Orabona, C., Vacca, C., Bianchi, R., Belladonna, M. L., Fioretti, M. C., Alegre, M. L., and Puccetti, P. (2003). Modulation of tryptophan catabolism by regulatory T cells. Nature Immunology *4*, 1206-1212.

Fallarino, F., Grohmann, U., You, S., McGrath, B. C., Cavener, D. R., Vacca, C., Orabona, C., Bianchi, R., Belladonna, M. L., Volpi, C.*, et al.* (2006). The combined effects of tryptophan starvation and tryptophan catabolites down-regulate T cell receptor zeta-chain and induce a regulatory phenotype in naive T cells. Journal of Immunology *176*, 6752-6761.

Fallarino, F., and Puccetti, P. (2006). Toll-like receptor 9-mediated induction of the immunosuppressive pathway of tryptophan catabolism. European Journal of Immunology *36*, 8-11.

Fallarino, F., Vacca, C., Orabona, C., Belladonna, M. L., Bianchi, R., Marshall, B., Keskin, D. B., Mellor, A. L., Fioretti, M. C., Grohmann, U., and Puccetti, P. (2002a). Functional expression of indoleamine 2,3-dioxygenase by murine CD8 alpha(+) dendritic cells. International Immunology *14*, 65-68.

Fallarino, I., Grohmann, U., Vacca, C., Bianchi, R., Orabona, C., Spreca, A., Fioretti, M. C., and Puccetti, P. (2002b). T cell apoptosis by tryptophan catabolism. Cell Death and Differentiation *9*, 1069-1077.

Fenczik, C. A., Sethi, T., Ramos, J. W., Hughes, P. E., and Ginsberg, M. H. (1997). Complementation of dominant suppression implicates CD98 in integrin activation. Nature *390*, 81-85.

Feral, C. C., Nishiya, N., Fenczik, C. A., Stuhlmann, H., Slepak, M., and Ginsberg, M. H. (2005). CD98hc (SLC3A2) mediates integrin signaling. Proc Natl Acad Sci U S A *102*, 355-360.

Ferrand, J., and Ferrero, R. L. (2013). Recognition of Extracellular Bacteria by NLRs and Its Role in the Development of Adaptive Immunity. Front Immunol *4*, 344.

Forouhar, F., Anderson, J. L. R., Mowat, C. G., Vorobiev, S. M., Hussain, A., Abashidze, M., Bruckmann, C., Thackray, S. J., Seetharaman, J., Tucker, T.*, et al.* (2007). Molecular

insights into substrate recognition and catalysis by tryptophan 2,3-dioxygenase. Proc Natl Acad Sci U S A *104*, 473-478.

Fox, J. M., Crabtree, J. M., Sage, L. K., Tompkins, S. M., and Tripp, R. A. (2015). Interferon Lambda Upregulates IDO1 Expression in Respiratory Epithelial Cells After Influenza Virus Infection. Journal of interferon & cytokine research : the official journal of the International Society for Interferon and Cytokine Research *35*, 554-562.

Friberg, M., Jennings, R., Alsarraj, M., Dessureault, S., Cantor, A., Extermann, M., Mellor, A. L., Munn, D. H., and Antonia, S. J. (2002). Indoleamine 2,3-dioxygenase contributes to tumor cell evasion of T cell-mediated rejection. International Journal of Cancer *101*, 151-155.

Frumento, G., Rotondo, R., Tonetti, M., Damonte, G., Benatti, U., and Ferrara, G. B. (2002). Tryptophan-derived catabolites are responsible for inhibition of T and natural killer cell proliferation induced by indoleamine 2,3-dioxygenase. Journal of Experimental Medicine *196*, 459-468.

Fuchs, B. C., and Bode, B. P. (2005). Amino acid transporters ASCT2 and LAT1 in cancer: Partners in crime? Seminars in Cancer Biology *15*, 254-266.

Fuchs, B. C., Finger, R. E., Onan, M. C., and Bode, B. P. (2007). ASCT2 silencing regulates mammalian target-of-rapamycin growth and survival signaling in human hepatoma cells. American Journal of Physiology-Cell Physiology *293*, C55-C63.

Fujigaki, H., Saito, K., Fujigaki, S., Takemura, M., Sudo, K., Ishiguro, H., and Seishima, M. (2006). The signal transducer and activator of transcription 1 alpha and interferon regulatory factor 1 are not essential for the induction of indoleamine 2,3-dioxygenase by lipopolysaccharide: Involvement of p38 mitogen-activated protein kinase and nuclear Factor-kappa B pathways, and synergistic effect of several proinflammatory cytokines. Journal of Biochemistry *139*, 655-662.

Fukunaga, M., Yamamoto, Y., Kawasoe, M., Arioka, Y., Murakami, Y., Hoshi, M., and Saito, K. (2012). Studies on Tissue and Cellular Distribution of Indoleamine 2,3-Dioxygenase 2: The Absence of IDO1 Upregulates IDO2 Expression in the Epididymis. Journal of Histochemistry & Cytochemistry *60*, 854-860.

Funatake, C. J., Marshall, N. B., Steppan, L. B., Mourich, D. V., and Kerkvliet, N. I. (2005). Cutting edge: Activation of the aryl hydrocarbon receptor by 2,3,7,8-tetrachlorodibenzo-p-dioxin generates a population of CD4(+)CD25(+) cells with characteristics of regulatory T cells. Journal of Immunology *175*, 4184-4188.

Gaide, O., Favier, B., Legler, D. F., Bonnet, D., Brissoni, B., Valitutti, S., Bron, C., Tschopp, J., and Thome, M. (2002). CARMA1 is a critical lipid raft-associated regulator of TCR-induced NF-kappa B activation. Nature Immunology *3*, 836-843.

Ganapathy, V., Thangaraju, M., and Prasad, P. D. (2009). Nutrient transporters in cancer: relevance to Warburg hypothesis and beyond. Pharmacol Ther *121*, 29-40.

Gandhi, R., Kumar, D., Burns, E. J., Nadeau, M., Dake, B., Laroni, A., Kozoriz, D., Weiner, H. L., and Quintana, F. J. (2010). Activation of the aryl hydrocarbon receptor induces human type 1 regulatory T cell-like and Foxp3(+) regulatory T cells. Nature Immunology *11*, 846-853.

Gao, Y.-F., Peng, R.-Q., Li, J., Ding, Y., Zhang, X., Wu, X.-J., Pan, Z.-Z., Wan, D.-S., Zeng, Y.-X., and Zhang, X.-S. (2009). The paradoxical patterns of expression of indoleamine 2,3-dioxygenase in colon cancer. Journal of Translational Medicine *7*.

Ge, K., DuHadaway, J., Du, W., Herlyn, M., Rodeck, U., and Prendergast, G. C. (1999). Mechanism for elimination of a tumor suppressor: Aberrant splicing of a brain-specific exon causes loss of function of Bin1 in melanoma. Proc Natl Acad Sci U S A *96*, 9689-9694.

Ge, K., Duhadaway, J., Sakamuro, D., Wechsler-Reya, R., Reynolds, C., and Prendergast, G. C. (2000a). Losses of the tumor suppressor BIN1 in breast carcinoma are frequent and reflect deficits in programmed cell death capacity. International Journal of Cancer *85*, 376-383.

Ge, K., Minhas, F., Duhadaway, J., Mao, N. C., Wilson, D., Buccafusca, R., Sakamuro, D., Nelson, P., Malkowicz, S. B., Tomaszewski, J., and Prendergast, G. C. (2000b). Loss of heterozygosity and tumor suppressor activity of BIN1 in prostate carcinoma. International Journal of Cancer *86*, 155-161.

Gibney, G., Hamid, O., Lutzky, J., Olszanski, A., Gangadhar, T., Gajewski, T., Chmielowski, B., Hanks, B., Boasberg, P., Zhao, Y., *et al.* (2015). Updated results from a phase 1/2 study of epacadostat (INCB024360) in combination with ipilimumab in patients with metastatic melanoma. European Journal of Cancer *51*, S106-S107.

Giovarelli, M., Musiani, P., Garotta, G., Ebner, R., Di Carlo, E., Kim, Y., Cappello, P., Rigamonti, L., Bernabei, P., Novelli, F., *et al.* (1999). A "stealth effect": Adenocarcinoma cells engineered to express TRAIL elude tumor-specific and allogeneic T cell reactions. Journal of Immunology *163*, 4886-4893.

Girardi, M., Oppenheim, D. E., Steele, C. R., Lewis, J. M., Glusac, E., Filler, R., Hobby, P., Sutton, B., Tigelaar, R. E., and Hayday, A. C. (2001). Regulation of cutaneous malignancy by gamma delta T cells. Science *294*, 605-609.

Gjymishka, A., Palii, S. S., Shan, J., and Kilberg, M. S. (2008). Despite increased ATF4 binding at the C/EBP-ATF composite site following activation of the unfolded protein response, system A transporter 2 (SNAT2) transcription activity is repressed in HepG2 cells. Journal of Biological Chemistry *283*, 27736-27747.

Godfrey, V. L., Wilkinson, J. E., and Russell, L. B. (1991). X-linked lymphoreticular disease in the scurfy (sf) mutant mouse. American Journal of Pathology *138*, 1379-1387.

Grewer, C., and Grabsch, E. (2004). New inhibitors for the neutral amino acid transporter ASCT2 reveal its Na+-dependent anion leak. Journal of Physiology *557*, 747-759.

Grohmann, U., Fallarino, F., Bianchi, R., Orabona, C., Vacca, C., Fioretti, M. C., and Puccetti, P. (2003). A defect in tryptophan catabolism impairs tolerance in nonobese diabetic mice. Journal of Experimental Medicine *198*, 153-160.

Grohmann, U., Orabona, C., Fallarino, F., Vacca, C., Calcinaro, F., Falorni, A., Candeloro, P., Belladonna, M. L., Bianchi, R., Fioretti, M. C., and Puccetti, P. (2002). CTLA-4-Ig regulates tryptophan catabolism in vivo. Nature Immunology *3*, 1097-1101.

Grohmann, U., Volpi, C., Fallarino, F., Bozza, S., Bianchi, R., Vacca, C., Orabona, C., Belladonna, M. L., Ayroldi, E., Nocentini, G., *et al.* (2007). Reverse signaling through GITR ligand enables dexamethasone to activate IDO in allergy. Nature Medicine *13*, 579-586.

Guillemin, G. J. (2012). Quinolinic acid, the inescapable neurotoxin. Febs Journal *279*, 1356-1365.

Gurtner, G. J., Newberry, R. D., Schloemann, S. R., McDonald, K. G., and Stenson, W. F. (2003). Inhibition of indoleamine 2,3-dioxygenase augments trinitrobenzene sulfonic acid colitis in mice. Gastroenterology *125*, 1762-1773.

Haber, R., Bessette, D., Hulihangiblin, B., Durcan, M. J., and Goldman, D. (1993). Identification of tryptophan 2,3-dioxygenase RNA in rodent brain. Journal of Neurochemistry *60*, 1159-1162.

Hahne, M., Rimoldi, D., Schroter, M., Romero, P., Schreier, M., French, L. E., Schneider, P., Bornand, T., Fontana, A., Lienard, D.*, et al.* (1996). Melanoma cell expression of Fas(Apo-1/CD95) ligand: Implications for tumor immune escape. Science *274*, 1363-1366.

Hamilton, K. S., Phong, B., Corey, C., Cheng, J., Gorentla, B., Zhong, X. P., Shiva, S., and Kane, L. P. (2014). T Cell Receptor-Dependent Activation of mTOR Signaling in T Cells Is Mediated by Carma1 and MALT1, But Not Bcl10. Science Signaling *7*.

Han, A. P., Yu, C., Lu, L. R., Fujiwara, Y., Browne, C., Chin, G., Fleming, M., Leboulch, P., Orkin, S. H., and Chen, J. J. (2001). Heme-regulated eIF2 alpha kinase (HRI) is required for translational regulation and survival of erythroid precursors in iron deficiency. Embo Journal *20*, 6909-6918.

Han, J., Backa, S. H., Hur, J., Lin, Y.-H., Gildersleeve, R., Shan, J., Yuan, C. L., Krokowski, D., Wang, S., Hatzoglou, M.*, et al.* (2013). ER-stress-induced transcriptional regulation increases protein synthesis leading to cell death. Nature Cell Biology *15*, 481-490.

Hanahan, D., and Weinberg, R. A. (2011). Hallmarks of Cancer: The Next Generation. Cell *144*, 646-674.

Hao, Y. J., Samuels, Y., Li, Q. L., Krokowski, D., Guan, B. J., Wang, C., Jin, Z. C., Dong, B. H., Cao, B., Feng, X. J.*, et al.* (2016). Oncogenic PIK3CA mutations reprogram glutamine metabolism in colorectal cancer. Nature Communications *7*.

Hara, K., Yonezawa, K., Weng, Q. P., Kozlowski, M. T., Belham, C., and Avruch, J. (1998). Amino acid sufficiency and mTOR regulate p70 S6 kinase and eIF-4E BP1 through a common effector mechanism. Journal of Biological Chemistry *273*, 14484-14494.

Harding, H. P., Novoa, I., Zhang, Y. H., Zeng, H. Q., Wek, R., Schapira, M., and Ron, D. (2000a). Regulated translation initiation controls stress-induced gene expression in mammalian cells. Mol Cell *6*, 1099-1108.

Harding, H. P., Zhang, Y. H., Bertolotti, A., Zeng, H. Q., and Ron, D. (2000b). Perk is essential for translational regulation and cell survival during the unfolded protein response. Mol Cell *5*, 897-904.

Harding, H. P., Zhang, Y. H., and Ron, D. (1999). Protein translation and folding are coupled by an endoplasmic-reticulum-resident kinase. Nature *397*, 271-274.

Harding, H. P., Zhang, Y. H., Zeng, H. Q., Novoa, I., Lu, P. D., Calfon, M., Sadri, N., Yun, C., Popko, B., Paules, R.*, et al.* (2003). An integrated stress response regulates amino acid metabolism and resistance to oxidative stress. Mol Cell *11*, 619-633.

Hassanein, M., Hoeksema, M. D., Shiota, M., Qian, J., Harris, B. K., Chen, H., Clark, J. E., Alborn, W. E., Eisenberg, R., and Massion, P. P. (2013). SLC1A5 Mediates Glutamine Transport Required for Lung Cancer Cell Growth and Survival. Clinical Cancer Research *19*, 560-570.

Hassanein, M., Qian, J., Hoeksema, M. D., Wang, J., Jacobovitz, M., Ji, X., Harris, F. T., Harris, B. K., Boyd, K. L., Chen, H.*, et al.* (2015). Targeting SLC1a5-mediated glutamine dependence in non-small cell lung cancer. International Journal of Cancer *137*, 1587-1597.

Hayashi, K., Ouchi, M., Endou, H., and Anzai, N. (2016). HOXB9 acts as a negative regulator of activated human T cells in response to amino acid deficiency. Immunology and Cell Biology *94*, 612-617.

Hayashi, T., Mo, J. H., Gong, X., Rossetto, C., Jang, A., Beck, L., Elliott, G. I., Kufareva, I., Abagyan, R., Broide, D. H.*, et al.* (2007). 3-Hydroxyanthranilic acid inhibits PDK1 activation and suppresses experimental asthma by inducing T cell apoptosis. Proc Natl Acad Sci U S A *104*, 18619-18624.

He, L., Vasiliou, K., and Nebert, D. W. (2009). Analysis and update of the human solute carrier (SLC) gene superfamily. Human genomics *3*, 195-206.

Hill, M., Pereira, V., Chauveau, C., Zagani, R., Remy, S., Tesson, L., Mazal, D., Ubillos, L., Brion, R., Ashgar, K.*, et al.* (2005). Heme oxygenase-1 inhibits rat and human breast cancer cell proliferation: mutual cross inhibition with indoleamine 2,3-dioxygenase. Faseb J *19*, 1957-1968.

Hill, M., Tanguy-Royer, S., Royer, P., Chauveau, C., Asghar, K., Tesson, L., Lavainne, F., Remy, S., Brion, R., Huber, F. X.*, et al.* (2007). IDO expands human CD4(+)CD25(high) regulatory T cells by promoting maturation of LPS-treated dendritic cells. European Journal of Immunology *37*, 3054-3062.

Hissong, B. D., Byrne, G. I., Padilla, M. L., and Carlin, J. M. (1995). Up-regulation of interferon-induced indoleamine 2,3-dioxygenase in human macrophgae cultures by lipopolysaccharide, muramyl tripeptide, and interleukin-1. Cellular Immunology *160*, 264-269.

Hissong, B. D., and Carlin, J. M. (1997). Potentiation of interferon-induced indoleamine 2,3-dioxygenase mRNA in human mononuclear phagocytes by lipopolysaccharide and interleukin-1. Journal of Interferon and Cytokine Research *17*, 387-393.

Holmgaard, R. B., Zamarin, D., Li, Y. Y., Gasmi, B., Munn, D. H., Allison, J. P., Merghoub, T., and Wolchok, J. D. (2015). Tumor-Expressed IDO Recruits and Activates MDSCs in a Treg-Dependent Manner. Cell Reports *13*, 412-424.

Holmgaard, R. B., Zamarin, D., Munn, D. H., Wolchok, J. D., and Allison, J. P. (2013). Indoleamine 2,3-dioxygenase is a critical resistance mechanism in antitumor T cell immunotherapy targeting CTLA-4. Journal of Experimental Medicine *210*, 1389-1402.

Holz, M. K., Ballif, B. A., Gygi, S. P., and Blenis, J. (2005). mTOR and S6K1 mediate assembly of the translation preinitiation complex through dynamic protein interchange and ordered phosphorylation events. Cell *123*, 569-580.

Hoshi, M., Saito, K., Hara, A., Taguchi, A., Ohtaki, H., Tanaka, R., Fujigaki, H., Osawa, Y., Takemura, M., Matsunami, H.*, et al.* (2010). The Absence of IDO Upregulates Type I

IFN Production, Resulting in Suppression of Viral Replication in the Retrovirus-Infected Mouse. Journal of Immunology *185*, 3305-3312.

Hou, D.-Y., Muller, A. J., Sharma, M. D., DuHadaway, J., Banerjee, T., Johnson, M., Mellor, A. L., Prendergasts, G. C., and Munn, D. H. (2007). Inhibition of indoleamine 2,3-dioxygenase in dendritic cells by stereoisomers of 1-methyl-tryptophan correlates with antitumor responses. Cancer Research *67*, 792-801.

Hsu, P. D., Scott, D. A., Weinstein, J. A., Ran, F. A., Konermann, S., Agarwala, V., Li, Y., Fine, E. J., Wu, X., Shalem, O.*, et al.* (2013). DNA targeting specificity of RNA-guided Cas9 nucleases. Nature Biotechnology *31*, 827-832.

Hu, B. G., Hissong, B. D., and Carlin, J. M. (1995). Interleukin-1 enhances indoleamine 2,3-dioxygenase activity by increasing specific messenger-RNA expression in human mononuclear phagocytes. Journal of Interferon and Cytokine Research *15*, 617-624.

Hu, H., Takano, N., Xiang, L., Gilkes, D. M., Luo, W., and Semenza, G. L. (2014). Hypoxia-inducible factors enhance glutamate signaling in cancer cells. Oncotarget *5*, 8853-8868.

Huang, A., Fuchs, D., Widner, B., Glover, C., Henderson, D. C., and Allen-Mersh, T. G. (2002). Serum tryptophan decrease correlates with immune activation and impaired quality of life in colorectal cancer. British Journal of Cancer *86*, 1691-1696.

Huang, F., Zhao, Y., Zhao, J., Wu, S., Jiang, Y., Ma, H., and Zhang, T. (2014). Upregulated SLC1A5 promotes cell growth and survival in colorectal cancer. International Journal of Clinical and Experimental Pathology *7*, 6006-6014.

Hwang, S. L., Chung, N. P. Y., Chan, J. K. Y., and Lin, C. L. S. (2005). Indoleamine 2,3-dioxygenase (IDO) is essential for dendritic cell activation and chemotactic responsiveness to chemokines. Cell Research *15*, 167-175.

Igarashi, T., Izumi, H., Uchiumi, T., Nishio, K., Arao, T., Tanabe, M., Uramoto, H., Sugio, K., Yasumoto, K., Sasaguri, Y.*, et al.* (2007). Clock and ATF4 transcription system regulates drug resistance in human cancer cell lines. Oncogene *26*, 4749-4760.

Iken, K., Liu, K. F., Liu, H. Z., Bizargity, P., Wang, L. Q., Hancock, W. W., and Visner, G. A. (2012). Indoleamine 2,3-Dioxygenase and Metabolites Protect Murine Lung Allografts and Impair the Calcium Mobilization of T Cells. American Journal of Respiratory Cell and Molecular Biology *47*, 405-416.

Inaba, T., Ino, K., Kajiyama, H., Yamamoto, E., Shibata, K., Nawa, A., Nagasaka, T., Akimoto, H., Takikawa, O., and Kikkawa, F. (2009). Role of the immunosuppressive enzyme indoleamine 2,3-dioxygenase in the progression of ovarian carcinoma. Gynecologic Oncology *115*, 185-192.

Ino, K., Yamamoto, E., Shibata, K., Kajiyama, H., Yoshida, N., Terauchi, M., Nawa, A., Nagasaka, T., Takikawa, O., and Kikkawa, F. (2008). Inverse correlation between tumoral indoleamine 2,3-dioxygenase expression and tumor-infiltrating lymphocytes in endometrial cancer: Its association with disease progression and survival. Clinical Cancer Research *14*, 2310-2317.

Ino, K., Yoshida, N., Kajiyama, H., Shibata, K., Yamamoto, E., Kidokoro, K., Takahashi, N., Terauchi, M., Nawa, A., Nomura, S.*, et al.* (2006). Indoleamine 2,3-dioxygenase is a novel prognostic indicator for endometrial cancer. British Journal of Cancer *95*, 1555-1561.

Ishimoto, T., Nagano, O., Yae, T., Tamada, M., Motohara, T., Oshima, H., Oshima, M., Ikeda, T., Asaba, R., Yagi, H.*, et al.* (2011). CD44 variant regulates redox status in cancer cells by stabilizing the xCT subunit of system xc(-) and thereby promotes tumor growth. Cancer Cell *19*, 387-400.

Jensen, S., Guskov, A., Rempel, S., Hanelt, I., and Slotboom, D. J. (2013). Crystal structure of a substrate-free aspartate transporter. Nature structural & molecular biology *20*, 1224-1226.

Jeon, Y. J., Khelifa, S., Ratnikov, B., Scott, D. A., Feng, Y., Parisi, F., Ruller, C., Lau, E., Kim, H., Brill, L. M.*, et al.* (2015). Regulation of Glutamine Carrier Proteins by RNF5 Determines Breast Cancer Response to ER Stress-Inducing Chemotherapies. Cancer Cell *27*, 354-369.

Jeong, Y. I., Kim, S. W., Jung, I. D., Lee, J. S., Chang, J. H., Lee, C. M., Chun, S. H., Yoon, M. S., Kim, G. T., Ryu, S. W.*, et al.* (2009). Curcumin Suppresses the Induction of

Indoleamine 2,3-Dioxygenase by Blocking the Janus-activated Kinase-Protein Kinase C delta-STAT1 Signaling Pathway in Interferon-gamma-stimulated Murine Dendritic Cells. Journal of Biological Chemistry *284*, 3700-3708.

Jha, G. G., and Miller, J. S. (2014). A randomized, double-blind phase 2 study of sipuleucel-T followed by indoximod or placebo in the treatment of patients with asymptomatic or minimally symptomatic metastatic castration-resistant prostate cancer. Journal of Clinical Oncology *32*.

Jiang, H. Y., and Wek, R. C. (2005). GCN2 phosphorylation of eIF2 alpha activates NF-kappa B in response to UV irradiation. Biochemical Journal *385*, 371-380.

Jiang, H. Y., Wek, S. A., McGrath, B. C., Lu, D., Hai, T. W., Harding, H. P., Wang, X. Z., Ron, D., Cavener, D. R., and Wek, R. C. (2004). Activating transcription factor 3 is integral to the eukaryotic initiation factor 2 kinase stress response. Molecular and Cellular Biology *24*, 1365-1377.

Jiang, L., Kon, N., Li, T., Wang, S. J., Su, T., Hibshoosh, H., Baer, R., and Gu, W. (2015). Ferroptosis as a p53-mediated activity during tumour suppression. Nature *520*, 57-62.

Johnsen, A. K., Templeton, D. J., Sy, M. S., and Harding, C. V. (1999). Deficiency of transporter for antigen presentation (TAP) in tumor cells allows evasion of immune surveillance and increases tumorigenesis. Journal of Immunology *163*, 4224-4231.

June, C. H., Bluestone, J. A., Nadler, L. M., and Thompson, C. B. (1994). The B7 and CD28 receptor families. Immunology Today *15*, 321-331.

Jurgens, B., Hainz, U., Fuchs, D., Felzmann, T., and Heitger, A. (2009). Interferon-gamma-triggered indoleamine 2,3-dioxygenase competence in human monocyte-derived dendritic cells induces regulatory activity in allogeneic T cells. Blood *114*, 3235-3243.

Kai, S., Goto, S., Tahara, K., Sasaki, A., Kawano, K., and Kitano, S. (2003). Inhibition of indoleamine 2,3-dioxygenase suppresses NK cell activity and accelerates tumor growth. Journal of experimental therapeutics & oncology *3*, 336-345.

Kai, S., Goto, S., Tahara, K., Sasaki, A., Tone, S., and Kitano, S. (2004). Indoleamine 2,3-dioxygenase is necessary for cytolytic activity of natural killer cells. Scandinavian Journal of Immunology *59*, 177-182.

Kanai, M., Funakoshi, H., Takahashi, H., Hayakawa, T., Mizuno, S., Matsumoto, K., and Nakamura, T. (2009). Tryptophan 2,3-dioxygenase is a key modulator of physiological neurogenesis and anxiety-related behavior in mice. Mol Brain *2*.

Kanai, Y., Clemencon, B., Simonin, A., Leuenberger, M., Lochner, M., Weisstanner, M., and Hediger, M. A. (2013). The SLC1 high-affinity glutamate and neutral amino acid transporter family. Molecular Aspects of Medicine *34*, 108-120.

Kanai, Y., and Hediger, M. A. (2004). The glutamate/neutral amino acid transporter family SLC1: molecular, physiological and pharmacological aspects. Pflugers Archiv-European Journal of Physiology *447*, 469-479.

Kanai, Y., Segawa, H., Miyamoto, K., Uchino, H., Takeda, E., and Endou, H. (1998). Expression cloning and characterization of a transporter for large neutral amino acids activated by the heavy chain of 4F2 antigen (CD98). Journal of Biological Chemistry *273*, 23629-23632.

Kaplan, D. H., Shankaran, V., Dighe, A. S., Stockert, E., Aguet, M., Old, L. J., and Schreiber, R. D. (1998). Demonstration of an interferon gamma-dependent tumor surveillance system in immunocompetent mice. Proc Natl Acad Sci U S A *95*, 7556-7561.

Kawano, T., Cui, J. Q., Koezuka, Y., Toura, I., Kaneko, Y., Motoki, K., Ueno, H., Nakagawa, R., Sato, H., Kondo, E.*, et al.* (1997). CD1d-restricted and TCR-mediated activation of V(alpha)14 NKT cells by glycosylceramides. Science *278*, 1626-1629.

Kekuda, R., Prasad, P. D., Fei, Y. J., TorresZamorano, V., Sinha, S., YangFeng, T. L., Leibach, F. H., and Ganapathy, V. (1996). Cloning of the sodium-dependent, broad-scope, neutral amino acid transporter B-O from a human placental choriocarcinoma cell line. Journal of Biological Chemistry *271*, 18657-18661.

Kent, W. J., Sugnet, C. W., Furey, T. S., Roskin, K. M., Pringle, T. H., Zahler, A. M., and Haussler, D. (2002). The human genome browser at UCSC. Genome Research *12*, 996-1006.

Khan, J. A., Forouhar, F., Tao, X., and Tong, L. (2007). Nicotinamide adenine dinucleotide metabolism as an attractive target for drug discovery. Expert Opinion on Therapeutic Targets *11*, 695-705.

Kim, C. S., Cho, S. H., Chun, H. S., Lee, S. Y., Endou, H., Kanai, Y., and Kim, D. K. (2008a). BCH, an inhibitor of system L amino acid transporters, induces apoptosis in cancer cells. Biological & pharmaceutical bulletin *31*, 1096-1100.

Kim, E., Goraksha-Hicks, P., Li, L., Neufeld, T. P., and Guan, K. L. (2008b). Regulation of TORC1 by Rag GTPases in nutrient response. Nature Cell Biology *10*, 935-945.

Kim, H., Chen, L., Lim, G., Sung, B., Wang, S. X., McCabe, M. F., Rusanescu, G., Yang, L. L., Tian, Y. H., and Mao, J. R. (2012). Brain indoleamine 2,3-dioxygenase contributes to the comorbidity of pain and depression. Journal of Clinical Investigation *122*, 2940-2954.

Kim, S., Kim, D. H., Jung, W. H., and Koo, J. S. (2013). Expression of glutamine metabolism-related proteins according to molecular subtype of breast cancer. Endocrine-related cancer *20*, 339-348.

Kinjo, Y., Wu, D., Kim, G. S., Xing, G. W., Poles, M. A., Ho, D. D., Tsuji, M., Kawahara, K., Wong, C. H., and Kronenberg, M. (2005). Recognition of bacterial glycosphingolipids by natural killer T cells. Nature *434*, 520-525.

Knox, W. E. (1966). The regulation of tryptophan pyrrolase activity by tryptophan. Advances in enzyme regulation *4*, 287-297.

Knox, W. E., and Mehler, A. H. (1950). The conversion of tryptophan to kynurenine in liver. 1. The coupled tryptophan peroxidase-oxidase system forming formylkynurenine. Journal of Biological Chemistry *187*, 419-430.

Kobayashi, K., Ohnishi, A., Promsuk, J., Shimizu, S., Kanai, Y., Shiokawa, Y., and Nagane, M. (2008). Enhanced tumor growth elicited by L-type amino acid transporter 1 in human malignant glioma cells. Neurosurgery *62*, 493-504.

Kobayashi, T., Shimabukuro-Demoto, S., Yoshida-Sugitani, R., Furuyama-Tanaka, K., Karyu, H., Sugiura, Y., Shimizu, Y., Hosaka, T., Goto, M., Kato, N.*, et al.* (2014). The

histidine transporter SLC15A4 coordinates mTOR-dependent inflammatory responses and pathogenic antibody production. Immunity *41*, 375-388.

Koblish, H. K., Hansbury, M. J., Bowman, K. J., Yang, G. J., Neilan, C. L., Haley, P. J., Burn, T. C., Waeltz, P., Sparks, R. B., Yue, E. W.*, et al.* (2010). Hydroxyamidine Inhibitors of Indoleamine-2,3-dioxygenase Potently Suppress Systemic Tryptophan Catabolism and the Growth of IDO-Expressing Tumors. Molecular Cancer Therapeutics *9*, 489-498.

Kokame, K., Agarwala, K. L., Kato, H., and Miyata, T. (2000). Herp, a new ubiquitin-like membrane protein induced by endoplasmic reticulum stress. Journal of Biological Chemistry *275*, 32846-32853.

Kolaczkowska, E., and Kubes, P. (2013). Neutrophil recruitment and function in health and inflammation. Nature reviews Immunology *13*, 159-175.

Kolesnikova, T. V., Mannion, B. A., Berditchevski, F., and Hemler, M. E. (2001). Beta1 integrins show specific association with CD98 protein in low density membranes. BMC biochemistry *2*.

Konan, K. V., and Taylor, M. W. (1996). Importance of the two interferon-stimulated response-element (ISRE) sequences in the regulation of the human indoleamine 2,3-dioxygenase gene. Journal of Biological Chemistry *271*, 19140-19145.

Koumenis, C., Naczki, C., Koritzinsky, M., Rastani, S., Diehl, A., Sonenberg, N., Koromilas, A., and Wouters, B. G. (2002). Regulation of protein synthesis by hypoxia via activation of the endoplasmic reticulum kinase PERK and phosphorylation of the translation initiation factor eIF2 alpha. Molecular and Cellular Biology *22*, 7405-7416.

Kropf, P., Baud, D., Marshall, S. E., Munder, M., Mosley, A., Fuentes, J. M., Bangham, C. R., Taylor, G. P., Herath, S., Choi, B. S.*, et al.* (2007). Arginase activity mediates reversible T cell hyporesponsiveness in human pregnancy. Eur J Immunol *37*, 935-945.

Krummel, M. F., and Allison, J. P. (1995). CD28 and CTLA-4 have opposing effects on the response of T-cells to stimulation. Journal of Experimental Medicine *182*, 459-465.

Kudo, Y. (2013). The role of placental indoleamine 2,3-dioxygenase in human pregnancy. Obstetrics & gynecology science *56*, 209-216.

Kudo, Y., Boyd, C. A. R., Sargent, I. L., and Redman, C. W. G. (2001). Tryptophan degradation by human placental indoleamine 2,3-dioxygenase regulates lymphocyte proliferation. Journal of Physiology *535*, 207-215.

Kudo, Y., Boyd, C. A. R., Spyropoulou, I., Redman, C. W. G., Takikawa, O., Katsuki, T., Hara, T., Ohama, K., and Sargent, I. L. (2004). Indoleamine 2,3-dioxygenase: distribution and function in the developing human placenta. Journal of Reproductive Immunology *61*, 87-98.

Kumar, S., Malachowski, W. P., DuHadaway, J. B., LaLonde, J. M., Carroll, P. J., Jaller, D., Metz, R., Prendergast, G. C., and Muller, A. J. (2008). Indoleamine 2,3-dioxygenase is the anticancer target for a novel series of potent naphthoquinone-based inhibitors. Journal of Medicinal Chemistry *51*, 1706-1718.

Kurian, M. A., Zhen, J., Cheng, S. Y., Li, Y., Mordekar, S. R., Jardine, P., Morgan, N. V., Meyer, E., Tee, L., Pasha, S.*, et al.* (2009). Homozygous loss-of-function mutations in the gene encoding the dopamine transporter are associated with infantile parkinsonism-dystonia. The Journal of clinical investigation *119*, 1595-1603.

Kwidzinski, E., Bunse, J., Aktas, O., Richter, D., Mutlu, L., Zipp, F., Nitsch, R., and Bechmann, I. (2005). Indolamine 2,3-dioxygenase is expressed in the CNS and down-regulates autoimmune inflammation. Faseb J *19*, 1347-1349.

Laval, J., Touhami, J., Herzenberg, L. A., Conrad, C., Taylor, N., Battini, J.-L., Sitbon, M., and Tirouvanziam, R. (2013). Metabolic Adaptation of Neutrophils in Cystic Fibrosis Airways Involves Distinct Shifts in Nutrient Transporter Expression. Journal of Immunology *190*, 6043-6050.

Leach, D. R., Krummel, M. F., and Allison, J. P. (1996). Enhancement of antitumor immunity by CTLA-4 blockade. Science *271*, 1734-1736.

Lee, J. R., Dalton, R. R., Messina, J. L., Sharma, M. D., Smith, D. M., Burgess, R. E., Mazzella, F., Antonia, S. J., Mellor, A. L., and Munn, D. H. (2003). Pattern of recruitment of immunoregulatory antigen-presenting cells in malignant melanoma. Laboratory Investigation *83*, 1457-1466.

Lee, S. M., Lee, Y. S., Choi, J. H., Park, S. G., Choi, I. W., Joo, Y. D., Lee, W. S., Lee, J. N., Choi, I., and Seo, S. K. (2010). Tryptophan metabolite 3-hydroxyanthranilic acid selectively induces activated T cell death via intracellular GSH depletion. Immunology Letters *132*, 53-60.

Lee, S. Y., Choi, H. K., Lee, K. J., Jung, J. Y., Hur, G. Y., Jung, K. H., Kim, J. H., Shin, C., Shim, J. J., In, K. H.*, et al.* (2009). The Immune Tolerance of Cancer is Mediated by IDO That is Inhibited by COX-2 Inhibitors Through Regulatory T Cells. Journal of Immunotherapy *32*, 22-28.

Lehman, S. L., Ryeom, S., and Koumenis, C. (2015). Signaling through alternative Integrated Stress Response pathways compensates for GCN2 loss in a mouse model of soft tissue sarcoma. Scientific Reports *5*.

Leonhardt, R. M., Lee, S.-J., Kavathas, P. B., and Cresswell, P. (2007). Severe tryptophan starvation blocks onset of conventional persistence and reduces reactivation of Chlamydia trachomatis. Infection and Immunity *75*, 5105-5117.

Lewkowicz, N., Klink, M., Mycko, M. P., and Lewkowicz, P. (2013). Neutrophil-CD4(+)CD25(+) T regulatory cell interactions: A possible new mechanism of infectious tolerance. Immunobiology *218*, 455-464.

Li, M., Bolduc, A. R., Hoda, M. N., Gamble, D. N., Dolisca, S. B., Bolduc, A. K., Hoang, K., Ashley, C., McCall, D., Rojiani, A. M.*, et al.* (2014). The indoleamine 2,3-dioxygenase pathway controls complement-dependent enhancement of chemo-radiation therapy against murine glioblastoma. Journal for immunotherapy of cancer *2*.

Li, W., Li, B., Fan, W., Geng, L., Li, X., Li, L., Huang, Z., and Li, S. (2009). CTLA4Ig gene transfer alleviates abortion in mice by expanding CD4(+)CD25(+) regulatory T cells and inducing indoleamine 2,3-dioxygenase. Journal of Reproductive Immunology *80*, 1-11.

Ling, W. F., Zhang, J. M., Yuan, Z. R., Ren, G. W., Zhang, L. Y., Chen, X. D., Rabson, A. B., Roberts, A. I., Wang, Y., and Shi, Y. F. (2014). Mesenchymal Stem Cells Use IDO to Regulate Immunity in Tumor Microenvironment. Cancer Research *74*, 1576-1587.

Littlejohn, T. K., Takikawa, O., Truscott, R. J. W., and Walker, M. J. (2003). Asp(274) and His(346) are essential for heme binding and catalytic function of human indoleamine 2,3-dioxygenase. Journal of Biological Chemistry *278*, 29525-29531.

Liu, V. C., Wong, L. Y., Jang, T., Shah, A. H., Park, I., Yang, X., Zhang, Q., Lonning, S., Teicher, B. A., and Lee, C. (2007). Tumor evasion of the immune system by converting CD4(+) CD25(-) T cells into CD4(+) CD25(+) T regulatory cells: Role of tumor-derived TGF-beta. Journal of Immunology *178*, 2883-2892.

Liu, X. D., Shin, N., Koblish, H. K., Yang, G. J., Wang, Q., Wang, K., Leffet, L., Hansbury, M. J., Thomas, B., Rupar, M.*, et al.* (2010). Selective inhibition of IDO1 effectively regulates mediators of antitumor immunity. Blood *115*, 3520-3530.

Liu, X. Q., Lu, K., Feng, L. L., Ding, M., Gao, J. M., Ge, X. L., and Wang, X. (2014). Up-regulated expression of indoleamine 2,3-dioxygenase 1 in non-Hodgkin lymphoma correlates with increased regulatory T-cell infiltration. Leukemia & Lymphoma *55*, 405-414.

Liu, Y., Yang, L., An, H., Chang, Y., Zhang, W., Zhu, Y., Xu, L., and Xu, J. (2015). High expression of Solute Carrier Family 1, member 5 (SLC1A5) is associated with poor prognosis in clear-cell renal cell carcinoma. Sci Rep *5*, 16954.

Lob, S., Konigsrainer, A., Zieker, D., Brucher, B., Rammensee, H. G., Opelz, G., and Terness, P. (2009). IDO1 and IDO2 are expressed in human tumors: levo- but not dextro-1-methyl tryptophan inhibits tryptophan catabolism. Cancer Immunology Immunotherapy *58*, 153-157.

Lu, P. D., Harding, H. P., and Ron, D. (2004). Translation reinitiation at alternative open reading frames regulates gene expression in an integrated stress response. Journal of Cell Biology *167*, 27-33.

Ma, Y., and Hendershot, L. M. (2003). Delineation of a negative feedback regulatory loop that controls protein translation during endoplasmic reticulum stress. The Journal of biological chemistry *278*, 34864-34873.

MacIver, N. J., Michalek, R. D., and Rathmell, J. C. (2013). Metabolic Regulation of T Lymphocytes. Annual Review of Immunology *31*, 259-283.

Makala, L. H. C., Baban, B., Lemos, H., El-Awady, A. R., Chandler, P. R., Hou, D. Y., Munn, D. H., and Mellor, A. L. (2011). Leishmania major Attenuates Host Immunity by Stimulating Local Indoleamine 2,3-Dioxygenase Expression. Journal of Infectious Diseases *203*, 715-725.

Malavasi, E. L., Ogawa, F., Porteous, D. J., and Millar, J. K. (2012). DISC1 variants 37W and 607F disrupt its nuclear targeting and regulatory role in ATF4-mediated transcription. Human molecular genetics *21*, 2779-2792.

Mansfield, A. S., Heikkila, P. S., Vaara, A. T., von Smitten, K. A. J., Vakkila, J. M., and Leidenius, M. H. K. (2009). Simultaneous Foxp3 and IDO expression is associated with sentinel lymph node metastases in breast cancer. BMC Cancer *9*.

Marin, M., Lavillette, D., Kelly, S. M., and Kabat, D. (2003). N-linked glycosylation and sequence changes in a critical negative control region of the ASCT1 and ASCT2 neutral amino acid transporters determine their retroviral receptor functions. J Virol *77*, 2936-2945.

Mastroberardino, L., Spindler, B., Pfeiffer, R., Skelly, P. J., Loffing, J., Shoemaker, C. B., and Verrey, F. (1998). Amino-acid transport by heterodimers of 4F2hc/CD98 and members of a permease family. Nature *395*, 288-291.

Matteoli, G., Mazzini, E., Iliev, I. D., Mileti, E., Fallarino, F., Puccetti, P., Chieppa, M., and Rescigno, M. (2010). Gut CD103(+) dendritic cells express indoleamine 2,3-dioxygenase which influences T regulatory/T effector cell balance and oral tolerance induction. Gut *59*, 595-604.

Mattner, J., DeBord, K. L., Ismail, N., Goff, R. D., Cantu, C., Zhou, D. P., Saint-Mezard, P., Wang, V., Gao, Y., Yin, N., *et al.* (2005). Exogenous and endogenous glycolipid antigens activate NKT cells during microbial infections. Nature *434*, 525-529.

McEwen-Smith, R. M., Salio, M., and Cerundolo, V. (2015). The regulatory role of invariant NKT cells in tumor immunity. Cancer Immunol Res *3*, 425-435.

Mellman, I., and Steinman, R. M. (2001). Dendritic cells: specialized and regulated antigen processing machines. Cell *106*, 255-258.

Mellor, A. L., Baban, B., Chandler, P., Marshall, B., Jhaver, K., Hansen, A., Koni, P. A., Iwashima, M., and Munn, D. H. (2003). Cutting Edge: Induced Indoleamine 2,3 Dioxygenase Expression in Dendritic Cell Subsets Suppresses T Cell Clonal Expansion. The Journal of Immunology *171*, 1652-1655.

Mellor, A. L., Sivakumar, J., Chandler, P., Smith, K., Molina, H., Mao, D. L., and Munn, D. H. (2001). Prevention of T cell-driven complement activation and inflammation by tryptophan catabolism during pregnancy. Nature Immunology *2*, 64-68.

Merlo, L. M. F., Pigott, E., DuHadaway, J. B., Grabler, S., Metz, R., Prendergast, G. C., and Mandik-Nayak, L. (2014). IDO2 Is a Critical Mediator of Autoantibody Production and Inflammatory Pathogenesis in a Mouse Model of Autoimmune Arthritis. Journal of Immunology *192*, 2082-2090.

Metz, R., DuHadaway, J. B., Kamasani, U., Laury-Kleintop, L., Muller, A. J., and Prendergast, G. C. (2007). Novel tryptophan catabolic enzyme IDO2 is the preferred biochemical target of the antitumor indoleamine 2,3-dioxygenase inhibitory compound D-1-methyl-tryptophan. Cancer Research *67*, 7082-7087.

Metz, R., DuHadaway, J. B., Rust, S., Munn, D. H., Muller, A. J., Mautino, M., and Prendergast, G. C. (2010). Zinc Protoporphyrin IX Stimulates Tumor Immunity by Disrupting the Immunosuppressive Enzyme Indoleamine 2,3-Dioxygenase. Molecular Cancer Therapeutics *9*, 1864-1871.

Metz, R., Rust, S., DuHadaway, J. B., Mautino, M. R., Munn, D. H., Vahanian, N. N., Link, C. J., and Prendergast, G. C. (2012). IDO inhibits a tryptophan sufficiency signal that stimulates mTOR A novel IDO effector pathway targeted by D-1-methyl-tryptophan. Oncoimmunology *1*, 1460-1468.

Metz, R., Smith, C., DuHadaway, J. B., Chandler, P., Baban, B., Merlo, L. M. F., Pigott, E., Keough, M. P., Rust, S., Mellor, A. L.*, et al.* (2014). IDO2 is critical for IDO1-mediated T-cell regulation and exerts a non-redundant function in inflammation. International Immunology *26*, 357-367.

Meurs, E., Chong, K., Galabru, J., Thomas, N. S. B., Kerr, I. M., Williams, B. R. G., and Hovanessian, A. G. (1990). Molecular-cloning and characterization of the human double-stranded-RNA activated protein-kinase induced by interferon. Cell *62*, 379-390.

Mezrich, J. D., Fechner, J. H., Zhang, X. J., Johnson, B. P., Burlingham, W. J., and Bradfield, C. A. (2010). An Interaction between Kynurenine and the Aryl Hydrocarbon Receptor Can Generate Regulatory T Cells. Journal of Immunology *185*, 3190-3198.

Miki, T., Sun, H., Lee, Y. H., Tandin, A., Kovscek, A. M., Subbotin, V., Fung, J. J., and Valdivia, L. A. (2001). Blockade of tryptophan catabolism prevents spontaneous tolerogenicity of liver allografts. Transplantation Proceedings *33*, 129-130.

Milne, T. A., Zhao, K., and Hess, J. L. (2009). Chromatin immunoprecipitation (ChIP) for analysis of histone modifications and chromatin-associated proteins. Methods in molecular biology (Clifton, NJ) *538*, 409-423.

Mizoguchi, H., O'Shea, J. J., Longo, D. L., Loeffler, C. M., McVicar, D. W., and Ochoa, A. C. (1992). Alterations in signal transduction molecules in T lymphocytes from tumor-bearing mice. Science *258*, 1795-1798.

Moennikes, O., Loeppen, S., Buchmann, A., Andersson, P., Ittrich, C., Poellinger, L., and Schwarz, M. (2004). A constitutively active dioxin/aryl hydrocarbon receptor promotes hepatocarcinogenesis in mice. Cancer Research *64*, 4707-4710.

Molano, A., Illarionov, P. A., Besra, G. S., Putterman, C., and Porcelli, S. A. (2008). Modulation of invariant natural killer T cell cytokine responses by indoleamine 2,3-dioxygenase. Immunology Letters *117*, 81-90.

Muller, A. J., DuHadaway, J. B., Donover, P. S., Sutanto-Ward, E., and Prendergast, G. C. (2005). Inhibition of indoleamine 2,3-dioxygenase, an immunoregulatory target of the cancer suppression gene Bin1, potentiates cancer chemotherapy. Nature Medicine *11*, 312-319.

Muller, A. J., DuHadaway, J. B., Jaller, D., Curtis, P., Metz, R., and Prendergast, G. C. (2010). Immunotherapeutic Suppression of Indoleamine 2,3-Dioxygenase and Tumor Growth with Ethyl Pyruvate. Cancer Research *70*, 1845-1853.

Muller, A. J., Sharma, M. D., Chandler, P. R., DuHadaway, J. B., Everhart, M. E., Johnson, B. A., Kahler, D. J., Pihkala, J., Soler, A. P., Munn, D. H., *et al.* (2008). Chronic inflammation that facilitates tumor progression creates local immune suppression by inducing indoleamine 2,3 dioxygenase. Proc Natl Acad Sci U S A *105*, 17073-17078.

Munder, M., Schneider, H., Luckner, C., Giese, T., Langhans, C. D., Fuentes, J. M., Kropf, P., Mueller, I., Kolb, A., Modolell, M., and Ho, A. D. (2006). Suppression of T-cell functions by human granulocyte arginase. Blood *108*, 1627-1634.

Munn, D. H., Shafizadeh, E., Attwood, J. T., Bondarev, I., Pashine, A., and Mellor, A. L. (1999). Inhibition of T cell proliferation by macrophage tryptophan catabolism. Journal of Experimental Medicine *189*, 1363-1372.

Munn, D. H., Sharma, M. D., Baban, B., Harding, H. P., Zhang, Y. H., Ron, D., and Mellor, A. L. (2005). GCN2 kinase in T cells mediates proliferative arrest and anergy induction in response to indoleamine 2,3-dioxygenase. Immunity *22*, 633-642.

Munn, D. H., Sharma, M. D., Hou, D., Baban, B., Lee, J. R., Antonia, S. J., Messina, J. L., Chandler, P., Koni, P. A., and Mellor, A. L. (2004a). Expression of indoleamine 2,3-dioxygenase by plasmacytoid dendritic cells in tumor-draining lymph nodes. Journal of Clinical Investigation *114*, 280-290.

Munn, D. H., Sharma, M. D., Lee, J. R., Jhaver, K. G., Johnson, T. S., Keskin, D. B., Marshall, B., Chandler, P., Antonia, S. J., Burgess, R., *et al.* (2002). Potential regulatory function of human dendritic cells expressing indoleamine 2,3-dioxygenase. Science *297*, 1867-1870.

Munn, D. H., Sharma, M. D., and Mellor, A. L. (2004b). Ligation of B7-1/B7-2 by human CD4(+) T cells triggers indoleamine 2,3-dioxygenase activity in dendritic cells. Journal of Immunology *172*, 4100-4110.

Munn, D. H., Zhou, M., Attwood, J. T., Bondarev, I., Conway, S. J., Marshall, B., Brown, C., and Mellor, A. L. (1998). Prevention of allogeneic fetal rejection by tryptophan catabolism. Science *281*, 1191-1193.

Mussai, F., De Santo, C., Abu-Dayyeh, I., Booth, S., Quek, L., McEwen-Smith, R. M., Qureshi, A., Dazzi, F., Vyas, P., and Cerundolo, V. (2013). Acute myeloid leukemia creates an arginase-dependent immunosuppressive microenvironment. Blood *122*, 749-758.

Musso, T., Gusella, G. L., Brooks, A., Longo, D. L., and Varesio, L. (1994). Interleukin-4 inhibits indoleamine 2,3-dioxygenase expression in human monocytes. Blood *83*, 1408-1411.

Nabi, R., Serajee, F. J., Chugani, D. C., Zhong, H. L., and Huq, A. (2004). Association of tryptophan 2,3 dioxygenase gene polymorphism with autism. American Journal of Medical Genetics Part B-Neuropsychiatric Genetics *125B*, 63-68.

Nagata, S., and Golstein, P. (1995). The Fas death factor. Science *267*, 1449-1456.

Nakamura, T., Shima, T., Saeki, A., Hidaka, T., Nakashima, A., Takikawa, O., and Saito, S. (2007). Expression of indoleamine 2, 3-dioxygenase and the recruitment of Foxp3-expressing regulatory T cells in the development and progression of uterine cervical cancer. Cancer Science *98*, 874-881.

Nakashima, M., Sonoda, K., and Watanabe, T. (1999). Inhibition of cell growth and induction of apoptotic cell death by the human tumor-associated antigen RCAS1. Nature Medicine *5*, 938-942.

Nakaya, M., Xiao, Y., Zhou, X., Chang, J.-H., Chang, M., Cheng, X., Blonska, M., Lin, X., and Sun, S.-C. (2014). Inflammatory T Cell Responses Rely on Amino Acid Transporter ASCT2 Facilitation of Glutamine Uptake and mTORC1 Kinase Activation. Immunity *40*, 692-705.

Natali, P. G., Nicotra, M. R., Bigotti, A., Venturo, I., Marcenaro, L., Giacomini, P., and Russo, C. (1989). Selective changes in expression of HLA class I polymorphic determinants in human solid tumors. Proc Natl Acad Sci U S A *86*, 6719-6723.

Nicklin, P., Bergman, P., Zhang, B., Triantafellow, E., Wang, H., Nyfeler, B., Yang, H., Hild, M., Kung, C., Wilson, C.*, et al.* (2009). Bidirectional Transport of Amino Acids Regulates mTOR and Autophagy. Cell *136*, 521-534.

Ninomiya, S., Narala, N., Huye, L., Yagyu, S., Savoldo, B., Dotti, G., Heslop, H. E., Brenner, M. K., Rooney, C. M., and Ramos, C. A. (2015). Tumor indoleamine 2,3-dioxygenase (IDO) inhibits CD19-CAR T cells and is downregulated by lymphodepleting drugs. Blood *125*, 3905-3916.

Nishikawa, H., and Sakaguchi, S. (2010). Regulatory T cells in tumor immunity. International Journal of Cancer *127*, 759-767.

Nothmann, D., Leinenweber, A., Torres-Salazar, D., Kovermann, P., Hotzy, J., Gameiro, A., Grewer, C., and Fahlke, C. (2011). Hetero-oligomerization of Neuronal Glutamate Transporters. Journal of Biological Chemistry *286*, 3935-3943.

Novoa, I., Zeng, H., Harding, H. P., and Ron, D. (2001). Feedback inhibition of the unfolded protein response by GADD34-mediated dephosphorylation of eIF2alpha. The Journal of cell biology *153*, 1011-1022.

Obojes, K., Andres, O., Kim, K. S., Daubener, W., and Schneider-Schaulies, R. (2005). Indoleamine 2,3-dioxygenase mediates cell type-specific anti-measles virus activity of gamma interferon. Journal of Virology *79*, 7768-7776.

Oda, K., Hosoda, N., Endo, H., Saito, K., Tsujihara, K., Yamamura, M., Sakata, T., Anzai, N., Wempe, M. F., Kanai, Y., and Endou, H. (2010). L-type amino acid transporter 1 inhibitors inhibit tumor cell growth. Cancer Sci *101*, 173-179.

Odemuyiwa, S. O., Ghahary, A., Li, Y. Y., Puttagunta, L., Lee, J. E., Musat-Marcu, S., Ghahary, A., and Moqbel, R. (2004). Cutting edge: Human eosinophils regulate T cell subset selection through indoleamine 2,3-dioxygenase. Journal of Immunology *173*, 5909-5913.

Ogmundsdottir, M. H., Heublein, S., Kazi, S., Reynolds, B., Visvalingam, S. M., Shaw, M. K., and Goberdhan, D. C. I. (2012). Proton-Assisted Amino Acid Transporter PAT1 Complexes with Rag GTPases and Activates TORC1 on Late Endosomal and Lysosomal Membranes. Plos One *7*.

Ohoka, N., Yoshii, S., Hattori, T., Onozaki, K., and Hayashi, H. (2005). TRB3, a novel ER stress-inducible gene, is induced via ATF4-CHOP pathway and is involved in cell death. The EMBO journal *24*, 1243-1255.

Okamoto, A., Nikaido, T., Ochiai, K., Takakura, S., Saito, M., Aoki, Y., Ishii, N., Yanaihara, N., Yamada, K., Takikawa, O.*, et al.* (2005). Indoleamine 2,3-dioxygenase serves as a marker of poor prognosis in gene expression profiles of serous ovarian cancer cells. Clinical Cancer Research *11*, 6030-6039.

Onodera, T., Jang, M. H., Guo, Z. J., Yamasaki, M., Hirata, T., Bai, Z. B., Tsuji, N. M., Nagakubo, D., Yoshie, O., Sakaguchi, S.*, et al.* (2009). Constitutive Expression of IDO by Dendritic Cells of Mesenteric Lymph Nodes: Functional Involvement of the CTLA-4/B7 and CCL22/CCR4 Interactions. Journal of Immunology *183*, 5608-5614.

Opitz, C. A., Litzenburger, U. M., Sahm, F., Ott, M., Tritschler, I., Trump, S., Schumacher, T., Jestaedt, L., Schrenk, D., Weller, M.*, et al.* (2011). An endogenous tumour-promoting ligand of the human aryl hydrocarbon receptor. Nature *478*, 197-203.

Orabona, C., Pallotta, M. T., Volpi, C., Fallarino, F., Vacca, C., Bianchi, R., Belladonna, M. L., Fioretti, M. C., Grohmann, U., and Puccetti, P. (2008). SOCS3 drives proteasomal degradation of indoleamine 2,3-dioxygenase (IDO) and antagonizes IDO-dependent tolerogenesis. Proc Natl Acad Sci U S A *105*, 20828-20833.

Orabona, C., Puccetti, P., Vacca, C., Bicciato, S., Luchini, A., Fallarino, F., Bianchi, R., Velardi, E., Perruccio, K., Velardi, A.*, et al.* (2006). Toward the identification of a tolerogenic signature in IDO-competent dendritic cells. Blood *107*, 2846-2854.

Oxenkrug, G. F. (2010). Metabolic syndrome, age-associated neuroendocrine disorders, and dysregulation of tryptophan-kynurenine metabolism. Annals of the New York Academy of Sciences *1199*, 1-14.

Pallotta, M. T., Orabona, C., Volpi, C., Vacca, C., Belladonna, M. L., Bianchi, R., Servillo, G., Brunacci, C., Calvitti, M., Bicciato, S.*, et al.* (2011). Indoleamine 2,3-dioxygenase is a signaling protein in long-term tolerance by dendritic cells. Nature Immunology *12*, 870-878.

Pantoja, L. G., Miller, R. D., Ramirez, J. A., Molestina, R. E., and Summersgill, J. T. (2000). Inhibition of Chlamydia pneumoniae replication in human aortic smooth muscle cells by gamma interferon-induced indoleamine 2,3-dioxygenase activity. Infection and Immunity *68*, 6478-6481.

Pfefferkorn, E. R. (1984). Interferon gamma blocks the growth of Toxoplasma gondii in human fibroblasts by inducing the host cells to degrade tryptophan. Proceedings of the National Academy of Sciences of the United States of America-Biological Sciences *81*, 908-912.

Phan, L., Chou, P. C., Velazquez-Torres, G., Samudio, I., Parreno, K., Huang, Y., Tseng, C., Vu, T., Gully, C., Su, C. H.*, et al.* (2015). The cell cycle regulator 14-3-3sigma opposes and reverses cancer metabolic reprogramming. Nat Commun *6*, 7530.

Pietra, G., Manzini, C., Rivara, S., Vitale, M., Cantoni, C., Petretto, A., Balsamo, M., Conte, R., Benelli, R., Minghelli, S.*, et al.* (2012). Melanoma cells inhibit natural killer cell function by modulating the expression of activating receptors and cytolytic activity. Cancer Res *72*, 1407-1415.

Pilotte, L., Larrieu, P., Stroobant, V., Colau, D., Dolusic, E., Frederick, R., De Plaen, E., Uyttenhove, C., Wouters, J., Masereel, B., and Van den Eynde, B. J. (2012). Reversal of tumoral immune resistance by inhibition of tryptophan 2,3-dioxygenase. Proc Natl Acad Sci U S A *109*, 2497-2502.

Pineda, M., Fernandez, E., Torrents, D., Estevez, R., Lopez, C., Camps, M., Lloberas, J., Zorzano, A., and Palacin, M. (1999). Identification of a membrane protein, LAT-2, that co-expresses with 4F2 heavy chain, an L-type amino acid transport activity with broad specificity for small and large zwitterionic amino acids. Journal of Biological Chemistry *274*, 19738-19744.

Pingitore, P., Pochini, L., Scalise, M., Galluccio, M., Hedfalk, K., and Indiveri, C. (2013). Large scale production of the active human ASCT2 (SLC1A5) transporter in Pichia pastoris - functional and kinetic asymmetry revealed in proteoliposomes. Biochimica Et Biophysica Acta-Biomembranes *1828*, 2238-2246.

Pochini, L., Scalise, M., Galluccio, M., and Indiveri, C. (2014). Membrane transporters for the special amino acid glutamine: structure/function relationships and relevance to human health. Frontiers in Chemistry *2*.

Porton, B., Greenberg, B. D., Askland, K., Serra, L. M., Gesmonde, J., Rudnick, G., Rasmussen, S. A., and Kao, H. T. (2013). Isoforms of the neuronal glutamate transporter

gene, SLC1A1/EAAC1, negatively modulate glutamate uptake: relevance to obsessive-compulsive disorder. Translational Psychiatry *3*.

Poulos, M. G., Guo, P. P., Kofler, N. M., Pinho, S., Gutkin, M. C., Tikhonova, A., Aifantis, I., Frenette, P. S., Kitajewski, J., Rafii, S., and Butler, J. M. (2013). Endothelial Jagged-1 Is Necessary for Homeostatic and Regenerative Hematopoiesis. Cell Reports *4*, 1022-1034.

Qiu, H., Dong, J., Hu, C., Francklyn, C. S., and Hinnebusch, A. G. (2001). The tRNA-binding moiety in GCN2 contains a dimerization domain that interacts with the kinase domain and is required for tRNA binding and kinase activation. Embo Journal *20*, 1425-1438.

Qiu, H. F., Garcia-Barrio, M. T., and Hinnebusch, A. G. (1998). Dimerization by translation initiation factor 2 kinase GCN2 is mediated by interactions in the C-terminal ribosome-binding region and the protein kinase domain. Molecular and Cellular Biology *18*, 2697-2711.

Rask-Andersen, M., Masuram, S., Fredriksson, R., and Schioth, H. B. (2013). Solute carriers as drug targets: current use, clinical trials and prospective. Mol Aspects Med *34*, 702-710.

Rasko, J. E. J., Battini, J. L., Gottschalk, R. J., Mazo, I., and Miller, A. D. (1999). The RD114 simian type D retrovirus receptor is a neutral amino acid transporter. Proc Natl Acad Sci U S A *96*, 2129-2134.

Ravishankar, B., Liu, H. Y., Shinde, R., Chandler, P., Baban, B., Tanaka, M., Munn, D. H., Mellor, A. L., Karlsson, M. C. I., and McGaha, T. L. (2012). Tolerance to apoptotic cells is regulated by indoleamine 2,3-dioxygenase. Proc Natl Acad Sci U S A *109*, 3909-3914.

Rebsamen, M., Pochini, L., Stasyk, T., de Araujo, M. E. G., Galluccio, M., Kandasamy, R. K., Snijder, B., Fauster, A., Rudashevskaya, E. L., Bruckner, M.*, et al.* (2015). SLC38A9 is a component of the lysosomal amino acid sensing machinery that controls mTORC1. Nature *519*, 477–481.

Reddy, P., Sun, Y. P., Toubai, T., Duran-Struuck, R., Clouthier, S. G., Weisiger, E., Maeda, Y., Tawara, I., Krijanovski, O., Gatza, E.*, et al.* (2008). Histone deacetylase inhibition modulates indoleamine 2,3-dioxygenase-dependent DC functions and regulates

experimental graft-versus-host disease in mice. Journal of Clinical Investigation *118*, 2562-2573.

Ren, P., Yue, M., Xiao, D., Xiu, R., Gan, L., Liu, H., and Qing, G. (2015). ATF4 and N-Myc coordinate glutamine metabolism in MYCN-amplified neuroblastoma cells through ASCT2 activation. Journal of Pathology *235*, 90-100.

Restifo, N. P., Esquivel, F., Kawakami, Y., Yewdell, J. W., Mule, J. J., Rosenberg, S. A., and Bennink, J. R. (1993). Identification of human cancers deficient in antigen processing. Journal of Experimental Medicine *177*, 265-272.

Reyes, N., Ginter, C., and Boudker, O. (2009). Transport mechanism of a bacterial homologue of glutamate transporters. Nature *462*, 880-885.

Reynolds, M. R., Lane, A. N., Robertson, B., Kemp, S., Liu, Y., Hill, B. G., Dean, D. C., and Clem, B. F. (2014). Control of glutamine metabolism by the tumor suppressor Rb. Oncogene *33*, 556-566.

Rivera, S., Lopezsoriano, F. J., Azconbieto, J., and Argiles, J. M. (1987). Blood amino acid compartmentation in mice bearing Lewis lung carcinoma. Cancer Research *47*, 5644-5646.

Robinson, C. M., Hale, P. T., and Carlin, J. M. (2006). NF-kappa B activation contributes to indoleamine dioxygenase transcriptional synergy induced by IFN-gamma and tumor necrosis factor-alpha. Cytokine *35*, 53-61.

Robinson, C. M., Shirey, K. A., and Carlin, J. M. (2003). Synergistic transcriptional activation of indoleamine dioxygenase by IFN-gamma and tumor necrosis factor-alpha. Journal of Interferon and Cytokine Research *23*, 413-421.

Rodriguez, P. C., Zea, A. H., Culotta, K. S., Zabaleta, J., Ochoa, J. B., and Ochoa, A. C. (2002). Regulation of T cell receptor CD3zeta chain expression by L-arginine. J Biol Chem *277*, 21123-21129.

Romani, L., Fallarino, F., De Luca, A., Montagnoli, C., D'Angelo, C., Zelante, T., Vacca, C., Bistoni, F., Fioretti, M. C., Grohmann, U*., et al.* (2008). Defective tryptophan catabolism underlies inflammation in mouse chronic granulomatous disease. Nature *451*, 211-215.

Romano, P. R., Garcia-Barrio, M. T., Zhang, X. L., Wang, Q. Z., Taylor, D. R., Zhang, F., Herring, C., Mathews, M. B., Qin, J., and Hinnebusch, A. G. (1998). Autophosphorylation in the activation loop is required for full kinase activity in vivo of human and yeast eukaryotic initiation factor 2 alpha kinases PKR and GCN2. Molecular and Cellular Biology *18*, 2282-2297.

Rossier, G., Meier, C., Bauch, C., Summa, V., Sordat, B., Verrey, F., and Kuhn, L. C. (1999). LAT2, a new basolateral 4F2hc/CD98-associated amino acid transporter of kidney and intestine. Journal of Biological Chemistry *274*, 34948-34954.

RotemYehudar, R., Groettrup, M., Soza, A., Kloetzel, P. M., and Ehrlich, R. (1996). LMP-associated proteolytic activities and TAP-dependent peptide transport for class I MHC molecules are suppressed in cell lines transformed by the highly oncogenic adenovirus 12. Journal of Experimental Medicine *183*, 499-514.

Sada-Ovalle, I., Chiba, A., Gonzales, A., Brenner, M. B., and Behar, S. M. (2008). Innate Invariant NKT Cells Recognize Mycobacterium tuberculosis-Infected Macrophages, Produce Interferon-gamma, and Kill Intracellular Bacteria. Plos Pathogens *4*.

Sakurai, K., Zou, J. P., Tschetter, J. R., Ward, J. M., and Shearer, G. M. (2002). Effect of indoleamine 2,3-dioxygenase on induction of experimental autoimmune encephalomyelitis. Journal of Neuroimmunology *129*, 186-196.

Sancak, Y., Bar-Peled, L., Zoncu, R., Markhard, A. L., Nada, S., and Sabatini, D. M. (2010). Ragulator-Rag Complex Targets mTORC1 to the Lysosomal Surface and Is Necessary for Its Activation by Amino Acids. Cell *141*, 290-303.

Sancak, Y., Peterson, T. R., Shaul, Y. D., Lindquist, R. A., Thoreen, C. C., Bar-Peled, L., and Sabatini, D. M. (2008). The Rag GTPases bind raptor and mediate amino acid signaling to mTORC1. Science *320*, 1496-1501.

Sanjana, N. E., Shalem, O., and Zhang, F. (2014). Improved vectors and genome-wide libraries for CRISPR screening. Nature Methods *11*, 783-784.

Santillan, M. K., Pelham, C. J., Ketsawatsomkron, P., Santillan, D. A., Davis, D. R., Devor, E. J., Gibson-Corley, K. N., Scroggins, S. M., Grobe, J. L., Yang, B.*, et al.* (2015).

Pregnant mice lacking indoleamine 2,3-dioxygenase exhibit preeclampsia phenotypes. Physiological reports *3*.

Sarkar, S. A., Wong, R., Hackl, S. I., Moua, O., Gill, R. G., Wiseman, A., Davidson, H. W., and Hutton, J. C. (2007). Induction of indoleamine 2,3-dioxygenase by interferon-gamma in human islets. Diabetes *56*, 72-79.

Sato, H., Tamba, M., Ishii, T., and Bannai, S. (1999). Cloning and expression of a plasma membrane cystine/glutamate exchange transporter composed of two distinct proteins. Journal of Biological Chemistry *274*, 11455-11458.

Sayama, S., Yoshida, R., Oku, T., Imanishi, J., Kishida, T., and Hayaishi, O. (1981). Inhibition of interferon-mediated induction of indoleamine 2,3-dioxygenase in mouse lung by inhibitors of prostaglandin biosynthesis. Proceedings of the National Academy of Sciences of the United States of America-Biological Sciences *78*, 7327-7330.

Scalise, M., Pochini, L., Panni, S., Pingitore, P., Hedfalk, K., and Indiveri, C. (2014). Transport mechanism and regulatory properties of the human amino acid transporter ASCT2 (SLC1A5). Amino Acids *46*, 2463-2475.

Schimke, R. T., Sweeney, E. W., and Berlin, C. M. (1965). Roles of synthesis and degradation in control of rat liver tryptophan pyrrolase. Journal of Biological Chemistry *240*, 322-331.

Scortegagna, M., Morris, M. A., Oktay, Y., Bennett, M., and Garcia, J. A. (2003). The HIF family member EPAS1/HIF-2alpha is required for normal hematopoiesis in mice. Blood *102*, 1634-1640.

Sedlmayr, P., Blaschitz, A., Wintersteiger, R., Semlitsch, M., Hammer, A., MacKenzie, C. R., Walcher, W., Reich, O., Takikawa, O., and Dohr, G. (2002). Localization of indoleamine 2,3-dioxygenase in human female reproductive organs and the placenta. Molecular Human Reproduction *8*, 385-391.

Segawa, H., Fukasawa, Y., Miyamoto, K., Takeda, E., Endou, H., and Kanai, Y. (1999). Identification and functional characterization of a Na+-independent neutral amino acid transporter with broad substrate selectivity. Journal of Biological Chemistry *274*, 19745-19751.

Seow, H. F., Broer, S., Broer, A., Bailey, C. G., Potter, S. J., Cavanaugh, J. A., and Rasko, J. E. (2004). Hartnup disorder is caused by mutations in the gene encoding the neutral amino acid transporter SLC6A19. Nat Genet *36*, 1003-1007.

Shalem, O., Sanjana, N. E., Hartenian, E., Shi, X., Scott, D. A., Mikkelsen, T. S., Heckl, D., Ebert, B. L., Root, D. E., Doench, J. G., and Zhang, F. (2014). Genome-Scale CRISPR-Cas9 Knockout Screening in Human Cells. Science *343*, 84-87.

Shankaran, V., Ikeda, H., Bruce, A. T., White, J. M., Swanson, P. E., Old, L. J., and Schreiber, R. D. (2001). IFN gamma and lymphocytes prevent primary tumour development and shape tumour immunogenicity. Nature *410*, 1107-1111.

Sharma, M. D., Baban, B., Chandler, P., Hou, D.-Y., Singh, N., Yagita, H., Azurna, M., Blazar, B. R., Mellor, A. L., and Munn, D. H. (2007). Plasmacytoid dendritic cells from mouse tumor-draining lymph nodes directly activate mature Tregs via indoleamine 2,3-dioxygenase. Journal of Clinical Investigation *117*, 2570-2582.

Sharma, M. D., Hou, D. Y., Baban, B., Koni, P. A., He, Y. K., Chandler, P. R., Blazar, B. R., Mellor, A. L., and Munn, D. H. (2010). Reprogrammed Foxp3(+) Regulatory T Cells Provide Essential Help to Support Cross-presentation and CD8(+) T Cell Priming in Naive Mice. Immunity *33*, 942-954.

Sharma, M. D., Hou, D. Y., Liu, Y. J., Koni, P. A., Metz, R., Chandler, P., Mellor, A. L., He, Y., and Munn, D. H. (2009). Indoleamine 2,3-dioxygenase controls conversion of Foxp3(+) Tregs to TH17-like cells in tumor-draining lymph nodes. Blood *113*, 6102-6111.

Shimizu, K., Kaira, K., Tomizawa, Y., Sunaga, N., Kawashima, O., Oriuchi, N., Tominaga, H., Nagamori, S., Kanai, Y., Yamada, M*., et al.* (2014). ASC amino-acid transporter 2 (ASCT2) as a novel prognostic marker in non-small cell lung cancer. Br J Cancer *110*, 2030-2039.

Shimode, S., Nakaoka, R., Shogen, H., and Miyazawa, T. (2013). Characterization of feline ASCT1 and ASCT2 as RD-114 virus receptor. The Journal of general virology *94*, 1608-1612.

Sidransky, H. (1976). Nutritional disturbances of protein-metabolism in liver. American Journal of Pathology *84*, 649-667.

Silk, J. D., Lakhal, S., Laynes, R., Vallius, L., Karydis, I., Marcea, C., Boyd, C. A. R., and Cerundolo, V. (2011). IDO Induces Expression of a Novel Tryptophan Transporter in Mouse and Human Tumor Cells. Journal of Immunology *187*, 1617-1625.

Simon, D. B., Nelson-Williams, C., Bia, M. J., Ellison, D., Karet, F. E., Molina, A. M., Vaara, I., Iwata, F., Cushner, H. M., Koolen, M.*, et al.* (1996). Gitelman's variant of Bartter's syndrome, inherited hypokalaemic alkalosis, is caused by mutations in the thiazide-sensitive Na-Cl cotransporter. Nat Genet *12*, 24-30.

Sinclair, L. V., Rolf, J., Emslie, E., Shi, Y.-B., Taylor, P. M., and Cantrell, D. A. (2013). Control of amino-acid transport by antigen receptors coordinates the metabolic reprogramming essential for T cell differentiation. Nature Immunology *14*, 500-508.

Siu, F., Bain, P. J., LeBlanc-Chaffin, R., Chen, H., and Kilberg, M. S. (2002). ATF4 is a mediator of the nutrient-sensing response pathway that activates the human asparagine synthetase gene. Journal of Biological Chemistry *277*, 24120-24127.

Smith, C., Chang, M. Y., Parker, K. H., Beury, D. W., DuHadaway, J. B., Flick, H. E., Boulden, J., Sutanto-Ward, E., Soler, A. P., Laury-Kleintop, L. D.*, et al.* (2012). IDO Is a Nodal Pathogenic Driver of Lung Cancer and Metastasis Development. Cancer Discovery *2*, 722-735.

Smyth, M. J., Crowe, N. Y., and Godfrey, D. I. (2001). NK cells and NKT cells collaborate in host protection from methylcholanthrene-induced fibrosarcoma. Int Immunol *13*, 459-463.

Smyth, M. J., Swann, J., Cretney, E., Zerafa, N., Yokoyama, W. M., and Hayakawa, Y. (2005). NKG2D function protects the host from tumor initiation. Journal of Experimental Medicine *202*, 583-588.

Smyth, M. J., Thia, K. Y. T., Street, S. E. A., Cretney, E., Trapani, J. A., Taniguchi, M., Kawano, T., Pelikan, S. B., Crowe, N. Y., and Godfrey, D. I. (2000). Differential tumor surveillance by natural killer (NK) and NKT cells. Journal of Experimental Medicine *191*, 661-668.

Soliman, H. H., Jackson, E., Neuger, T., Dees, E. C., Harvey, R. D., Han, H., Ismail-Khan, R., Minton, S., Vahanian, N. N., Link, C.*, et al.* (2014a). A first in man phase I trial of the

oral immunomodulator, indoximod, combined with docetaxel in patients with metastatic solid tumors. Oncotarget *5*, 8136-8146.

Soliman, H. H., Minton, S. E., Ismail-Khan, R., Han, H. S., Janssen, W., Vahanlan, N. N., Link, C. J., Strelcher, H., Sullivan, D., and Antonia, S. J. (2014b). A phase 2 study of Ad.p53 DC vaccine in combination with indoximod in metastatic solid tumors. Journal of Clinical Oncology *32*.

Soliman, H. H., Minton, S. E., Ismail-Khan, R., Han, H. S., Vahanian, N. N., Link, C. J., Kennedy, G., Streicher, H., Sullivan, D., and Antonia, S. J. (2015). A phase 1/2 study of Ad.p53 DC vaccine with indoximod immunotherapy in metastatic breast cancer. Cancer Research *75*.

Sono, M., Taniguchi, T., Watanabe, Y., and Hayaishi, O. (1980). Indoleamine 2,3-dioxygenase -equilibrium studies of the tryptophan binding to the ferric, ferrous, and CO-bound enzymes. Journal of Biological Chemistry *255*, 1339-1345.

Speeckaert, R., Vermaelen, K., van Geel, N., Autier, P., Lambert, J., Haspeslagh, M., van Gele, M., Thielemans, K., Neyns, B., Roche, N.*, et al.* (2012). Indoleamine 2,3-dioxygenase, a new prognostic marker in sentinel lymph nodes of melanoma patients. European Journal of Cancer *48*, 2004-2011.

Spindel, O. N., World, C., and Berk, B. C. (2012). Thioredoxin Interacting Protein: Redox Dependent and Independent Regulatory Mechanisms. Antioxidants & Redox Signaling *16*, 587-596.

Spranger, S., Spaapen, R. M., Zha, Y., Williams, J., Meng, Y., Ha, T. T., and Gajewski, T. F. (2013). Up-Regulation of PD-L1, IDO, and T-regs in the Melanoma Tumor Microenvironment Is Driven by CD8(+) T Cells. Science Translational Medicine *5*.

St-Arnaud, R., Mandic, V., and Elchaarani, B. (2010). FIAT, the factor-inhibiting ATF4-mediated transcription, also represses the transcriptional activity of the bZIP factor FRA-1. Annals of the New York Academy of Sciences *1192*, 338-343.

Staveley-O'Carroll, K., Sotomayor, E., Montgomery, J., Borrello, I., Hwang, L., Fein, S., Pardoll, D., and Levitsky, H. (1998). Induction of antigen-specific T cell anergy: An early event in the course of tumor progression. Proc Natl Acad Sci U S A *95*, 1178-1183.

Street, S. E. A., Cretney, E., and Smyth, M. J. (2001). Perforin and interferon-gamma activities independently control tumor initiation, growth, and metastasis. Blood *97*, 192-197.

Street, S. E. A., Trapani, J. A., MacGregor, D., and Smyth, M. J. (2002). Suppression of lymphoma and epithelial malignancies effected by interferon gamma. Journal of Experimental Medicine *196*, 129-134.

Sugimoto, H., Oda, S. I., Otsuki, T., Hino, T., Yoshida, T., and Shiro, Y. (2006). Crystal structure of human indoleamine 2,3-dioxygenase: Catalytic mechanism of O-2 incorporation by a heme-containing dioxygenase. Proc Natl Acad Sci U S A *103*, 2611-2616.

Sundrud, M. S., Koralov, S. B., Feuerer, M., Calado, D. P., Kozhaya, A. E., Rhule-Smith, A., Lefebvre, R. E., Unutmaz, D., Mazitschek, R., Waldner, H.*, et al.* (2009). Halofuginone Inhibits T(H)17 Cell Differentiation by Activating the Amino Acid Starvation Response. Science *324*, 1334-1338.

Tailor, C. S., Nouri, A., Zhao, Y. A., Takeuchi, Y., and Kabat, D. (1999). A sodium-dependent neutral-amino-acid transporter mediates infections of feline and baboon endogenous retroviruses and simian type D retroviruses. Journal of Virology *73*, 4470-4474.

Tajiri, T., Liu, X. Y., Thompson, P. M., Tanaka, S., Suita, S., Zhao, H. Q., Maris, J. M., Prendergast, G. C., and Hogarty, M. D. (2003). Expression of a MYCN-interacting isoform of the tumor suppressor BIN1 is reduced in neuroblastomas with unfavorable biological features. Clinical Cancer Research *9*, 3345-3355.

Takamatsu, M., Hirata, A., Ohtaki, H., Hoshi, M., Hatano, Y., Tomita, H., Kuno, T., Saito, K., and Hara, A. (2013). IDO1 Plays an Immunosuppressive Role in 2,4,6-Trinitrobenzene Sulfate-Induced Colitis in Mice. Journal of Immunology *191*, 3057-3064.

Takao, M., Okamoto, A., Nikaido, T., Urashima, M., Takakura, S., Saito, M., Saito, M., Okamoto, S., Takikawa, O., Sasaki, H.*, et al.* (2007). Increased synthesis of indoleamine-2,3-dioxygenase protein is positively associated with impaired survival in patients with serous-type, but not with other types of, ovarian cancer. Oncology Reports *17*, 1333-1339.

Takeda, K., Kaisho, T., and Akira, S. (2003). Toll-like receptors. Annu Rev Immunol *21*, 335-376.

Takikawa, O., Kuroiwa, T., Yamazaki, F., and Kido, R. (1988). Mechanism of interferon-gamma action - characterization of indoleamine 2,3-dioxygenase in cultured human cells induced by interferon-gamma and evaluation of the enzyme-mediated tryptophan degradation in its anticellular activity. Journal of Biological Chemistry *263*, 2041-2048.

Terness, P., Bauer, T. M., Rose, L., Dufter, C., Watzlik, A., Simon, H., and Opelz, G. (2002). Inhibition of allogeneic T cell proliferation by indoleamine 2,3-dioxygenase-expressing dendritic cells: Mediation of suppression by tryptophan metabolites. Journal of Experimental Medicine *196*, 447-457.

Theate, I., van Baren, N., Pilotte, L., Moulin, P., Larrieu, P., Renauld, J.-C., Herve, C., Gutierrez-Roelens, I., Marbaix, E., Sempoux, C., and Van den Eynde, B. J. (2015). Extensive Profiling of the Expression of the Indoleamine 2,3-Dioxygenase 1 Protein in Normal and Tumoral Human Tissues. Cancer Immunology Research *3*, 161-172.

Thomas, L. (1959). Discussion. In Cellular and Humoral Aspects of the Hypersensitive States, (New York: Hoeber-Harper), pp. 529–532.

Thomas, S. R., and Stocker, R. (1999). Redox reactions related to indoleamine 2,3-dioxygenase and tryptophan metabolism along the kynurenine pathway. Redox Report *4*, 199-220.

Thomson, A. W., Turnquist, H. R., and Raimondi, G. (2009). Immunoregulatory functions of mTOR inhibition. Nature Reviews Immunology *9*, 324-337.

Timmerman, L. A., Holton, T., Yuneva, M., Louie, R. J., Padro, M., Daemen, A., Hu, M., Chan, D. A., Ethier, S. P., van 't Veer, L. J.*, et al.* (2013). Glutamine sensitivity analysis identifies the xCT antiporter as a common triple-negative breast tumor therapeutic target. Cancer Cell *24*, 450-465.

Toyoda, M., Kaira, K., Ohshima, Y., Ishioka, N. S., Shino, M., Sakakura, K., Takayasu, Y., Takahashi, K., Tominaga, H., Oriuchi, N.*, et al.* (2014). Prognostic significance of amino-acid transporter expression (LAT1, ASCT2, and xCT) in surgically resected tongue cancer. Br J Cancer *110*, 2506-2513.

Trapnell, C., Pachter, L., and Salzberg, S. L. (2009). TopHat: discovering splice junctions with RNA-Seq. Bioinformatics *25*, 1105-1111.

Trapnell, C., Williams, B. A., Pertea, G., Mortazavi, A., Kwan, G., van Baren, M. J., Salzberg, S. L., Wold, B. J., and Pachter, L. (2010). Transcript assembly and quantification by RNA-Seq reveals unannotated transcripts and isoform switching during cell differentiation. Nature Biotechnology *28*, 511-515.

Ueno, A., Cho, S., Cheng, L., Wang, J. X., Hou, S., Nakano, H., Santarnaria, P., and Yang, Y. (2007). Transient upregulation of indoleamine 2,3-dioxygenase in dendritic cells by human chorionic gonadotropin downregulates autoimmune diabetes. Diabetes *56*, 1686-1693.

Utsunomiya-Tate, N., Endou, H., and Kanai, Y. (1996). Cloning and functional characterization of a system ASC-like Na+-dependent neutral amino acid transporter. Journal of Biological Chemistry *271*, 14883-14890.

Uyttenhove, C., Pilotte, L., Theate, I., Stroobant, V., Colau, D., Parmentier, N., Boon, T., and Van den Eynde, B. J. (2003). Evidence for a tumoral immune resistance mechanism based on tryptophan degradation by indoleamine 2,3-dioxygenase. Nature Medicine *9*, 1269-1274.

van Geldermalsen, M., Wang, Q., Nagarajah, R., Marshall, A. D., Thoeng, A., Gao, D., Ritchie, W., Feng, Y., Bailey, C. G., Deng, N.*, et al.* (2016). ASCT2/SLC1A5 controls glutamine uptake and tumour growth in triple-negative basal-like breast cancer. Oncogene *35*, 3201-3208.

Vantourout, P., and Hayday, A. (2013). Six-of-the-best: unique contributions of gammadelta T cells to immunology. Nature reviews Immunology *13*, 88-100.

Vattem, K. M., and Wek, R. C. (2004). Reinitiation involving upstream ORFs regulates ATF4 mRNA translation in mammalian cells. Proc Natl Acad Sci U S A *101*, 11269-11274.

Verbist, K. C., Guy, C. S., Milasta, S., Liedmann, S., Kaminski, M. M., Wang, R. N., and Green, D. R. (2016). Metabolic maintenance of cell asymmetry following division in activated T lymphocytes. Nature *532*, 389-393.

Verdon, G., Oh, S., Serio, R. N., and Boudker, O. (2014). Coupled ion binding and structural transitions along the transport cycle of glutamate transporters. eLife *3*, e02283.

Verrey, F. (2003). System L: heteromeric exchangers of large, neutral amino acids involved in directional transport. Pflugers Archiv-European Journal of Physiology *445*, 529-533.

Verrey, F., Closs, E. I., Wagner, C. A., Palacin, M., Endou, H., and Kanai, Y. (2004). CATs and HATs: the SLC7 family of amino acid transporters. Pflugers Archiv-European Journal of Physiology *447*, 532-542.

Volpi, C., Fallarino, F., Bianchi, R., Orabona, C., De Luca, A., Vacca, C., Romani, L., Gran, B., Grohmann, U., Puccetti, P., and Belladonna, M. L. (2012). A GpC-Rich Oligonucleotide Acts on Plasmacytoid Dendritic Cells To Promote Immune Suppression. Journal of Immunology *189*, 2283-2289.

von Bergwelt-Baildon, M. S., Popov, A., Saric, T., Chemnitz, J., Classen, S., Stoffel, M. S., Fiore, F., Roth, U., Beyer, M., Debey, S.*, et al.* (2006). CD25 and indoleamine 2,3-dioxygenase are up-regulated by prostaglandin E2 and expressed by tumor-associated dendritic cells in vivo: additional mechanisms of T-cell inhibition. Blood *108*, 228-237.

Wainwright, D. A., Balyasnikova, I. V., Chang, A. L., Ahmed, A. U., Moon, K. S., Auffinger, B., Tobias, A. L., Han, Y., and Lesniak, M. S. (2012). IDO Expression in Brain Tumors Increases the Recruitment of Regulatory T Cells and Negatively Impacts Survival. Clinical Cancer Research *18*, 6110-6121.

Waldhauer, I., and Steinle, A. (2008). NK cells and cancer immunosurveillance. Oncogene *27*, 5932-5943.

Wang, D., Saga, Y., Mizukami, H., Sato, N., Nonaka, H., Fujiwara, H., Takei, Y., Machida, S., Takikawa, O., Ozawa, K., and Suzuki, M. (2012). Indoleamine-2,3-dioxygenase, an immunosuppressive enzyme that inhibits natural killer cell function, as a useful target for ovarian cancer therapy. International journal of oncology *40*, 929-934.

Wang, Q., Beaumont, K. A., Otte, N. J., Font, J., Bailey, C. G., van Geldermalsen, M., Sharp, D. M., Tiffen, J. C., Ryan, R. M., Jormakka, M.*, et al.* (2014). Targeting glutamine transport to suppress melanoma cell growth. International Journal of Cancer *135*, 1060-1071.

Wang, Q., Hardie, R.-A., Hoy, A. J., van Geldermalsen, M., Gao, D., Fazli, L., Sadowski, M. C., Balaban, S., Schreuder, M., Nagarajah, R.*, et al.* (2015a). Targeting ASCT2-mediated glutamine uptake blocks prostate cancer growth and tumour development. Journal of Pathology *236*, 278-289.

Wang, R. N., Dillon, C. P., Shi, L. Z., Milasta, S., Carter, R., Finkelstein, D., McCormick, L. L., Fitzgerald, P., Chi, H. B., Munger, J., and Green, D. R. (2011). The Transcription Factor Myc Controls Metabolic Reprogramming upon T Lymphocyte Activation. Immunity *35*, 871-882.

Wang, S. Y., Tsun, Z. Y., Wolfson, R. L., Shen, K., Wyant, G. A., Plovanich, M. E., Yuan, E. D., Jones, T. D., Chantranupong, L., Comb, W.*, et al.* (2015b). Lysosomal amino acid transporter SLC38A9 signals arginine sufficiency to mTORC1. Science *347*, 188-194.

Wang, X. Z., Kuroda, M., Sok, J., Batchvarova, N., Kimmel, R., Chung, P., Zinszner, H., and Ron, D. (1998). Identification of novel stress-induced genes downstream of chop. Embo Journal *17*, 3619-3630.

Wang, Y. T., Liu, H. Z., McKenzie, G., Witting, P. K., Stasch, J. P., Hahn, M., Changsirivathanathamrong, D., Wu, B. J., Ball, H. J., Thomas, S. R.*, et al.* (2010). Kynurenine is an endothelium-derived relaxing factor produced during inflammation. Nature Medicine *16*, 279-285.

Wang, Z., Cao, Y., Albino, A. P., Zeff, R. A., Houghton, A., and Ferrone, S. (1993). Lack of HLA class I antigen expression by melanoma cells SK-MEL-33 caused by a reading frameshift in beta 2-microglobulin messenger RNA. Journal of Clinical Investigation *91*, 684-692.

Waterhouse, P., Penninger, J. M., Timms, E., Wakeham, A., Shahinian, A., Lee, K. P., Thompson, C. B., Griesser, H., and Mak, T. W. (1995). Lymphoproliferative disorders with early lethality in mice deficient in CTLA-4. Science *270*, 985-988.

Wek, S. A., Zhu, S. H., and Wek, R. C. (1995). The histidyl-transfer-RNA synthetase-related sequence in the EIF-2-alpha protein-kinase GCN2 interacts with transfer-RNA and is required for activation in response to starvation for different amino-acids. Molecular and Cellular Biology *15*, 4497-4506.

Wildin, R. S., Ramsdell, F., Peake, J., Faravelli, F., Casanova, J. L., Buist, N., Levy-Lahad, E., Mazzella, M., Goulet, O., Perroni, L.*, et al.* (2001). X-linked neonatal diabetes mellitus, enteropathy and endocrinopathy syndrome is the human equivalent of mouse scurfy. Nature Genetics *27*, 18-20.

Wilkinson, A. C., Ballabio, E., Geng, H., North, P., Tapia, M., Kerry, J., Biswas, D., Roeder, R. G., Allis, C. D., Melnick, A.*, et al.* (2013). RUNX1 is a key target in t(4;11) leukemias that contributes to gene activation through an AF4-MLL complex interaction. Cell Rep *3*, 116-127.

Willems, L., Jacque, N., Jacquel, A., Neveux, N., Maciel, T. T., Lambert, M., Schmitt, A., Poulain, L., Green, A. S., Uzunov, M.*, et al.* (2013). Inhibiting glutamine uptake represents an attractive new strategy for treating acute myeloid leukemia. Blood *122*, 3521-3532.

Wise, D. R., DeBerardinis, R. J., Mancuso, A., Sayed, N., Zhang, X.-Y., Pfeiffer, H. K., Nissim, I., Daikhin, E., Yudkoff, M., McMahon, S. B., and Thompson, C. B. (2008). Myc regulates a transcriptional program that stimulates mitochondrial glutaminolysis and leads to glutamine addiction. Proc Natl Acad Sci U S A *105*, 18782-18787.

Witkiewicz, A., Potoczek, M., Berger, A., Sato, T., Brody, J., and Constantino, C. (2009a). Expression of indoleamine 2,3-dioxygenase in malignant melanoma. Journal of Cutaneous Pathology *36*.

Witkiewicz, A. K., Costantino, C. L., Metz, R., Muller, A. J., Prendergast, G. C., Yeo, C. J., and Brody, J. R. (2009b). Genotyping and Expression Analysis of IDO2 in Human Pancreatic Cancer: A Novel, Active Target. Journal of the American College of Surgeons *208*, 781-787.

Wojtal, K. A., Eloranta, J. J., Hruz, P., Gutmann, H., Drewe, J., Staumann, A., Beglinger, C., Fried, M., Kullak-Ublick, G. A., and Vavricka, S. R. (2009). Changes in mRNA Expression Levels of Solute Carrier Transporters in Inflammatory Bowel Disease Patients. Drug Metabolism and Disposition *37*, 1871-1877.

Wollscheid, B., Bausch-Fluck, D., Henderson, C., O'Brien, R., Bibel, M., Schiess, R., Aebersold, R., and Watts, J. D. (2009). Mass-spectrometric identification and relative quantification of N-linked cell surface glycoproteins. Nat Biotechnol *27*, 378-386.

Xiao, B. G., Liu, X., and Link, H. (2004). Antigen-specific T cell functions are suppressed over the estrogen-dendritic cell-indoleamine 2,3-dioxygenase axis. Steroids *69*, 653-659.

Xiao, Y. G., Christou, H., Liu, L., Visner, G., Mitsialis, S. A., Kourembanas, S., and Liu, H. Z. (2013). Endothelial Indoleamine 2,3-Dioxygenase Protects against Development of Pulmonary Hypertension. American Journal of Respiratory and Critical Care Medicine *188*, 482-491.

Xu, D. S., and Hemler, M. E. (2005). Metabolic activation-related CD147-CD98 complex. Molecular & Cellular Proteomics *4*, 1061-1071.

Yan, Y. P., Zhang, G. X., Gran, B., Fallarino, F., Yu, S., Li, H. M., Cullimore, M. L., Rostami, A., and Xu, H. (2010). IDO Upregulates Regulatory T Cells via Tryptophan Catabolite and Suppresses Encephalitogenic T Cell Responses in Experimental Autoimmune Encephalomyelitis. Journal of Immunology *185*, 5953-5961.

Ye, J., Kumanova, M., Hart, L. S., Sloane, K., Zhang, H., De Panis, D. N., Bobrovnikova-Marjon, E., Diehl, J. A., Ron, D., and Koumenis, C. (2010). The GCN2-ATF4 pathway is critical for tumour cell survival and proliferation in response to nutrient deprivation. Embo Journal *29*, 2082-2096.

Yernool, D., Boudker, O., Jin, Y., and Gouaux, E. (2004). Structure of a glutamate transporter homologue from Pyrococcus horikoshii. Nature *431*, 811-818.

Yeung, A. W. S., Wu, W., Freewan, M., Stocker, R., King, N. J. C., and Thomas, S. R. (2012). Flavivirus infection induces indoleamine 2,3-dioxygenase in human monocyte-derived macrophages via tumor necrosis factor and NF-kappa B. Journal of Leukocyte Biology *91*, 657-666.

Yu, J. P., Sun, J. Y., Wang, S. E., Li, H., Cao, S., Cong, Y. Z., Liu, J. T., and Ren, X. B. (2011). Upregulated Expression of Indoleamine 2, 3-Dioxygenase in Primary Breast Cancer Correlates with Increase of Infiltrated Regulatory T Cells In Situ and Lymph Node Metastasis. Clinical & Developmental Immunology, 469135.

Yun, D. W., Lee, S. A., Park, M. G., Kim, J. S., Yu, S. K., Park, M. R., Kim, S. G., Oh, J. S., Kim, C. S., Kim, H. J.*, et al.* (2014). JPH203, an L-type amino acid transporter 1-

selective compound, induces apoptosis of YD-38 human oral cancer cells. Journal of pharmacological sciences *124*, 208-217.

Zakharia, Y., Drabick, J., Khleif, S., Munn, D., Link, C., Vahanian, N., Kennedy, E., Rixe, O., and Milhem, M. (2015). Results of Phase 1b trial of the Indoleamine 2,3-dioxygenase (IDO) Pathway Inhibitor Indoximod plus Ipilimumab for the treatment of unresectable stage III or IV melanoma. European Journal of Cancer *51*.

Zhang, P. C., McGrath, B. C., Reinert, J., Olsen, D. S., Lei, L., Gill, S., Wek, S. A., Vattem, K. M., Wek, R. C., Kimball, S. R.*, et al.* (2002). The GCN2 eIF2 alpha kinase is required for adaptation to amino acid deprivation in mice. Molecular and Cellular Biology *22*, 6681-6688.

Zhao, E. H., Ding, J., Xia, Y. F., Liu, M. L., Ye, B. W., Choi, J. H., Yan, C. H., Dong, Z., Huang, S., Zha, Y. H.*, et al.* (2016). KDM4C and ATF4 Cooperate in Transcriptional Control of Amino Acid Metabolism. Cell Reports *14*, 506-519.

Zhu, W. H., Lu, C. Z., Huang, Y. M., Link, H., and Xiao, B. G. (2007). A putative mechanism on remission of multiple sclerosis during pregnancy: estrogen-induced indoleamine 2,3-dioxygenase by dendritic cells. Multiple Sclerosis *13*, 33-40.

Zinszner, H., Kuroda, M., Wang, X. Z., Batchvarova, N., Lightfoot, R. T., Remotti, H., Stevens, J. L., and Ron, D. (1998). CHOP is implicated in programmed cell death in response to impaired function of the endoplasmic reticulum. Genes & Development *12*, 982-995.

Zoncu, R., Bar-Peled, L., Efeyan, A., Wang, S. Y., Sancak, Y., and Sabatini, D. M. (2011). mTORC1 Senses Lysosomal Amino Acids Through an Inside-Out Mechanism That Requires the Vacuolar H+-ATPase. Science *334*, 678-683.

Zou, W. P. (2005). Immunosuppressive networks in the tumour environment and their therapeutic relevance. Nature Reviews Cancer *5*, 263-274.

Zou, W. P. (2006). Regulatory T cells, tumour immunity and immunotherapy. Nature Reviews Immunology *6*, 295-307.